

AD 670961

FOREIGN TECHNOLOGY DIVISION



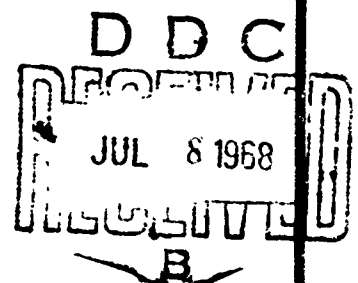
MATHEMATICAL MODELS FOR CALCULATION OF ELECTRICAL AND MAGNETIC FIELDS

by

O. V. Tozoni



GOLDEN ANNIVERSARY
FOREIGN TECHNOLOGY DIVISION



Distribution of this document is unlimited. It may be released to the Clearinghouse, Department of Commerce, for sale to the general public.

Reproduced by the
CLEARINGHOUSE
for Federal Scientific & Technical
Information Springfield Va 22151

309

This document is a machine translation of Russian text which has been processed by the AN/GSQ-16(XW-2) Machine Translator, owned and operated by the United States Air Force. The machine output has been post-edited to correct for major ambiguities of meaning, words missing from the machine's dictionary, and words out of the context of meaning. The sentence word order has been partially rearranged for readability. The content of this translation does not indicate editorial accuracy, nor does it indicate USAF approval or disapproval of the material translated.

ACCESSION FOR	
CFSI	WHITE SECTION <input checked="" type="checkbox"/>
DDC	BUFF SECTION <input type="checkbox"/>
UNANNOUNCED	<input type="checkbox"/>
JUSTIFICATION	
BY	
FOR BUTION AVAILABILITY CODE	
1	AVAIL. and or SPECIAL

EDITED MACHINE TRANSLATION

MATHEMATICAL MODELS FOR CALCULATION OF ELECTRICAL
AND MAGNETIC FIELDS

By: O. V. Tozoni

English pages: 300

TM6501691

THIS TRANSLATION IS A RENDITION OF THE ORIGINAL FOREIGN TEXT WITHOUT ANY ANALYTICAL OR EDITORIAL COMMENT. STATEMENTS OR THEORIES ADVOCATED OR IMPLIED ARE THOSE OF THE SOURCE AND DO NOT NECESSARILY REFLECT THE POSITION OR OPINION OF THE FOREIGN TECHNOLOGY DIVISION.

PREPARED BY:

TRANSLATION DIVISION
FOREIGN TECHNOLOGY DIVISION
WP-APB, OHIO.

Akademiya Nauk Ukrainskoy SSR
Institut Kibernetiki

Tozoni O. B.

MATEMATICHESKIYE MODELI DLYA RASCHETA
ELEKTRICHESKIKH I MAGNITNYKH
POLEY

Kiyev-1964
Pages 304

ITIS INDEX CONTROL FORM

01 Acc Nr TM6501691	68 Translation Nr MT6600086	65 X Ref Acc Nr AM4047286	76 Reel/Frame Nr 1654 1573
97 Header Clas UNCL	63 Clas UNCL, 0	64 Control Markings 0	94 Expansion UR
02 Ctry UR	03 Ref 0000	04 Yr 64	05 Vol 000
06 Iss 000	07 B. Pg. 0001	45 B. Pg. 0304	10 Date NONE

Transliterated Title

SEE SOURCE

09 English Title
MATHEMATICAL MODELS FOR CALCULATION OF ELECTRICAL AND MAGNETIC FIELDS

43 Source (RUSSIAN)
MATEMATICHESKIYE MODELI DLYA RASCHETA ELEKTRICHESKIKH I MAGNITNYKH POLEY

42 Author 98 Document Location

TOZONI, O. V.

16 Co-Author 47 Subject Codes

NONE

12, 20, 09

16 Co-Author 39 Topic Tags: mathematic model, electric field, magnetic field, electronic computer

NONE

16 Co-Author

NONE

16 Co-Author

NONE

ABSTRACT: This monograph presents new methods of calculating electromagnetic fields using modeling and electronic computers, describes the operating principles and the design of models of the most complex mathematical operations, and examines the methods of calculating specialized modeling machines for calculating electromagnetic fields. The last chapter considers the theory of models of spatial static fields with an optimal boundary structure. Examples are included of the calculation and building of models with minimum distorting boundary and new methods of modeling. The book contains basically original material which can be used in the design of new types of electromagnetic equipment. The book is intended for researchers and engineers concerned with calculating electromagnetic fields and developing and designing new types of electrical and radio equipment.

TABLE OF CONTENTS [abridged]:

Preface

Chapter I. Analytic Functions and Flat Field

Chapter II. Modeling of Conformally Mapping Functions

Chapter III. Calculation of Electrical and Magnetic Fields With the Help of Simulation of Conformal Mapping

Chapter IV. Integrators for Calculation of Flat Fields and Their Application

Chapter V. Model For Investigation of Volumetric Fields

Literature

English translation: 299 pages.

TABLE OF CONTENTS

Preface.....	1
CHAPTER I	
Analytic Functions and Flat Field	
§ 1. Harmonic Functions on Plane.....	5
§ 2. Functions of Flux and Complex Potential in a Flat Field.....	8
§ 3. Plane-Parallel Electrostatic Field.....	11
§ 4. Plane-Parallel Magnetic Field.....	13
§ 5. Conformal Transformations.....	19
§ 6. Invariance of the Laplace Equation During.....	23
§ 7. Conformal Transformation of a Circle of Radius R to a Circle of the Same Radius with Translation of Point $z_0 = re^{i\theta}$ to the Center of Circle.....	25
§ 8. Solution of the Dirichlet Problem for the Circle. Integral of Poisson.....	27
§ 9. Poisson Integral for the Upper Half-Plane.....	28
§ 10. Poisson Integral for an Infinite Band.....	29
§ 11. Normal Derivative of Potential on the Boundary of the Band.....	31
§ 12. Solution of the Dirichlet Problem in a Biconnected Region Using Conformal Transformation.....	36
§ 13. Transformation of Ring onto a Band.....	38
§ 14. Determining Maximum Values of Potential When Solving the Modified Dirichlet Problem in a Biconnected Region.....	41
§ 15. Example of the Calculation of the Field of a Charged Axis in an Annular Gap Between Two Concentric Cylinders.....	46
CHAPTER II	
Modeling of Conformally Mapping Functions	
§ 16. Electrical Field of Current in a Conducting Sheet.....	53
§ 17. Simulation of a Function Conformally Depicting a Singly-Connected Region on a Band.....	59
§ 18. Determination of Constants of the Christoffel Formula for Region Bounded by a Closed, Nonintersecting Broken Line.....	65
§ 19. Modeling of a Function Infinite-Sheetly, Conformally Mapping a Bicoupled Region Onto a Band.....	67

CHAPTER III
Calculation of Electrical and Magnetic Fields With
the Help of Simulation of Conformal Mapping

§ 20.	Calculation of the Field of a Charged Conductor.....	79
§ 21.	Calculating the Magnetic Field of a DC Machine by Modeling of a Conformal Mapping. Formulation of Problem.....	83
§ 22.	Calculation of Induction on the Armature of an Unsaturated Machine not Having Gaps between the Yoke and Cores of Additional Poles.....	9-
§ 23.	Calculation of Induction on the Armature of an Unsaturated Machine with Gaps Between Yoke and Cores of Additional Poles.....	104

CHAPTER IV
Integrators for Calculation of Flat Fields and Their Application

§ 24.	Electrointegrator for Simulation of Particular Solution of Poisson Equation.....	115
§ 25.	Modeling Errors.....	122
§ 26.	Electrointegrator for Solution of the Dirichlet and Neumann Problems.....	132
§ 27.	Electrointegrator Resolution.....	140
§ 28.	Calculation of the Magnetic Field in the Gap of a Saturated Magnetic System.....	167
§ 29.	On Electromodeling of a Magnetic Field and on the Possibility of Computer Calculation of Static Fields in Nonlinear Media.....	176
§ 30.	Electrosimulation of Distribution of Sinusoidal Current in Current Carriers.....	193
§ 31.	Computer Calculation of Parameters of a Three- Phase System of Current Carrier.....	209

CHAPTER V
Model for Investigation of Volumetric Fields

§ 32.	Difficulties of Modeling.....	219
§ 33.	Green's Theorem.....	221
§ 34.	Formulation of the Problem of Construct of a Model Element of Unlimited Space.....	224
§ 35.	Basic Geometric Presentations.....	227
§ 36.	Model with Minimum of Average Value or Absolute Magnitude of Potential of Distortion.....	230
§ 37.	Model with Zero Meaning Value of Potential of Distortion.....	236
§ 38.	On Accuracy of Modeling.....	243

§ 39. Model of an Element of Unbounded Space Having the Form of a Rectangle.....	248
§ 40. Models for Calculation of Space Fields.....	258
§ 41. Simulation of Field of Stray Currents in the Networks of Electrified Railroads and Underground Pipelines.....	277
§ 42. Model for Calculating Electrotection of Underground Constructions from Corrosion.....	290
Literature.....	296
U. S. Board on Geographic Names Transliteration System.....	299
Designations of the Trigonometric Functions.....	300

In monograph are presented new methods of calculation of electromagnetic fields with the help of simulation and electronic computers, are described principles of action and construction of models of separate most complicated mathematical operations, are given methods of design of specialized analog computers for calculation of electromagnetic fields. In last chapter is presented theory of models of space static fields with optimum structure of boundary. Are given examples of calculation and construction of models with minimumly distorting boundary and new methods of simulation.

Book contains basically original material which it is possible to use when designing new types of electromagnetic devices.

It is intended for scientists and engineers occupied with calculations of electromagnetic fields and also developing and designing of new types of electro- and radiotechnical devices.

Editor-in-Chief
Associate Member of Ukrainian
Academy of Sciences
G. Ye. Pukhov

PREFACE

Calculation of electromagnetic fields in linear media usually reduces to solution of boundary value problems for partial differential equations of elliptic type. Analytic solution of these problems as a rule is very complicated and is labor-consuming. Technology presents ever more stringent requirements on speed and accuracy of calculation of fields. Distribution of field determines all properties and characteristics of any electromagnetic mechanism, therefore creation of new electrical machine or installation is inconceivably without preliminary calculation and analysis of picture of electromagnetic field in it. Earlier during designing of one or another electromagnetic mechanism it was possible to be satisfied with qualitative character of distribution of field and for calculation to use set of experimentally obtained relationships very approximately reflecting essence of phenomenon. At present the power of electromagnetic devices has grown so much that an error during their design of several percents in determination of field leads to impermissible losses of energy in the prepared device or to the device not satisfying its technical requirements.

These circumstances cause necessity of developing effective methods of calculation of electromagnetic fields based on strict mathematical relationships and creation of specialized computers to sufficiently accurately and rapidly realizing these methods. Application of universal computers discrete action for calculation of fields frequently turns out to be unjustified since it requires great expenditure of time on programming of every concrete problem and large machine time expended on its solution. For complicated forms of investigated regions which usually are met in practical problems, the necessary accuracy of solution

is not ensured because of the impossibility to operate with large numbers of initial data with a limited fast store in the machine.

The best solution would be simulation of the calculated field by a field of another physical nature in an analog model. However there exist fields for simulation of which it is not possible to construct analog model. Besides, even for those fields which it is possible to model, to construct model ensuring assigned accuracy is costly and complicated. Expenditure of labor on manufacture of model would be justified if it in a certain sense was universal, i.e., allowed simple change of circuit of region of investigated field and boundary conditions on it and, due to this, could be used for solution of many practical problems of the same kind. However, to construct such a model has not yet been managed.

In connection with this there is a rational solution of problem of calculation of a field by complex means, i.e., analytic calculation should be combined with simulation of separate, most complicated and labor-consuming operations. For this is required to construct algorithm of solution of problem such that it consists of small number of well modeled mathematical operations common to the given class of problems, combined with simple and efficient arithmetical calculations. Similar structures of electromagnetic fields different in nature permits constructing an algorithm satisfying these requirements. Models of separate operations entering into it can be made sufficiently accurate and either universal, in the sense of simplicity of change of boundary conditions, or simple and cheap.

Advantage of proposed algorithmic method of simulation is possibility of appraisal of upper limit of methodical error of obtained solution with limitations, put on boundary conditions, satisfied in the majority of practical cases. This makes solution of problem with the help of simulation not less reliable than when using direct analytic methods.

At present has appeared possibility of creating complex of modelling devices for calculation of electromagnetic plane-parallel fields. Such a complex can be considered as a specialized computer whose elements are adjusted for simulation of limited number of complicated mathematical operations. From sequence of these operations it is possible to construct algorithm of solution of majority

of problems of calculation of plane-parallel electromagnetic fields met in practice.

In book are presented element of theory of devices simulating mathematical operations encountered during calculation of fields, the construction and principle of operation of these devices are described and algorithms are given of solution of separate problems by calculation of fields, adjusted for realization of them with the help of analog computers and on universal computers.

Analytic methods of calculation of volume fields are developed considerably worse than methods of calculation of flat fields. Up to now to the most effective means of determination of space static fields has been their simulation in a conducting medium or in a volume grid by a direct current field. However during simulation also appear difficulties connected with unlimited extent of the field.

It is impossible to present an infinite model. Boundary of model, being interface of two different media, distorts modelled field. The error appearing here frequently attains an inadmissible magnitude. It is of great interest to construct a model in which boundary would not introduce distortions.

It is known that it is impossible to construct a model of volume field in which completely absent will be distortions introduced by its boundary without application of active element, of adjusted every time for maintenance of concrete boundary conditions. However if one were to definitely select the form and structure of boundary of model then error introduced by boundary can be made small, independently of distribution of sources of modelled field. A theory of models for investigation of space fields possessing such properties is discussed in the last chapter of this book. In it is considered how to determine form and structure of boundary of model ensuring expedient minimum of distortions of modelled field in assigned region, independent of location of field sources and properties of medium in which it is modelled. On the basis of solution of this problem was developed a new analog computer for calculation and design of optimum electro-protection of the underground pipeline or cable network from soil corrosion and from corrosion caused by stray currents of electrified railroads, a new method of simulation of volume fields of great extent by sections was presented, attenuators for volume grids and electrolytic baths was designed.

Book is intended for engineers-electricians therefore author strives, with ideas lying at basis of analytic methods of calculation of fields, to give physical or geometric interpretation. With this goal in first chapter are given necessary relationships from field theory and the connection is shown between plane-parallel electromagnetic fields and the theory of analytic functions of complex variable.

CHAPTER I

ANALYTIC FUNCTIONS AND FLAT FIELD

§ 1. Harmonic Functions on Plane

Potential of electrostatic field of charges distributed in space satisfies the Poisson equation

$$\operatorname{div} \operatorname{grad} U = -\frac{\rho}{\epsilon} \quad (1.1)$$

Here U — potential; ρ — volume density of charge; ϵ — dielectric constant of medium.

For plane-parallel field this relationship in right-angle coordinates is recorded so:

$$\frac{\partial^2 U}{\partial x^2} + \frac{\partial^2 U}{\partial y^2} = -\frac{\tau}{\epsilon}, \quad (1.2)$$

where τ — limit of relation of magnitude of charge in volume of filament with cross section ΔS and unit length to area of cross section ΔS as $\Delta S \rightarrow 0$. In that part of space where charges are lacking ($\tau = 0$) potential satisfies the Laplace equation

$$\Delta U = \frac{\partial^2 U}{\partial x^2} + \frac{\partial^2 U}{\partial y^2} = 0. \quad (1.3)$$

A function satisfying the Laplace equation is called harmonic. Since subsequently we will frequently need to deal with harmonious functions, let us consider their characteristic properties.

A harmonic function can have neither a maximum nor a minimum at any of the internal points of the region since for an absolute maximum or minimum of a

harmonic function in any point it is necessary that all its partial derivatives of second order be, at this point, either negative only or positive only and this is incompatible with the Laplace equation.

It follows from this that potential - harmonic function - can take a maximum and minimum value only at the boundary of the region (for instance on surface of charged conductors) with the exception of that case when it is constant in the entire region (e.g., inside a conductor).

Let us write the Laplace equation on a plane in polar coordinates

$$\Delta U = \frac{\partial^2 U}{\partial r^2} + \frac{1}{r} \frac{\partial U}{\partial r} + \frac{\partial^2 U}{r^2 \partial \theta^2} = 0. \quad (1.4)$$

Here

$$r = \sqrt{x^2 + y^2}; \quad \theta = \arctg \frac{y}{x}.$$

Let us select some point on the plane as the origin of coordinates and plot a circle of radius R with its center at this point (Fig. 1). Since potential is a single-valued function, on this circle $U(r, \theta) = U(r, \theta + 2k\pi)$ (k - whole number), i.e., potential is a periodic function of θ with a period of 2π . This permits representing it in the form of a Fourier series whose coefficients will be functions only of the radius of the circle.

$$U(r, \theta) = R_0(r) + \sum_{n=1}^{\infty} [R_n(r) \cos n\theta + S_n(r) \sin n\theta]. \quad (1.5)$$

Let us find these functions. We differentiate expression (1.5) and substitute in equation (1.4):

$$\begin{aligned} \frac{\partial U}{\partial r} &= R'_0 + \sum_{n=1}^{\infty} [R'_n \cos n\theta + S'_n \sin n\theta], \\ \frac{\partial U}{\partial \theta} &= R'_0 + \sum_{n=1}^{\infty} [R'_n \cos n\theta + S'_n \sin n\theta], \\ \frac{\partial^2 U}{\partial \theta^2} &= - \sum_{n=1}^{\infty} n^2 [R_n \cos n\theta + S_n \sin n\theta], \\ \Delta U &= R''_0 + \frac{1}{r} R'_0 + \sum_{n=1}^{\infty} \left(R''_n + \frac{1}{r} R'_n - \frac{n^2}{r^2} R_n \right) \cos n\theta + \\ &+ \sum_{n=1}^{\infty} \left(S''_n + \frac{1}{r} S'_n - \frac{n^2}{r^2} S_n \right) \sin n\theta = 0. \end{aligned} \quad (1.6)$$

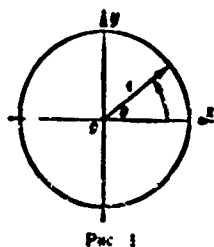


Fig. 1.

This equality will be satisfied for any θ only under the condition that all amplitudes of harmonics equal zero, i.e., if

$$\begin{aligned} R_0' + \frac{1}{r} R_0' &= 0, \\ R_n' + \frac{1}{r} R_n' - \frac{n^2}{r^2} R_n &= 0, \\ S_n + \frac{1}{r} S_n - \frac{n^2}{r^2} S_n &= 0. \end{aligned} \quad (1.7)$$

Solving these equations we find an expression for the coefficients of series (1.5).

We set $R_0' = y$, then $R_0'' = \frac{dy}{dr}$ and

$$-\frac{y}{r} = \frac{dy}{dr}; \quad -\frac{dr}{r} = \frac{dy}{y},$$

hence $-\ln r = \ln y - \ln B_0 = \ln \frac{R_0'}{B_0}$, $R_0' = \frac{B_0}{r}$

or

$$dR_0 = B_0 \frac{dr}{r^2}$$

and

$$R_0(r) = A_0 + B_0 \ln r. \quad (1.8)$$

Multiplying the second of equations (1.7) by r^2 ($r > 0$) we reduce it to the well-known Euler equation

$$r^2 R_n'' + r R_n' - n^2 R_n = 0.$$

Let us seek a solution in the form $R_n(r) = r^k$. Placing this solution in the equation we obtain

$$k(k-1)r^k + kr^k - n^2 r^k = 0,$$

or, eliminating r^k ,

$$k^2 - n^2 = 0, \quad k_{1,2} = \pm n.$$

Consequently

$$R_n(r) = A_n r^n + B_n r^{-n}, \quad (1.9)$$

analogously

$$S_n(r) = C_n r^n + D_n r^{-n}. \quad (1.10)$$

Placing these values in series (1.5) we have

$$U(r, \theta) = A_0 + B_0 \ln r + \sum_{n=1}^{\infty} (A_n r^n + B_n r^{-n}) \cos n\theta + \quad (1.11)$$

$$+ \sum_{n=1}^{\infty} (C_n r^n + D_n r^{-n}) \sin n\theta. \quad (1.11)$$

(Cont'd)

Thus potential of plane-parallel electrostatic field in uniform isotropic dielectric can be represented in the form of series (1.11).

Let us assume that origin of coordinates is selected at point of field M. Potential at this point is limited and $r = 0$, therefore we should have

$$B_0 = B_n = D_n = 0, \quad U(M) = U(0) = A_0.$$

Potential in neighborhood of point M will be in the form of series

$$U(r, \theta) = U(M) + \sum_{n=1}^{\infty} (A_n r^n \cos n\theta + C_n r^n \sin n\theta). \quad (1.12)$$

Let us show now that the value of the harmonic function — potential — at the center of the circle is equal to the mean value on the circumference. Let us superimpose the origin of coordinates with the center of the circle (point M).

On circumference of radius ρ we have

$$\frac{1}{2\pi\rho} \oint U(\rho, \theta) d\theta = \frac{1}{2\pi} \int_{-\pi}^{\pi} \left[U(M) + \sum_{n=1}^{\infty} (A_n \rho^n \cos n\theta + C_n \rho^n \sin n\theta) \right] d\theta = U(M),$$

or

$$U(M) = \frac{1}{2\pi\rho} \oint U(\rho, \theta) d\theta = \frac{1}{2\pi} \int_{-\pi}^{\pi} U(\theta) d\theta. \quad (1.13)$$

§ 2. Functions of Flux and Complex Potential in a Flat Field

Let us consider a field of two parallel charged cylinders (Fig. 2). Surfaces of equal potential in it are cylindrical with generatrices parallel to the cylinder axes (axis oz). Lines of force also form cylindrical surfaces. Flux Ψ through any cylindrical surface, path of which coincides with lines of force, obviously is equal to zero. At every point on such a surface the vector E is tangent to it. Let us select one of the surfaces, formed by a set of force lines, as the initial surface — the boundary of a tube of flux. Let us agree to measure flux counterclockwise from it. Let us plot through point $M(x, y)$ a line of force and a cylindrical surface corresponding to it. The magnitude of flux in the tube formed by this surface and the initial surface will depend on coordinates of point $M(x, y)$. Flux occurring at a unit depth of the tube in the direction of axis

of conductor we will call the function of flux and will designate by $V(x, y)$. The function of flux at point $M(x, y)$ is an electrostatic flux the depth of which is equal to one while the shores are the initial line of force and the line of force passing through point M . Consequently, at any point lying on a line of force, the function of flux is identical and the equation of the line of force may be written:

$$V(x, y) = V_1 = \text{const}$$

During bypass around a charged conductor with charge τ per unit length, the function of flux will obtain an increase equal, according to Gaussian theory, to $\frac{\tau}{\epsilon}$. Consequently in this case the function of flux is multivalued. Let us find the connection between the function of flux V and potential U . Potential decreases in the direction of vector E , therefore

$$E_x = -\frac{\partial U}{\partial x}; \quad E_y = -\frac{\partial U}{\partial y}. \quad (2.1)$$

Let us consider two infinitely close force lines $V = V_1$ and $V = V_1 + dV$ (Fig. 3). The flux dV between these lines equals

$$dV = -E_x dx = E_y dy,$$

since the function of flux decreases during motion in the positive direction along the ox axis. These relationships yield

$$E_x = \frac{\partial V}{\partial y}; \quad E_y = -\frac{\partial V}{\partial x}. \quad (2.2)$$

Comparing expressions (2.1) and (2.2) we obtain

$$\frac{\partial V}{\partial x} = \frac{\partial U}{\partial y}; \quad \frac{\partial V}{\partial y} = -\frac{\partial U}{\partial x}. \quad (2.3)$$

Relationships (2.3) are called the Cauchy-Riemann conditions. By differentiating conditions (2.3) it is easy to show that U and V satisfy the Laplace equation

$$\frac{\partial^2 U}{\partial x^2} + \frac{\partial^2 U}{\partial y^2} = 0; \quad \frac{\partial^2 V}{\partial x^2} + \frac{\partial^2 V}{\partial y^2} = 0. \quad (2.4)$$

The two functions satisfying the Cauchy-Riemann conditions are called conjugate harmonic functions. Conditions (2.3) are conditions of orthogonality of curves $U = \text{const}$ and $V = \text{const}$.

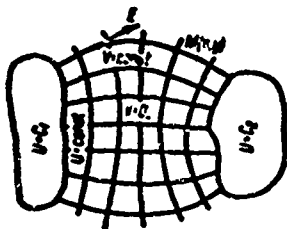


Fig. 2.

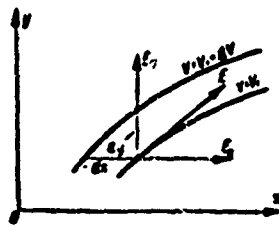


Fig. 3.

For depicting a plane-parallel field graphically it is agreed to plot equipotential and force lines in such manner so that during transition from any line to a neighboring one the same increase of potential or function of flux is obtained. Equations $U(x, y) = \text{const}$ and $V(x, y) = \text{const}$ determine two families curves crossing everywhere at right angles, i.e., forming in plane xoy an orthogonal grid. As can be seen from the definition of functions of flux and potential, measurement of their magnitudes (or their change) in the field is made in two mutually perpendicular directions: V is measured along lines of equal potential ($U = \text{const}$), U along lines of force ($V = \text{const}$), as the coordinates x and y are measured on the plane. Every point in the field can be characterized by a pair coordinates x and y and pair of magnitudes V and U in it. Similarly, both a point on the plane can be defined by one complex coordinate $z = x + iy$, and a point in the electrostatic field can be defined by one complex value $W = V + iU$ called the complex potential of the electrostatic field.

Let us demonstrate that the complex potential W may be considered as a differentiable function of one complex coordinate of the point $z = x + iy$, similar to a function in one real variable. For this it is sufficient to show that the derivative $\frac{dW}{dz}$ does not depend on the direction of differentiation of complex plane (Z). Let us assume that direction of increase ΔZ coincides in direction with the axis ox . Then

$$\frac{dW}{dz} = \frac{dW}{dx} = \frac{\partial V}{\partial x} + i \frac{\partial U}{\partial x} = i \frac{\partial U}{\partial y} + \frac{\partial V}{\partial y} = \frac{dW}{dy},$$

i.e., derivatives with respect to two mutually perpendicular directions are equal. Let differentiation now be carried out in an arbitrary direction ne^i , $dz = e^i dn$

$$\begin{aligned}\frac{dW}{dz} &= e^{-i\theta} \frac{dW}{dn} = e^{-i\theta} \left(\frac{dW}{dx} \cos \theta + i \frac{dW}{dy} \sin \theta \right) = \\ &= e^{-i\theta} (\cos \theta + i \sin \theta) \frac{dW}{dx} = \frac{dW}{dx}.\end{aligned}\quad (2.5)$$

i.e., the derivative with respect to any direction $ne^{i\theta}$ on the complex plane is equal to the derivative along the ox axis. It follows from this that complex potential $W = V + iU$ may be considered as differentiable function of one complex coordinate $z = x + iy$ of the point in the plane. Such a function of complex variable z is called holomorphic or analytic.

If the complex potential of electrostatic field is known then it is easy to construct the field pattern and to determine all of the interesting quantities. Lines of force are plotted according to the equation

$$\operatorname{Re}\{W(z)\} = V(x, y) = \text{const};$$

equipotential lines according to the equation

$$\operatorname{Im}\{W(z)\} = U(x, y) = \text{const}.$$

Field strength is found from the formulas

$$\begin{aligned}E &= \left| \frac{dW}{dz} \right| = \sqrt{\left(\frac{\partial U}{\partial x} \right)^2 + \left(\frac{\partial U}{\partial y} \right)^2}; \\ E &= i \frac{d\bar{W}}{dz} = i \frac{\partial V}{\partial x} + \frac{\partial U}{\partial x}.\end{aligned}\quad (2.6)$$

Consequently calculation of a flat field reduces to finding complex potential $W(z)$.

§ 3. Plane-Parallel Electrostatic Field

If it is necessary to find the field of a system of parallel charged conductors separated by distances considerably exceeding the dimensions of their cross sections then in approximation the conductors can be replaced by infinitely thin filaments and the field of the system of charged filaments considered. The complex potential of a field of charged filaments with charges τ_k located at points z_{0k} will be defined thus:

$$W(z) = -\frac{i}{2\pi\epsilon} \sum_{k=1}^n \tau_k \ln(z - z_{0k}) + c. \quad (3.1)$$

If the field close to the surface of conductors at distances commensurable with dimensions of cross sections is considered such replacement is not permissible.

Let us formulate the problem of calculation of the field in this case. The distribution of charges on the surface of the conductors as a rule is unknown. Only potentials of the conductors, the shapes of their cross sections and their mutual location are known. Outside the wire there is no charge and the potential satisfies the Laplace equation, on the surface of the conductors (contours of cross sections of cylinders L_k) potential takes the assigned values c_k . Thus calculation of the field reduces to a solution of the following problem known as the Dirichlet problem: to find the harmonic function — potential $U(x, y)$ — in a multiply connected region, taking constant values c_k on each of the curves L_k of the corresponding contour.

The case of charged filaments located near uncharged cylinders is of interest. It is possible to consider the field as the result of superposition of two fields. Sources of one are charges of the filament, sources of the other, charges induced on conductors. The potential of the field of induced charges $\varphi(x, y)$ can be found by solution of the boundary value problem. Let us formulate it.

On contours of the cross sections of cylinders L_k the electrical potential U of the resultant field takes constant values c_k which are not previously known

$$U/L_k = c_k = u/L_k + \varphi/L_k = u(t_k) + \varphi(t_k),$$

whence

$$\varphi(t_k) = c_k - u(t_k), \quad (3.2)$$

t_k — point of contour L_k .

Inasmuch as the potential on each of circuits contains an unknown constant c_k additional conditions are required for a unique solution to the problem. Let us find these. The complex potential of the field of induced charges $\Omega(z)$ is a holomorphic function outside of the conductors:

$$\Omega(z) = \Psi(x, y) + i\varphi(x, y). \quad (3.3)$$

Here $\Psi(x, y)$ is a function of the flux of the induced charge field conjugate to the electrical potential $\varphi(x, y)$. By the Gauss theorem for any circuit L_k we have

$$\oint_{L_k} \frac{\partial \Psi}{\partial n} dt = \oint_{L_k} \frac{\partial \varphi}{\partial t} dt = 0, \quad (3.4)$$

such that there are no free charges on the cylinders. Consequently the function of flux Ψ just as the potential ϕ are single-valued functions. The complex potential $Q(z)$ will also be single-valued. This is therefore, the additional condition.

Thus the problem of calculating the field of induced charges reduces to what is known in mathematics as the "modified Dirichlet problem" as follows: to find analytical function (complex potential), holomorphic and single-valued in multiply-connected region, if on each of curves L_k comprising the contour, the imaginary part of this function $\varphi(t)$ is given with an accuracy of the constant component c_k [15].

In a plane-parallel field it is necessary to consider the possibility of an irregular solution resulting from the abstraction which we introduce in replacing the real field with a flat one. If according to the conditions of the problem the total charge of the conductors located on a unit of their length differs from zero then the potential of the field at infinity increases without limit and the solution becomes irregular. Actually the potential cannot increase without limit with distance from the charged bodies. Irregularity is obtained as a result of the unlimited length of the cylinders which we admit by substituting a plane-parallel field.

§ 4. Plane-Parallel Magnetic Field

The field of a system of threads of current. Complex potential $W_m(z)$ of the field of a rectilinear filament of current I in a uniform isotropic medium with permeability μ has the form

$$W_m(z) = V_m(x, y) + iU_m(x, y) = -\frac{I}{2\pi} \ln(z - z_0) + c. \quad (4.1)$$

Here $z_0 = x_0 + iy_0$ - coordinate of point in which is located filament; V_m - function of magnetic flux; U_m - scalar magnetic potential; c - complex constant: $c = c_1 + ic_2$. Assuming $z - z_0 = re^{it}$, we obtain

$$W_m(z) = -\frac{I}{2\pi} \ln r - i\frac{I}{2\pi} \theta + c = -\frac{I}{2\pi} \ln r + c_1 - i\left(\frac{I}{2\pi} \theta - c_2\right). \quad (4.2)$$

whence

$$V_m(x, y) = -\frac{I}{2\pi} \ln r + c_1; \quad U_m(x, y) = -\frac{I}{2\pi} \theta + c_2. \quad (4.3)$$

The equation of lines of force is $V_m = \text{const}$ or $r = \text{const}$. Lines of force constitute concentric circles with center at point z_0 . The equation of lines of equal potential is $U_m = \text{const}$ or $\theta = \text{const}$. Lines of equal potential constitute rays emanating from point z_0 . As $r \rightarrow 0$ and $r \rightarrow \infty$, i.e., upon approach to points z_0 and ∞ the function of magnetic flux increases without limit, the complex potential at these points has logarithmic peculiarities.

Considering $c_1 = 0$, we obtain on circumference $r = 1$, $V_m = 0$, i.e., circumference $r = 1$ is an initial force line. Assuming $c_2 = 0$ we obtain on straight line $\theta = 0$, $U_m = 0$, i.e., ray $\theta = 0$ is a line of zero potential.

It is required to find the field of a system of parallel wires with currents, where the distance between wires considerably exceeds the dimensions of their cross sections, then in approximation the wire can be replaced by infinitely thin

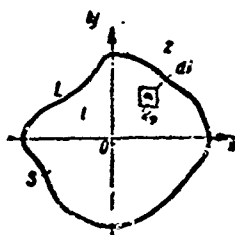


Fig. 4.

filaments located at the centers of gravity of the cross sections and the field of this system of filaments of current may then be considered. Such a replacement will not lead to essential errors if one limits consideration to the field at a region external with respect to the circles with centers at points of location of the filaments and radii equal to distances from the filament to the most remote point of the cross section of its wire.

The field of a system of n parallel filaments with currents I_k located in points z_{0k} we find by applying the method of superposition

$$W_m(z) = -\frac{I}{2\pi} \sum_{k=1}^n I_k \ln(z - z_{0k}) + c. \quad (4.4)$$

A magnetic field outside wires of any cross section with currents I_k . Let us consider a magnetic field of current I flowing in a long rectilinear wire of cross section S (Fig. 4). Let us place the origin of coordinates at the center of gravity of the cross section. We then divide the wire into infinitely fine parallel filaments of cross section dS with coordinates $z_0 = x_0 + iy_0$. Every such

filament is a linear conductor with current $di = \delta dS$, the current density δ being constant. The component of complex potential at point $z = x + iy$ from filament with current $di = \delta dS$ will be

$$dW_m(z) = -\frac{\delta}{2\pi} \ln(z - z_0) dS. \quad (4.5)$$

Summing the components of complex potential from all filaments over cross section S of the wire we obtain a complex potential W_m at point z :

$$\begin{aligned} W_m(z) &= -\frac{\delta}{2\pi} \iint_S \ln(z - z_0) dS + \\ &+ c = -\frac{\delta}{2\pi} \iint_S \ln z dS - \\ &-\frac{\delta}{2\pi} \iint_S \ln\left(1 - \frac{z_0}{z}\right) dS + c. \end{aligned}$$

During integration over dS the variable is z_0 , therefore

$$\frac{\delta}{2\pi} \iint_S \ln z dS = \frac{\delta S}{2\pi} \ln z = \frac{I}{2\pi} \ln z$$

and

$$W_m(z) = -\frac{I}{2\pi} \ln z - \frac{\delta}{2\pi} \iint_S \ln\left(1 - \frac{z_0}{z}\right) dS + c. \quad (4.6)$$

In this expression under the double integral stand the analytic function outside of cross section S ,

$$f(z_0) = \ln\left(1 - \frac{z_0}{z}\right).$$

We take the Green formula [22] and demonstrate that the complex integral over area S of analytic function $f(z_0)$ can be replaced by complex integral over contour L delimiting this area. Let us calculate the integral $\iint_S f(z) dS$, where $f(z) = V(x, y) + iU(x, y)$.

Let us put set $f(z) = \frac{d\Omega}{dz} = \Omega'(z)$, $\Omega(z) = v(x, y) + i\psi(x, y)$ and consequently

$$f(z) = V + iU = \frac{\partial v}{\partial x} + i \frac{\partial \psi}{\partial x} = -i \frac{\partial v}{\partial y} + \frac{\partial \psi}{\partial y}.$$

$$\begin{aligned}
\iint f(z) dS &= \int_{\gamma} dx \int_{\gamma} (V + iU) dy = \int_{\gamma} dx \left(-i \int_{\gamma} \frac{\partial v}{\partial y} dy + \right. \\
&+ \left. \int_{\gamma} \frac{\partial u}{\partial y} dy \right) = -i \int_{\gamma} [v(x, y_2) - v(x, y_1)] dx + \int_{\gamma} [u(x, y_2) - \\
&- u(x, y_1)] dx = i \oint_{\gamma} v(x, y) dx - \oint_{\gamma} u(x, y) dx = \\
&= i \oint_{\gamma} (v + ie) dx = i \oint_{\gamma} \Omega dx.
\end{aligned} \tag{4.7}$$

Altering the order of integration we obtain

$$\begin{aligned}
\iint f(z) dS &= \int_{\gamma} dy \int_{\gamma} (V + iU) dx = \int_{\gamma} dy \left[\int_{\gamma} \frac{\partial v}{\partial x} dx + \right. \\
&+ \left. i \int_{\gamma} \frac{\partial u}{\partial x} dx \right] = \oint_{\gamma} v(x, y) dy + i \oint_{\gamma} u(x, y) dy = \\
&= \oint_{\gamma} (v + ie) dy = \oint_{\gamma} \Omega dy.
\end{aligned} \tag{4.8}$$

Combining the results obtained and bisecting we find [24]

$$\iint f(z) dS = \frac{1}{2} \oint_{\gamma} \Omega (ix + dy) = \frac{i}{2} \oint_{\gamma} \Omega(z) dz, \tag{4.9}$$

or

$$\iint f(z) dS = \frac{i}{2} \oint_{\gamma} f(z) dz, \tag{4.10}$$

Applying this formula for calculating the complex potential of the magnetic field of a wire with current, we obtain

$$W_m(z) = -\frac{i}{2\pi} \ln z - \frac{i\theta}{4\pi} \oint_{\gamma} \left[\int \ln \left(1 - \frac{z_0}{z} \right) dz_0 \right] d\bar{z}_0 + c. \tag{4.11}$$

But

$$\int \ln \left(1 - \frac{z_0}{z} \right) dz_0 = (z_0 - z) \ln \left(1 - \frac{z_0}{z} \right) - z_0$$

and

$$W_m(z) = -\frac{i}{2\pi} \ln z - i \frac{\theta}{4\pi} \oint_{\gamma} \left[(z_0 - z) \ln \left(1 - \frac{z_0}{z} \right) - z_0 \right] d\bar{z}_0 + c. \tag{4.12}$$

When the field is defined for a region where $|z| > z_0$ is the maximum distance from the center of gravity to the boundary of the wire cross section, we have

$$\ln\left(1 - \frac{z_0}{z}\right) = - \sum_{n=1}^{\infty} \frac{1}{n} \left(\frac{z_0}{z}\right)^n,$$

$$\int \ln\left(1 - \frac{z_0}{z}\right) dz_0 = - \sum_{n=1}^{\infty} \frac{1}{n(n+1)} \cdot \frac{z_0^{n+1}}{z^n}.$$

whence

$$W_m(z) = - \frac{I}{2\pi} \left[\ln z - i \sum_{n=1}^{\infty} \frac{1}{n(n+1)} \oint \frac{z_0^{n+1}}{z^n} dz_0 \right]. \quad (4.13)$$

The field of a system of wires of different cross section can be determined by applying the method of superposition.

Field of current carrying wires located near ferromagnetic cylinders. As in the electrostatic problem, the field may be represented in the form of a superpositioning of two fields. The sources of one are currents in wires, source of the others is magnetization of the ferromagnetic cylinders. The potential of the field of currents flowing in the wires can be calculated by the formulas of the preceding paragraph. The field of magnetization can be found by solving the boundary value problem. Let us formulate it. Sources of the magnetization field — elementary currents of iron — are inside cross sections of the ferromagnetic bodies. Therefore field of magnetization outside these sections can be described by a scalar potential function $\varphi_m(x, y)$, satisfying the Laplace equation

$$\frac{\partial^2 \varphi_m}{\partial x^2} + \frac{\partial^2 \varphi_m}{\partial y^2} = 0. \quad (4.14)$$

If the distribution of potential over the contour of cross sections of the ferromagnetic bodies were known then the potential $\varphi_m(x, y)$ in all regions outside these sections would be uniquely defined. The distribution of potential $\varphi_m(l)$ over the contour of cross sections of ferromagnetic bodies can be found with sufficient accuracy and simplicity only when it is previously known that induction within the ferromagnetic bodies does not exceed 1 Wb/m^2 . Here the permeability of iron is everywhere much greater than the permeability of air and it is possible to set

$\mu_a = \infty$. If on the contour there are no currents from external sources then

$H_{ta} = H_t$, where $H_{ta} = B_{ta} \frac{1}{\mu_a}$ and $H_t = B_t \frac{1}{\mu_a}$ are tangential components of full intensity on the contour of ferromagnetic bodies in iron and air respectively. On the other hand, for $\mu_a = \infty$, and a limited induction in iron $B_{ta} H_{ta} = 0$, whence

$$H_{ta} = H_t = 0 \quad (4.15)$$

Taking into consideration that the resultant component of intensity \vec{H} consists of the intensity H_0 caused by the field of eddy currents in the wires and H_m caused by the intensity of magnetization, we obtain $H_0 + H_m = 0$, or finally

$$H_m = -H_0 \quad (4.16)$$

i.e., on contour of ferromagnetic bodies the tangential component of intensity H_m of the field of intensity of magnetization is equal and opposite to the tangential component H_{0t} of the field of currents in the wires.

Integrating H_m over the contour we obtain the distribution by potential of the field of magnetization $\varphi_m(t)$. The result of such integration with an accuracy to the constant will give a value of potential at a point on the contour t in the form of the imaginary part of a complex potential $W_m(t)$ of the magnetic field of currents in the wires

$$\int H_m dt = - \int H_0 dt = \varphi_m(t) = - \operatorname{Im} [W_m(t)] + c_k \quad (4.17)$$

where c_k is an unknown constant which differs for each contour of the cross section. As can be seen from this expression, the distribution of potential $\varphi_m(t)$ can be found with an accuracy to the constants c_k , therefore for unique solution of the problem additional conditions are necessary. Let us clarify them.

The field of magnetization intensity outside the cross sections of cylinders can be characterized by complex potential

$$W_m(z) = \Psi_m + i\varphi_m \quad (4.18)$$

where Ψ_m - function of flux conjugate to the scalar magnetic potential φ_m .

Applying the total current law and considering that in any problem the total current through a cross section normal to the axes of the wires is equal to zero

for any cross section contour of the ferromagnetic body, we can write

$$\oint_L H_z dt = \oint_L \frac{\partial \Psi_z}{\partial t} dt = 0. \quad (4.19)$$

Consequently the scalar potential of the magnetization field outside cross sections of the ferromagnetic bodies is a single-valued function. Analogously, from the principle of continuity of magnetic lines for any contour L we have

$$\oint_L \frac{\partial \Psi_z}{\partial n} dt = \oint_L \frac{\partial \Psi_z}{\partial t} dt = 0, \quad (4.20)$$

i.e., the function of flux Ψ_z of the magnetization field is also a single-valued function. Consequently the complex potential $W_z(t)$ will also be single-valued. Thus the problem of calculating the magnetization field in a multicoupled region beyond the cross section of ferromagnetic bodies reduces to the modified Dirichlet problem [28]:

"To find an analytic function (complex magnetic potential), holomorphic and single-valued, in a multiply connected region if on each of the curves L_k comprising the contour the imaginary part of this function $\Psi_z(t)$ is given with an accuracy to the constant c_k ."

§ 5. Conformal Transformations

Let us consider complex potential $W = V + iU$ as the complex coordinate of a point on the new plane (W) on which, along the real axis, are plotted values of the function of flux V, and along the imaginary axis values of potential U. On plane (W) points which earlier filled region D of the field (on plane Z), fill a new region D_1 , differing in general from region D. We shall consider region D_1 as a geometric transformation of region D, i.e., a transformation of region D from plane (Z) to region D_1 of plane (W).

As we clarified earlier, harmonic functions V and U can take maximum and minimum values only on circuit the contour [boundary] of the region just as the coordinates x and y. Therefore points of the contour of region D during transformation can cross only to points of the region D_1 contour. Internal points convert to internal points, and the transformation will be single-valued.

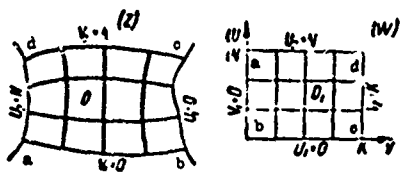


Fig. 5.

Let us consider the region D included between two equipotential surfaces of conductors and two force lines (Fig. 5). Let us assume that $U_1 = 0$, $U_2 = N$, $V_1 = 0$ and $V_2 = K$. On plane (W) region D will convert to a rectangle with sides $U_1 = 0$, $V_1 = 0$, $U_2 = N$, $V_2 = K$. In reality all points of line ab have values of the flux function $V_1 = 0$, the potential on this line when going from a to b changes from $U_2 = N$ to $U_1 = 0$, all points of line bc have a potential $U_1 = 0$, functions of flux when going from b to c change from $V_1 = 0$ to $V_2 = K$, etc. Consequently, the boundary of region D on plane (Z) will convert to the outline of a rectangle on the plane (W). All internal points of region D have values of potential greater than zero and less than N whole values of function of flux is greater than zero and less than K, consequently, on plane (W) they also will be internal points of rectangle D_1 . Lines of force of plane (Z) convert to straight lines, parallel to the ordinates axis on plane (W), lines of equal potential to straight lines parallel to the axis of abscissas. Curvilinear squares formed by the intersection of lines of force and equipotential lines on the plane (Z) will be converted to rectilinear squares on plane (W). But then in the rectangle on the plane (W) the lines $x = \text{const}$ and $y = \text{const}$ will be curves. Like lines $U = \text{const}$ and $V = \text{const}$ of plane (Z), they will form an orthogonal grid since on plane (W) x and y will be conjugate harmonic functions of the coordinates V and U . For them the Cauchy-Riemann conditions and Laplace equation also hold:

$$\frac{\partial x}{\partial V} = \frac{\partial y}{\partial U}; \quad \frac{\partial x}{\partial U} = -\frac{\partial y}{\partial V}; \quad \Delta_V U x = 0. \quad \Delta_V U y = 0. \quad (5.1)$$

Thus complex potential of electrostatic field $W(z) = V(x, y) + iU(x, y)$ — an analytic function of a complex variable — accomplishes a geometric transformation of region D of plane (Z) into a rectangle of plane (W). This transformation has one characteristic peculiarity. Infinitesimal sections of the transformed region retains its form after transformation. This infinitesimal curvilinear squares remain squares after transformation. Therefore such a transformation is called conformal.

Let us now clarify what the complex potential $W(z)$ will convert the entire

part of plane (Z), external with respect to conductors, into. Complex potential $W = V + iU$ outside the conductors is an analytic function whose imaginary part takes the constant values $U = 0$ and $U = N$ on cross sectional contours L_1 and L_2 of the conductors. Let us consider the properties of this function. From the property of a harmonic function to take a maximum or minimum value on the contour of the region it follows that on L_1 values $U = N$ are maximum values in the region, on L_2 , $U = 0$ are minimum values. Therefore the sign of the normal derivative $\frac{\partial U}{\partial n}$ is the same in any point of contour L_1 and since $\frac{\partial U}{\partial n} = \frac{\partial V}{\partial t}$, we have

$$\oint_{L_1} \frac{\partial U}{\partial n} dt = \oint_{L_1} \frac{\partial V}{\partial t} dt = C = \frac{\tau}{\epsilon} \quad (\text{by theorem of Gauss}). \quad (5.2)$$

Thus the real part of function $W(z)$ during a circuit along the contour L_1 undergoes an increase equal to $\frac{\tau}{\epsilon}$, and consequently, the value of the real part of V at any point z of the region is infinitely defined and equal to $V + k \frac{\tau}{\epsilon}$ (k - an integer) which means that $W(z) = V + k \frac{\tau}{\epsilon} + iU$ is also infinitely defined, its values differing from one another by multiples of $\frac{\tau}{\epsilon}$.

In order to avoid ambiguity we will proceed in the following way. Let us imagine a surface in the form of a spiral with an infinite number of turns of embracing each contour L_1 and L_2 such that every turn constitutes a sheet coinciding with a region outside L_1 and L_2 . We will consider that the region of definition of $W(z)$ is such a surface. We will isolate the line $V = 0 \left(V = \frac{\tau}{\epsilon} \right)$ and segment this line as a result of segmenting the entire infinite-sheet surface will break down into separate sheets. On plane (W) every such sheet will correspond to a rectangle enclosed between straight lines $U = 0$, $U = N$, $V = k \frac{\tau}{\epsilon}$ and $V = (k+1) \frac{\tau}{\epsilon}$.

The entire infinite-sheet surface will correspond to an infinite band between straight lines $U = 0$ and $U = N$. Taking as the domain of definition of function $W(z)$ that infinite-sheet surface called the Riemannian surface, we thereby obtain a one-to-one correspondence between points on different sheets of the Riemannian surface and points of the infinite band on plane (W). The function $W(z)$ as where it is looked on as a spiral of the Riemannian surface conformally depicting it on an infinite band. The inverse function $z(W)$ will be single-valued since every value of W on the band corresponds to only one value z on the plane (Z).

Let us consider some examples.

Complex potential of a field of charged filament. Expression for complex potential will be written thus:

$$\begin{aligned} W(z) &= -\frac{\tau}{2\pi\epsilon} (\operatorname{arctg} \frac{y}{x} - i \ln \sqrt{x^2 + y^2}) = \\ &= -i \frac{\tau}{2\pi\epsilon} \ln z = -i \frac{\tau}{2\pi\epsilon} (\ln r + i\theta). \end{aligned} \quad (5.3)$$

Lines of equal potential $\ln r = \text{const}$ are circles with centers at the origin of coordinates, force lines $\theta = \text{const}$ are rays extending from the origin of coordinates. Function $W(z) = -i \frac{\tau}{2\pi\epsilon} \ln z$ goes to infinity at two points: for $z = 0$ and $z = \infty$, i.e., has logarithmic peculiarities in these points. The entire plane (Z), with the exception of these points, conformally maps function $W(z)$ on an infinite band of width $\frac{\tau}{\epsilon}$ from $U = -\infty$ ($r = \infty$) to $U = \infty$ ($r = 0$). This function maps a circle of radius r on a semiband of width $\frac{\tau}{\epsilon}$ from $U = \infty$ to $U' = -\frac{\tau}{2\pi\epsilon} \ln r$.

The part of the plane bounded by two rays (angle between them equal to θ), emanating from point $z = 0$ is also mapped by the function $W(z)$ on an infinite band of width $\frac{\tau\theta}{2\pi\epsilon}$. The domain of definition of $W(z)$ is an infinite-sheet Riemannian surface each sheet of which coincides with the entire plane (Z).

Complex potential field of two charged filaments. Let us assume a distance between filaments of $2b$. Applying the superposition principle we find

$$W(z) = -i \frac{\tau_1}{2\pi\epsilon} \ln(z - z_1) - i \frac{\tau_2}{2\pi\epsilon} \ln(z - z_2) + c.$$

We take $\tau_1 = -\tau_2 = \tau$, $z_1 = -b$, $z_2 = b$. Then

$$W(z) = -\frac{\tau}{2\pi\epsilon} \ln \frac{z+b}{z-b} + c. \quad (5.4)$$

We designate $z+b = r_1 e^{i\theta_1}$; $z-b = r_2 e^{i\theta_2}$, then

$$V = -\frac{\tau}{2\pi\epsilon} (\theta_2 - \theta_1) + c; \quad U = \frac{\tau}{2\pi\epsilon} \ln \frac{r_2}{r_1} + c. \quad (5.5)$$

Setting $c_2 = 0$ we obtain $U = 0$ for $r_1 = r_2$, i.e., the axis of ordinates will be a line of equal potential. Setting $c_1 = 0$ we obtain $V = 0$ for $\theta_2 = \theta_1$, i.e., the initial line of force will be a segment of the axis of abscissas going out from the filaments to infinity on both sides. The equation of the lines of force

$\theta_2 - \theta_1 = \text{const}$ is the equation of a circle with its center on the oy axis, passing through the filaments. The equation of equipotentials is also the equation of a circle with its center on the ox axis

$$U(x, y) = \frac{\tau}{2\pi\epsilon} \ln \frac{r_2}{r_1} = \text{const} \quad \text{or} \quad \frac{(x+b)^2 + y^2}{(x-b)^2 + y^2} = c^2.$$

Hence

$$\left(x - \frac{1+c^2}{1-c^2}b\right)^2 + y^2 = \left(\frac{2cb}{1-c^2}\right)^2. \quad (5.6)$$

coordinates of the center of the circle

$$x_0 = \frac{1+c^2}{1-c^2}b, \quad y_0 = 0. \quad (5.7)$$

radius

$$R = \frac{2cb}{1-c^2}. \quad (5.8)$$

The function $W(z) = -i \frac{\tau}{2\pi\epsilon} \ln \frac{z+b}{z-b}$ goes infinity at two points: at $z = b$ $W(b) = -\infty$ and $z = -b$ $W(-b) = \infty$. At these points the function has logarithmic characteristics. The entire plane (Z), with the exception of singular points, function $W(z)$ conformally maps on an infinite band of width $\frac{\tau}{\epsilon}$ from $U = -\infty$ to $U = \infty$.

The circle of radius R with its center at the point (x_0, y_0) is mapped by this function on the semiband from $U = -\infty$ to $U = \frac{\tau}{2\pi\epsilon} \ln \left[\sqrt{\frac{b^2}{R^2} + 1} - \frac{b}{R} \right]$. The circle of radius b with center at the origin of coordinates is mapped by the function $W(z)$ on an infinite band of width $\frac{\tau}{2\pi\epsilon}$ from $U = -\infty$ to $U = \infty$.

§ 6. Invariance of the Laplace Equation During Conformal Transformation

Let us consider an important property of conformal transformation of regions. Let us show what if in region D is assigned a harmonic function $\varphi(x, y)$ and the region is conformally transformed to another region D_1 then if at points D_1 corresponding during transformation to points D, values of the function are maintained as before, the function $\varphi_1(V, U)$ in region D_1 remains harmonic. In

other words the Laplace equation will not be changed during conformal transformation of the region [12].

Let us assume that in region D on plane (Z) there is distributed a potential $\varphi(x, y)$ which is a harmonic function of coordinates x, y of points in the region. Let us transform region D conformally into some other region D_1 with the help of analytic function $w = u + iv$. On plane (W) the coordinates of any point will be u and v which on plane (Z) were conjugate harmonic functions of coordinates x and y and satisfied there the Cauchy-Riemann conditions

$$\frac{\partial u}{\partial x} = \frac{\partial v}{\partial y}; \quad \frac{\partial u}{\partial y} = -\frac{\partial v}{\partial x}. \quad (6.1)$$

Let us substitute coordinates in the Laplace equation, i.e., clarify what equation will satisfy function φ after conformal transformation of the region. On plane (Z) we had

$$\frac{\partial^2 \varphi}{\partial x^2} + \frac{\partial^2 \varphi}{\partial y^2} = 0. \quad (6.2)$$

Converting to new coordinates u and v we obtain:

$$\begin{aligned} \frac{\partial \varphi}{\partial x} &= \frac{\partial \varphi}{\partial u} \frac{\partial u}{\partial x} + \frac{\partial \varphi}{\partial v} \frac{\partial v}{\partial x}; \quad \frac{\partial \varphi}{\partial y} = \frac{\partial \varphi}{\partial u} \frac{\partial u}{\partial y} + \frac{\partial \varphi}{\partial v} \frac{\partial v}{\partial y}; \\ \frac{\partial^2 \varphi}{\partial x^2} &= \frac{\partial^2 \varphi}{\partial u^2} \left(\frac{\partial u}{\partial x} \right)^2 + 2 \frac{\partial^2 \varphi}{\partial u \partial v} \frac{\partial u}{\partial x} \frac{\partial v}{\partial x} + \\ &+ \frac{\partial^2 \varphi}{\partial v^2} \left(\frac{\partial v}{\partial x} \right)^2 + \frac{\partial \varphi}{\partial u} \frac{\partial^2 u}{\partial x^2} + \frac{\partial \varphi}{\partial v} \frac{\partial^2 v}{\partial x^2}; \\ \frac{\partial^2 \varphi}{\partial y^2} &= \frac{\partial^2 \varphi}{\partial u^2} \left(\frac{\partial u}{\partial y} \right)^2 + 2 \frac{\partial^2 \varphi}{\partial u \partial v} \frac{\partial u}{\partial y} \frac{\partial v}{\partial y} + \frac{\partial^2 \varphi}{\partial v^2} \left(\frac{\partial v}{\partial y} \right)^2 + \\ &+ \frac{\partial \varphi}{\partial u} \frac{\partial^2 u}{\partial y^2} + \frac{\partial \varphi}{\partial v} \frac{\partial^2 v}{\partial y^2}. \end{aligned}$$

Combining second derivatives we obtain

$$\begin{aligned} \frac{\partial^2 \varphi}{\partial x^2} + \frac{\partial^2 \varphi}{\partial y^2} &= \left(\frac{\partial^2 \varphi}{\partial u^2} + \frac{\partial^2 \varphi}{\partial v^2} \right) \left[\left(\frac{\partial u}{\partial x} \right)^2 + \left(\frac{\partial u}{\partial y} \right)^2 \right] + \\ &+ \frac{\partial \varphi}{\partial u} \Delta u + \frac{\partial \varphi}{\partial v} \Delta v = 0. \end{aligned}$$

Thus for $\Delta u = 0, \Delta v = 0$, and $|\text{grad } u|^2 = \left[\left(\frac{\partial u}{\partial x} \right)^2 + \left(\frac{\partial u}{\partial y} \right)^2 \right] \neq 0$, we obtain

$$\frac{\partial^2 \varphi}{\partial u^2} + \frac{\partial^2 \varphi}{\partial v^2} = 0. \quad (6.3)$$

Thus, after conformal transformation of region D to region D_1 the potential remains a harmonic function of the new coordinates u and v . Conformal transformation does not alter the Laplace equation. This property of conformal transformation permits calculation of a field in any complex region leads to calculation of a field in a simple region where the expression for potential is known.

§ 7. Conformal Transformation of a Circle of Radius R to a Circle of the Same Radius With Translation of Poin. $z_0 = re^{i\theta}$ to the Center of Circle

To obtain a transformation of a function we use the pictures of fields of one and two charged filaments considered earlier. The complex potential of the field of one charged filament with charge $\tau = -2\pi\epsilon$

$$W(z) = i \ln z \quad (7.1)$$

maps a circle $|z| < R$ on an infinite semiband of width 2π . In this case the center of the circle $\zeta = 0$ passes to point $W = -\infty$, circle $|z| = R$ to a segment of the straight line $U = \ln R$. The complex potential of a field of two charged filaments also depicts a circle $|z| < R$ limited by equipotential $U = \text{const}$ on an infinite semiband; translates point $z = z_0$, in which is located the filament, to point $W = -\infty$ and circle $|z| = R$ to a segment of straight line $U = \text{const}$ (Fig. 6).

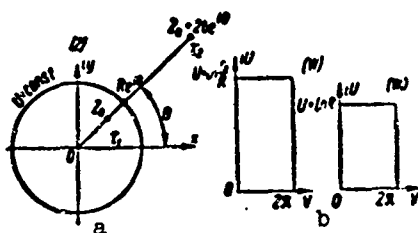


Fig. 6.

Applying consecutively these transformations we transform circle $|z| = R$ to a semiband and then the semiband again to circle $|z| = R$, but in such a manner that the center of the first circle $\zeta = 0$ falls on the point z_0 of the second circle.

Let us assume that at points $z_0 = re^{i\theta}$ and $z_0 + 2be^{i\theta}$ are placed charged filaments whose linear charge densities equal $\tau_1 = 2\pi\epsilon$ and $\tau_2 = -2\pi\epsilon$ (Fig. 6). The complex potential of field of these charges will be:

$$W(z) = V + iU = i \ln \frac{z - z_0}{z - z_0 - 2be^{i\theta}} \quad (7.2)$$

From the picture of the field of two charged filaments considered earlier we have

$$R = \frac{2cb}{1-c^2}; \quad r_0 + 2b = z_0 + b = \frac{1+c^2}{1-c^2} b + b = \frac{2b}{1-c^2},$$

whence

$$c = \frac{R}{r_0 + 2b}; \quad R = \frac{2bR}{(r_0 + 2b) \left[1 - \frac{R^2}{(r_0 + 2b)^2} \right]}; \quad (7.3)$$

$$r_0 + 2b = \frac{R^2}{r_0 + 2b} = 2b; \quad r_0 + 2br_0 = R^2; \quad 2b = \frac{R^2 - r_0^2}{r_0}.$$

Consequently, so that on circle of radius R the potential U will be constant, it is necessary that the equality $2b = \frac{R^2 - r_0^2}{r_0}$. At the point $z = Re^{it}$

$$\begin{aligned} W(z) &= i \ln \frac{Re^{it} - r_0 e^{it}}{\left(R - r_0 - \frac{R^2 - r_0^2}{r_0} \right) e^{it}} = i \ln \frac{R - r_0}{R - r_0 - \frac{R^2 - r_0^2}{r_0}} = \\ &= i \ln \frac{r_0(R - r_0)}{R(R - r_0)} = i \ln \frac{r_0}{R} = \pi. \end{aligned} \quad (7.4)$$

Consequently on the circle $|z| = R$, potential $U = \ln \frac{r_0}{R}$. Thus, the function

$$\begin{aligned} W(z) &= i \ln \frac{z - z_0}{z - z_0 - 2be^{it}} = i \ln \frac{z - z_0}{z - z_0 - \frac{R^2 - r_0^2}{r_0} e^{it}} = \\ &= i \ln \frac{r_0(z - z_0)}{r_0 z - r_0 z_0 - \frac{R^2 - r_0^2}{r_0} e^{it}} = i \ln e^{it(n-1)} \frac{r_0(z - z_0)}{R^2 - z z_0} \end{aligned} \quad (7.5)$$

conformally maps circle $|z| < R$ onto an infinite band of width 2π on plane (W), point z_0 translating to point $W = -\infty$ and circumference $|z| = R$ to segment $U_1 = \ln \frac{r_0}{R}$. The function $W_1 = i \ln \zeta$ conformally maps the circle $|\zeta| < R$ onto an infinite semiband of width 2π and translates point $\zeta = 0$ into point $W_1 = -\infty$ and circumference $|\zeta| = R$ into segment $U_2 = \ln R$. We superimpose both semibands on plane (W) in such a manner that line $U_1 = \ln \frac{r_0}{R}$ and $U_2 = \ln R$ coincided. For this semiband, on which the function $W_1 = i \ln \zeta$ maps the circle $|\zeta| < R$, we shift downward a distance $U_2 - U_1$, transferring the origin of coordinates. Here we obtain

$$W = W_1 - iU_1 + iU_2 = i \ln \zeta - i \ln R + i \ln \frac{r_0}{R} = i \ln \frac{r_0}{R^2} \zeta. \quad (7.6)$$

Equating now both expression for W , we find the sought transformation

$$i \ln e^{it(n-1)} \frac{r_0(z - z_0)}{R^2 - z z_0} = i \ln \frac{r_0}{R^2} \zeta. \quad (7.7)$$

whence

$$\zeta = e^{i(\theta-\phi)} \frac{R^2(z-z_0)}{R^2-z\bar{z}_0} \quad (7.8)$$

§ 8. Solution of the Dirichlet Problem for the Circle. Integral of Poisson

The value of a harmonic function at the center of a circle is equal to its mean value on the circumference [13]

$$\varphi(0) = \frac{1}{2\pi R} \oint \varphi(R, \alpha) |dl|. \quad (8.1)$$

Conformally mapping a circle of radius R onto a circle of the same radius in such a manner so that point z_0 is transferred to the center of the circle $\zeta = 0$ we can find the value of the harmonic function at any point in the circle z_0 from values of the function on the circumference, i.e., we can solve the Dirichlet problem for the circle.

The formula conformally transforming the circle $|z| < R$ into the circle $|\zeta| < R$ and transferring the point z_0 to the center of circle $\zeta = 0$, was found earlier:

$$\zeta = e^{i(\theta-\phi)} \frac{R^2(z-z_0)}{R^2-z\bar{z}_0} \quad (8.2)$$

In order to find the value of the function $\varphi(0)$ at the center of circle $|z| < R$, it is sufficient to take the integral over the circumference $|z| = R$. On this circumference we have $|dl| = R d\alpha = d\zeta$.

Passing to plane (Z) we obtain

$$\begin{aligned} |dl| &= \left| d \frac{R^2(z-z_0)}{R^2-z\bar{z}_0} \right| = R^2 \left| \frac{R^2 - \bar{z}_0 z + (z-z_0)\bar{z}_0}{(R^2-z\bar{z}_0)^2} \right| dz = \\ &= R^2 \frac{R^2 - |z_0|^2}{|R^2 - z\bar{z}_0|^2} |dz|. \end{aligned} \quad (8.3)$$

On the circle $z = Re^{i\psi}$, $dz = Rd\psi$. We set $z_0 = re^{i\phi}$, then

$$|dl| = R^2 \frac{(R^2 - r^2) R d\psi}{R^2 (R^2 - re^{i(\psi-\phi)})^2} = \frac{R^2 - r^2}{R^2 - 2rR \cos(\psi-\phi) + r^2} R d\psi \quad (8.4)$$

Substituting this value for $|dl|$ in the integral (8.1) we obtain an expression for

the potential $\varphi(z_0)$ at any internal point of the circle $|z| = R$ in terms of the value of potential on the circumference - integral of Poisson for the circle

$$\varphi(r, \theta) = \frac{1}{2\pi} \int_0^{2\pi} \varphi(R, \gamma) \frac{R^2 - r^2}{R^2 - 2Rr \cos(\gamma - \theta) + r^2} d\gamma.$$

Here r, θ - coordinates of a point in the circle in which for the potential φ is sought; $\varphi(R, \gamma)$ - values of potential on a circumference of radius R .

§ 9. Poisson Integral for the Upper Half-Plane

Let us find a function conformally mapping the upper half-plane of plane (Z) on the circle $|z| = R$ and translating the real axis into the circumference $|z| = R$ and point $z_0 = x + iy$ into the center of the circle $\zeta = 0$. As is easily seen, the complex potential of the field of two charged axes located at points z_0 and \bar{z}_0 with charges on them of $\tau_1 = 2\pi\epsilon$ and $\tau_2 = -2\pi\epsilon$,

$$W(z) = V + iU = i \ln \frac{z - z_0}{z - \bar{z}_0} \quad (9.1)$$

conformally maps the entire half-plane ($y > 0$) onto an infinite semiband of width 2π and translates the entire real axis $y = 0$ to a segment of the axis $U = 0$ and the point $z = z_0$ to the point $W = -\infty$. The complex potential of a field of one charged axis with charge $\tau = -2\pi\epsilon$

$$W_1(\zeta) = i \ln \frac{\zeta}{R} \quad (9.2)$$

maps a circle radius R on the same semiband, circumference $|z| = R$ being translated into a segment of the axis $U_1 = 0$ and the point $\zeta = 0$ into point $W_1 = -\infty$. Combining both transformations we obtain

$$i \ln \frac{z - z_0}{z - \bar{z}_0} = i \ln \frac{\zeta}{R}, \quad \zeta = R \frac{z - z_0}{z - \bar{z}_0} \quad (9.3)$$

Thus the function conformally mapping the upper half-plane of plane (Z) onto the circle $|z| = R$ of plane (ζ) and translating the point z_0 to the center of circle $\zeta = 0$ has the form

$$\zeta = R \frac{z - z_0}{z - \bar{z}_0} \quad (9.4)$$

Using the expression for the value of the harmonic function at the center of the circle in terms of its value on the circumference, we find a solution to the Dirichlet problem (Poisson integral) for the half-plane. On the boundary of the upper half-plane $z = t$, $dz = dt$

$$|dl| = |dz| = \left| dR \frac{z - z_0}{z - \bar{z}_0} \right| = R \left| \frac{z - z_0}{(z - z_0)^2} dz \right| = R \frac{2y dt}{(t - x)^2 + y^2} \quad (9.5)$$

Converting to new variables under the integral sign we obtain

$$\varphi(0) = \frac{1}{2\pi R} \oint \varphi(R, u) dl = \varphi(x, y) = \frac{1}{\pi} \int_{-\infty}^{\infty} \varphi(t) \frac{y dt}{(t - x)^2 + y^2} \\ \varphi(x, y) = \frac{1}{\pi} \int_{-\infty}^{\infty} \varphi(t) \frac{y dt}{(t - x)^2 + y^2} \quad (9.6)$$

Here (x, y) are the coordinates of the point on the upper half-plane at which is sought the potential φ ; t the present coordinate of the real axis and $\varphi(t)$ the value of potential on the boundary of the upper half-plane.

§ 10. Poisson Integral for an Infinite Band

In preceding paragraph we saw that a function conformally mapping the upper half-plane of the plane (Z) onto the circle $|z| = R$ and translating point z_0 to the center of the circle $\xi = 0$ has the form

$$\xi = R \frac{z - z_0}{z - \bar{z}_0} \quad (9.7)$$

On the other hand we know that the complex potential of the field of a charged filament placed at the coordinate origin $z = 0$ with a charge $\tau = -2\pi\epsilon$,

$$W = i \ln z = V + iU$$

conformally maps the entire upper half-plane $\text{Im} z > 0$ onto an infinite band of width π . The inverse function

$$z = e^{-iW} = e^{-i(V+iU)} = e^{-iV} e^{-U} \quad (10.1)$$

conformally maps an infinite band of width π onto the upper half-plane and translates a point of band $W_0 = V_0 + iU_0$ into a point of half-plane $z_0 = x + iy$. Combining these two transformations we obtain a function which conformally maps a band of width π of plane (W) onto a circle of radius R of plane (ζ) and which translates point $W_0 = V_0 + iU_0$ to the center of circle $\zeta = 0$,

$$\zeta = R \frac{e^{-iV} - e^{i'V} e^{-iU}}{e^{-iU} - e^{i'U} e^{-iV}} \quad (10.2)$$

Using the expression for the value of the harmonic function at the center of the circle in terms of its value on the circumference, we find a solution to the Dirichlet problem (Poisson integral) for an infinite band.

On the left boundary of band $W = i \ln t = i\tau$, $dW = i d\tau$ in it will cross point $t > 0$ of the positive real semiaxis of plane $|Z|$. On the right boundary of band $W = i \ln(-t) = i\tau - \pi$, $dW = i d\tau$ it will cross point of the semiaxis $t < 0$. Consequently, on one semicircle of $|\zeta| = R$ of plane (ζ)

$$\zeta = R \frac{e^{\tau - iU_0} - e^{i'U_0} e^{-iV_0}}{e^{\tau - iU_0} - e^{i'U_0} e^{-iV_0}} = R \frac{e^{\tau - iU_0} - e^{-iV_0}}{e^{\tau - iU_0} - e^{-iV_0}} \quad (10.3)$$

$$|d\zeta| = R \left| d \frac{e^{\tau - iU_0} - e^{-iV_0}}{e^{\tau - iU_0} - e^{-iV_0}} \right| = R \left| e^{\tau - iU_0} \frac{-2i \sin V_0}{e^{\tau - iU_0} - 2e^{\tau - iU_0} \cos V_0 + 1} \right| d\tau =$$

$$= R \frac{\sin V_0}{\operatorname{ch}(\tau - U_0) - \cos V_0} d\tau. \quad (10.4)$$

On the other semicircle of $|\zeta| = R$ of plane (ζ)

$$\zeta = R \frac{e^{\tau - iU_0} - e^{i'U_0} e^{-iV_0}}{e^{\tau - iU_0} - e^{i'U_0} e^{-iV_0}} = R \frac{e^{\tau} + e^{i'U_0} e^{-iV_0}}{e^{\tau} + e^{i'U_0} e^{-iV_0}} =$$

$$= R \frac{e^{\tau - U_0} + e^{-iV_0}}{e^{\tau - U_0} + e^{-iV_0}} \quad (10.5)$$

$$|d\zeta| = R \left| d \frac{e^{\tau - U_0} + e^{-iV_0}}{e^{\tau - U_0} + e^{-iV_0}} \right| = R \frac{\sin V_0}{\operatorname{ch}(\tau - U_0) + \cos V_0} d\tau \quad (10.6)$$

Converting in integral (8.1) to new variables we obtain

$$\varphi(0) = \frac{1}{2\pi R} \oint \varphi(R, \alpha) d\zeta = \varphi(V, U) = \frac{1}{2\pi} \int_{-\pi}^{\pi} \varphi(i\tau) \frac{\sin V d\tau}{\operatorname{ch}(\tau - U) - \cos V} + \frac{1}{2\pi} \int_{-\pi}^{\pi} \varphi(-\pi + i\tau) \frac{\sin V d\tau}{\operatorname{ch}(\tau - U) + \cos V}. \quad (10.7)$$

If one were to multiply by $(-i)$, turn the band by an angle $-\frac{\pi}{2}$ and alter its width from π to h units, then we obtain [20]

$$\begin{aligned} q(U, V) = & \frac{1}{2h} \int_{-\infty}^{\infty} q(\tau) \frac{\sin kV d\tau}{\operatorname{ch} k(\tau - U) - \cos kV} + \\ & + \frac{1}{2h} \int_{-\infty}^{\infty} q(\tau + i h) \frac{\sin kV d\tau}{\operatorname{ch} k(\tau - U) + \cos kV}, \end{aligned} \quad (10.8)$$

where $k = \frac{\pi}{h}$ and h the width of the band.

§ 11. Normal Derivative of Potential on the Boundary of the Band

In application frequent the problem of calculation of a field reduces to finding the normal derivative of potential on the contour of the region. If we know the function $z = f(\zeta)$ which conformally maps the considered region onto a canonical region, or at least its limiting values on the contour $t = f(\tau)$, then knowing the normal derivative of potential on the boundary of the canonical region it is easy to find the normal derivative on the boundary of the given region also.

Actually, let us assume that in region D we are given the analytic function — complex potential

$$W(z) = V(x, y) + i\varphi(x, y). \quad (11.1)$$

where $V(x, y)$ — function of flow

$\varphi(x, y)$ — potential.

Introducing conformally mapping function $z = f(\zeta)$, we obtain the distribution of the complex potential in the canonical region

$$W(z) = W(f(\zeta)) = W_1(\zeta) \quad (11.2)$$

Taking the derivative with respect to ζ we obtain

$$W_1'(\zeta) = W'(f(\zeta)) = W'(z) f'(\zeta). \quad (11.3)$$

whence

$$W'(z) = \frac{1}{f'(\zeta)} W_1'(\zeta). \quad (11.4)$$

Taking into account that the modulus of the derivative of complex potential is

equal to the modulus of the gradient of potential $\varphi(x, y)$, we have

$$|\text{grad } \varphi| = \frac{1}{|f'(\zeta)|} |\text{grad } \varphi_1|. \quad (11.5)$$

Hence, due to conformity transformation, for the normal derivatives of potential we obtain

$$\frac{\partial \varphi}{\partial n} = \frac{1}{|f'(\zeta)|} \frac{\partial \varphi_1}{\partial v}. \quad (11.6)$$

where ∂v is an element of the normal to the contour of the canonical region.

Since function $f(\zeta)$ is holomorphic and is continuous up to the contours of D_1 , the value of the modulus of its derivative on the contour does not depend on direction of differentiation and can be obtained by differentiation over the contour

$$|f'(\zeta)| = |f'(\tau)| = \left| \frac{dt}{d\tau} \right|, \quad (11.7)$$

where dt is an element of contour length of the assigned region D corresponding during conformal transformation to an element of length $d\tau$ of boundary of the canonical region D_1 .

Consequently

$$\lim_{n \rightarrow \infty} \frac{\partial \varphi}{\partial n} = \left| \frac{d\tau}{dt} \right| \lim_{\tau \rightarrow \infty} \frac{\partial \varphi_1}{\partial v}, \quad \frac{\partial \varphi}{\partial n} = \left| \frac{d\tau}{dt} \right| \frac{\partial \varphi_1}{\partial v}. \quad (11.8)$$

Let us derive a formula for the normal derivative of potential on the boundary of the band. Taking the derivative with respect to V under the integral sign of formula (10.8), we obtain

$$\begin{aligned} \frac{\partial \varphi_1}{\partial V} = \frac{k}{2h} \left\{ \int_{-\infty}^{\infty} \varphi_1(\tau) \frac{\text{ch } k(\tau - U) \cos kV - 1}{[\text{ch } k(\tau - U) - \cos kV]^2} d\tau + \right. \\ \left. + \int_{-\infty}^{\infty} \varphi_1(\tau + ih) \frac{\text{ch } k(\tau - U) \cos kV + 1}{[\text{ch } k(\tau - U) + \cos kV]^2} d\tau \right\}. \end{aligned} \quad (11.9)$$

In the first of the integrals, to the integrand we add and subtract $\varphi_1(U)$, in the second we add and subtract $\varphi_1(U + ih)$:

$$\begin{aligned}
& \int_{-\infty}^{\infty} \varphi_1(\tau) \frac{\operatorname{ch} k(\tau-U) \cos kV - 1}{[\operatorname{ch} k(\tau-U) - \cos kV]^2} d\tau = \\
& = \varphi_1(U) \int_{-\infty}^{\infty} \frac{\operatorname{ch} k(\tau-U) \cos kV - 1}{[\operatorname{ch} k(\tau-U) - \cos kV]^2} d\tau + \\
& + \int_{-\infty}^{\infty} [\varphi_1(\tau) - \varphi_1(U)] \frac{\operatorname{ch} k(\tau-U) \cos kV - 1}{[\operatorname{ch} k(\tau-U) - \cos kV]^2} d\tau = \\
& = -\frac{2}{k} \varphi_1(U) + \int_{-\infty}^{\infty} [\varphi_1(\tau) - \varphi_1(U)] \frac{\operatorname{ch} k(\tau-U) \cos kV - 1}{[\operatorname{ch} k(\tau-U) - \cos kV]^2} d\tau.
\end{aligned} \tag{11.10}$$

Analogously

$$\begin{aligned}
& \int_{-\infty}^{\infty} \varphi_1(\tau + ih) \frac{\operatorname{ch} k(\tau-U) \cos kV + 1}{[\operatorname{ch} k(\tau-U) + \cos kV]^2} d\tau = \\
& = \frac{2}{k} \varphi_1(U + ih) + \int_{-\infty}^{\infty} [\varphi_1(\tau + ih) - \varphi_1(U + ih)] \times \\
& \times \frac{\operatorname{ch} k(\tau-U) \cos kV + 1}{[\operatorname{ch} k(\tau-U) + \cos kV]^2} d\tau,
\end{aligned} \tag{11.11}$$

since

$$\begin{aligned}
& \int_{-\infty}^{\infty} \frac{\operatorname{ch} k(\tau-U) \cos kV - 1}{[\operatorname{ch} k(\tau-U) - \cos kV]^2} d\tau = \\
& = \frac{2}{k} \frac{1 - e^{2k(U-L)}}{e^{2k(U-L)} - 2e^{k(U-L)} \cos kV + 1} \Big|_{-\infty}^{\infty} = -\frac{2}{k};
\end{aligned} \tag{11.12}$$

$$\begin{aligned}
& \int_{-\infty}^{\infty} \frac{\operatorname{ch} k(\tau-U) \cos kV + 1}{[\operatorname{ch} k(\tau-U) + \cos kV]^2} d\tau = \\
& = -\frac{2}{k} \frac{1 + e^{2k(U-L)}}{e^{2k(U-L)} + 2e^{k(U-L)} \cos kV + 1} \Big|_{-\infty}^{\infty} = \frac{2}{k}.
\end{aligned} \tag{11.13}$$

Passing to a limit $V \rightarrow 0$ for the normal derivative $\frac{\partial \varphi_1}{\partial V}$ on the lower boundary of the band, we obtain

$$\begin{aligned}
& \lim_{V \rightarrow 0} \frac{\partial \varphi_1}{\partial V} = \frac{1}{k} [\varphi_1(U + ih) - \varphi_1(U)] + \\
& + \frac{k}{2h} \int_{-\infty}^{\infty} \frac{\varphi_1(\tau) - \varphi_1(U)}{\operatorname{ch} k(\tau-U) - 1} d\tau + \frac{k}{2h} \int_{-\infty}^{\infty} \frac{\varphi_1(\tau + ih) - \varphi_1(U + ih)}{\operatorname{ch} k(\tau-U) + 1} d\tau
\end{aligned} \tag{11.14}$$

Let us introduce the new variable $\alpha = \tau - U$ and present functions $\varphi_1(\tau)$ and $\varphi_1(\tau + ih)$ in the form of sums of their even and odd parts:

$$\begin{aligned}\varphi_1(\tau) &= \frac{\varphi_1(U + \alpha) + \varphi_1(U - \alpha)}{2} + \frac{\varphi_1(U + \alpha) - \varphi_1(U - \alpha)}{2}, \\ \varphi_1(\tau + ih) &= \frac{\varphi_1(U + \alpha + ih) + \varphi_1(U - \alpha + ih)}{2} + \\ &+ \frac{\varphi_1(U + \alpha + ih) - \varphi_1(U - \alpha + ih)}{2}.\end{aligned}\quad (11.15)$$

Substituting values (11.15) in formula (11.14) we obtain

$$\begin{aligned}\lim_{h \rightarrow 0} \frac{\partial \varphi_1}{\partial V} &= \frac{1}{h} [\varphi_1(U + ih) - \varphi_1(U)] + \\ &+ \frac{k}{2h} \int_0^\infty \frac{\varphi_1(U + \alpha) + \varphi_1(U - \alpha) - 2\varphi_1(U)}{\operatorname{ch} ka - 1} d\alpha + \\ &+ \frac{k}{2h} \int_0^\infty \frac{\varphi_1(U + \alpha + ih) + \varphi_1(U - \alpha + ih) - 2\varphi_1(U + ih)}{\operatorname{ch} ka + 1} d\alpha.\end{aligned}\quad (11.16)$$

Due to oddness of the integrands,

$$\begin{aligned}\int_0^\infty \frac{\varphi_1(U + \alpha) - \varphi_1(U - \alpha)}{\operatorname{ch} ka - 1} d\alpha &\approx 0, \\ \int_0^\infty \frac{\varphi_1(U + \alpha + ih) - \varphi_1(U - \alpha + ih)}{\operatorname{ch} ka + 1} d\alpha &= 0.\end{aligned}\quad (11.17)$$

Analogously, for the normal derivative of potential on the upper boundary of the band we have

$$\begin{aligned}\lim_{h \rightarrow 0} \frac{\partial \varphi_1}{\partial V} &= \frac{1}{h} [\varphi_1(U + ih) - \varphi_1(U)] + \\ &+ \frac{k}{2h} \int_0^\infty \frac{\varphi_1(U + \alpha) + \varphi_1(U - \alpha) - 2\varphi_1(U)}{\operatorname{ch} ka + 1} d\alpha + \\ &+ \frac{k}{2h} \int_0^\infty \frac{\varphi_1(U + \alpha + ih) + \varphi_1(U - \alpha + ih) - 2\varphi_1(U + ih)}{\operatorname{ch} ka - 1} d\alpha\end{aligned}\quad (11.18)$$

Let us designate known functions, standing in numerator of integrands (11.16) and (11.18), thus:

$$\begin{aligned}\varphi_1(U + \alpha) + \varphi_1(U - \alpha) - 2\varphi_1(U) &= f_1(ka), \\ \varphi_1(U + \alpha + ih) + \varphi_1(U - \alpha + ih) - 2\varphi_1(U + ih) &= f_2(ka).\end{aligned}\quad (11.19)$$

We take integrals by parts

$$k \int_0^{\infty} \frac{f_1(ka) da}{\operatorname{ch} ka - 1} = -f_1(ka) \operatorname{cth} \frac{ka}{2} \Big|_0^{\infty} + \\ + k \int_0^{\infty} f_1'(ka) \operatorname{cth} \frac{ka}{2} da; \quad (11.20)$$

$$k \int_0^{\infty} \frac{f_2(ka) da}{\operatorname{ch} ka + 1} = f_2(ka) \operatorname{th} \frac{ka}{2} \Big|_0^{\infty} - k \int_0^{\infty} f_2'(ka) \operatorname{th} \frac{ka}{2} da. \quad (11.21)$$

We expand $\operatorname{cth} \frac{ka}{2}$ and $\operatorname{th} \frac{ka}{2}$ into a series of exponential functions:

$$\operatorname{cth} \frac{ka}{2} = 1 + 2 \sum_{n=1}^{\infty} \frac{1}{e^{nka}}; \quad \operatorname{th} \frac{ka}{2} = 1 + 2 \sum_{n=1}^{\infty} \frac{(-1)^n}{e^{nka}}; \quad (11.22)$$

$$k \int_0^{\infty} \frac{f_1(ka) da}{\operatorname{ch} ka - 1} = -f_1(ka) \operatorname{cth} \frac{ka}{2} \Big|_0^{\infty} + k \int_0^{\infty} f_1'(ka) da + \\ + 2k \sum_{n=1}^{\infty} \int_0^{\infty} \frac{f_1(ka) da}{e^{nka}} = f_1(ka) \left(1 - \operatorname{cth} \frac{ka}{2} \right) \Big|_0^{\infty} + \\ + 2 \sum_{n=1}^{\infty} \int_0^{\infty} \frac{f_1'(ka) d(ka)}{e^{nka}}; \quad (11.23)$$

$$k \int_0^{\infty} \frac{f_2(ka) da}{\operatorname{ch} ka + 1} = f_2(ka) \operatorname{th} \frac{ka}{2} \Big|_0^{\infty} - \int_0^{\infty} f_2'(ka) d(ka) - \\ - 2 \sum_{n=1}^{\infty} (-1)^n \int_0^{\infty} \frac{f_2(ka) d(ka)}{e^{nka}} = f_2(ka) \left(\operatorname{th} \frac{ka}{2} - 1 \right) \Big|_0^{\infty} - \\ - 2 \sum_{n=1}^{\infty} (-1)^n \int_0^{\infty} \frac{f_2'(ka) d(ka)}{e^{nka}}. \quad (11.24)$$

If the function $\varphi_1(U)$ is continuous and has a continuous derivative then the second derivative $\varphi_1''(U)$ is limited and

$$\varphi_1''(U) = \lim_{a \rightarrow 0} \frac{\varphi_1(U+a) + \varphi_1(U-a) - 2\varphi_1(U)}{a^2} = c$$

or

$$\lim_{a \rightarrow 0} \frac{f_{1,2}(ka)}{a^2} = c. \quad (11.25)$$

Hence

$$\lim_{a \rightarrow 0} f_{1,2}(ka) = c, a^2 = 0 \quad \text{and} \quad \lim_{a \rightarrow 0} f'(ka) = ca = 0. \quad (11.26)$$

Therefore we have

$$\begin{aligned} f_1(ka) \left(1 - \operatorname{cth} \frac{ka}{2} \right) \Big|_0^\infty &= 0 - \lim_{a \rightarrow 0} f(ka) \left(1 - \operatorname{cth} \frac{ka}{2} \right) = \\ &= \lim_{a \rightarrow 0} 2f_1(ka) \operatorname{ch}^2 \frac{ka}{2} = 0; \end{aligned} \quad (11.27)$$

$$f_2(ka) \left(\operatorname{th} \frac{ka}{2} - 1 \right) \Big|_0^\infty = 0 - \lim_{a \rightarrow 0} f_2(ka) \left(\operatorname{th} \frac{ka}{2} - 1 \right) = 0. \quad (11.28)$$

Consequently

$$\begin{aligned} \lim_{h \rightarrow 0} \frac{\partial \varphi_1}{\partial U} &= \frac{1}{h} \left[\varphi_1(U + ih) - \varphi_1(U) + \sum_{n=1}^{\infty} \int_0^{\infty} \frac{f_1(ka) d(ka)}{e^{nka}} - \right. \\ &\quad \left. - \sum_{n=1}^{\infty} (-1)^n \int_0^{\infty} \frac{f_2(ka) d(ka)}{e^{nka}} \right] = \frac{1}{h} \left[\varphi_1(U + ih) - \varphi_1(U) + \right. \\ &\quad \left. + \sum_{n=1}^{\infty} n \int_0^{\infty} \frac{f_1(ka) d(ka)}{e^{nka}} - \sum_{n=1}^{\infty} (-1)^n n \int_0^{\infty} \frac{f_2(ka) d(ka)}{e^{nka}} \right]; \end{aligned} \quad (11.29)$$

$$\begin{aligned} \lim_{h \rightarrow 0} \frac{\partial \varphi_2}{\partial U} &= \frac{1}{h} \left[\varphi_2(U + ih) - \varphi_2(U) + \sum_{n=1}^{\infty} \int_0^{\infty} \frac{f_2(ka) d(ka)}{e^{nka}} - \right. \\ &\quad \left. - \sum_{n=1}^{\infty} (-1)^n \int_0^{\infty} \frac{f_1(ka) d(ka)}{e^{nka}} \right] = \frac{1}{h} \left[\varphi_2(U + ih) - \varphi_2(U) + \right. \\ &\quad \left. + \sum_{n=1}^{\infty} n \int_0^{\infty} \frac{f_2(ka) d(ka)}{e^{nka}} - \sum_{n=1}^{\infty} (-1)^n n \int_0^{\infty} \frac{f_1(ka) d(ka)}{e^{nka}} \right]. \end{aligned} \quad (11.30)$$

§ 12. Solution of the Dirichlet Problem in a Biconnected Region Using Conformal Transformation

From all of the preceding material it is clear that the Dirichlet problem for any singly-connected (i.e., limited by one closed contour) region can be solved as follows:

1. Conformally convert given region into any canonical region: circle, upper half-plane, or infinite band; in other words find an analytic function establishing a one-to-one correspondence of the given and canonical regions.

2. Transfer boundary values of the sought harmonic function – potential – to corresponding (during conformal transformation) points of the boundary of the canonical region.

3. With the help of the Poisson integral calculate values of potential at internal points of the canonical region.

4. Knowing the conformally-mapping function transfer values of potential found at points of the canonical region to their corresponding points in the assigned region and thereby obtain a solution to the problem.

Let us demonstrate that the Dirichlet problem for a biconnected region can be solved using infinite sheet conformal mapping of it onto a canonical single-connected region where, in turn, the Poisson integral yields a solution [29].

Let there be assigned a biconnected region D limited by external L_1 and internal L_2 contours (Fig. 7a). We assume that in D there is an analytic function

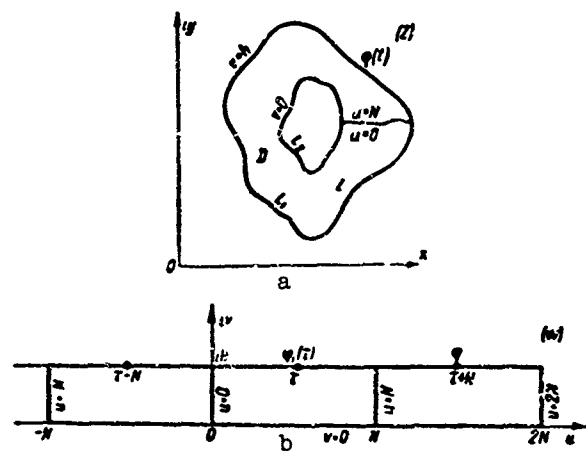


Fig. 7.

virtue of the fact that $\frac{\partial v}{\partial n} = \frac{\partial u}{\partial t}$ (u and v) – conformal harmonic functions

$$\oint_L \left| \frac{\partial v}{\partial n} \right| dt = \oint_L \left| \frac{\partial u}{\partial t} \right| dt = \oint_L du = N \neq 0 \quad (12.1)$$

Thus the real part of function $w(z)$ when going around contour L_1 undergoes an increase equal to N and, consequently, the value of the real part of u at any point z of the region is infinitely-valued and equal to $u + kN$ (k – an integer) which means that $w = u + kN + iv$ is also infinitely-valued. Therefore the region of definition of function $w(z)$ on plane (z) will be an infinite-sheet Riemann

surface every sheet of which coincides with region D. Let us isolate in D the line $u = 0$ and make a cut coinciding with this line. As a result of the cut the entire infinite-sheet Riemannian surface is broken up into separate sheets. On plane (w) to every such sheet there will correspond a rectangle contained between straight lines $v = 0$, $v = h$, $u = kN$ and $u = (k+1)N$ (k — an integer) (Fig. 7b). The entire infinite-sheet Riemannian surface will correspond to an infinite band between straight lines $v = 0$ and $v = h$. Inverse function $z(w)$ will be single-valued every value w on the band corresponds to only one value of z . It follows from this that values of single-valued harmonic function $\varphi(x, y)$ in region D will equal values of $\varphi_1(u, v)$ at corresponding points on the band. It is easy to show that the function $\varphi_1(u, v)$ will also be harmonic and single-valued. Actually harmonic function $\varphi(x, y)$ can be regarded as the imaginary portion of analytic function $\Omega(z)$. By virtue of uniqueness of analytic function $z(w)$, function $\Omega(z) = \Omega[z(w)] = \Omega_1(w)$ will also be analytic and its imaginary part $\varphi_1(u, v)$ — harmonic and single-valued. At points of the band w corresponding to points z of region D, values of $\varphi_1(u, v)$ will equal values of $\varphi(x, y)$, values of $\varphi_1(\tau)$ on boundaries of the band will equal values of $\varphi(t)$ at corresponding points of the contour of region D. But from values of the single-valued harmonic function, on boundaries of the infinite band, by the Poisson integral for the band, are determined values of the function inside the region, i.e., the Dirichlet problem is solved. From the reasoning presented it follows that if an analytic function w is known whose imaginary part v takes constant values on the external and internal contours of region D, then such a function conformally maps the biconnected region on a band, translating the external and internal contour of the region to the boundaries of the band. With the help of this function the Dirichlet problem in the biconnected region can be solved just, as in a singly-connected one, with the help of the Poisson integral.

§ 13. Transformation of Ring Onto a Band

Let us consider the function

$$w(z) = u + iv = i \ln \frac{z}{a} \quad (13.1)$$

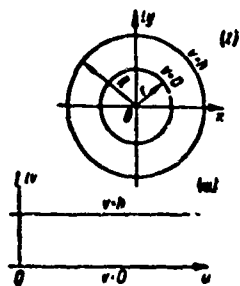


Fig. 8.

Assuming $z = re^{i\theta}$, we obtain

$$w = i \ln \frac{R}{r} e^{i\theta} = -\theta + i \ln \frac{R}{r} = u + iv.$$

Hence

$$u = -\theta, \quad v = \ln \frac{R}{r}. \quad (13.2)$$

On circumference $|z| = r$ the imaginary part of this function takes a constant value equal to zero:

$$v = \ln \frac{R}{r} = 0. \quad (13.3)$$

On circumference $|z| = R$ the imaginary part also takes a constant value,

$$v = \ln \frac{R}{r} = h. \quad (13.4)$$

Consequently the function $w(z) = i \ln \frac{z}{R}$ accomplishes infinite-sheet conformal mapping of a ring formed by two concentric circles of radius r and R onto an infinite band of width $h = \ln \frac{R}{r}$ (Fig. 8).

Let us construct a function infinite-sheet, conformally depicting a ring formed by two nonconcentric circumferences of radii R_1 and R_2 , the distance between whose centers equals δ , on an infinite band (Fig. 9). Let us consider the function

$$W(z) = i \ln \frac{z+b}{z-b} + ik = u + iv. \quad (13.5)$$

As was earlier clarified the line $v = \text{const}$ of this function are circumferences with centers on the ox axis at the points

$$x_0 = \frac{1+c^2}{1-c^2} b, \quad y_0 = 0 \text{ and radii } R = \frac{2cb}{1-c^2}, \text{ where } c = \frac{z-b}{z+b}.$$

Let us assume a circle of radius R_1 with its center at the point $x_0, v = 0$.

From this condition we find the constant k :

$$\begin{aligned} v &= \ln \left| \frac{z+b}{z-b} \right| + k = \ln \left| \frac{x_0 + R_1 e^{i\theta} + b}{x_0 + R_1 e^{i\theta} - b} \right| + k = \\ &= \ln \left| \frac{\frac{1+c_1^2}{1-c_1^2} b + b + \frac{2c_1 b}{1-c_1^2} e^{i\theta}}{\frac{1+c_1^2}{1-c_1^2} b - b + \frac{2c_1 b}{1-c_1^2} e^{i\theta}} \right| + k = \\ &= \ln \left| \frac{1+c_1 e^{i\theta}}{c_1 + e^{i\theta}} \right| \cdot \frac{1}{c_1} + k = -\ln c_1 + k = 0. \end{aligned} \quad (13.5)$$

whence $k = \ln c_1$.

On a circle of radius R_2 with its center at the point x_{02}

$$\begin{aligned} \theta &= \ln \left| \frac{z+b}{z-b} \right| c_1 = \ln c_1 \left| \frac{x_{02} + R_2 e^{i\theta} + b}{x_{02} + R_2 e^{i\theta} - b} \right| = \\ &= \ln \frac{c_1}{c_2} \left| \frac{1 + c_2 e^{i\theta}}{c_2 + e^{i\theta}} \right| = \ln \frac{c_1}{c_2}. \end{aligned} \quad (13.6)$$

We express c_1 , c_2 and b in terms of the given values of R_1 , R_2 and δ . From the relationship $R = \frac{2b}{1-c^2}$ we find

$$b = \frac{\sqrt{R^2 + b^2} - b}{R}.$$

then

$$c_1 = \frac{\sqrt{R_1^2 + b^2} - b}{R_1}, \quad c_2 = \frac{\sqrt{R_2^2 + b^2} - b}{R_2}. \quad (13.7)$$

From the relationship

$$\begin{aligned} \delta = x_{02} - x_{01} &= b \left(\frac{1+c_2^2}{1-c_2^2} - \frac{1+c_1^2}{1-c_1^2} \right) = R c_2 - R c_1 = \\ &= \sqrt{R_2^2 + b^2} - \sqrt{R_1^2 + b^2}. \end{aligned} \quad (13.8)$$

After conversion we find

$$b = \frac{\sqrt{(R_1^2 + R_2^2 - \delta^2) - 4R_1^2 R_2^2}}{2\delta}. \quad (13.9)$$

Thus,

$$\begin{aligned} c_1 &= \frac{\sqrt{R_1^2 + b^2} - b}{R_1} = \\ &= \frac{R_2^2 - R_1^2 - \delta^2 - \sqrt{(R_1^2 + R_2^2 - \delta^2) - 4R_1^2 R_2^2}}{2\delta R_1}. \end{aligned} \quad (13.10)$$

$$c_2 = \frac{R c_1 + b}{R_2}; \quad \frac{c_2}{c_1} = \frac{c_1 R_2}{c_1 R_1 + b} = \frac{R_2}{R_1} \cdot \frac{1}{1 + \frac{\delta}{c_1 R_1}}. \quad (13.11)$$

Placing the origin of coordinates on the center of the small circle at the point x_{01} , we will have $z = x_0 + \zeta$ and

$$W(\zeta) = i \ln \frac{x_0 + b + \zeta}{x_0 - b + \zeta} + i \ln c_1 = i \ln \frac{\left(\frac{c_1^2 + 1}{1 - c_1^2} + 1 \right) b + \zeta}{\left(\frac{1 + c_1^2}{1 - c_1^2} - 1 \right) b + \zeta} c_1 = i \ln \frac{\frac{2b}{1 - c_1^2} + \zeta}{\frac{2bc_1^2}{1 - c_1^2} + \zeta} c_1 = i \ln \frac{R_1 + c_1 \zeta}{R c_1 + \zeta}. \quad (13.12)$$

Thus the function

$$W(z) = i \ln \frac{R_1 + z_0 \bar{z}}{R_1 z + \bar{z}}$$

infinite-sheetly, conformally depicts a ring formed by two circumferences R_1 and R_2 , the distance between whose centers equals δ , on an infinite band of width

$$k = \ln \frac{R_2}{R_1} \cdot \frac{1}{1 + \frac{\delta}{c_1 R_1}}. \quad (13.13)$$

Here c_1 is expressed by formula (13.10).

§ 14. Determining Maximum Values of Potential When Solving the Modified Dirichlet Problem in a Biconnected Region

Let us consider the field of charged filaments located near two conducting cylinders. Field will consist of two components. Sources of one will be the charges of the filaments, sources of other — charges induced on the conducting cylinders. Complex potential of field $W(z)$ equals the sum of the complex potentials of each component of the field. On the surfaces of the cylinders (contours L_1 and L_2) its imaginary part (electrical potential) takes constant values c_1 and c_2 . The electrical potential of the field of charged filaments is easily determined:

$$U(x, y) = \operatorname{Im} [W_1(z)] = -\frac{1}{2\pi\epsilon} \sum_{k=1}^n \tau_k \ln |z - z_{0k}|. \quad (14.1)$$

On the surfaces of the conductors at points t_1 and t_2 its values equal:

$$\begin{aligned} U_1(t_1) &= -\frac{1}{2\pi\epsilon} \sum_{k=1}^n \tau_k \ln |t_1 - z_{0k}| \\ U_1(t_2) &= -\frac{1}{2\pi\epsilon} \sum_{k=1}^n \tau_k \ln |t_2 - z_{0k}| \end{aligned} \quad (14.2)$$

Subtracting them from constant values c_1 and c_2 of the resultant potential, we obtain limiting values of field potential of charges induced on the conductors

$$U_2(t_1) = c_1 - U_1(t_1); \quad U_2(t_2) = c_2 - U_1(t_2). \quad (14.3)$$

Considering that the potential is determined with an accuracy to the constant, we take $c_2 = 0$. Constant c_1 , as already indicated in § 3 is determined from the condition of single-valuedness of the function of flux of the field of induced charges. Let us define this constant [28].

The total induced charge on each of the cylinders is equal to zero, therefore on the basis of Gauss' theorem we have

$$\oint_{L_k} E_n dl = \oint_{L_k} \frac{\partial U_2}{\partial n} dl = 0 \quad (k = 1, 2). \quad (14.4)$$

But $\frac{\partial U_2}{\partial n} = \frac{\partial V_2}{\partial l}$, where V_2 — a function of flux of field of charges induced on the cylinders — is a harmonic function conjugate to the electrical potential.

We have

$$\oint_{L_k} \frac{\partial U_2}{\partial n} dl = \oint_{L_k} \frac{\partial V_2}{\partial l} dl = 0, \quad (14.5)$$

i.e., the function of flux V_2 is single-valued in region D.

Let us take c_1 also equal to zero. Then the limiting values of potential U^* will be

$$U^*(l_1) = -U_1(l_1); \quad U^*(l_2) = -U_1(l_2). \quad (14.6)$$

Potential U^* , defined in region D by its limiting values (14.6), will be a single-valued function of coordinates, its limiting values assigned single-valuedly, however, its conjugate function of flux V^* simple will not be single-valued since for uniqueness of V^* is necessary a fully defined unique value of constant c_1 but we arbitrarily have taken it equal to zero.

It is natural to assume that the magnitude constant c_1 is determined by the form of the region contour and by the distribution of potential U_1 on it. Having mapped region D onto an infinite band and thereby excluded the influence of contour form of the region on the magnitude of c_1 it is possible for us to express c_1 as a function only of distribution of potential on the boundaries of the band. Let us show this.

Taking the derivative of potential $U^*(z)$ with respect to the normal to one of the contours and integrating over the contour we obtain

$$\oint_{L_k} \frac{\partial U^*}{\partial n} dl = M \neq 0. \quad (14.7)$$

We will represent potential $U^*(z)$ in the form of the sum of two components

$$U^*(z) = U_2(z) + U_1^*(z). \quad (14.8)$$

Here $U_2(z)$ is the sought potential satisfying the condition

$$\oint_{L_1} \frac{\partial U_2}{\partial n} dl = 0 \quad (14.9)$$

and taking on the contours the values

$$U_2(t_1) = c_1 - U_1(t_1) \text{ and } U_2(t_2) = -U_1(t_2). \quad (14.10)$$

Potential $U_2^*(z)$ is stipulated by the selection of constant c_1 , equal to zero, and takes on the contours the values

$$U_2^*(t_1) = U^*(t_1) - U_1(t_1) = -c_1; \quad U_2^*(t_2) = U^*(t_2) - U_1(t_2) = 0 \quad (14.11)$$

Equality (14.7) can now be written thus:

$$\oint_{L_1} \frac{\partial U^*}{\partial n} dl = \oint_{L_1} \frac{\partial U_2}{\partial n} dl + \oint_{L_1} \frac{\partial U_2^*}{\partial n} dl = M, \quad (14.12)$$

whence

$$\oint_{L_1} \frac{\partial U_2^*}{\partial n} dl = M \quad (14.13)$$

We depict region D infinite-sheetly on a band. Every sheet of the Riemannian surface, coinciding with D, will be depicted on a rectangle with sides N and h. The potential on the mapped region - band - we designate by the subscript n. Obviously

$$\oint_{L_1} \frac{\partial U_n^*}{\partial n} dl = \int_0^N \left[\frac{\partial U_n^*}{\partial u} \right]_{u=0} du = M, \quad (14.14)$$

since motion along the Riemannian surface from the left shore of the cut to the right corresponds to motion on the band from $u = 0$ to $u = N$. But on the band we have

$$\left[\frac{\partial U_n^*}{\partial n} \right]_{u=0} = \frac{0 - (-c_1)}{h} = \frac{c_1}{h}; \quad M = \frac{c_1}{h} \int_0^N du = \frac{N}{h} c_1. \quad (14.15)$$

whence

$$c_1 = \frac{h}{N} M. \quad (14.16)$$

On the other hand,

$$M = \oint_L \frac{\partial U^*}{\partial n} dl = \int_0^N \left[\frac{\partial U^*}{\partial v} \right]_{v=0} du = \int_0^N \left[\frac{\partial U^*}{\partial v} \right]_{v=\frac{1}{2}} du \quad (14.17)$$

and this means we can write

$$c_1 = \frac{h}{N} \int_0^N \left[\frac{\partial U^*}{\partial v} \right]_{v=\frac{1}{2}} du. \quad (14.18)$$

The quantity $\left[\frac{\partial U^*}{\partial v} \right]_{v=\frac{1}{2}}$ is not difficult to find if one were to use formula (11.10), connecting the derivative of potential normal to the boundary with its limiting values on the boundaries of the band.

For $v = \frac{h}{2} \cos kv = \cos \frac{\pi}{2} = 0$ and, consequently,

$$\left[\frac{\partial U^*}{\partial v} \right]_{v=\frac{1}{2}} = \frac{k}{2h} \int_{-\infty}^{\infty} \frac{U_a^*(\tau + ih) - U_a^*(\tau)}{\operatorname{ch}^2 k(\tau - u)} d\tau \quad \left(k = \frac{\pi}{h} \right). \quad (14.19)$$

Substituting this value in the expression for c_1 we obtain

$$c_1 = \frac{h}{N} \int_0^N du \cdot \frac{k}{2h} \int_{-\infty}^{\infty} \frac{U_a^*(\tau + ih) - U_a^*(\tau)}{\operatorname{ch}^2 k(\tau - u)} d\tau \quad (14.20)$$

The magnitude of integral (14.20) does not depend on the order of integration, therefore

$$\begin{aligned} c_1 &= \frac{h}{2N} \int_{-\infty}^{\infty} [U_a^*(\tau + ih) - U_a^*(\tau)] d\tau \int_0^N \frac{du}{\operatorname{ch}^2 k(\tau - u)} = \\ &= \frac{1}{2N} \int_{-\infty}^{\infty} [U_a^*(\tau + ih) - U_a^*(\tau)] [\operatorname{th} k(\tau - N) - \operatorname{th} k\tau] d\tau = \\ &= -\frac{\operatorname{sh} kN}{N} \int_{-\infty}^{\infty} \frac{U_a^*(\tau + ih) - U_a^*(\tau)}{\operatorname{ch} k(2\tau - N) \operatorname{ch} kN} d\tau \end{aligned} \quad (14.21)$$

Earlier we took

$$U^*(u_1) = -U_1(u_1), \quad U^*(u_2) = -U_2(u_2).$$

consequently, on boundaries of the band also will be

$$U'_a(\tau + ih) = -U_{ia}(\tau + ih); \quad U'_a(\tau) = -U_{ia}(\tau). \quad (14.22)$$

Therefore we obtain

$$c_1 = \frac{sh kN}{N} \int_{-\infty}^{\infty} \frac{U_{ia}(\tau + ih) - U_{ia}(\tau)}{ch k(2\tau - N) + ch kN} d\tau. \quad (14.23)$$

The difference of limiting values of potential

$$\Delta U_a = U_{ia}(\tau + ih) - U_{ia}(\tau)$$

is a periodic function with period equal to N (Fig. 7b). We represent it in the form of the Fourier series

$$\Delta U_a = a_0 + \sum_{v=1}^{\infty} a_v \cos v\omega\tau + \sum_{v=1}^{\infty} b_v \sin v\omega\tau \quad \left(\text{for } \omega = \frac{2\pi}{N} \right) \quad (14.24)$$

and substitute in expression (14.23)

$$\begin{aligned} c_1 &= a_0 \frac{sh kN}{N} \int_{-\infty}^{\infty} \frac{d\tau}{ch k(2\tau - N) + ch kN} + \\ &+ \frac{sh kN}{N} \sum_{v=1}^{\infty} a_v \int_{-\infty}^{\infty} \frac{\cos v\omega\tau d\tau}{ch k(2\tau - N) + ch kN} + \\ &+ \frac{sh kN}{N} \sum_{v=1}^{\infty} b_v \int_{-\infty}^{\infty} \frac{\sin v\omega\tau d\tau}{ch k(2\tau - N) + ch kN}. \end{aligned} \quad (14.25)$$

Let us consider integrals standing under the summation signs. We introduce a new variable according to the formula

$$\tau = \xi + \frac{N}{2}, \quad (14.26)$$

then

$$\int_{-\infty}^{\infty} \frac{\sin v\omega\tau d\tau}{ch k(2\tau - N) + ch kN} = \int_{-\infty}^{\infty} \frac{(-1)^v \sin v\omega\xi d\xi}{ch 2k\xi + ch kN} = 0, \quad (14.27)$$

since the function under the integral is odd, and the integral is taken between symmetric limits.

Similarly we obtain

$$\begin{aligned} \operatorname{sh} kN \int_{-\infty}^{\infty} \frac{\cos \omega \tau d\tau}{\operatorname{ch} k(2\tau - N) + \operatorname{ch} kN} &= -\frac{1}{2} \int_{-\infty}^{\infty} \cos v\omega \tau [\operatorname{th} k(\tau - N) - \\ &- \operatorname{th} k\tau] d\tau = \frac{1}{2} \int_{-\infty}^{\infty} \cos v\omega \tau \operatorname{th} k\tau d\tau - \frac{1}{2} \int_{-\infty}^{\infty} \cos v\omega \tau \operatorname{th} k(\tau - N) d\tau = 0. \end{aligned} \quad (14.28)$$

Consequently

$$\begin{aligned} c_1 &= a_0 \frac{\operatorname{sh} kN}{N} \int_{-\infty}^{\infty} \frac{d\tau}{\operatorname{ch} k(2\tau - N) + \operatorname{ch} kN} = \\ &= \frac{a_0}{kN} \operatorname{sh} kN \int_0^{\infty} \frac{dx}{\operatorname{ch} x + \operatorname{ch} kN} = \frac{a_0}{kN} \left[\ln \operatorname{ch} \frac{x + kN}{2} - \right. \\ &\quad \left. - \ln \operatorname{ch} \frac{x - kN}{2} \right]_0^{\infty} = a_0. \end{aligned} \quad (14.29)$$

But a_0 is a constant component of the periodic potential difference ΔU_n equal to the mean value of this difference on segment N , therefore [4]

$$c_1 = a_0 = \frac{1}{N} \int_0^N [U_{1n}(\tau + ih) - U_{1n}(\tau)] d\tau. \quad (14.30)$$

Thus to determine the constant c_1 we must: 1) map region D infinite-sheetly on a band in such a manner that every sheet of the Riemannian surface is mapped onto a rectangle by dimensions $h \times N$; 2) transfer values of potential U_1 on the boundary of the band, calculated from (14.2), to points on the contours L_1 and L_2 ; 3) find the constant component of the periodic difference of potentials on the boundary of the band. Limiting values of the potential of the field of induced charges on contours of region D are then determined thus:

$$\begin{aligned} U_2(t_1) &= \frac{1}{N} \int_0^N [U_{1n}(\tau + ih) - U_{1n}(\tau)] d\tau - U_1(t_1), \\ U_2(t_2) &= -U_1(t_1). \end{aligned} \quad (14.31)$$

§ 15. Example of the Calculation of the Field of a Charged Axis in an Annular Gap Between Two Concentric Cylinders

We use the derived formulas for calculating the electrostatic field of a charged axis in the gap between two concentric conducting cylinders. The charge per unit length of axis equals σ , the radii of the cylinders — R_1 and R_2 , the axis

is at point $z_0 = qe^{i\psi}$, the origin of coordinates on the axis of the cylinders.

Electrical potential of a charged axis

$$U_1(x, y) = -\frac{\sigma}{2\pi\epsilon} \ln |z - z_0|. \quad (15.1)$$

On circumferences L_1 and L_2 its values are:

$$\begin{aligned} U_1(R_1, \theta) &= -\frac{\sigma}{2\pi\epsilon} \ln |R_1 e^{i\theta} - qe^{i\psi}| = \\ &= -\frac{\sigma}{2\pi\epsilon} \ln \sqrt{R_1^2 - 2R_1 q \cos(\theta - \psi) + q^2}. \end{aligned} \quad (15.2)$$

$$\begin{aligned} U_2(R_2, \theta) &= -\frac{\sigma}{2\pi\epsilon} \ln |R_2 e^{i\theta} - qe^{i\psi}| = \\ &= -\frac{\sigma}{2\pi\epsilon} \ln \sqrt{R_2^2 - 2R_2 q \cos(\theta - \psi) + q^2}. \end{aligned} \quad (15.3)$$

The function, infinite-sheetly, conformally depicting a ring on a band of width $k = \ln \frac{R_2}{R_1}$, has the form

$$\Omega(z) = i \ln \frac{z}{R}. \quad (15.4)$$

On circumferences L_1 and L_2 its values are

$$\Omega(R_1, e^{i\theta}) = i \ln \frac{R_1}{R_1} e^{i\theta} = -\theta + i \ln \frac{R_1}{R_1} = \tau + ih; \quad (15.5)$$

$$\Omega(R_2, e^{i\theta}) = i \ln \frac{R_2}{R_1} e^{i\theta} = -\theta + \tau. \quad (15.6)$$

Consequently, on the boundaries of the band the distribution of potential will be such:

$$U_1(\tau + ih) = -\frac{\sigma}{2\pi\epsilon} \ln \sqrt{R_1^2 - 2R_1 q \cos(\tau + \psi) + q^2}, \quad (15.7)$$

$$U_2(\tau) = -\frac{\sigma}{2\pi\epsilon} \ln \sqrt{R_2^2 - 2R_2 q \cos(\tau + \psi) + q^2}. \quad (15.8)$$

We represent the difference of these values in the form of a Fourier series

$$\begin{aligned} \Delta U_{in} = U_{in}(\tau + ih) - U_{in}(\tau) &= \frac{\sigma}{2\pi\epsilon} \left[\ln \frac{q}{R_1} + \ln \sqrt{\frac{1 - 2 \frac{R_2}{q} \cos(\tau + \psi) + \frac{R_2^2}{q^2}}{1 - 2 \frac{q}{R_1} \cos(\tau + \psi) + \frac{q^2}{R_1^2}}} \right] = -\frac{\sigma}{2\pi\epsilon} \ln \frac{R_1}{q} - \\ &- \frac{\sigma}{2\pi\epsilon} \sum_{k=1}^{\infty} \left(\frac{R_2^k}{q^k} - \frac{q^k}{R_1^k} \right) \frac{\cos k(\tau + \psi)}{k}. \end{aligned} \quad (15.9)$$

The constant component of the periodic difference of potentials ΔU_{1n} , and consequently, the constant c_1 , will equal

$$c_1 = c_0 = -\frac{\sigma}{2\pi\epsilon} \ln \frac{R_1}{\rho}. \quad (15.10)$$

Hence for limiting values of field of potential charges induced on the conductors, we obtain:

$$U_1(R_1, \psi) = \frac{\sigma}{2\pi\epsilon} \left[\ln \sqrt{R_1^2 - 2R_1\rho \cos(\psi - \varphi) + \rho^2} - \ln \frac{R_1}{\rho} \right], \quad (15.11)$$

$$U_2(R_2, \theta) = \frac{\sigma}{2\pi\epsilon} \ln \sqrt{R_2^2 - 2R_2\rho \cos(\theta - \varphi) + \rho^2} \quad (15.12)$$

These values on boundaries of the band:

$$\begin{aligned} U_n(\tau + ih) &= \frac{\sigma}{2\pi\epsilon} \left[\ln \rho + \ln \sqrt{1 - 2\frac{\rho}{R_1} \cos(\tau + \varphi) + \frac{\rho^2}{R_1^2}} \right] = \\ &= \frac{\sigma}{2\pi\epsilon} \left[\ln \rho - \sum_{k=1}^{\infty} \frac{\rho^k}{R_1^k} \frac{\cos k(\tau + \varphi)}{k} \right], \end{aligned} \quad (15.13)$$

$$\begin{aligned} U_n(\tau) &= \frac{\sigma}{2\pi\epsilon} \ln \rho \sqrt{1 - 2\frac{R_2}{\rho} \cos(\tau + \varphi) + \frac{R_2^2}{\rho^2}} = \\ &= \frac{\sigma}{2\pi\epsilon} \left[\ln \rho - \sum_{k=1}^{\infty} \frac{R_2^k}{\rho^k} \frac{\cos k(\tau + \varphi)}{k} \right]. \end{aligned} \quad (15.14)$$

Let us find the distribution of the normal component of intensity on the surface of the cylinders. By formula (11.29), on the boundary of the band we have

$$\begin{aligned} \frac{\partial U_n}{\partial \nu} \Big|_{\nu=0} &= \frac{1}{h} \left[U_n(u + ih) - U_n(u) + \right. \\ &\left. + \sum_{n=1}^{\infty} n \int_0^{\pi} \frac{f_1(a) da}{e^{na}} - \sum_{n=1}^{\infty} (-1)^n \int_0^{\pi} \frac{f_2(a) da}{e^{na}} \right], \end{aligned} \quad (15.15)$$

$$\begin{aligned} f_1(a) &= \frac{\sigma}{2\pi\epsilon} \sum_{k=1}^{\infty} \frac{R_1^k}{k\rho^k} [2 \cos k(u + \varphi) - \cos k(u + \varphi + a) - \cos k(u + \\ &+ \varphi - a)] = \frac{\sigma}{\pi\epsilon} \sum_{k=1}^{\infty} \frac{R_1^k}{\rho^k} \cdot \frac{\cos k(u + \varphi)}{k} (1 - \cos ka), \end{aligned} \quad (15.16)$$

$$f_2(a) = \frac{\sigma}{\pi e} \sum_{k=1}^{\infty} \frac{q^k}{R_1^k} \cdot \frac{\cos k(u + \psi)}{k} (1 - \cos ka), \quad (15.17)$$

$$\begin{aligned} \frac{\partial U_{2n}}{\partial v} \Big|_{v=0} = & \frac{\sigma}{\pi e h} \left[\frac{1}{2} \ln \sqrt{\frac{1 - 2 \frac{q}{R_1} \cos(u + \psi) + \frac{q^2}{R_1^2}}{1 - 2 \frac{R_2}{q} \cos(u + \psi) + \frac{R_2^2}{q^2}}} + \right. \\ & + \sum_{n=1}^{\infty} n \int_0^{\pi} \frac{\sum_{k=1}^{\infty} \frac{R_2^k}{q^k} \cdot \frac{\cos k(u + \psi)}{k} (1 - \cos ka)}{e^{na}} da - \\ & - \sum_{n=1}^{\infty} (-1)^n \int_0^{\pi} \frac{\sum_{k=1}^{\infty} \frac{q^k}{R_1^k} \cdot \frac{\cos k(u + \psi)}{k} (1 - \cos ka)}{e^{na}} da \Big] = \\ & = \frac{\sigma}{\pi e h} \left[\frac{1}{2} \ln \sqrt{\frac{1 - 2 \frac{q}{R_1} \cos(\tau + \psi) + \frac{q^2}{R_1^2}}{1 - 2 \frac{R_2}{q} \cos(\tau + \psi) + \frac{R_2^2}{q^2}}} + \right. \\ & + \sum_{n=1}^{\infty} n \sum_{k=1}^{\infty} \frac{R_2^k}{q^k} \cdot \frac{\cos k(u + \psi)}{k} \int_0^{\pi} \frac{1 - \cos ka}{e^{na}} da - \\ & - \sum_{n=1}^{\infty} (-1)^n \sum_{k=1}^{\infty} \frac{q^k}{R_1^k} \cdot \frac{\cos k(u + \psi)}{k} \int_0^{\pi} \frac{1 - \cos ka}{e^{na}} da \Big]. \quad (15.18) \end{aligned}$$

But

$$\begin{aligned} \int_0^{\pi} \frac{1 - \cos ka}{e^{na}} da &= -\frac{1}{ne^{na}} \Big|_0^{\pi} - \frac{k \sin ka - n \cos ka}{(n^2 + k^2) e^{na}} \Big|_0^{\pi} = \\ &= \frac{1}{n} - \frac{n}{n^2 + k^2} = \frac{k^2}{n(n^2 + k^2)}. \quad (15.19) \end{aligned}$$

$$\begin{aligned} \frac{\partial U_{2n}}{\partial v} \Big|_{v=0} = & \frac{\sigma}{\pi e h} \left[\frac{1}{2} \ln \sqrt{\frac{1 - 2 \frac{q}{R_1} \cos(u + \psi) + \frac{q^2}{R_1^2}}{1 - 2 \frac{R_2}{q} \cos(u + \psi) + \frac{R_2^2}{q^2}}} + \right. \\ & + \sum_{n=1}^{\infty} \sum_{k=1}^{\infty} k \frac{R_2^k}{q^k} \cdot \frac{\cos k(u + \psi)}{n^2 + k^2} - \\ & - \sum_{n=1}^{\infty} (-1)^n \sum_{k=1}^{\infty} k \frac{q^k}{R_1^k} \cdot \frac{\cos k(u + \psi)}{n^2 + k^2} \Big] \quad (15.20) \end{aligned}$$

Considering the absolute convergence of series we change the order of summation:

$$\begin{aligned}
 \sum_{k=1}^{\infty} \sum_{n=1}^{\infty} k \frac{R_2^2}{e^2} \cdot \frac{\cos k(u+\psi)}{n^2+k^2} &= \sum_{k=1}^{\infty} k \frac{R_2^2}{e^2} \cos k(u+\psi) \sum_{n=1}^{\infty} \frac{1}{n^2+k^2} = \\
 &= \sum_{k=1}^{\infty} \frac{R_2^2}{e^2} \cos k(u+\psi) \left[\pi \operatorname{cth} k\pi - \frac{1}{k} \right] \cdot \frac{1}{2} = \\
 &= \frac{\pi}{2} \sum_{k=1}^{\infty} \frac{R_2^2}{e^2} \operatorname{cth} k\pi \cos k(u+\psi) - \frac{1}{2} \sum_{k=1}^{\infty} \frac{R_2^2}{e^2} \cdot \frac{\cos k(u+\psi)}{k} = \\
 &= \frac{\pi}{2} \sum_{k=1}^{\infty} \frac{R_2^2}{e^2} \operatorname{cth} k\pi \cos k(u+\psi) + \\
 &+ \frac{1}{2} \ln \left| 1 - 2 \frac{R_2}{e} \cos(u+\psi) + \frac{R_2^2}{e^2} \right|. \quad (15.21)
 \end{aligned}$$

$$\begin{aligned}
 \sum_{k=1}^{\infty} (-1)^k \sum_{n=1}^{\infty} k \frac{e^2}{k_1^2} \cdot \frac{\cos k(u+\psi)}{n^2+k^2} &= \\
 &= \sum_{k=1}^{\infty} k \frac{e^2}{k_1^2} \cos k(u+\psi) \sum_{n=1}^{\infty} \frac{(-1)^k}{n^2+k^2} = \\
 &= \sum_{k=1}^{\infty} \frac{e^2}{k_1^2} \cos k(u+\psi) \frac{1}{2} \left(\frac{\pi}{\operatorname{sh} k\pi} - \frac{1}{k} \right) = \frac{\pi}{2} \sum_{k=1}^{\infty} \frac{e^2}{k_1^2} \frac{\cos k(u+\psi)}{\operatorname{sh} k\pi} + \\
 &+ \frac{1}{2} \ln \left| 1 - 2 \frac{e}{R_1} \cos(u+\psi) + \frac{e^2}{R_1^2} \right|. \quad (15.22)
 \end{aligned}$$

Substituting these values in formula (15.20) we obtain

$$\begin{aligned}
 \frac{\partial U_{2n}}{\partial v} \Big|_{v=0} &= \frac{\sigma}{2\pi h} \left[\sum_{k=1}^{\infty} \frac{R_2^2}{e^2} \operatorname{cth} k\pi \cos k(u+\psi) - \right. \\
 &\left. - \sum_{k=1}^{\infty} \frac{e^2}{k_1^2} \cdot \frac{\cos k(u+\psi)}{\operatorname{sh} k\pi} \right]. \quad (15.23)
 \end{aligned}$$

Taking into consideration that with high accuracy

$$\begin{aligned}
 \sum_{k=1}^{\infty} \frac{R_2^2}{e^2} \operatorname{cth} k\pi \cos k(u+\psi) &\approx \frac{R_2}{e} \operatorname{cth} \pi \cos(u+\psi) + \sum_{k=1}^{\infty} \frac{R_2^2}{e^2} \cos k(u+\psi) = \frac{R_2}{e} \operatorname{cth} \pi \cos(u+\psi) + \\
 + \frac{1 - \frac{R_2}{e} \cos(u+\psi)}{1 - 2 \frac{R_2}{e} \cos(u+\psi) + \frac{R_2^2}{e^2}} - 1 &= \frac{R_2}{e} \cos(u+\psi) = \frac{R_2}{e} \operatorname{cth} \pi \cos(u+\psi) \div \frac{R_2^2}{e^2} \cdot \frac{\cos 2(u+\psi) - \frac{R_2}{e} \cos(u+\psi)}{1 - 2 \frac{R_2}{e} \cos(u+\psi) + \frac{R_2^2}{e^2}} \\
 & \quad (15.24)
 \end{aligned}$$

and

$$\sum_{n=1}^{\infty} \frac{e^n}{R_1^n} \cdot \frac{\cos k(u + \varphi)}{\operatorname{sh} k\pi} \approx \frac{e}{R_1} \cdot \frac{\cos(u + \varphi)}{\operatorname{sh} \pi}. \quad (15.25)$$

will obtain

$$\begin{aligned} \frac{\partial U_{\Sigma}}{\partial v} \Big|_{v=0} = & \frac{e}{2\pi \ln \frac{R_1}{R_2}} \left[\left(\frac{R_2}{e} \operatorname{cth} \pi - \frac{e}{R_1} \frac{1}{\operatorname{sh} \pi} \right) \cos(u + \varphi) + \right. \\ & \left. + \frac{R_2^2}{e^2} \cdot \frac{\cos 2(u + \varphi) - \frac{R_2}{e} \cos(u + \varphi)}{1 - 2 \frac{R_2}{e} \cos(u + \varphi) + \frac{R_2^2}{e^2}} \right]. \end{aligned} \quad (15.26)$$

Analogously, for the normal derivative of potential on the upper boundary of the band we obtain

$$\begin{aligned} \frac{\partial U_{\Sigma}}{\partial v} \Big|_{v=\pi} = & \frac{e}{2\pi \ln \frac{R_1}{R_2}} \left[\left(\frac{e}{R_1} \operatorname{cth} \pi - \frac{R_1}{e} \frac{1}{\operatorname{sh} \pi} \right) \cos(u + \varphi) + \right. \\ & \left. + \frac{e^2}{R_1^2} \cdot \frac{\cos 2(u + \varphi) - \frac{e}{R_1} \cos(u + \varphi)}{1 - 2 \frac{e}{R_1} \cos(u + \varphi) + \frac{e^2}{R_1^2}} \right]. \end{aligned} \quad (15.27)$$

The normal derivative of the potential of the field of induced charges on the surface of the inner conducting cylinder has the form

$$\begin{aligned} \frac{\partial U_2}{\partial n} \Big|_{R_1} = & \frac{d\tau}{dt} \cdot \frac{\partial U_{\Sigma}}{\partial v} \Big|_{v=0} = \left| \frac{d \left(\ln \frac{z}{R_2} \right)}{dz} \right|_{z=R_1} \cdot \frac{\partial U_{\Sigma}}{\partial v} \Big|_{v=0} = \\ = & \frac{1}{R_1} \cdot \frac{\partial U_{\Sigma}}{\partial v} \Big|_{v=0}. \end{aligned} \quad (15.28)$$

On the surface of the outer conducting cylinder the normal derivative of potential of field of induced charges is:

$$\frac{\partial U_2}{\partial n} \Big|_{R_2} = \frac{1}{R_1} \cdot \frac{\partial U_{\Sigma}}{\partial v} \Big|_{v=\pi}. \quad (15.29)$$

The normal derivative of potential of field of charged axis on the surface of the inner cylinder is written thus:

$$\begin{aligned} \frac{\partial U_1}{\partial R} \Big|_{R=R_2} &= -\frac{e}{2\pi} \cdot \frac{R_1 - e \cos(\theta - \varphi)}{R_1^2 - 2R_1 e \cos(\theta - \varphi) + e^2} = \\ &= -\frac{e}{2\pi R_2} \cdot \frac{1 - \frac{e}{R_1} \cos(\theta - \varphi)}{1 - 2 \frac{e}{R_1} \cos(\theta - \varphi) + \frac{e^2}{R_1^2}}. \end{aligned} \quad (15.30)$$

and on the surface of the outer cylinder

$$\begin{aligned} \frac{\partial U_1}{\partial R} \Big|_{R=R_1} &= -\frac{e}{2\pi} \cdot \frac{R_1 - e \cos(\theta - \varphi)}{R_1^2 - 2R_1 e \cos(\theta - \varphi) + e^2} = \\ &= -\frac{e}{2\pi R_1} \cdot \frac{1 - \frac{e}{R_1} \cos(\theta - \varphi)}{1 - 2 \frac{e}{R_1} \cos(\theta - \varphi) + \frac{e^2}{R_1^2}}. \end{aligned} \quad (15.31)$$

CHAPTER II

MODELING OF CONFORMALLY MAPPING FUNCTIONS

§ 16. Electrical Field of Current in a Conducting Sheet

Plane-parallel electro- and magnetostatic fields in a dielectric, strictly speaking, do not exist since there cannot be infinite sources of these fields and there is no media with zero electrical or magnetic permeabilities. On the contrary, the field of current in conductors can be plane-parallel since the current can concentrate in a bounded domain limiting this region with an insulating surface. On the interface between the conductor and dielectric the normal component of current density is equal to zero, the vector of current density lies in a plane tangent to the interface and consequently the surface of conductor may be regarded as a surface formed by the totality of flow lines. The field of current in a thin conducting sheet will be plane-parallel.

From the principle of continuity of flow lines it follows

$$\operatorname{div} \bar{\delta} = 0, \quad (16.1)$$

where $\bar{\delta}$ — vector of current density.

In a uniform isotropic medium, according to Ohm's law, the density of current is proportional to intensity \bar{E}

$$\bar{\delta} = \gamma \bar{E} = -\gamma \operatorname{grad} U. \quad (16.2)$$

Substituting expression (16.2) in (16.1) we will obtain

$$\operatorname{div} \bar{\delta} = \gamma \operatorname{div} \operatorname{grad} U = \gamma \Delta U = 0, \quad (16.3)$$

i.e., potential of field of direct current in conducting medium satisfies the Laplace equation. When deriving expression (16.3) we did not consider magnetic

interaction of currents which in general affects distribution of current density in conductor and, consequently, the potential. Let us estimate magnitude of this interaction.

Let us consider two charges q_1 and q_2 moving in a conducting medium in one direction with a speed v . The distance between charges is r . The force of electrical interaction of charges, determining distribution of field in conductor, according to equation (16.3) has the form [18]

$$|f_e| = \frac{1}{4\pi\epsilon_0} \cdot \frac{q_1 q_2}{r^2}. \quad (16.4)$$

The force of magnetic interaction of moving charges distorting this distribution of the field is written thus:

$$|f_m| = |q_1 [\vec{v} \cdot \vec{B}]|. \quad (16.5)$$

The induction B of the magnetic field of a moving charge q_2 at a distance r from it equals

$$B = \mu_0 \frac{q_2 v}{4\pi r^2} \quad (16.6)$$

and is directed along the normal to the plane of vectors \vec{v} and \vec{r} . Placing this value of induction in expression (16.5) we obtain

$$|f_m| = q_1 v B = \mu_0 \frac{q_1 q_2 v^2}{4\pi r^2}. \quad (16.7)$$

Consequently we write the relationship between the electrical and magnetic intensities affecting the distribution of current density in the conductor

$$\left| \frac{f_e}{f_m} \right| = \frac{1}{v^2 \epsilon_0 \mu_0} = \frac{c^2}{v^2}. \quad (16.8)$$

where $c = \frac{1}{\sqrt{\epsilon_0 \mu_0}} = 3 \cdot 10^8$ m/s - velocity of light in emptiness.

It is known that the average speed of directed motion of charges in metal does not exceed 1 m/s, i.e., $v^2 \approx 1$ m²/s and consequently the forces of electrical interaction of charges moving in the conductor are in $9 \cdot 10^{16}$ times greater than the forces of magnetic interaction. Influence of the magnetic field on distribution of direct current in the conductor is so insignificant that it can always be disregarded and it may be considered that the electrical potential of the field in a medium with constant conductivity satisfies the Laplace equation.

Let us consider uniform flat conducting sheet of constant thickness Δ and unlimited extent (Fig. 10). At point O we connect to the sheet a thin conductor and



Fig. 10.

pass through the sheet a constant current I (it is assumed that the return wire is connected infinitely far away). Let us draw a circle l of radius r with its center at the point O . In accordance with the principle of continuity of current we have

$$\oint \delta_n dl = \oint \gamma E_n dl = I; \quad (16.9)$$

$$\delta_n = \delta_n' \Delta = \gamma' \Delta E_n = \gamma E_n.$$

Here

δ_n' — density of current normal to circle l ;

Δ — thickness of sheet;

γ' — conductivity of material of sheet;

$\gamma = \gamma' \Delta$ — conductivity of unit of surface of sheet.

Due to symmetry, on the circle l $E_n = E = \text{const}$ and $I = \gamma E \cdot 2\pi r$. Hence

$$\vec{E} = -\text{grad } U = \frac{\vec{r}_0}{2\pi\gamma r}, \quad (16.10)$$

\vec{r}_0 — unit direction vector of \vec{r} .

Let us assume at some point, at a distance r_1 from point O , a potential to equal to zero: $U(r_1) = 0$. Then potential U at any point of the sheet at the distance r from point O will be determined thus:

$$U(r) = \int \vec{E} d\vec{r} = \frac{I}{2\pi\gamma} \int \frac{dr}{r} = \frac{I}{2\pi\gamma} (\ln r_1 - \ln r) =$$

$$= -\frac{I}{2\pi\gamma} \ln r + c. \quad (16.11)$$

Lines of equal potential will be concentric circles with their centers at point O , current lines will be rays radiating from point O . Precisely such picture has the field of a charged axis, the expression for potential of which differs from (16.11) only in that it includes a linear charge τ instead of current I and ϵ instead of γ . Consequently field of current in sheet in this case can serve as an analog of the electrostatic field of a charged axis in a dielectric.

Let us assume that now current is brought in to a section S of the surface of the sheet so that to each element of area dS is brought a current $di = \delta dS$. The component of potential dU giving rise to a current di at a distance r from it

equals

$$dU = -\frac{1}{2\pi\gamma} dl \ln r = -\frac{\delta ds}{2\pi\gamma} \ln r. \quad (16.12)$$

Potential caused by all current I brought to S has the form

$$U = -\frac{1}{2\pi\gamma} \int_S \delta \ln r dS + c_1. \quad (16.13)$$

There is an analogous formula for potential of a flat electrostatic field in a dielectric and for the vector potential of a magnetic field in a uniform medium.

The analogy between a field of direct current in a flat conducting sheet and plane-parallel electrostatic and magnetostatic fields is used for modeling electro- and magnetostatic fields. In this respect the field of current possesses great advantages over other physical fields. The field is easily produced and its intensity easily measured at any place.

Potential U of current field in a sheet is a harmonic function and has its conjugate function of flux (or current). By value of function of current J at point (x, y) of the sheet we understand the magnitude of current I through any section connecting point (x, y) with initial line of current (on which is taken $j = 0$) divided by the conductivity of a unit surface of the sheet

$$J(x, y) = \frac{I(x, y)}{\gamma}. \quad (16.14)$$

Conjugate harmonic functions U and J can be represented in the form of imaginary and real parts of an analytic function — complex potential Ω

$$\Omega(z) = J(x, y) + iU(x, y). \quad (16.15)$$

From everything that has been said one may see that the field of direct current in a sheet can be used for simulation of any flat physical field described by harmonic function $\varphi(x, y)$.

Let us consider the possibility of solving the Dirichlet problem by simulation the sought function φ with an electrical field of current in a conducting sheet [36].

Stationary plane-parallel field of current in a conducting sheet is characterized by two conjugate harmonic functions — electrical potential U and function of currents J , each of which can be selected for modeling. In Fig. 11 is given the fundamental diagram for simulation of searched in region D of harmonic

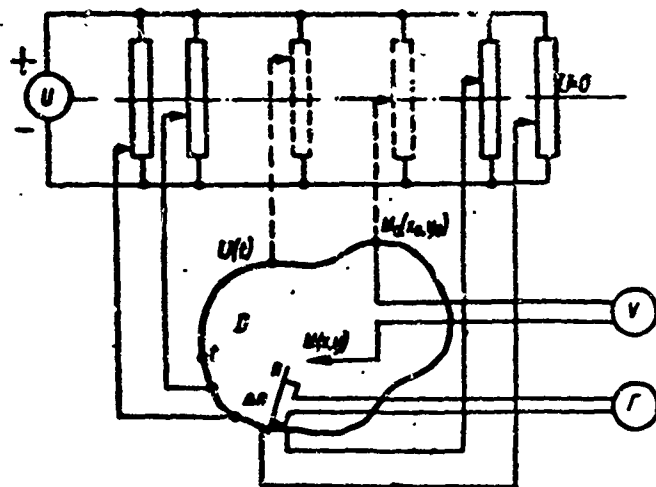


Fig. 11.

function $\varphi(x, y)$ by an electrical potential $U(x, y)$ on a conducting sheet cut in the form of an assigned region D . Function φ is given on the contour l by values of electrical potential $U(t) = \varphi(t)$. The value of potential at any point $M(x, y)$ of the region, is proportional to the value of $\varphi(x, y)$, can be measured with an accuracy of the constant by a voltmeter connected between the point $M(x, y)$ and the

point $M_0(x_0, y_0)$ at which the potential is taken equal to zero.

In the majority of practical problems we are not interested in the harmonic function φ , itself but in its gradient and in particular the normal derivative on boundary $\frac{\partial \varphi}{\partial n}$. This quantity can be measured, as shown on the diagram with a galvanometer and the help of a double probe the distance Δn between whose needles is precisely held:

$$\alpha_r = \frac{\partial U}{\partial n} \Delta n \equiv \frac{\partial \varphi}{\partial n}. \quad (16.16)$$

Practical set-up of an installation for simulation of a potential function is difficult: in order to ensure independent assignment of potential at every point of the boundary, the model should be prepared from a conducting material with a high specific electrical resistance, otherwise upon establishing the potential at any one point of the model contour the potentials of all neighboring points will be changed. Metallic sheets possessing good homogeneity have a low specific resistance but existing conducting papers are nonuniform and potential of field of current in them differs from harmonic. During measurement of gradient of potential on a model of paper this difference leads to impermissible error.

It is considerably more convenient and more exact to model a harmonic function φ of a current function J in a metallic sheet. In Fig. 12 is shown fundamental diagram of such a modeling. Boundary values $\varphi(t)$ of the sought function $\varphi(x, y)$ are given by the magnitude of current supplied to the model circuit. Here, for an increase of threshold function on a certain section of the

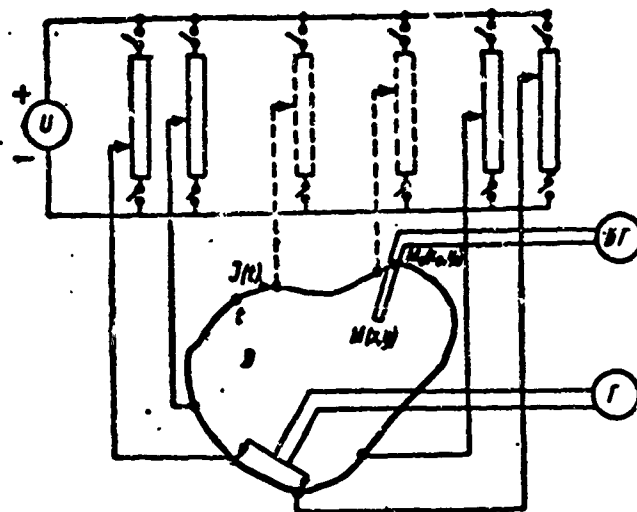


Fig. 12.

boundary we obtain

$$\Delta \varphi(t) = \Delta J(t) = \frac{i}{\gamma}, \quad (16.17)$$

where i — current supplied to given section of boundary, γ — conductivity of unit of surface of sheet.

Measurement of current function in any point of the region can be made either with a special magnetic band connected to a ballistic galvanometer

$$\alpha_{0,r} = \oint \vec{H} d\vec{l} = i = \gamma J(x, y) \equiv \varphi(x, y), \quad (16.18)$$

or with a double probe connected to a voltmeter. For this we present $J(x, y)$ in the form of an integral taken along the line connecting section of contour L on which $J = 0$, with point (z) ,

$$J(z) = \int_L^z \frac{\partial J}{\partial n} dt = \int_L^z \frac{\partial U}{\partial n} dt. \quad (16.19)$$

Replacing the integral by a final sum and considering $\Delta n = \Delta t$, we obtain

$$J(z) \approx \sum_{k=1}^n \frac{\Delta U_k}{\Delta n} \Delta t = \sum_{k=1}^n \Delta U_k. \quad (16.20)$$

Component ΔU_k is measured with a special double probe which breaks the line into m parts each equal to the distance between needles. The probe is mounted in such a manner so that the average distance between needles coincided with the middle of section of straight line and needle are disposed on a perpendicular to this

section. Measurement of the normal derivative of current $\frac{\partial J}{\partial n}$ on the boundary is made with a galvanometer connected to the double probe. In virtue of the conjugation of functions U and J normal derivative of current is equal to the tangential derivative electrical potential

$$\left| \frac{\partial J}{\partial n} \right| = \left| \frac{\partial U}{\partial \tau} \right| \quad (16.21)$$

and consequently the voltage drop measured over a sufficiently small section Δt along the boundary of the region is proportional to the derivative of current on this section:

$$a_r = \frac{\partial U}{\partial \tau} \Delta t = \frac{\partial \varphi}{\partial n}. \quad (16.22)$$

Simulation according to the diagram shown in Fig. 12 also contains essential deficiencies:

- 1 - for every concrete problem it is necessary to prepare its own region model which, when requirements for accuracy of simulation are high, requires a great expenditure of qualified labor;
- 2 - for obtaining accuracy of simulation it is necessary to ensure sufficiently accurate assignment of boundary values of modeling function over the entire contour of the region; for this a large number of current sources is required;
- 3 - appraisal of accuracy of simulation for an arbitrary the region is hampered; use of the idea of conformal transformation [25, 37, 38, 42] would permit avoidance of these difficulties and creation of universal analog computers for solution of Dirichlet and Neumann problems.

§ 17. Simulation of a Function Conformally Depicting a Singly-Connected Region on a Band

Let there be given a region D bounded piecewise by smooth contour L . Let us perform the following experiment. From a thin uniform conducting sheet we cut a model in the form of region D (Fig. 13). To two points of the model contour, A and B , we connect a dc source. Let us consider the field of current in the model. The normal component of current density δ_n on the model contour is absent ($\delta_n = 0$), consequently on the contour $\delta = \delta_t$. Let us take contour line AmB as the initial line, i.e., on it we set $J = 0$. Then value of stream function J in any point M of the model will equal current I flowing through any section connecting point M with section of contour AmB divided by conductivity of a unit

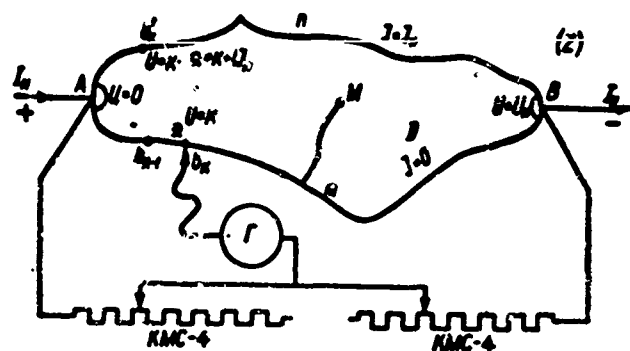


Fig. 13.

surface of sheet γ

$$J = \frac{I}{\gamma}. \quad (17.1)$$

Let us take also potential of point C, lying near point A, equal to zero. Then potential U at point M will be equal to the voltage between points M and C. On section of contour AnB of stream functions we take the value

$$J_N = \frac{I_N}{\gamma}, \quad (17.2)$$

where I_N — total current through the model.

We assume that contact is made at geometric points A and B. Let us consider the environment of the point of contact. In it converge two boundary flow lines

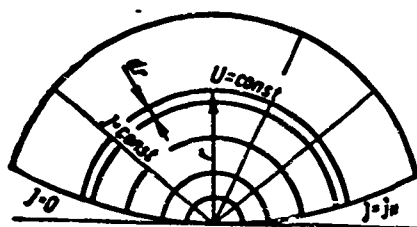


Fig. 14.

$J = 0$ and $J = J_N$ (Fig. 14) and, consequently, all intermediate lines. Field pattern in environment of point of contact is similar to field pattern of charged axis and lines of equal potential differ little from concentric circles with centers at the point of contact. Let us find the resistance of environment of the point of contact. Resistance of band of width dr and radius r equals

$$dR = \frac{dr}{2\pi\gamma}. \quad (17.3)$$

Resistance of the entire environment of the point of contact is

$$R = \int \frac{dr}{\pi\gamma r} = \frac{1}{\pi\gamma} \ln r \Big|_0^\infty = \frac{1}{\pi\gamma} \ln r + \infty = \infty, \quad (17.4)$$

i.e., resistances of contact points are equal to infinity. This means that with a

finite quantity of current through the model the potential U at points of contact should be infinitely great ($U_k = \pm\infty$).

Thus the complex potential of the current field in the model $\Omega = j + iU$ takes the following boundary values.

1. On section of contour AmB real part of J takes constant value $J = 0$, the imaginary part U varies from $-\infty$ at point A to $+\infty$ at point B .
2. On section of contour AnB the real part of J takes constant value $J = J_N$, the imaginary part of U also changes from $-\infty$ to $+\infty$.

Consequently on plane (Ω) region D is converted into a vertical infinite band of width $J_N = h$ between lines $J = 0$ and $J = J_N$. Complex potential $\Omega = J + iU$ is a function conformally depicting region D on an infinite band. For convenience of depicting on figures U and J in expression for Ω we change places.

Field of current in model will not change if contacts A and B are made on equipotential lines $U = 0$ and $U = U_N$. The form of these lines near points A and B can be indicated beforehand, namely, does the point of contact lie on a smooth part of the contour or coincide with its angular point. At its intersection the line $U = \text{const}$ will differ very little from arcs of a circle with its center at the point of contact since the point of contact for function Ω is a singular point of logarithmic type. In this case the part of the model, not occupied by contacts, on plane (Ω) will be depicted on a rectangle between straight lines $J = 0$, $U = U_N$, $J = J_N$, $U = 0$. The analytic function — complex potential of field of current in model $\Omega(z)$ — being analytically continued through lines of contacts on sections of the model under contacts, will map these segments on two infinite semi-bands of width $J_N = h$ supplementing the rectangle to infinite band in both directions (Fig. 15).

The accuracy of simulation will depend on homogeneity of sheet from which is prepared model, accuracy of preparation of model contour, and degree of coincidence of circumference of contact with line $U = \text{const}$ of the field of current in the model if current is brought in at two geometric points of the contour.

Let us consider now how it is possible to model a function conformally mapping a singly-connected region D , external with respect to closed contour L , onto a band (Fig. 16a). Reasoning just as in preceding case, for this it is

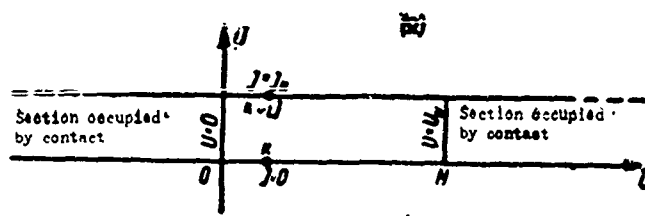


Fig. 15.

necessary to make a model from a conducting sheet in the form of the considered region and to two points of model contour introduce a direct current. Complex potential field of current in such a model will be a function conformally mapping region D onto a band. Contacts may also be made along two small arcs of circles with centers at the points of contour A and B .

However during preparation of such a model an essential difficulty arises. Region D is infinitely large but the external dimensions of the model must be limited. The external contour of the model will introduce distortion in field of current in it since on it is constrained the establishment of a constant value

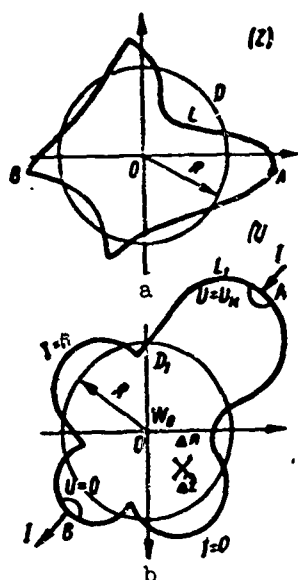


Fig. 16.

of current function $J = \text{const}$. The error introduced by the external contour of the model when its radius is small can be so great as to essentially distort the mapping function not only in points of region remote from contour L also on the actual contour. Let us estimate the magnitude of this error. If the model were of unlimited dimensions then the complex potential of the field of current in it would have by its own sources of contact charges to which a direct current is supplied and the distributed charges applied to the contour L are determined by value $J = \text{const}$ on the contour L . Let the external contour of the model now be made in the form of a circle of radius R with center in middle of the segment connecting the most remote points of contour L . Let us join the contacts of the source of current to these points.

On the external circuit also is constrained satisfaction of the condition $J = \text{const}$, i.e., there will appear an induced charge. Let us estimate the distorting influence of this charge. For simplicity of consideration we will limit ourselves to an appraisal of the influence of only that part of the induced

charges on the external circuit which are produced by charges of the model contacts.

Applying the method of mirror images, we find the complex potential of the field of charges induced on the contour of the model by charges of the contacts. Let us assume that the origin of coordinates coincides with the center of external circle R and the contacts with charges $\pm\tau$ are situated at points $\pm r$. Then the complex potential of the field of induced charges will be written thus:

$$\Delta\Omega(z) = -i \frac{\tau}{2\pi\gamma} \ln \frac{z - \frac{R^2}{r}}{z + \frac{R^2}{r}} = -i \frac{\tau}{2\pi\gamma} \ln \frac{\frac{z}{R^2} - 1}{\frac{z}{R^2} + 1}. \quad (17.5)$$

The modulus of this quantity at point t of contour L has the form

$$|\Delta\Omega(t)| = \frac{\tau}{2\pi\gamma} \left| \ln \frac{1 - i \frac{rt}{R^2}}{1 + i \frac{rt}{R^2}} \right| \approx \frac{\tau}{\pi\gamma} \cdot \frac{r|t|}{R^2}. \quad (17.6)$$

We approximately replace the mapping function by the complex potential of field of charges on contacts on an unlimited model

$$\Omega(z) = -i \frac{\tau}{2\pi\gamma} \ln \frac{z - r}{z + r} = -i \frac{\tau}{2\pi\gamma} \ln \frac{\frac{z}{r} - 1}{\frac{z}{r} + 1}. \quad (17.7)$$

At point t of contour L we define the modulus of this quantity

$$|\Omega(t)| = \frac{\tau}{2\pi\gamma} \left| \ln \frac{1 - \frac{t}{r}}{1 + \frac{t}{r}} \right| \approx \frac{\tau}{\pi\gamma} \frac{|t|}{r}. \quad (17.8)$$

The relative error introduced by the outer contour of the model at point t equals

$$\delta = \frac{|\Delta\Omega(t)|}{|\Omega(t)|} \approx \frac{r^2|t|}{R^2|t|} = \frac{r^2}{R^2}. \quad (17.9)$$

So that this error will be less than 1% it is necessary that the radius of the outer contour of the model be more than

$$R_1 = \frac{r}{\sqrt{0.01}} = 10r. \quad (17.10)$$

This error can be eliminated without increasing the dimensions of the model. For this it is sufficient to perform a double transformation: analytically with the help of function $\zeta = \frac{R^2}{z}$ to map region D, external to contour L, onto internal region region D_1 limited by new contour L_1 then the conformally transform region D_1 onto an infinite band by modeling on a model of a conducting sheet. For this is selected inside contour L a point in which is considered $z = 0$. Expediently this point is selected in such a manner so that circumference of radius with center at this point coincides as near as possible with contour L. As was noted, with the help of function $\zeta(z) = \frac{R^2}{z}$ region D, external to circuit contour L, is mapped onto region D_1 , bounded by contour L_1 (Fig. 16b). Here point $z = \infty$ shifts to point $\zeta = 0$. From a conducting sheet is cut a model in the form of region D_1 . To two, remote from each other, sections of the model contour are soldered contacts in the form of round washers of small diameter and a direct current passed through the model. The complex potential of field of current in the model $W(\zeta) = W\left(\frac{R^2}{z}\right)$, considered as a function of points z of region D, will be a function conformally mapping region D onto an infinite band of width $h = \frac{1}{\gamma}$ and translating point

$z = \infty$ to point $\Omega_0 = J_0 + iU_0$.

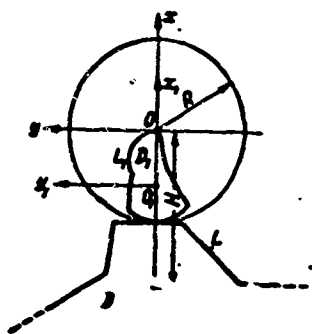


Fig. 17.

By the same method, applying preliminary inversion with respect to a circle of radius R, is modeled a conformal mapping of semi-infinite region D with assigned boundary L (Fig. 17). For this semi-infinite region D with boundary L of plane (z) is converted to limited singly-connected region D_1 with boundary L_1 of plane ζ by simple inversion with respect to a circle of radius R [39]:

$$\zeta = \frac{R^2}{z} + \frac{R^2}{H}; \quad z = \frac{R^2}{\zeta - \frac{R^2}{H}}. \quad (17.11)$$

Here end-point $z = \infty$ passes to end-point $\zeta = R^2/H$ and internal point $z = -H$ of region D passes to internal point of region D_1 coinciding with origin of coordinates $\zeta = 0$. The indicated transformation is conformal and in order to find the conformal mapping of semi-infinite region D onto a band of width h it is now sufficient to determine the conformal mapping of region D_1 onto an infinite band.

§ 18. Determination of Constants of the Christoffel Formula
for Region Bounded by a Closed, Nonintersecting
Broken Line

By the presented method of simulation of conformal transformation easily can be found the constants of the Christoffel-Schwarz formula both for internal and also for external regions [20].

Let us assume attempt to find an expression for a function conformally mapping the upper half-plane onto the interior of polygon L. For this from a conducting sheet will be cut a model in the form of region D (Fig. 18) and at two remote angles z_1 and z_m to it are joined contacts in the form of washers of small diameter. Through model is passed a direct current and determined the potentials U_k of angular points z_k of contour of region D in fractions of total potential drop U_N between contacts of the model. Let us assume that they are equal, respectively, to $U_2, U_3, \dots, U_{m-1}, U_{m+1}, \dots, U_n$. With the help of function $\zeta = \xi + i\eta = e^{\pi/h \cdot \Omega}$ we map band of width h on upper half-plane (ζ). Let us designate constant $e^{\pi/h} = a$ and then $\zeta = a^\Omega$. Angular points of the contour of region D z_2, z_3, \dots, z_{m-1} (Fig. 18) after mapping onto a band will correspond to the point with coordinates $(U_k, 0)$, lying on lower bound of the band. By these points on the boundary of the upper half-plane will correspond to points with coordinates $a^{\Omega_2} = a^{U_2}, a^{\Omega_3} = a^{U_3}, \dots, a^{\Omega_{m-1}} = a^{U_{m-1}}$ (Fig. 19). Angular points z_{m+1}, \dots, z_n on the band will correspond to points with coordinates (U_k, h) , lying on the upper boundary of the band. On the boundary of the upper half-plane they will correspond to points with coordinates

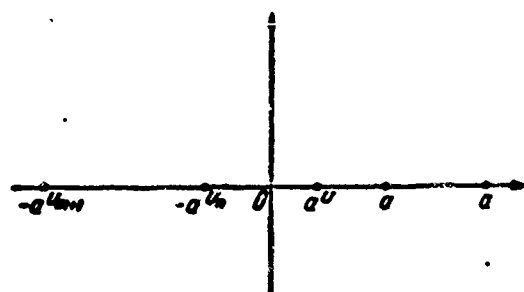
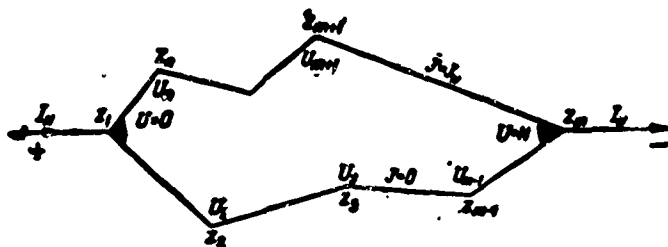
$$a^{\Omega_{m+1}} = a^{U_{m+1} + ih} = -a^{U_{m+1}}, \dots, a^{\Omega_n} = -a^{U_n}.$$

Angular points z_1 and z_2 potentials of which must be $U_1 = -\infty$ and $U_m = +\infty$ on band will correspond to points $\Omega_1 = -\infty$ and $\Omega_m = +\infty$. On the boundary of the upper half-plane they will correspond to points with coordinates

$$a^{\Omega_1} = a^{-\infty} = 0 \quad \text{and} \quad a^{\Omega_m} = a^{+\infty} = \infty.$$

Placing these coordinates in the Christoffel formula we obtain an expression for the function conformally mapping the upper half-plane onto region

$$Z(\Omega) = c \int \tau^{\alpha-1} (\tau - a^{U_2})^{\alpha_2-1} \dots (\tau - a^{U_{m-1}})^{\alpha_{m-1}-1} (\tau + a^{U_{m+1}})^{\alpha_{m+1}-1} \dots \\ \dots (\tau + a^{U_n})^{\alpha_n-1} d\tau. \quad (18.1)$$



Here $\alpha_1, \alpha_2, \dots, \alpha_n$ are angles between neighboring segments of the broken line in fractions of π , $a = e^{\pi/h}$; ζ the coordinate of the point of the upper half-plane; $z(\zeta)$ the coordinate of its corresponding point in region D.

If an expression for function conformally mapping the upper half-plane onto the exterior of polygon L is sought then we proceed in the following way.

1. Region D, external to polygonal contour L, with the help of function $\zeta = \frac{R^2}{z}$ is mapped onto region D_1 bounded by contour L_1 . Point $z = \infty$ will, in this case, go to point $\zeta = 0$ (Fig. 20a, b).

2. Region D_1 is mapped onto an infinite band of width h by means of modeling. Assume that the contacts are attached to the model on sections of contour ξ_n, ξ_1 and ξ_m, ξ_{m+1} , corresponding to sides z_n, z_1 and z_m, z_{m+1} of the polygon. On section of contour of model $\xi_1, \xi_2, \dots, \xi_m$ we take J equal to zero and on section ξ_n, ξ_1 potential of contact J also equal to zero. Then during

transformation points $\zeta_1, \zeta_2, \dots, \zeta_m$, corresponding to angular points of the polygon z_1, z_2, \dots, z_m will go to points U_1, U_2, \dots, U_m , lying on the lower boundary of band $J = 0$, points $\zeta_{m+1}, \dots, \zeta_n$ will go into points $(U_{m+1} + ih), \dots, (U_n + ih)$, lying on the upper boundary of the band, points $\zeta = 0$, corresponding to point $z = \infty$, will go to point $\Omega_0 = U_0 + iJ_0$ (Fig. 20c)

3. The band on the upper half-plane is mapped with the help of function $\zeta(\Omega) = e^{\frac{\pi}{h}\Omega}$ (Fig. 20). After mapping onto the boundary of the upper half-plane angular points of the contour L z_1, z_2, \dots, z_m will correspond to points with coordinates $-e^{\frac{\pi}{h}U_{m+1}}, -e^{\frac{\pi}{h}U_{m+2}}, \dots, -e^{\frac{\pi}{h}U_n}$, angular points $z_{m+1}, z_{m+2}, \dots, z_n$ will correspond to points with coordinates $-e^{\frac{\pi}{h}U_{m+1}}, -e^{\frac{\pi}{h}U_n}$. Point $z = \infty$ will correspond to point $\zeta_0 = e^{\frac{\pi}{h}\Omega_0}$. Substituting these values into the Christoffel formula we obtain an expression for the function conformally mapping the upper half-plane onto region D and translating point ζ_0 into an infinity distant point

$$z(\zeta) = c \int \frac{(\tau - a^{U_1})^{\alpha_1-1} (\tau - a^{U_2})^{\alpha_2-1} \dots (\tau - a^{U_m})^{\alpha_m-1} \times (\tau + a^{U_{m+1}})^{\alpha_{m+1}-1} \dots (\tau + a^{U_n})^{\alpha_n-1} d\tau}{(\tau - a^{\Omega_0})^2 (\tau - a^{\bar{\Omega}_0})^2} \quad (18.2)$$

Here $a = e^{\frac{\pi}{h}}$, $h = \frac{I}{\gamma}$, I is the current through the mod 1 of region D_1 ; $\alpha_1, \alpha_2, \dots, \alpha_n$ - external angles of the polygon measured in fractions of π ; U_1, U_2, \dots, U_n - potentials of points of model corresponding to angular points of polygon measured with respect to the contact where it is assumed $U = 0$.

§ 19. Modeling of a Function Infinite-Sheetly, Conformally Mapping a Bicoupled Region Onto a Band

Let there be given a bicoupled region $D = D_1 + D_2$ having one or several axes of symmetry (Fig. 21) and it is being required to find a function carrying out infinite-sheet conformal mapping of region D onto an infinite band. As was shown in §12, this function is determined by the constant values of its imaginary part on contours of the region. Let us prepare from a conducting sheet a model in the form of region D' equal to half of region D over the left side of the axis of symmetry. We realize contact along segments ab and de of the cut of region D and connect the model to a direct current circuit. Let us consider the field of current in the model. The magnitude of current I flowing through any line connecting point M of D with section δM of the contour, divided by the

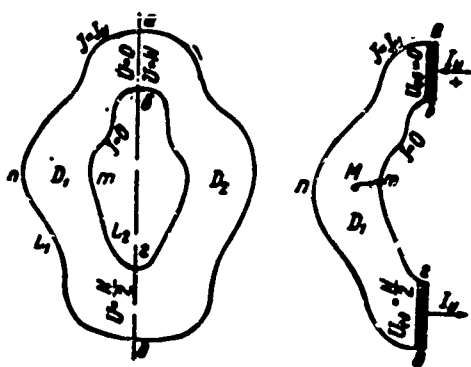


Fig. 21.

conductivity of a unit surface of the sheet γ , is equal to the function of current J at point $M \left(J = \frac{I}{\gamma} \right)$. The magnitude of voltage between point M and contact ab , on which is assumed $U = 0$ will be equal to potential of point M . From continuity of the normal component of current density δ_n on the model contour it follows that $\delta_n = 0$ and $\delta = \delta_t$, i.e., the model contour coincides with lines of current

$J = \text{const.}$ In other words, the imaginary part of analytic function Ω on contour section am is constant and equal to h : $J = \frac{I_N}{\gamma} = h$. On contour section bm , $j = 0$. Let us take the scale of potential such that the potential of contact rd equals $U_{rd} = \frac{N}{2}$ units. Let us assume that we performed the same experiment with a model in the form of region D'' (with the right side of region D) then considering, as in the first experiment, contact potential rd $U_{rd} = \frac{N}{2}$ and on section of internal contour $J = 0$, we obtain, considering the former direction of current, the potential of contact ab $U_{ab} = \frac{N}{2} + \frac{N}{2} = N$ and on section of external contour $J = h$. Due to symmetry the value of $\frac{\partial U}{\partial n}$ at the point of contact rd on model D' equals the value of $\frac{\partial U}{\partial n}$ at the same point of contact rd on model D'' . Assuming that $\frac{\partial U}{\partial n} = \frac{\partial J}{\partial t}$, we obtain that at points of intersection rd with both sides of the of the cross section of the function $\Omega = U + iJ$ coincide and, consequently, Ω can be extended from D' into D'' , i.e., D' and D'' may be electrically connected along rd after such connection of the field in models D' and D'' no longer changed.

Let us consider section ab . Due to symmetry of values of J on both sides of the section also coincide, values of U are different. On the side D' , $U = 0$ on the side D'' $U = N$, i.e., during passage along internal (or external) contour real part U of function Ω undergoes an increase equal to N units. We take still according to the example models D'_1 , and D''_1 and combine them with the first examples D' and D'' in such a manner so that model D''_1 falls under D'' and D'_1 falls on D' . We connect electrically along sections ab , D' with D''_1 and D'_1 with D'' , then, passing to section rd , we obtain on D''_1 $U_{rd} = \frac{N}{2}$ on D'_1 $U_{rd} = \frac{3}{2} N$.

Continuing such an operation an infinite number of times we obtain an infinite number of electrically united examples of models of region D superimposed one on the other. In other words, function Ω in region D is infinitely valued with a real period N. Assuming what values of the imaginary part of this function on the external L_1 and internal L_2 contours are constant and equal $J = h$ and $J = 0$ we conclude that function $\Omega = U + iJ$ — the complex potential of the field of direct current in the model — will be sought.

Let us turn to simulation of a mapping function for a bicoupled asymmetrical region [30].

Let us consider region D, limited by two contours L_1 and L_2 . Let contour L_1 embrace contour circuit L_2 . As is known, function $\Omega = v + iJ$, infinite-sheetly conformally mapping region D onto a band of width h, is defined in D by the following limiting values of its imaginary part on contours of the region:

$$\text{on } L_1 \ J = h, \text{ on } L_2 \ J = 0. \quad (19.1)$$

For brevity we shall call Ω simply a mapping function.

Mapping function Ω can be modeled with a complex potential of field of current in a model prepared in the form of region D from a conducting sheet. With the help of contacts in the form of contours L_1 and L_2 made from material with conductivity γ_k many times greater than the conductivity γ of the sheet and connected to the model along L_1 and L_2 , we connect the model to a source of direct current. Through the model will flow a direct current whose field will be characterized by analytic function $\Omega_1 = v_1 + iJ_1$, a complex potential, where

$$\text{on } L_1 \ v_1 = v_{N_1} \text{ and on } L_2 \ v_1 = 0. \quad (19.2)$$

From comparison of (10.2) with (19.1) one may see that for function Ω_1 on the boundary is determined real part and for function Ω — correspondingly the imaginary part. Consequently, Ω and Ω_1 will be orthogonal where v_1 corresponds to J and J_1 corresponds to v .

As can be seen, the problem of simulation of a mapping function for doubly connected region D in principle is solved very simply. In practice however the matter is complicated by the fact that measurement of values of complex potential Ω at points of the model is hampered. Simulation of a mapping function by complex

potential Ω_1 permits simply measuring in every point of region D only magnitude v_1 , corresponding to imaginary part J mapping function Ω , and to find only one coordinate of point Ω on the band corresponding to point z in region D. The problem could be solved constructing the second model in the form of region D and assigning to function Ω_2 boundary conditions (19.1), in which h is connected with v_{N1} in (19.2), so that functions Ω_2 and Ω_1 are not only orthogonal but also have identical scales. This would be easy to carry out if we knew the position of at least one line $J_1 = \text{const}$ of the field of current Ω_1 on the model. Then having cut the model along this line (first removing contacts on L_1 and L_2) and joining both sides of the cut contacts prepared in the form of the line of cut it would be possible to pass through the model a direct current whose field is characterized by the function Ω .

If region D has an axis of symmetry then it is known beforehand that the cut must be made on the segment of this axis between L_1 and L_2 since on the indicated segment $J_1 = \text{const}$, consequently, $v = \text{const}$ also. On such a model is measured the real part v of mapping function Ω , after which function Ω may be defined inasmuch as its imaginary part w measured on the first model. If, however, there is no axis of symmetry the line $J_1 = \text{const}$ cannot be found precisely and, consequently, it is impossible to model the mapping function Ω in region D. In the literature is described a method of constructing lines $J_1 = \text{const}$ as follows: With the help of contacts of great conductivity there are applied to each of contours L_1 and L_2 of a model made in the form of region D_1 , constant potentials v' and v'' . Then with a probe connected through a measuring instrument to one of the contacts are plotted a number of equipotential lines and then is constructed a line normal to them, taking it as the line $J_1 = \text{const}$. The accuracy of construction by this method obviously depends on subjective peculiarities of the performer and an appraisal of error of such a construction cannot be calculated.

Let us consider in principle an excellent method of determination of line $v = \text{const}$ mapping function $\Omega = v + iJ$ in two-connected region D.

Let us take region D, bounded by external L_1 and internal L_2 contours. We prepare from a conducting sheet a model in the form of region D and make a cut along straight line ab connecting L_1 and L_2 (Fig. 22). To both sides of cut ab we attach contacts, preparing them from a material whose conductivity γ_k is much greater than the conductivity of the sheet γ . We pass through the model a direct

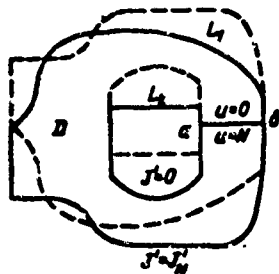


Fig. 22.

current. Complex potential of field of current in the model $\Omega' = u + J'$ will be a function carrying out conformal mapping of region D with cut ab onto a rectangle bounded by straight lines $J' = 0$, $u = 0$, $J' = h$ and $u = N$ (Fig. 23). It is not

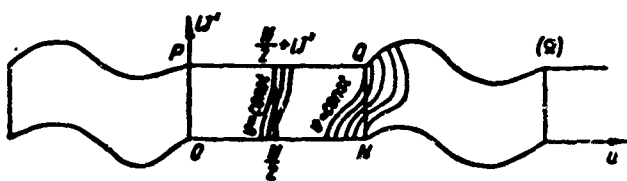


Fig. 23.

difficult to show that although the imaginary part of function Ω' takes constant values $J' = 0$ and $J' = h$ on contours of the region L_1 and L_2 , Ω' will not equal the mapping function $\Omega = v + iJ$.

Indeed, boundary conditions for Ω' in region D with a cut are equal to boundary conditions for Ω since the cut was made arbitrarily and does not coincide with line $v = \text{const}$. Continuing symmetrically function Ω' through line of cut ab we notice that contours of neighboring (from above and from below) sheets of the Riemannian surface, being the domain of definition of function Ω' do not coincide with the contour of region D (Fig. 22, dotted line) and, consequently, values of the imaginary part J' function Ω' at points of contours L_1 and L_2 on neighboring sheets of the Riemannian surface will not be constant and equal to $J' = 0$ and $J' = h$. Hence one may see that function Ω' maps D not onto a band but onto a region limited by two nonintersecting curves passing periodically in segments of parallel lines (Fig. 23).

Making arbitrary cut ab (Fig. 22) we intersected line $v = \text{const}$ of sought function Ω with the line of cut. Obviously the divergence of functions Ω' and Ω is bigger the greater the divergence between the line of cut $u = \text{const}$ and the lines $v = \text{const}$. The latter may be characterized by the maximum value of derivative $\frac{\partial v}{\partial l}$ on the line of cut (dl - element of line of cut).

In actuality $\frac{\partial v}{\partial l} = |\text{grad } v| \sin \theta$ is proportional to the sine of angle θ between tangents to the lines $v = \text{const}$ and $u = \text{const}$ at their point of intersection. At the limit where $\theta = 0$ $\frac{\partial v}{\partial l} = 0$ both the line $v = \text{const}$ and $u = \text{const}$ coincide. Due to conformity mapping onto plane Ω' of the angle between lines $v_{\Pi} = \text{const}$ and $u = \text{const}$ at their points of intersection is everywhere preserved (v_{Π} designates the value of v on Π in Ω). Taking into account the fact that on plane Ω' element dl will correspond to element dJ' , we conclude that divergence between the lines $v_{\Pi} = \text{const}$ and the straight line $u = \text{const}$ may also be characterized by the maximum value of derivative $\frac{\partial v_{\Pi}}{\partial J'} = |\text{grad } v_{\Pi}| \sin \theta$. At the limit where $\theta = 0$ $\frac{\partial v_{\Pi}}{\partial J'} = 0$ the lines $v_{\Pi} = \text{const}$ convert to straight lines $u = \text{const}$.

Let us show that the greatest divergence between lines $v_{\Pi} = \text{const}$ and the line $u = \frac{N}{2}$, intersecting them is less than the biggest divergence between lines $v_{\Pi} = \text{const}$ and the line intersecting them, $u = N$ (or $u = 0$). Really the boundary conditions for Ω' on contours L_1 and L_2 coincide with boundary conditions of the sought function

$$\frac{\partial J}{\partial t} = \frac{\partial J'}{\partial t} \quad \text{or} \quad \frac{\partial v}{\partial n} = \frac{\partial u}{\partial n}, \quad (19.3)$$

in other words the lines $v = \text{const}$ and $u = \text{const}$ intersect contours L_1 and L_2 at right angles. On plane Ω' L_1 and L_2 will be converted into straight lines $J' = J_N$ and $J' = 0$, and element normal to them dn into element dJ' . Consequently, on plane Ω' we have $\frac{\partial v_{\Pi}}{\partial J'} = 0$ on both straight lines $J = J_N$ and $J = 0$.

Let us assume that the greatest divergence between line $u = N$ and lines $v_{\Pi} = \text{const}$ intersecting it will equal $\left[\frac{\partial v_{\Pi}}{\partial J'} \right]_{\text{max}} = m$, then on the entire contour of rectangle $OPQN$ (Fig. 23) into which will be transformed region D with cut ab , values of the quantity $\frac{\partial v_{\Pi}}{\partial J'}$ will be determined. But $\frac{\partial v_{\Pi}}{\partial J'}$ in the rectangle is a harmonic function (real part of analytic function $\frac{d\Omega_{\Pi}}{d\Omega'} = \frac{\partial v_{\Pi}}{\partial J'} + i \frac{\partial J_{\Pi}}{\partial J'}$) and consequently, can be determined within the rectangle by its own values on its contour.

Let us estimate the biggest magnitude of divergence $\left[\frac{\partial v_{\Pi}}{\partial J'} \right]_{\text{max}}$ on the line $u = \frac{N}{2}$. For this we map the rectangle onto the upper half-plane $\zeta = x + iy$ in such a manner so that point $\Omega' = \frac{N}{2}$ goes to point $\zeta = 0$, point $\Omega' = \frac{N}{2} + iJ_N$ passes to

point $\zeta = \infty$, and point $\Omega = N$ to point $\zeta = 1$. Then on boundary of upper half-plane segment $\left[0, \frac{N}{2}\right]$ will pass to segment $[-1, 0]; \left[\frac{N}{2}, N\right]$ - to segment $[0, 1]$. Segments OP and NQ, will become respectively $\left[-1, -\frac{1}{k}\right]$ and $\left[1, \frac{1}{k}\right]$, the remaining part of the real axis will correspond to segment PQ. Here the line $u = \frac{N}{2}$ will correspond to imaginary axis $\varepsilon = 0$ (Fig. 24).

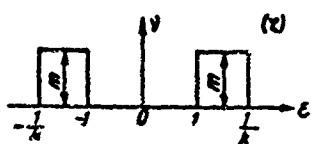


Fig. 24.

At corresponding points of the rectangle and the upper half-plane values of function $\left[\frac{\partial v_n}{\partial J'}\right]$ will be retained.

Let us estimate the greatest value of $\left[\frac{\partial v_n}{\partial J'}\right]_{\max}$ on the

axis $\varepsilon = 0$ corresponding to the line $u = \frac{N}{2}$, increasing a fortiori the divergence on line $u = 0$ ($u = N$) taking it constant and equal to the greatest value of m . Applying the integral of Poisson for the upper half-plane we have

$$\begin{aligned} \left[\frac{\partial v_n}{\partial J'}\right](0, v) &\leq \frac{1}{\pi} \int_{-\frac{1}{k}}^{-1} m \frac{v d\xi}{\xi^2 + v^2} + \frac{1}{\pi} \int_1^{\frac{1}{k}} m \frac{v d\xi}{\xi^2 + v^2} = \\ &= \frac{m}{\pi} \left[\operatorname{arctg} \frac{\xi}{v} \Big|_{-\frac{1}{k}}^{-1} + \operatorname{arctg} \frac{\xi}{v} \Big|_1^{\frac{1}{k}} \right] = 2 \frac{m}{\pi} \left[\operatorname{arctg} \frac{1}{kv} - \right. \\ &\left. - \operatorname{arctg} \frac{1}{v} \right] = 2 \frac{m}{\pi} \operatorname{arctg} \frac{\left(\frac{1}{k} - 1\right)v}{v^2 + \frac{1}{k}} = 2 \frac{m}{\pi} \operatorname{arctg} \frac{(1-k)v}{kv^2 + 1}. \end{aligned} \quad (19.4)$$

For $v = 0$ and $v = \infty$ this magnitude is equal to zero and, consequently, on the axis $\varepsilon = 0$ has a maximum. Let us take the derivative of argument $\frac{(1-k)v}{kv^2 + 1}$ with respect to v and equate it to zero

$$\frac{\left(\frac{1}{k} - 1\right)\left(v^2 + \frac{1}{k}\right) - \left(\frac{1}{k} - 1\right)2v^2}{\left(v^2 + \frac{1}{k}\right)^2} = 0, \quad (19.5)$$

whence

$$v^2 = \frac{1}{k} \text{ and } v = \pm \sqrt{\frac{1}{k}}.$$

Consequently, maximum value $\left[\frac{\partial v_n}{\partial J'} \right]_{u=\frac{N}{2}}^{\max}$ on line $u = \frac{N}{2}$ will be

$$\left[\frac{\partial v_n}{\partial J'} \right]_{u=\frac{N}{2}}^{\max} \leq \frac{2}{\pi} m \operatorname{arctg} \frac{\frac{1}{k} - 1}{2\sqrt{\frac{1}{k}}} = \frac{2}{\pi} m \operatorname{arctg} \frac{1-k}{2\sqrt{k}}, \quad (19.6)$$

where by condition

$$0 < k < 1. \quad (19.7)$$

Let us determine the value of k , at which $\left[\frac{\partial v_n}{\partial J'} \right]_{u=\frac{N}{2}}^{\max} = m$. Obviously this will be under the condition

$$\operatorname{arctg} \frac{1-k}{2\sqrt{k}} = \frac{\pi}{2}, \quad (19.8)$$

or

$$\operatorname{tg} \frac{\pi}{2} = \frac{1-k}{2\sqrt{k}} = \infty \text{ or } k = 0.$$

Thus with any ratio of sides of the rectangle $\frac{J_N}{N}$ the maximum value of $\left[\frac{\partial v_n}{\partial J'} \right]_{u=\frac{N}{2}}^{\max}$ will be less than the maximum value of $\left[\frac{\partial v_n}{\partial J'} \right]_{u=N}^{\max} = m$. Hence we conclude that for any two-connected region D the divergence between lines $v = \text{const}$ and $u = \frac{N}{2}$ is always smaller than the divergence between lines $v = \text{const}$ and $u = N (u = 0)$.

Example 1. Let us assume that the ratio between sides N and J_N of a rectangle on plane Ω' equals two. The function depicting on the rectangle an annulus with external R and internal r radii, cut along the radius $\theta = 0$, has the form

$$\Omega' = i \ln \frac{z}{r}. \quad (19.9)$$

Point $z_1 = re^{i0}$ it translates to vertex $\Omega'_1 = 0$, point $z_2 = Re^{i0}$ to vertex $\Omega'_2 = i \ln \frac{R}{r} = iJ_N$ and finally point $z_3 = re^{i2\pi}$ to vertex $\Omega'_3 = -2\pi = N$.

The ratio of sides of the rectangle $N = 2J_N$ will correspond to a ratio of radii of the ring

$$\frac{2\pi}{\ln \frac{R}{r}} = 2, \quad \pi = \ln \frac{R}{r},$$

whence $R = re^{\pi} \approx 23r$. On plane ζ after transformation of the rectangle into the upper half-plane in such a manner so that point $\Omega' = \frac{N}{2}$ goes to point $\zeta = 0$ and $\Omega' = \frac{N}{2} + iJ_N$ to point $\zeta = \infty$, vertices of the rectangle will correspond to the point $\frac{1}{k} = \sqrt{2}, 1$ [12]. Hence we obtain

$$\left[\frac{\partial v_n}{\partial J'} \right]_{u=\frac{N}{2}}^{\max} < \frac{2}{\pi} m \operatorname{arctg} \frac{\sqrt{2}-1}{2\sqrt{\sqrt{2}}} = \frac{2}{\pi} m \cdot 0,172 = 0,11m. \quad (19.10)$$

Consequently, at a ratio of radii of the ring $R = 23r$ the biggest possible divergence between lines $v = \text{const}$ and their intersecting line $u = \frac{N}{2}$ is almost 10 times less than the greatest divergence between lines $v = \text{const}$ and their intersecting line $u = N$. With decrease of the ratio of radii of the ring the divergence will decrease.

Example 2. Let us assume a relation of ring radii $R = 2r$. Then for the relation of sides of the rectangle we have

$$\frac{N}{J_N} = \frac{2\pi}{\ln 2} = \frac{2\pi}{0,6931} = 9,07.$$

The function which maps the upper half-plane of plane ζ onto the rectangle has the form

$$\Omega = A \int_0^{\zeta} \frac{d\zeta}{V(1-\zeta^2)(1-k^2\zeta^2)}. \quad (19.11)$$

The ratio of sides of the rectangle $\frac{N}{J_N}$ corresponds to the ratio of full elliptic integrals [23]

$$\frac{2K}{K'} = \frac{N}{J_N} = 9,07, \quad (19.12)$$

where

$$K = \int_0^1 \frac{d\zeta}{V(1-\zeta^2)(1-k^2\zeta^2)}, \quad K' = \int_0^1 \frac{dt}{V(1-t^2)(1-k_1^2 t^2)}, \quad (19.13)$$

$$k_1^2 = 1 - k^2.$$

The greatest value of ratio $\frac{2k}{k'}$, available in tables of elliptic integrals and equal to $\frac{2.4841}{1.571} = 6.16 < 9.07$, corresponds to values $k^2 = 0.999$ and $k_1^2 = 0.001$.

Consequently,

$$1 > k^2 > 0.999, \quad k > 0.9995, \quad \frac{1}{k} < 1.0005.$$

Hence for a maximum possible magnitude of divergence between lines $v = \text{const}$ and the line intersecting it $u = \frac{N}{2}$ we obtain

$$\left[\frac{\partial v}{\partial r} \right]_{\frac{N}{2}}^{\text{max}} < \frac{2}{\pi} m \operatorname{arctg} \frac{1.0003 - 1}{2\sqrt{1.0005}} < \frac{2}{\pi} m \operatorname{arctg} 0.0003 = 0.0002m. \quad (19.14)$$

In Fig. 25 is given a picture of the lines $v = \text{const}$ and $u = \text{const}$ on a model cut in the form of an annulus with the ratio $\frac{R}{r} = 2$. Here the line of contact

$u = 0$ and $u = N$ coincides with the tangent to the internal circumference of the ring, i.e., the divergence on the line of contact is the highest possible. From the given picture of lines $v = \text{const}$ and $u = \text{const}$ one may see that already at $u = 0.2N$ divergence is practically absent.

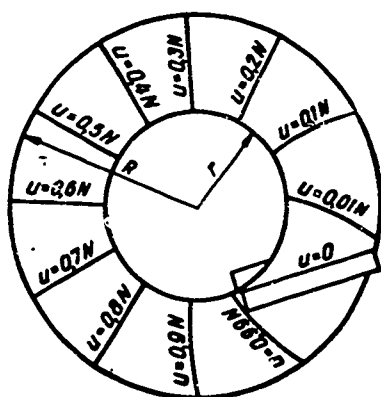


Fig. 25.

Thus, in order to model mapping function Ω in a two-connected region and to measure its value at any point it is necessary to assign constant potentials with help of contacts on contours of the region L_1 and L_2 and to measure the value of v_1 at all points of interest during calculation.

Then on another model of region D, similar to the first but without contacts, along L_1 and L_2 make a cut along a line approximately corresponding to the line $J' = \text{const}$. To both sides of the cut join contacts prepared in the form of the line of cut and pass a direct current through the model. Measuring N and J_N , calculate the highest possible divergence between lines $v = \text{const}$ and $u = \frac{N}{2}$. If magnitude of divergence does not exceed the permissible error then line $u = \frac{N}{2}$ is taken for the line $u = \text{const}$ and, making on the new model a cut along this line, constant potentials are applied to it by contacts. If however, magnitude of divergence exceeds the

permissible coinciding with line $u = \frac{N}{2}$ on the previous model, etc., so long as the divergence is greater than the permissible error.

In final analysis modeling of the mapping function is produced on two models of identical dimension prepared from one and the same conducting sheet. On the first model contacts are connected to contours L_1 and L_2 on the second — to the shores of a cut along the line corresponding to the line $J_1 = \text{const}$ of the first model and contours L_1 and L_2 free from contacts. On the first model with the help of a null-galvanometer, connected as a potentiometer, the family of lines $v_1 = \text{const}$ corresponding to the lines $J = \text{const}$ mapping the function Ω is plotted. Here a magnitude of interval Δv_1 between neighboring lines $v_1 = \text{const}$ is given. On the second model is plotted the family of lines $v = \text{const}$ also at a defined interval Δv between neighboring lines.

Let us consider under what conditions the real and imaginary components of mapping function Ω onto both models will be measured in the same scale.

Let us assume that on the first model the voltage applied to contacts along L_1 and L_2 equals U_N , the current through the model is I_N and the dc resistance of model is r . According to Ohm's law we have

$$u_N = I_N r, \quad \frac{I_N}{Y} = J_N. \quad (19.15)$$

Let us assume that now on the second model with contacts along the sides of line $J_1 = \text{const}$ the voltage between contacts equals v_N , the current through the model is I_N and the resistance of model R . According to Ohm's law

$$v_N = I_N R, \quad \frac{I_N}{Y} = J_N. \quad (19.16)$$

For coordination of scales of quantities v and J on both models it is necessary so that the magnitude of u_N of the first model equal the magnitude of J_N of the second model and, conversely, the magnitude of v_N of the second model equal to the magnitude of J_N of the first model, i.e.,

$$u_N = J_N = \frac{I_N}{Y} \text{ and } v_N = J_N = \frac{I_N}{Y}. \quad (19.17)$$

Substituting (19.15) and (19.16) in (19.17), we obtain

$$I_N r = \frac{v_N}{Y R} = v_N Y r.$$

whence

$$r = \frac{1}{\gamma R}, \quad u_N = \frac{v_N}{\gamma R}, \quad l_N = \frac{I_N}{\gamma r}. \quad (19.18)$$

Let the magnitude of v_N on the second model be taken equal to N units

$$v_N = N. \quad (19.19)$$

then the magnitude of u_N on the first model must be set equal to

$$u_N = \frac{N}{\gamma R} = N\gamma r. \quad (19.20)$$

Under conditions (19.19) and (19.20) the family of lines $v_1 = \text{const}$ on the first model and $v = \text{const}$ on the second model, built through the identical interval $\Delta v_1 = \Delta v$, in totality form a grid of orthogonal lines every cell of which is a curvilinear square.

The grid of orthogonal lines with square cells are on the constructed models thus:

1. Parallel to the second model to its contacts is connected a resistance of $N \Omega$. With the help of probe and null-galvanometer connected to the slider of this resistor, the lines $v = \text{const}$ are plotted. When plotting the k -th line $v = k$ the cursor is placed in such a manner so that the ratio of resistance branches equalled $k : (N - k)$. The following $(k + 1)$ -th line is plotted, preliminarily shifting the slider 1Ω and establishing a branch ratio of $(k + 1) : (N - k - 1)$, etc.

2. Parallel to contacts of the first model is connected a resistance equal to $N_1 = N\gamma r \Omega$, and as in the first case, the lines $v_1 = \text{const}$ corresponding to lines $J = \text{const}$ of the second model are plotted, moving the slider 1Ω for the construction of each subsequent following line.

For measurement of N_1 and J_N from the same sheet as the model is prepared a strip of length l and width h ($l \approx 10h$), to the ends of which are soldered copper contacts. Both models and the strip are connected in series and connected in a circuit of direct current I . A compensator is used to measure the magnitude of voltages u_N , v_N and v_{II} between contacts of the first model, the second model and the strip respectively. Then N_1 and J_N are calculated from the relationships:

$$J_N = \frac{I}{\gamma} = \frac{N}{R\gamma}, \quad \gamma = \frac{II}{v_N h}, \quad R = \frac{v_N}{I}, \quad J_N = \frac{N h \eta_{II}}{l v_N}. \quad (19.21)$$

$$N_1 = N\gamma r = N \frac{l}{v_n h} \cdot \frac{u_N}{l} = N \frac{l u_N}{h v_n}, \quad N_1 = N \frac{l u_N}{h v_n}. \quad (19.22)$$

Obviously mapping function Ω may be considered as the complex potential of an electrostatic field in a region bounded by two conducting cylindrical surfaces L_1 and L_2 . In this case grid of orthogonal lines will be constructed by the method outlined depict the electrostatic field of a cylindrical capacitor. Lines $J = \text{const}$ ($v_1 = \text{const}$) will correspond to equipotential lines of the field, lines $v = \text{const}$ to lines of force.

CHAPTER III

CALCULATION OF ELECTRICAL AND MAGNETIC FIELDS WITH THE HELP OF SIMULATION OF CONFORMAL MAPPING

§ 20. Calculation of the Field of a Charged Conductor

Calculation of the field of an isolated charged cylindrical conductor reduces to the solution of the Dirichlet problem for a function analytic everywhere outside the conductor except at an infinitely distant point where the function has a logarithmic singularity. The sought field may be modeled by a field of current in a conducting sheet, however, so that the simulation be sufficiently accurate it is necessary to form the external contour of model in the shape of a circle, with a bus of high conductivity soldered to it, and a radius 5-6 times greater than the biggest overall dimension of the conductor cross section. When the radius of the outer contour of the model is small it will strongly distort field of current in it. To the outer contour circuit of the model, being the contour of the conductor cross section, is also soldered a bus of high conductivity and between the buses in passed a direct current. The model becomes bulky and complicated in manufacture. Applying conformal mapping it is possible to simplify the model and to eliminate the distortion introduced by the outer contour.

Let us assume that the cross section of a cylindrical conductor with charge τ per unit length is limited by contour L . Complex potential of electrostatic field $\Phi(z)$ at infinity has a logarithmic singularity equivalent to the presence, a charge $-\tau$ of reverse sign. Let us depict region D external to contour L on the upper half plane of Ω with the help of conformal mapping $\Omega(z) = \mu + i\nu$. Contour L

with constant value of potential on it will be converted into the real axis $v = 0$, point $z = \infty$ with charge $-\tau$ will cross into point $\Omega_0 = \mu_0 + i\nu_0$. The complex potential of a charged filament-conducting plane system is written thus:

$$\Phi_1(\Omega) = i \frac{\tau}{2\pi\epsilon} \ln \frac{\Omega - \Omega_0}{\Omega - \bar{\Omega}_0}. \quad (20.1)$$

If the mapping function is known in placing it in formula (20.1), we obtain the sought field

$$\Phi(z) = \Phi_1[\Omega(z)].$$

In the general case we do not know an expression for the function $\Omega(z)$ however, this function can be found by modeling as follows.

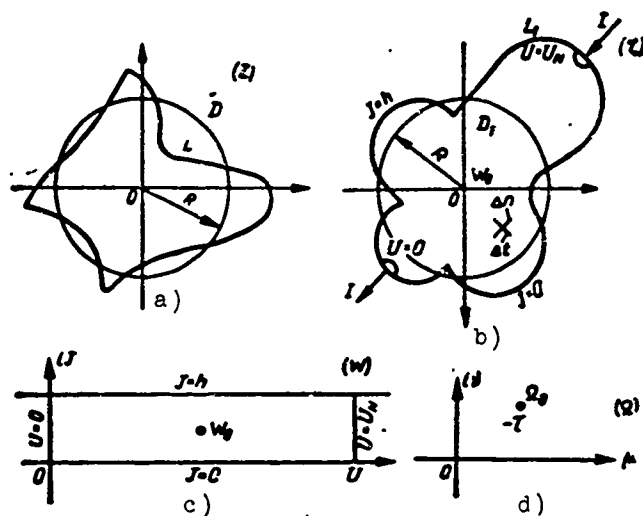


Fig. 26.

1. At any internal point of the cross section of the cylinder let us set $z = 0$. Point $z = 0$ is conveniently selected in such a manner so that a circle of radius R with its center at this point will as nearly as possible coincide with contour L (Fig. 26a).

2. Let us map with the help of function $\zeta = \frac{R^2}{z}$ the region D , external to contour L , onto region D_1 , bound by contour L_1 . Here point $z = \infty$, containing charge $-\tau$, will cross into point $\zeta = 0$ (Fig. 26b).

3. Let us map region D_1 onto an infinite band of width h . We obtain the mapping function by mapping as demonstrated in § 17. Let us cut from a conducting sheet a

model in the form of region D_1 . To two sections of the model contour remote from each other we solder contacts in the form of round disks of small diameter in such a manner so that the center of the disk falls on the contour of the model. We join the clamps from a source of current to the contacts and pass a direct current through the model. The complex potential of the current field in the model $W(\zeta)$ will be a function conformally depicting region D_1 onto an infinite band of width $h = \frac{I}{\gamma}$. Here I is the current through the model. On plane (W) the part of region D_1 , not occupied by contacts will be depicted on a rectangle of width h and length U_N (U_N - voltage between contacts of model). Sections occupied by contacts will be mapped onto two semi-bands supplementing the rectangle to a complete band in both sides.

Let us take the electrical potential of one of the contacts equal to zero ($U_k = 0$) and on the section of contour between contacts the value of the current function also equals zero ($J = 0$) (Fig. 26c). Coordinates of point W_0 may now be measured on the model. For this it is necessary: a) to measure the voltage U_0 between the contact where $U_k = 0$ and the point $\zeta = 0$; b) to measure the magnitude of the function of current J_0 at the point $\zeta = 0$.

4. Let us map, with the help of function $\Omega(W) = e^{\frac{\pi}{h}W}$ the infinite band onto the upper simiplane. During mapping point W_0 with charge $-\tau$ will go to the point

$$\Omega_0 = \mu_0 + i\nu_0 = e^{\frac{\pi}{h}(U_0 + iJ_0)} = e^{\frac{\pi}{h}U_0} \cos \frac{\pi}{h} J_0 + ie^{\frac{\pi}{h}U_0} \sin \frac{\pi}{h} J_0.$$

The upper bound of the band will convert to the negative real semiaxis, the lower bound - to the positive semiaxis (Fig. 26d). The function mapping region D onto the upper half-plane has the form

$$\Omega(z) = \Omega\{W[\zeta(z)]\} = e^{\frac{\pi}{h}W\left(\frac{R}{z}\right)}. \quad (20.2)$$

The complex potential of the sought field of a charged cylindrical conductor equals

$$\Phi(z) = i \frac{\tau}{2\pi\epsilon} \ln \frac{e^{\frac{\pi}{h}W} - e^{\frac{\pi}{h}W_0}}{e^{\frac{\pi}{h}W} - e^{\frac{\pi}{h}W_0}}. \quad (20.3)$$

During calculation of the static field the distribution of normal voltage on the surface of the conductor is of interest. Let us derive the formula for voltage on the surface.

Assuming that there is no tangential component of voltage on the surface of the conductor, we obtain

$$E_n = \left| \frac{d\Phi_1}{d\Omega} \right| \cdot \left| \frac{d\Omega}{dz} \right| = \left| \frac{d\Phi_1}{d\Omega} \right| \cdot \left| \frac{d\Omega}{dW} \right| \cdot \left| \frac{dW}{d\zeta} \right| \cdot \left| \frac{d\zeta}{dz} \right|. \quad (20.4)$$

Let us find the moduli of derivatives and substitute them in formula (20.4). On the real axis

$$\Omega = \mu = \pm e^{\frac{\pi}{h} U}. \quad (20.5)$$

$$\begin{aligned} \left| \frac{d\Phi_1}{d\Omega} \right| &= \frac{\tau}{2\pi\epsilon} \left| \frac{\Omega_0 - \bar{\Omega}_0}{(\Omega - \Omega_0)(\Omega - \bar{\Omega}_0)} \right| = \frac{\tau v_0}{\pi\epsilon[(\mu - \mu_0)^2 + v_0^2]} = \\ &= \frac{\tau e^{\frac{\pi}{h} U_0} \sin \frac{\pi}{h} J_0}{\pi\epsilon \left[\left(\pm e^{\frac{\pi}{h} U} - e^{\frac{\pi}{h} U_0} \cos \frac{\pi}{h} J_0 \right)^2 + e^{\frac{2\pi}{h} U_0} \sin^2 \frac{\pi}{h} J_0 \right]} = \\ &= \frac{\tau e^{\frac{\pi}{h} U_0} \sin \frac{\pi}{h} J_0}{2\pi\epsilon e^{\frac{\pi}{h}(U-U_0)} \left[\operatorname{ch} \frac{\pi}{h} (U - U_0) \mp \cos \frac{\pi}{h} J_0 \right]}, \end{aligned} \quad (20.6)$$

$$\left| \frac{d\Omega}{dW} \right| = \left| \frac{\pi}{h} e^{\frac{\pi}{h} W} \right| = \frac{\pi}{h} e^{\frac{\pi}{h} U}, \quad (20.7)$$

$$\left| \frac{dW}{d\zeta} \right| \approx \left| \frac{\Delta U}{q} \right| = \frac{|\Delta U|}{q}. \quad (20.8)$$

Here ΔU — voltage between needles of a double probe connected to the model contour on both sides of point U , q — distance between needles,

$$\left| \frac{d\zeta}{dz} \right| = \left| \frac{R^2}{z^2} \right| = \frac{R^2}{|z|^2}. \quad (20.9)$$

Substituting these values in formula (20.4) we obtain

$$E_n \approx \frac{\tau R^2 |\Delta U| \sin \frac{\pi}{h} J_0}{2\epsilon h q |z|^2 \left[\operatorname{ch} \frac{\pi}{h} (U - U_0) \mp \cos \frac{\pi}{h} J_0 \right]}. \quad (20.10)$$

Thus, voltage E_n on the surface of a charged cylindrical conductor can be found from a simple sheet model. As an example let us calculate by formula (20.10) the voltage on the surface of a cylinder of circular cross section.

The function conformally mapping a circle of radius R onto a band of width h , has the form

$$W(\zeta) = \frac{h}{\pi} \ln \frac{\zeta - R}{\zeta + R} - i \frac{h}{2}. \quad (20.11)$$

Point $\zeta = 0$ (corresponding to $z = \infty$) translates to the point

$$W_0 = W(0) = \frac{h}{\pi} \ln(-1) - i \frac{h}{2} = i \frac{h}{2}, \quad U_0 = 0, \quad J_0 = \frac{h}{2}. \quad (20.12)$$

On the circle $\zeta = Re^{i\theta}$, $|z|^2 = R^2$

$$\begin{aligned} \frac{|\Delta U|}{q} &= \left| \frac{dW}{d\zeta} \right| = \frac{2Rh}{\pi|\zeta^2 - R^2|} = \frac{2h}{\pi R |\cos 2\theta - 1 + i \sin 2\theta|} = \frac{h}{\pi R \sin \theta}, \\ \operatorname{ch} \frac{\pi}{h} (U - U_0) &= \operatorname{ch} \ln \left| \frac{Re^{i\theta} - R}{Re^{i\theta} + R} \right| = \operatorname{ch} \ln \sqrt{\frac{1 - \cos \theta}{1 + \cos \theta}} = \frac{1}{\sin \theta}. \end{aligned} \quad (20.13)$$

Substituting these values in formula (20.10), we find

$$E_n = \frac{\tau R^2 h \sin \frac{\pi h}{2h} \sin \theta}{2\epsilon h \pi R R^2 \sin \theta} = \frac{\tau}{2\pi \epsilon R}. \quad (20.14)$$

The well known result is obtained.

§ 21. Calculating the Magnetic Field of a DC Machine by Modeling of a Conformal Mapping. Formulation of Problem

During the design of dc electrical machines of especially traction motors, it is desirable to be able beforehand to calculate the distribution of the magnetic field in the air gap of the machine, especially near the commutation zone where the form of the magnetic field very strongly affects machine stability with respect to flashes and circular fire on the commutator.

Of great significance is the distribution curve of the radial component of induction along the circumference of the armature since it conditions the emf

distribution curve between neighboring commutator plates. The latter determines the inherent capability of traction motors to withstand overloads from the point of view of possibility of appearance of circular fire.

For calculation and plotting of operating characteristics of a motor it is necessary to know the magnitude of the working magnetic flux. It is possible to calculate the flux only when the magnetic field in the gap of the machine is defined, in particular if the distribution curve of the radial component induction along circumference of the armature [25] is plotted.

The magnetic field in the air gap of a machine will be considered flat and presented in the form of the superposition of two fields: a) vortex field created by currents in the windings of the machine and not depending on properties of the environment, i.e., such as would occur in the air gap of a machine built from material with a permeance $\mu = \mu_0$, equal to the permeance of air (it is called vortex due to closure of part of the lines of this field within limits of the region of the air gap of the machine and ambiguity of scalar magnetic potential U_m characterizing this field): b) field of magnetization of steel parts of the machine, i.e., such as would be in the air gap of the machine if all its steel parts were made from an absolutely permanent-magnet material and magnetized by working currents of machine, after which currents would be turned off. In § 4 it was shown that this problem can be solved it is known beforehand that the induction inside the magnetic circuit of the machine is small (does not exceed 1 Wb/m^2) and the permeance of the steel can be taken equal to infinity. The magnetic induction B in the air gap of the machine and the scalar magnetic potential U outside the cross section of the windings with current is written thus:

$$\begin{aligned}\bar{B} &= \bar{B}_\delta + \bar{B}_m, \\ U &= U_m + \varphi.\end{aligned}\tag{21.1}$$

where \bar{B}_δ is the component of induction of the vortex field of currents of density δ flowing in the windings; \bar{B}_m is the component of induction of the field of magnetization of steel parts of machine; U_m is the potential of vortex field; φ is the potential of field of magnetization.

Component of induction \bar{B}_δ and potential U_m outside the cross section of

conductors with currents can be found from the following relationships:

$$U_m(x, y) \operatorname{Im}[W_m] = \operatorname{Im} \left[\frac{1}{2\pi} \iint_S \delta \ln(z - z_0) dS \right], \quad (21.2)$$

$$\vec{B}_0 = -\mu_0 \operatorname{grad} U_m. \quad (21.3)$$

Here $W_m(z)$ is the complex magnetic potential of the vortex field of current in windings of the machine;

z is the complex coordinate of point at which potential $z = x + iy$; is defined:

z_0 is the current coordinate of filament of current $di = \delta dS$ in cross section S winding to current;

δ is the current density.

Calculation of $W_m(z)$ can be made by formula (4.13) with no great difficulty. Considerably more complicated in the determination of components of induction B_H and potential φ caused by magnetization of the steel. As was shown in § 4, potential φ in region of air gap satisfies the Laplace equation and its value on the surface of the magnetic circuit $\varphi(t)$ can be found with an accuracy to the constant from the expression

$$\varphi(t) = C - U_m(t). \quad (21.4)$$

In general the region of the air gap in a machine is multiply connected, limited by contours of the armature of stator and additional poles. On each of the contours the limiting values of potential will be:

$$\begin{aligned} \varphi(t_a) &= C_a - U_m(t_a), & \varphi(t_{cr}) &= C_{cr} - U_m(t_{cr}), \\ \varphi(t_{a,n}) &= C_{a,n} - U_m(t_{a,n}), \end{aligned} \quad (21.5)$$

where the constants C_a , C_{cr} and $C_{a,n}$ are not mutually equal and can be determined from the condition of uniqueness of complex potential $\mathcal{W} = \psi + i\varphi$. Calculation of the field of magnetization leads thus to a solution of the modified Dirichlet problem [28].

Let us determine the constants C . Let us assume initially that there are no gaps between yoke and the core of the additional poles. Region of the air gap in it is two-connected, symmetric with respect to the axis of poles and is bounded

by the outer contour of the stator and internal contour circuit of the armature. Distribution of potential on them equals respectively:

$$\varphi(s_a) = C_a - U_m(s_a), \quad \varphi(s_{cr}) = C_{cr} - U_m(s_{cr}). \quad (21.6)$$

Sections of windings with currents and direction of currents in them are symmetric with respect to the axis of poles, therefore, distribution of potential of field of currents of windings along contours of the region $U_m(s_a)$ and $U_m(s_{cr})$ satisfy the following condition:

$$U_m(s_a) = -U_m(-s_a); \quad U_m(s_{cr}) = -U_m(-s_{cr}). \quad (21.7)$$

Using symmetry we define constants C_a and C_{cr} . Let us map the region of the air gap of the machine onto a ring. The contour of the armature will translate into an internal circumference of radius r , the contour of the stator into an external circumference of radius R . We assume that $\zeta = \zeta(z) = \rho e^{i\theta}$ is a function mapping region of air gap onto a ring, $(\zeta)z = z$ being it reverse. Due to symmetry of the region of the air gap with respect to the axis we have

$$|\zeta'(s)| = |\zeta'(-s)|, \quad (21.8)$$

where s is an arc measured along contours of the armature or stator from the axis of symmetry. On circumferences of the ring the distribution of potential of field of magnetization will cross into

$$\varphi(s_a) = C_a - U_m[s_a(\zeta)] = C_a - U_{m1}(r, \theta) = \varphi_1(r, \theta), \quad (21.9)$$

$$\varphi(s_{cr}) = C_{cr} - U_m[s_{cr}(\zeta)] = C_{cr} - U_{m1}(R, \theta) = \varphi_1(R, \theta). \quad (21.10)$$

Here, as the result of mapping, the average value of distributions $\varphi(s_a)$ and $\varphi(s_{cr})$ do not change. Indeed,

$$rd\theta = |d\zeta| = |\zeta'(s)| ds \quad (21.11)$$

and

$$\begin{aligned} \frac{1}{2\pi r} \oint_{(a)} U_{m1}(r, \theta) r d\theta &= \frac{1}{2\pi r} \left[\int_0^{\frac{L}{2}} U_m(s_a) |\zeta'(s_a)| ds + \right. \\ &\quad \left. + \int_0^{\frac{L}{2}} U_m(-s_a) |\zeta'(-s_a)| ds \right] = 0, \end{aligned} \quad (21.12)$$

i.e.,

$$\frac{1}{2\pi} \int_0^{2\pi} U_{m1}(r, \theta) d\theta = 0, \quad (21.13)$$

and analogously

$$\frac{1}{2\pi} \int_0^{2\pi} U_{m1}(R, \theta) d\theta = 0. \quad (21.14)$$

For any closed contour embracing the armature we have

$$\oint_L \frac{\partial \varphi}{\partial n} dt = 0 \quad (21.15)$$

Crossing to the ring $\zeta = \varrho e^{i\theta}$, on internal the circumference ($\varrho = r$) we have

$$\oint_L \frac{\partial \varphi}{\partial n} dt = r \int_0^{2\pi} \left[\frac{\partial \varphi_1}{\partial \varrho} \right]_{\varrho=r} d\theta = 0, \quad (21.16)$$

and, consequently, for any $\varrho (r < \varrho < R)$

$$\frac{1}{2\pi} \int_0^{2\pi} \frac{\partial \varphi_1}{\partial \varrho} d\theta = 0. \quad (21.17)$$

Hence, the equality

$$\frac{1}{2\pi} \int_r^R d\varrho \int_0^{2\pi} \frac{\partial \varphi_1}{\partial \varrho} d\theta = 0. \quad (21.18)$$

The magnitude of integral (21.18) does not depend on the order of integration, therefore

$$\begin{aligned} \frac{1}{2\pi} \int_r^R d\varrho \int_0^{2\pi} \frac{\partial \varphi_1}{\partial \varrho} d\theta &= \frac{1}{2\pi} \int_0^{2\pi} d\theta \int_r^R \frac{d\varphi_1}{d\varrho} d\varrho = \frac{1}{2\pi} \int_0^{2\pi} \varphi_1(R, \theta) d\theta - \\ &- \frac{1}{2\pi} \int_0^{2\pi} \varphi_1(r, \theta) d\theta = C_{cr} - \frac{1}{2\pi} \int_0^{2\pi} U_{m1}(R, \theta) d\theta - C_n + \\ &+ \frac{1}{2\pi} \int_0^{2\pi} U_{m1}(r, \theta) d\theta = 0, \end{aligned} \quad (21.19)$$

whence, considering (21.13) and (21.14), we obtain

$$C_A = C_{CT} = 0,$$

i.e., constants C_A and C_{CT} are equal and during calculation can be assumed to equal zero.

Thus if in the machine there is no gap between the yoke and additional poles, the limiting values of potential of the field of magnetization on contours of the region of the air gap can be determined immediately from the expressions

$$\varphi(t_A) = -U_m(t_A), \quad \varphi(t_{CT}) = -U_m(t_{CT}). \quad (21.20)$$

Let us consider a quadripole machine with gaps between cores of additional poles and the yoke. The region of the air gap in it will be six-connected and upon mapping of it onto a ring cuts will appear into which contours of the additional poles will be transformed (Fig. 27a, b). Since the mapped region is symmetric all cuts will also be symmetric with respect to the axis of armature — the center of symmetry of the region, both points of crossing of the contour of the core of the additional pole with its axis merging into one point lying at the middle of the cut. Distribution of potential $U_m(s_{A,n})$ on cores of additional poles, due to symmetry of location of sections of windings, will satisfy either the condition

$$U_m(s_{A,n}) = -U_m(-s_{A,n}) \quad (21.21)$$

with a current in the windings of the main poles, or condition

$$U_m(s_{A,n}) = U_m(-s_{A,n}) \quad (21.22)$$

with a current in the windings of the additional poles and armature.

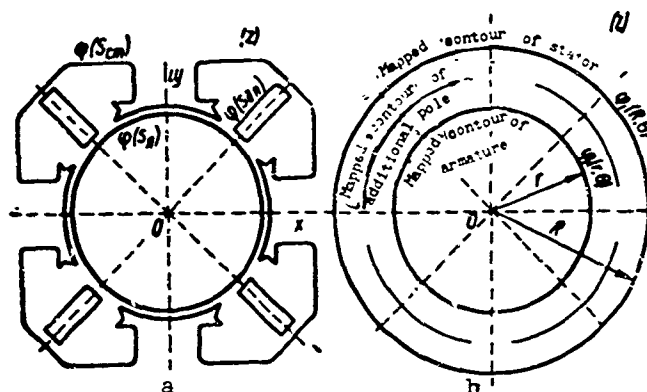


Fig. 27.

In the second case, as in the first, during mapping onto a ring potential jumps on neighboring cuts will be equal in magnitude and opposite in sign, therefore, during integration of expression (21.18) from r to R they are mutually compensated and thus, as in case of the two-connected region of an air gap, we have

$$C_a = C_{cr} = 0.$$

Let us turn to determination of limiting values of potential $\varphi(l_{a,n})$ on the contours of additional poles.

Mapping the region of the air gap onto a ring in such a manner so that the contour of the core of the additional pole converts into the internal circumference, the contour of the stator in the external circumference (Fig. 28) and applying

analogous reasoning when supplying windings of the main poles, i.e., under condition (21.21), we obtain the relationship

$$C_{a,n} = C_{cr} = C_a = 0. \quad (21.23)$$

When supplying the windings of additional poles and the armature

$$U_m(s_{a,n}) = U_m(-s_{a,n}). \quad (21.24)$$

therefore, we may not integrate expression (21.18) from r to R since on cuts into which will be transformed the contour circuit of the

Fig. 28.

armature and contours of the remaining additional poles, mutual compensation of potential jumps will not occur.

Using the symmetry of a six-connected region of air gap of machine and symmetry of distribution of potential along the contour bounding, the problem of calculation of constant $C_{a,n}$ in the six-connected region can be replaced by the corresponding problem in a two-connected region.

Limiting values of potential on the armature and stator are

$$\varphi(l_a) = -U_m(l_a),$$

$$\varphi(l_{cr}) = -U_m(l_{cr}).$$

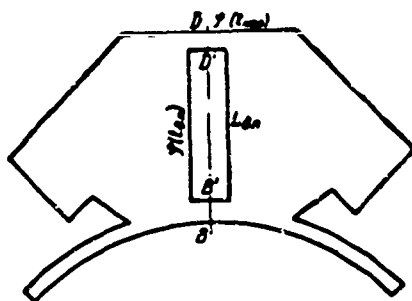


Fig. 29.

From the symmetry of distribution of potential $U_m(t)$ and symmetry of region of air gap with respect to axes of main pole it follows that the lines $\varphi = 0$ coincide with segments of the axes of main poles lying in the air gap. Making cuts along it we break the six-connected region of the air gap into four identical two-connected regions. Let us consider one of these regions (Fig. 29). Limiting values of potential on its contours equal:

$$\varphi(t_{nap}) = -U_m(t_{nap}), \quad \varphi(t_{a,n}) = C_{a,n} - U_m(t_{a,n}).$$

For determination of the constant $C_{a,n}$ with the help of results of § 14 it is sufficient to perform the following operation: calculate by formula (4.13) the value of potential $U_m(t)$ at points on the contour of region D; map region D infinite sheetly onto a band in such a manner that every sheet of the Riemannian surface is mapped onto a rectangle of dimensions $h \times N$; transfer values of potential U_m calculated from the formula (4.13) at points of the contour t_{nap} and $t_{a,n}$ into corresponding, during conformal mapping, points of boundaries of the band $\tau + ih$ and τ ; find the constant component of the periodic potential difference on the boundary of the band.

Constant $C_{a,n}$ is defined thus:

$$C_{a,n} = \frac{1}{N} \int_0^N [U_m(\tau + ih) - U_m(\tau)] d\tau, \quad (21.25)$$

and limiting values of potential of the field of magnetization are

$$\begin{aligned} \varphi(t_a) &= -U_m(t_a), & \varphi(t_{cr}) &= -U_m(t_{cr}), \\ \varphi(t_{a,n}) &= \frac{1}{N} \int_0^N [U_m(\tau + ih) - U_m(\tau)] d\tau - U_m(t_{a,n}). \end{aligned} \quad (21.26)$$

In § 23 an approximation formula for the determination of $C_{a.g.}$ is derived.

§ 22. Calculation of Induction on the Armature
of an Unsaturated Machine Not Having
Gaps Between the Yoke and Cores
of Additional Poles

In this case the region of the air gap of the machine is two-connected and constants C_R and C_{CT} equal zero. Limiting values of potential on armature and stator surfaces are immediately determined:

$$\psi(t_a) = -U_m(t_a), \quad \psi(t_{cr}) = -U_m(t_{cr}). \quad (21.20)$$

Solution of the Dirichlet problem, i.e. determination of potential in the region from its values on the contour can be obtained by means of conformal mapping of the two-connected symmetric region onto a band. Inasmuch as is necessary to determine the value of induction only on the contour, it is sufficient to find only the conformity of points of contours of these regions. Conformal mapping of the two-connected region of the air gap onto a band is performed with the help of modeling as described in § 19.

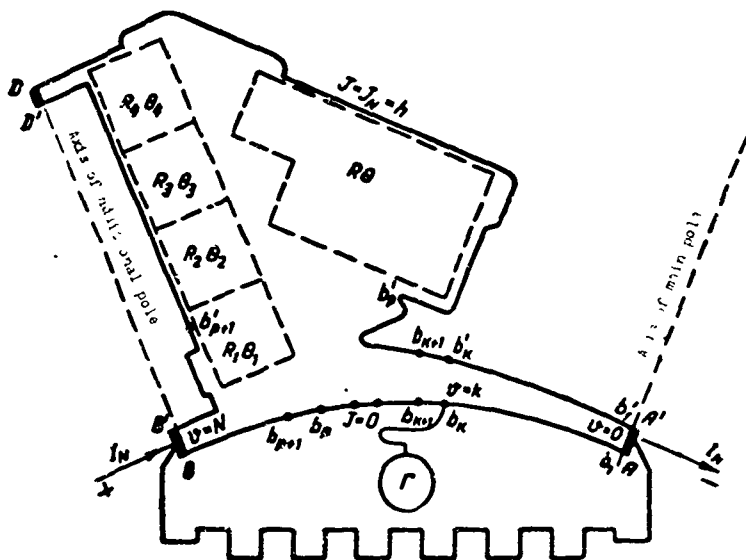


Fig. 30.

We prepare from sheet iron or thin dynamo steel a model in the form of part of the air gap of the machine between axes of the main and additional poles (Fig. 30). Along the line of axes AA' and BB' we solder copper contacts and connect the model to a dc circuit in series with a strip of the same dynamo steel as the model.

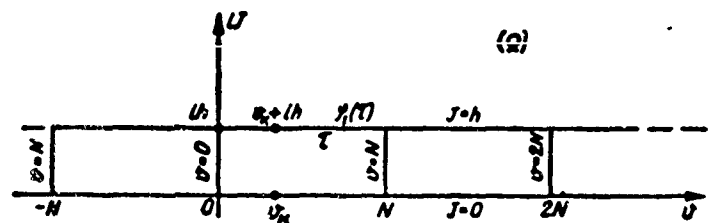


Fig. 31.

With help of zerogalvanometer Γ , connected in a potentiometer circuit, we find a series of points b_k and b'_k on the lower AB and upper A'B' sections of the model contour, starting from contact AA', such that the potential difference of two-neighboring points b_{k-1} and b_k , b'_{k-1} and b'_k is constant:

$$\Delta v = v_k - v_{k-1} = \text{const.}$$

It is convenient in practice to divide the entire voltage between contacts AA' and BB' into 100 equal parts, using for this purpose two resistance decades connected as a potentiometer. In order to fix the found points on the model contour, under the model is placed a sheet of heavy paper, the model contour is outlined in pencil and the points are inscribed directly on paper with a sharp probe and numbered. Setting $\Delta v = 1$ cm on the plane (Ω) , we find that v_k corresponds to a point on the axis of abscissas lying at a distance k cm from the origin ($\Omega = 0$) and $u_{BB'}$ is a point at a distance $N = 100$ cm from the origin.

Measuring the voltage between contacts of the model $u_m = u_{BB'}$, the voltage between contacts of the strip u_n and the dimensions of the strip $L \times H$ we find the width of the strip h . Indeed, from the obvious relationship

$$r_n = \frac{u_n}{I} = \frac{L}{\gamma H}; \quad J_N = \frac{I}{\gamma}; \quad \frac{h}{N} = \frac{J_N}{u_m}$$

it follows

$$h = N \frac{u_n H}{u_m L}. \quad (22.1)$$

Knowing the width of the band h , one can determine value of mapping function $\Omega = v + iJ$ at any found point b_k or b'_k . Thus, at point b_k , lying on a section of the model contour corresponding to armature, $J = 0$ and $\Omega_k = v_k = k$. At point b'_k lying on the section of the model contour corresponding to the stator, $J = h$ and

$\Omega = v_k + ih$. On the plane (Ω) points b_k of the inner contour of the region of the air gap (armature contour) will correspond to points of the real axis $J = 0$, points b_k' of the stator contour will correspond to points of the line $J = h$ (Fig. 31).

For finding the normal component of induction on the armature it is necessary to know magnitude of modulus of the derivative of the mapping function on the model contour

$$\left| \frac{d\Omega}{dz} \right|_t = \left| \frac{d\tau}{dt} \right|_t.$$

where dt is an element of length of the contour of the region of air gap corresponding during conformal mapping to an element of length $d\tau$ of the band boundary. Replacing infinitesimal increments by sufficiently small final ones, we can write

$$\left| \frac{d\tau}{dt} \right| \approx \left| \frac{\Delta\tau}{\Delta t} \right|.$$

This magnitude, it is possible to measure sufficiently accurately with a galvanometer connected to double probe with a fixed distance between needles equal to Δt .

Connecting the probe to the circuit of the model in such a manner so that point b_k (or b_k') coincides with the mean distance between needles, we measure the voltage between them Δv . The modulus of the derivative of the mapping function at point b_k (or b_k') will be determined thus:

$$\left| \frac{d\tau}{dt} \right| \approx \left| \frac{\Delta\tau}{\Delta t} \right| = \left| \frac{\Delta v}{\Delta t} \cdot \frac{N}{u_m} \right|. \quad (22.2)$$

Determining on the model the correspondance of points of contours of region of air gap and band, calculating value of potential $\varphi(t)$ at points of contour of air gap and transferring them to corresponding points of the boundary of the band, we obtain curves of potential distribution on boundaries of the band $\varphi_n(\tau)$. The normal component of induction at point b_n of the armature can now be found from relationship (11.8)

$$B_n(b_n) = -\mu_0 \frac{\partial \varphi}{\partial n} = -\mu_0 \left| \frac{d\tau}{dt} \right| \left| \frac{\partial \varphi_n}{\partial J} \right|_{J=0} \approx -\mu_0 \left| \frac{\Delta v}{\Delta t} \cdot \frac{N}{u_m} \right| \left| \frac{\partial \varphi_n}{\partial J} \right|_{J=0}. \quad (22.3)$$

Using formula (11.16) we obtain

$$\begin{aligned}
 B(b_n) = & -\frac{\mu_0}{h} \left| \frac{\Delta v}{\Delta t} \cdot \frac{N}{u_w} \right| \left[\varphi_n(n+ih) - \varphi_n(n) + \right. \\
 & + \frac{\pi}{2h} \int_0^\infty \frac{\varphi_n(n+\alpha) + \varphi_n(n-\alpha) - 2\varphi_n(n)}{\operatorname{ch} k\alpha - 1} d\alpha + \\
 & \left. + \frac{\pi}{2h} \int_0^\infty \frac{\varphi_n(n+\alpha+ih) + \varphi_n(n-\alpha+ih) - 2\varphi_n(n+ih)}{\operatorname{ch} k\alpha + 1} d\alpha \right]. \quad (22.4)
 \end{aligned}$$

Analysis of the field pattern of various types of salient-pole dc machines has shown that for technical calculations it is possible to take a simplified distribution of potential on boundaries of the band. The field potential of poles of the machine continuously changes over the surfaces of the armature and stator, however, the peculiarity of configuration of the air gap, especially its small magnitude under the poles and then its sharp growth between poles, leads to the fact that sections of the stator contour located under windings of poles, on which occurs the biggest change of potential, during mapping onto a band are practically drawn into a point and the potential on them changes in jumps sufficiently small so that it may be disregarded. Here it is possible to take the potential of the armature equal to zero and the potential of the surface of the pole applied to the armature constant and equal to the ampere-turns of the pole coil acting on the air gap $\varphi_n = I W_n$.

Let us assume that point on model b'_p the last on the main pole, has the number p , the following point b'_{p+1} falls on an additional pole. Then on the upper boundary of the band we may consider that the potential of the field of the main poles $\varphi(1)$ has a constant value equal to the ampere-turns acting on the air gap between points $(-p+ih)$ and $(p+ih)$. On the lower boundary of the band corresponding to the surface of the armature it is equal to zero. Analogously, the potential of the field of the additional bands on the upper boundary between points $[(p+1)+ih]$ and $[2N-(p+1)+ih]$ can be taken as constant, equal to the ampere-turns of pole, on the lower boundary - equal to zero.

The distribution of potential caused by current in the winding of the armature also may be simplified and considering that the potential of the stator is equal

to zero and the potential of the armature at point b_n is proportional to the distance along the circumference of the armature from the axis of the main pole to point b_n and attains a maximum equal to the ampere-turns of the armature under the axis of the auxiliary pole

$$\varphi_n(b_n) = \frac{b_n}{b_n} I W_{an}. \quad (22.5)$$

If point b_n on the circumference of the armature were disposed evenly over the entire section between axes of the main and auxiliary poles then the distribution of potential of the field of current in the armature on the lower boundary of the band could have been presented thus:

$$\varphi_1(n) = \frac{n}{N} I W_{an}. \quad (22.6)$$

In reality points b_n on the circumference of the armature are disposed nonuniformly and taking on the lower boundary of the band the distribution of potential (22.6), we allow a certain error. However, as will be clear below, it can in sufficient measure be eliminated. Let us apply the method of superposition and find the value of induction on the surface of the armature as the sum of inductions with potentials only on the main poles then with potentials only on the auxiliary poles and finally with a potential only on the armature. In order to facilitate calculation we first demonstrate that the influence of the potentials of the poles and armature located in the neighboring quadrant, on the magnitude of induction on the considered section of the armature is insignificant. To do this we demonstrate that a potential of finite value distributed on the boundaries of a band at a distance greater than $2h$, from the considered point $\Omega = n$ has practically no effect on the magnitude of the normal component of induction $B_n = \mu_0 \left[\frac{\partial \varphi_1}{\partial J} \right]$ at this point. Let potential $\varphi_1(\tau) = c$ be distributed on the segments $(-\infty, n-2h)$ and $(n+2h, \infty)$, potential $\varphi_1(\tau+ih) = c_2$ on the segments $(-\infty, n-2h+ih)$ and $(n+2h+ih, \infty)$, then:

$$\lim_{J \rightarrow 0} \left[\frac{\partial \varphi_1}{\partial J} \right]_1 = \frac{1}{h} [\varphi_1(n+ih) - \varphi_1(n)] + \\ + \frac{\pi}{2h^2} \int_0^\infty \frac{\varphi_1(n+\alpha) + \varphi_1(n-\alpha) - 2\varphi_1(n)}{\cosh k\alpha - 1} d\alpha +$$

$$\begin{aligned}
& + \frac{\pi}{2h^2} \int_{-2h}^{2h} \frac{\varphi_1(n+a+ih) + \varphi_1(n-a+ih) - 2\varphi_1(n+ih)}{\operatorname{ch} ka + 1} da = \\
& = \frac{\pi}{2h^2} \int_{-2h}^{2h} \frac{2c_1 da}{\operatorname{ch} ka - 1} + \frac{\pi}{2h^2} \int_{-2h}^{2h} \frac{2c_2 da}{\operatorname{ch} ka + 1} = -\frac{kc_1}{\pi} \operatorname{cth} \frac{ka}{2} \Big|_{-2h}^{2h} + \\
& + \frac{kc_2}{\pi} \operatorname{th} \frac{ka}{2} \Big|_{-2h}^{2h} = \frac{1}{h} \left(\frac{2c_1 e^{-2\pi}}{1+e^{-2\pi}} + \frac{2c_2 e^{-2\pi}}{1-e^{-2\pi}} \right) \approx \frac{c_1 + c_2}{h} 2e^{-2\pi} \approx \\
& \approx 3,75 \cdot 10^{-3} \frac{c_1 + c_2}{h}.
\end{aligned}$$

On the other hand the normal component of intensity $\left[\frac{\partial \varphi_1}{\partial y} \right]_2$ at point $\Omega = n$, caused by the distribution of potential $\varphi_1(\tau + ih) = c_2$ on the section of the upper boundary of the band between points $(n-2h)$ and $(n+2h)$, has the form

$$\begin{aligned}
\lim_{J \rightarrow 0} \left[\frac{\partial \varphi_1}{\partial J} \right]_2 &= \frac{c_2}{h} + \frac{\pi}{2h^2} \int_{-2h}^{2h} \frac{-2c_2 da}{\operatorname{ch} ka + 1} = \frac{c_2}{h} - \frac{c_2}{h} \operatorname{th} \frac{ka}{2} \Big|_{-2h}^{2h} = \frac{c_2}{h} - \\
&- \frac{c_2}{h} + \frac{c_2}{h} \cdot \frac{1-e^{-2\pi}}{1+e^{-2\pi}} \approx \frac{c_2}{h}.
\end{aligned} \tag{22.8}$$

Setting $c_3 = c_1 + c_2$, we obtain

$$\left[\frac{\partial \varphi_1}{\partial J} \right]_1 = 3,75 \cdot 10^{-3} \left[\frac{\partial \varphi_1}{\partial J} \right]_2. \tag{22.9}$$

i.e., the magnitude of the component of intensity (and, consequently, induction) at point $\Omega = n$ on the boundary of the band caused by the potential distributed along boundaries of the band at distance greater than $2h$ from point n is less than half of one percent of the magnitude of intensity at this point caused by difference of potential at points n and $n + ih$.

Consequently, the distribution of potential on boundaries of the band beyond the borders of section $-2h \leq a \leq 2h$ ($a = \tau - h$) cannot be taken into account without loss of calculation accuracy.

With the presence, in electrical machines, of a ratio of dimensions of diameter of armature and gap above pole of magnitude N not less than $10h$, and the number of points p , occurring on the main band lies in the range of 0.6 to $0.8N$. The potential of the neighboring pole on the upper boundary of the band, distributed

Therefore, on the considered section $0 \leq n \leq N$ the first integral in formula (22.4) differs little from zero, the second is equal to zero, and for the normal component of induction on armature at point b_n from (22.4) we obtain

$$B(b_n)_{p,n} = -\mu_0 \left| \frac{\Delta v N}{\Delta t u_m} \right| \frac{I W_{\pi, \max}}{h} \cdot \frac{n}{N}. \quad (22.12)$$

From expression (22.12) one may see that induction at point b_n is proportional to the accepted magnitude of potential on it. Substituting in (22.12) the value of potential at point b_n , equal to $I_{\pi, \max} \frac{b_n}{b_N}$, we obtain

$$B(b_n)_{p,n} = -\mu_0 \left| \frac{\Delta v N}{\Delta t u_m} \right| \frac{I W_{\pi, \max}}{h} \cdot \frac{b_n}{b_N}. \quad (22.13)$$

If on the model the serration of the armature is disregarded then that in the derived formulas (22.10), (22.11), and (22.12) it is necessary to introduce a teeth coefficient k_z , which can be calculated from the formula

$$k_{zn} = \frac{t_z + 10\delta_n}{b_z + 10\delta_n}. \quad (22.14)$$

Here t_z is the magnitude of tooth spacing on circumference of armature; b_z is the width of tooth on circumference of armature; δ_n is the magnitude of gap at point b_n , for which is calculated k_{zn} .

Taking into account the serration of the armature, for the induction established at point b_n on the surface of the armature of an unsaturated machine, designated by the constant $e^{\frac{\pi}{h}} = e^{\frac{\pi}{h}} = a$, we obtain:

a) field of main poles:

$$B(b_n)_{ra,n} = -\mu_0 \left| \frac{\Delta v N}{\Delta t u_m} \right| \frac{I W_{ra,n}}{k_{zn} h} \cdot \frac{1}{a^{n-p} + 1}; \quad (22.15)$$

b) field of additional poles:

$$B(b_n)_{a,n} = -\mu_0 \left| \frac{\Delta v N}{\Delta t u_m} \right| \frac{I W_{a,n}}{k_{zn} h} \cdot \frac{1}{a^{p+1-n} + 1}; \quad (22.16)$$

c) field of armature:

$$B(b_n)_a = -\mu_0 \left| \frac{\Delta v N}{\Delta t u_m} \right| \frac{I W_{\pi, \max}}{k_{zn} h} \cdot \frac{b_n}{b_N} \quad (22.17)$$

between points $(2N-p+ih)$ and $(2N+p+ih)$ will be located at a distance $l > (2N-p-n) > 20h-8h-10h=2h$, from the point under consideration $n (0 \leq n \leq N)$ and consequently, its influence on the magnitude of induction at the point n may be neglected. Let us proceed to a calculation of the induction on the armature. For this purpose we substitute simplified values of distribution of potential in one quadrant of the air gap of the machine into the formula for the normal derivative of potential on the boundary of the band.

Field of main terminals. Potential $\varphi_{ra,n} = IW_{ra,n}$ is distributed on the surface of pole between points b'_{-p} and b'_p . On the upper boundary of the band this corresponds to a distribution between points $(-p)$ and p . For determination of the normal component of induction at point b_n on the armature we use the formula (11.9):

$$\begin{aligned} B(b_n)_{ra,n} &= -\mu_0 \left| \frac{\Delta v}{\Delta t} \cdot \frac{N}{u_m} \right| \lim_{J \rightarrow 0} \left[\frac{IW_{ra,n} k^2}{2\pi} \int_{-p}^p \frac{\operatorname{ch} k(\tau-n) \cos kJ + 1}{[\operatorname{ch} k(\tau-n) + \cos kJ]^2} d\tau \right] = \\ &= -\mu_0 \left| \frac{\Delta v}{\Delta t} \cdot \frac{N}{u_m} \right| \frac{IW_{ra,n}}{2\pi} k^2 \int_{-p}^p \frac{d\tau}{\operatorname{ch} k(\tau-n) + 1} = \\ &= -\mu_0 \left| \frac{\Delta v}{\Delta t} \cdot \frac{N}{u_m} \right| \frac{IW_{ra,n}}{2h} \operatorname{th} \frac{k}{2} (\tau-n) \Big|_{-p}^p \cong -\mu_0 \left| \frac{\Delta v N}{\Delta t u_m} \right| \frac{IW_{ra,n}}{h} \cdot \frac{1}{1 + e^{k(n-p)}}, \\ \text{or} \\ B(b_n)_{ra,n} &= -\mu_0 \left| \frac{\Delta v N}{\Delta t u_m} \right| \frac{IW_{ra,n}}{h} \cdot \frac{1}{1 + e^{k(n-p)}} \left(k = \frac{\pi}{h} \right). \end{aligned} \quad (22.10)$$

Field of additional poles. Potential $\varphi_{a,n} = IW_{a,n}$ is distributed on the surface of a pole between points b'_{p+1} and b'_{2N-p-1} . On the upper boundary of the band this corresponds to a distribution between points $(p+1)$ and $(2N-p-1)$. Just as when calculating the induction of the field of the main poles we have

$$\begin{aligned} B(b_n)_{a,n} &= -\mu_0 \frac{IW_{a,n}}{2h} \left| \frac{\Delta v N}{\Delta t u_m} \right| \operatorname{th} \frac{k}{2} (\tau-n) \Big|_{p+1}^{2N-p-1} = \\ &= -\mu_0 \left| \frac{\Delta v N}{\Delta t u_m} \right| \frac{IW_{a,n}}{h} \cdot \frac{1}{1 + e^{k(p+1-n)}}. \end{aligned} \quad (22.11)$$

Field of armature reaction. The distribution of potential on the lower boundary of the band is taken as follows:

$$\varphi_1(n) = \frac{n}{N} IW_{s, \max}.$$

The resultant induction at point b_n on the armature equals:

$$B(b_n) = B(b_n)_{r,n} \mp B(b_n)_{a,n} \pm B(b_n)_s. \quad (22.18)$$

Here b_n is the distance from contact AA' to point b_n measured on the model along the circumference of the armature; p is the number of poing b_p , last on the main pole; h is the width of band $h = N \frac{u_n H}{u_m L}$; b_n is the distance along circumference of armature between contacts AA' and BB' of the model (Fig. 30); N is the number of points taken on the contour of the model armature; u_m and u_n is respectively, voltage measured between contacts of the model and a strip of dimensions $L \times H$; Δv is the voltage between needles of double probe applied to the model contour at point b_n ; Δt is the distance between needles of probe;

$$a = e^{\frac{\pi}{h}}.$$

Taking a simplified distribution of potential we thereby facilitate calculation of the magnitude of induction: the necessity of calculating the eddy component of induction on the armature is eliminated since an excessive potential difference between corresponding points of the armature and stator is knowingly taken.

Let us consider, for instance, the field of the main poles. As follows from the law of total current, potential difference of the field of magnetization between corresponding points of the armature and stator at the section of the armature under the pole is equal to the total ampere-turns of the pole minus the eddy potential drop U_m in the gap between points. It is accepted that this difference is equal to the total ampere-turns of the pole, i.e.,

$$\begin{aligned} IW_{r,n} &= IW_{r,n} - [U_m(b_n) - U_m(b_n)] + [U_m(b_n) - U_m(b_n)] = \\ &= [\varphi(b_n) - \varphi(b_n)] + [U_m(b_n) - U_m(b_n)]. \end{aligned} \quad (22.19)$$

Determining the normal component of induction of the field of main poles on the armature according to formula (22.15) for points under the pole, i.e., for $n \ll p$ we obtain

$$\begin{aligned} B(b_n) &= -\mu_0 \left| \frac{\Delta v N}{\Delta t u_m} \right| \frac{\varphi(b_n) + U_m(b_n) - U_m(b_n)}{h} \cdot \frac{1}{a^{n-p} + 1} = \\ &= -\mu_0 \left| \frac{\Delta v N}{\Delta t u_m} \right| \frac{\varphi(b_n)}{h} - \frac{\mu_0}{\delta} [U_m(b_n) - U_m(b_n)] \approx B_n(b_n) + B(b_n). \end{aligned} \quad (22.20)$$

The first member of the right half of equality (22.20) constitutes a main part of the magnitude of the normal component of induction of the field of magnetization, the second member may be considered equal to the normal component of induction of the eddy field of current in the pole windings. We reach a similar result when examining the field of additional poles.

Thus, formulas (22.15), (22.16), and (22.17) make it possible to determine the magnitude of total induction on the armature which includes both the component of induction of the field of magnetization and the component of the eddy field of currents in the machine windings.

The method presented for calculation of the magnetic field of dc machines has been repeatedly checked experimentally and confirmed by direct measurements of the magnitude of induction at points on the armature surface. For example we will give a comparison of values of induction, at points on the armature of dc machines of the firm AEG, type HN-300, 230 V, 130 A, 30 kW, 1100 r/min, measured and calculated by the described method, directly. Measurements of induction at points on the surface of the armature were made by the ballistic method. For this purpose on surface of armature of machine were glued four shifted measuring coils embracing each tooth-groove of armature at 90° intervals. During rotation of the armature with help of a turning attachment the measuring coils are moved along the circumference.

During transmission current along windings of machine, flux, occurring on a tooth division of the armature, permeated the circuit of the measuring coil. A change in direction of current in the windings of machine led to a change in direction of flux permeating the measuring coil and flow of induced charge through the ballistic galvanometer. Deflection of the galvanometer beam made it possible to measure the magnitude of flux penetrating the measuring coil and to determine the mean value of induction on the surface of the armature at the coil location. The distance along the surface of the armature between axes of neighboring main poles was divided into four approximately equal parts. Measurements of flux were made with coincidence of the axis of the measuring coil with the points of division. The turning attachment ensured the possibility of turn of the armature over an angle greater than 90° . Induction was measured during transmission of current along each of the machine windings separately (through windings of the

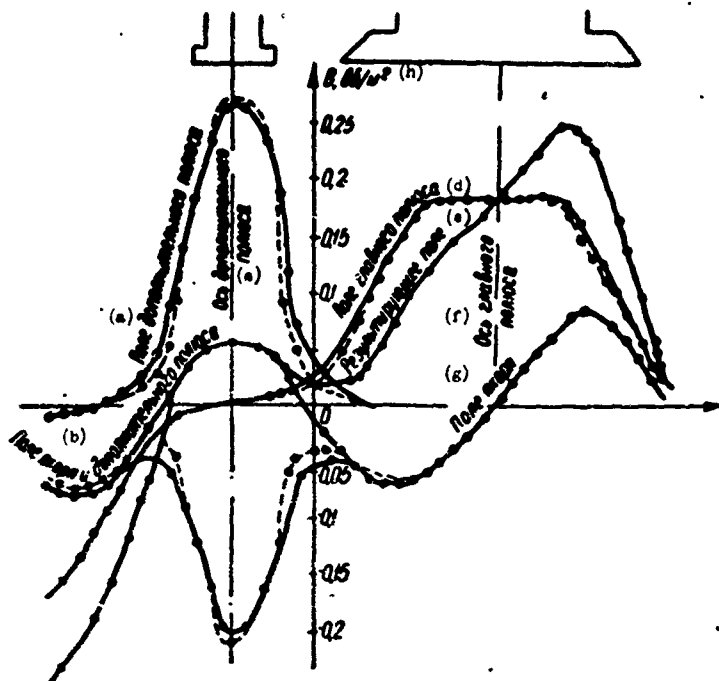


Fig. 32. KEY: (a) Field of additional pole; (b) Field of armature and additional pole; (c) Axis of auxiliary pole; (d) Field of main pole; (e) Resultant field; (f) Axis of main pole; (g) Field of armature; (h) Wb/m^2 .

main poles additional poles, and armature), through all windings of the machine simultaneously and through two windings - armature and additional poles. The results of measurements are given in the form of curves depicted in Fig. 32 by solid lines. Experimentally measured values of induction were collated with those calculated by the method presented. From a sheet of dynamo steel of thickness 0.5 mm was prepared a model of the cross section of the region of the air gap of the machine in a 3:1 scale and the band in the form of a rectangle (Fig. 33). The model is connected to a dc circuit and on sections of its contour points are contacted with a probe which correspond, during conformal mapping, to evenly spaced points on the boundaries of the band. At each point values of the modulus of the derivative of the mapping function were measured with a double probe. Coordinates of points on the expanded circumference of the armature and the value of the modulus of the derivative of the mapping function in them are given in Table 1, where S is the number selected for designating points on the armature; b_n is the distance measured on model from contact AA' to point of number n along the circumference of the armature.

Table 1.

S	n	b_n	$\frac{1}{3} \left \frac{\Delta v}{\Delta t} \cdot \frac{N}{u_m} \right $	S	n	b_n	$\frac{1}{3} \left \frac{\Delta v}{\Delta t} \cdot \frac{N}{u_m} \right $	S	n	b_n	$\frac{1}{3} \left \frac{\Delta v}{\Delta t} \cdot \frac{N}{u_m} \right $	S	n	b_n	$\frac{1}{3} \left \frac{\Delta v}{\Delta t} \cdot \frac{N}{u_m} \right $	S	n	b_n	$\frac{1}{3} \left \frac{\Delta v}{\Delta t} \cdot \frac{N}{u_m} \right $
0	7	0	11.75	6	43	112	10.52	11	65	202	4.72	16	74.5	300	3.61	17	300	319	7.8
1	15	18.1	11.75	7	49	132	9.4	12	68	224	3.41	18	83	319	10	19	336	356	11.64
2	22	39	11.75	8	54	151	8.11	13	70	244	2.4	19	90	336	12	20	356	378	12
3	29	57	11.75	9	58	167	7	14	71	257	2.17		99						
4	36	75	11.52	10	62	185	5.7	15	73	285	2.55								

Values measured on model: $u_m = 16.45$ mV, $p = 71$,
 $N = 100$. Values measured on the band (Fig. 33):
 $L = 201$ mm, $H = 20$ mm, $u_m = 7.12$ mV, and $I = 1$ A,

$$h = N \frac{u_m H}{u_m L} = 4.31, \quad a = e^{\frac{\pi}{h}} = e^{0.729} = 2.073.$$

Since the magnitude of the gap under the main pole is not identical, the coefficient k_z was determined for every point b_n . Here we proceeded from the following considerations. Considering that under the center of the main pole on the model the field of current is uniform conductivity of the tube of flux between lines $v = 0$ and $v = 1$ equals

$$\frac{b_1}{\delta} = \frac{1}{h},$$

where δ is the gap under the center of the main pole. Since conductivity of all tubes of the field of current on the models are equal, for tubes between lines $v = n + 1$ and $v = n - 1$ we obtain

$$\frac{|b_{n+1} - b_{n-1}|}{\delta_n} \approx \frac{2b_1}{\delta} = \frac{2}{h},$$

whence

$$\delta_{ns} \approx h \frac{|b_{n+1} - b_{n-1}|}{2},$$

or, assuming $|b_{n+1} - b_{n-1}| = |\Delta t|$, $2 = |\Delta v| \frac{N}{u_m}$,

$$\delta_{ns} \approx h \left| \frac{\Delta t}{\Delta v} \right| \frac{N}{u_m} \text{ and } k_z = \frac{t_z + 10\delta_{ns}}{b_z + 10\delta_{ns}}.$$

Here t_z is the tooth pitch (67.5×3); b_z is the width of tooth along the external diameter of the armature (40.5×3).

Values of coefficient k_z at different points on the armature are given in Table 2.

Table 2.

S	k_m	S	k_m	S	k_m	S	k_m
0	1.18	6	1.16	11	1.085	16	1.0
1	1.18	7	1.148	12	1.05	17	1.0
2	1.18	8	1.13	13	1.0	18	1.16
3	1.18	9	1.12	14	1.0	19	1.18
4	1.18	10	1.1	15	1.0	20	1.18
5	1.175						

Table 3.

S	B_s	S	B_s	S	B_s	S	B_s
0	1730	6	1529	11	760	16	46
1	1730	7	1440	12	510	17	16
2	1730	8	1260	13	283	18	8
3	1730	9	1090	14	190	19	4
4	1730	10	910	15	84.5	20	0
5	1720						

Table 4.

S	B_s	S	B_s	S	B_s	S	B_s
0	0	6	0	11	12	16	852
1	0	7	0	12	61	17	1795
2	0	8	0	13	158	18	2280
3	0	9	0	14	234	19	2610
4	0	10	2	15	500	20	2670
5	0						

Table 5.

S	B_s	S	B_s	S	B_s	S	B_s
0	0	6	670	11	576	16	620
1	120	7	710	12	470	17	1240
2	250	8	710	13	367	18	1660
3	370	9	680	14	340	19	2030
4	485	10	630	15	420	20	2220
5	600						

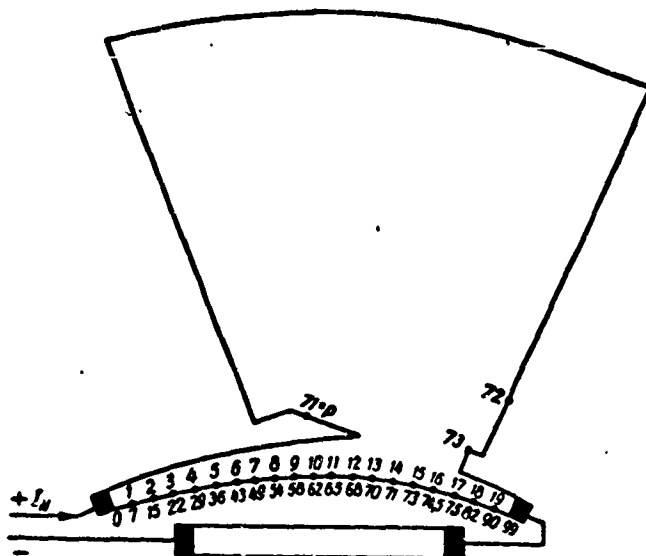


Fig. 33.

Value of induction (in Gauss) of the field of the main poles at points on the surface of the armature of an HN-300 motor calculated from formula (22.15), where $\mu_0=1,256$, $a=2,073$, $p=71$, $I W_{r.n.}=600$ A are given in Table 3.

In Table 4 are given values of the induction of the field of additional poles at points on the surface of the armature of an HN-300 motor calculated from formula (22.16) for $I W_{a.n.}=900$ A.

Values of induction of the armature field at points on the armature surface of the same motor, calculated from formula (22.17) for $I W_a=844$ A are given in Table 5 and results of calculation -- in the form of hachured curves on Fig. 32.

§ 23. Calculation of Induction on the Armature of an Unsaturated Machine with Gaps Between Yoke and Cores of Additional Poles

As already indicated in § 21, symmetry of the six-connected (in this case) region of the air gap of the machine and symmetry of the distribution of potential along contours bounding it, permits finding the line of equal potential, not calculating the field, make cuts along it and thereby reduce the problem to the calculation of the field in a two-connected region.

Calculation of the field when feed windings of the main poles. In this case

$$C_n = C_{cr} = C_{a.n.} = 0$$

and limiting values of potential on all contours are immediately determined

$$\begin{aligned}\varphi(t_n) &= -U_m(t_n), \quad \varphi(t_{cr}) = -U_m(t_{cr}), \\ \varphi(t_{a,n}) &= -U_m(t_{a,n}).\end{aligned}$$

Segments of the axes of additional poles, lying in the region of the air gap, coincide with lines $\varphi = 0$. Making four cuts along segments of axes between the yoke and cores of the poles (Fig. 27), we make region of the air gap two-connected. Here the limiting values of potential φ on the entire contour, including cuts, are determined, the problem being solved just as in § 22. The form of the model and location of contacts AA' and BB' on it for electrical modeling mapping the function in this case are shown in Fig. 30. Calculation may be made according to approximate formula (22.15).

Calculation of field with supply of windings of auxiliary poles and armature.

In this case

$$C_s = C_{cr} = 0$$

and limiting values of potential on the armature and stator are:

$$\varphi(t_n) = -U_m(t_n), \quad \varphi(t_{cr}) = -U_m(t_{cr}).$$

From conditions of symmetry it follows that the lines $\varphi = 0$ in this case coincide with segments of axes of main poles lying in the air gap. Making cuts along it, we split the six-connected region of the air gap into four identical two-connected regions (Fig. 27). For determination of constant $C_{д.п.}$ we use the same model to obtain conformal mapping as when calculating the field when feeding windings of the main poles, but contacts to it we connect along segments of the axis of the auxiliary pole BB' and DD'. Constant $C_{д.п.}$ can be found from formula (21.25) although, using the peculiarity of configuration of the air interval of dc machines and peculiarity of potential distribution along its contours, the expression for $C_{д.п.}$ may be simplified. Let us demonstrate this on the example of calculation of constant $C_{д.п.}$ for traction motor [NB-409/840] (HE-409/840).

Let us determine constant $C_{д.п.}$ when supplying windings of the auxiliary poles. The contour of the section of the air interval region and the cross section of the winding with current are shown in Fig. 30. The potential of the field of

current flowing in windings of auxiliary poles we define in the following way: we divide the cross section of the winding into $n = 4$ rectangles and replace each of their axes with a current coinciding with its center of gravity. Then for potential $U_m(x, y)$ we have

$$U_m = \sum_{k=1}^4 U_{mk}, \quad (23.1)$$

where each of potential U_{mk} is created by eighth current-carrying axes located at points of the eight cross sections of the windings of the additional poles symmetric with respect to the axis of the armature. Designating coordinates of these points $z_{k1}, z_{k2}, \dots, z_{k8}$, for potential U_{mk} we obtain

$$U_{mk}(x, y) = \text{Im} \left[\frac{iW}{8\pi} \ln \frac{(z - z_{k2})(z - z_{k3})(z - z_{k7})(z - z_{k8})}{(z - z_{k1})(z - z_{k4})(z - z_{k5})(z - z_{k6})} \right], \quad (23.2)$$

or, using the symmetry of location of the axes, the current-carrying after transformation we obtain

$$U_{mk}(\varrho, \gamma) = \frac{iW}{2\pi n} \text{arctg} \frac{4r_k^2(r_k^2 - 1) \sin 2\theta_k \cos 2\gamma}{r_k^4 + 1 + 2r_k^2(\cos 4\theta_k - 2 \cos^2 2\gamma)}. \quad (23.3)$$

Here $r_k = \frac{\varrho}{R_k}$, R_k and θ_k are the polar coordinates of the current-carrying axis $z_{k1} = R_k e^{i\theta_k}$, ϱ and γ are the polar coordinates of the point at which is determined potential $z = \varrho e^{i\gamma}$. Angles θ_k and γ are measured from the axis of the additional pole. For the potential from the entire current in windings of additional poles we have:

$$U_m(\varrho, \gamma) = \frac{iW}{2\pi n} \sum_{k=1}^4 \text{arctg} \frac{4r_k^2(r_k^2 - 1) \sin 2\theta_k \cos 2\gamma}{r_k^4 + 1 + 2r_k^2(\cos 4\theta_k - 2 \cos^2 2\gamma)}. \quad (23.4)$$

From the drawing of the motor it follows:

$$R_1 = 39 \text{ cm}; \quad R_2 = 42.3 \text{ cm}; \quad R_3 = 46.7 \text{ cm}; \quad R_4 = 51 \text{ cm};$$

$$\theta_1 = 8^\circ 18'; \quad \theta_2 = 7^\circ 34'; \quad \theta_3 = 6^\circ 50'; \quad \theta_4 = 6^\circ 14'.$$

We connect a model of half the considered two-connected region with contact BB' and DD' to a dc circuit (Fig. 30) and plot N points on each section of its contour through equal values of voltage drop Δv . We select a series of points

Table 6.

No. of points	ϱ	γ	ν	$-\frac{U_m}{W}$	No. of points	ϱ	γ	ν	$-\frac{U_m}{W}$
1	34	0°	95,5	0,841	9	43,4	4°51'	63,5	0,554
2	34	2°	87	0,843	10	45,3	4°5'	62	0,49
3	34,1	4°10'	77	0,853	11	47,1	3°55'	60	0,416
4	35,3	4°10'	79	0,826	12	49	3°45'	58	0,34
5	35,5	3°50'	70,3	0,815	13	51	3°35'	55	0,27
6	37,7	4°50'	69	0,797	14	52,5	3°30'	46	0,228
7	39,6	4°40'	65,5	0,72	15	52,5	1°45'	22	0,241
8	41,5	4°30'	65	0,64	16	52,5	0°	0	0,243

on the external and internal contours of the region and from formula (23.4) calculate the magnitude of the magnetic potential in them. Coordinates of points on the contour of the air gap region, coordinates of points corresponding to it on boundaries of an infinite band and calculated values of magnetic potential U_m on them are given in Table 6, (contour of core of additional pole $J = 0$) and Table 7 (external contour of region $J = h$). Curves of potential distribution $U_m(\tau)$, $U_m(\tau + ih)$ and $U_m(\tau + ih) - U_m(\tau)$ are shown in Fig. 34, plotted along points on the boundary of an infinite band ($0 \leq \tau \leq N$). Measurements on the model give; $h = 7.15$, $N = 95.5$, $2kN = 84$. For determination of constant $C_{d.n.}$ we use equation (14.30). Determining the area of curve $U_m(\tau + ih) - U_m(\tau)$ in the interval ($0 \leq \tau \leq N$), we obtain $S = 33,57/W$ and consequently

$$C_{d.n.} = \frac{S}{N} = \frac{33,57/W}{95,5} = 0,352/W \quad (23.5)$$

Replacing curve $U_m(\tau + ih) - U_m(\tau)$ with two rectangles as shown by the dotted line in Fig. 34, it is easy to derive a simple rule for approximate determination of the magnitude of $C_{d.n.}$ when supplying windings of the auxiliary poles equivalent to it in area.

Table 7.

No. of points	ϱ	γ	ν	$\frac{U_m}{W}$	No. of points	ϱ	γ	ν	$-\frac{U_m}{W}$
1	33	0	95,5	0,143	9	48,5	19°40'	63,7	0,02
2	33	4°30'	78	0,13	10	50,5	14°50'	61,5	0,05
3	33	9°	71	0,103	11	53,7	11°5'	58,5	0,087
4	33	13°30'	68,7	0,076	12	53,5	6°30'	55,5	0,157
5	33	22°30'	67,5	0,035	13	53,4	5°	53	0,1575
6	36,5	18°40'	67	0,042	14	53,2	3°30'	44,5	0,207
7	42	28°25'	65	0,0042	15	53,2	1°45'	22	0,2205
8	46,7	24°40'	64,5	-0,005	16	53,2	0	0	0,225

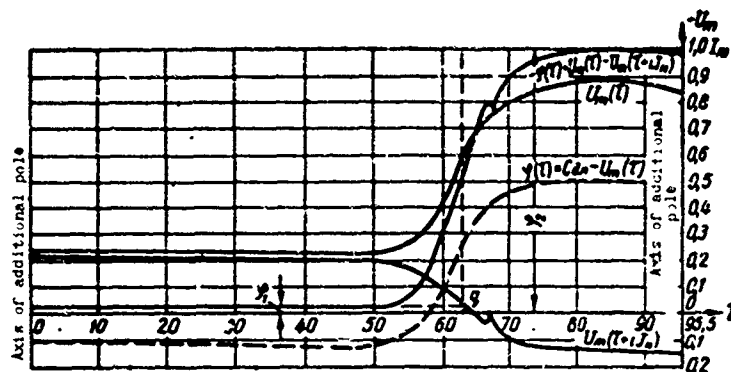


Fig. 34.

Indeed, the change of potential difference $U_{m1}(\tau+ih) - U_{m1}(\tau)$ occurs, as can be seen from Fig. 34, basically only on the lateral surface of the core of the additional pole under the coil with current. Therefore, the width of every rectangle equals the number of points occurring on half of the contour of the core of the additional pole.

Taking into account that the peculiarities of form of the curves shown in Fig. 34 are not specific only for the considered motor NB-409, but general for all existing designs, determination of $C_{\Delta, n}$ for a dc quadripole machine may be performed in the following way:

1) determine potential difference on the axis of the additional pole between the yoke and core

$$\varphi_1 = U_{m1}(0+ih) - U_{m1}(0) = U_m(\theta_{cr}, 0^\circ) - U_m(\theta_{\Delta, n, 1}, 0^\circ) \quad (23.6)$$

2) determine potential difference on the axis of the additional pole between the armature and core

$$\varphi_2 = U_{m1}(N+ih) - U_{m1}(N) = U_m(R_0, 0^\circ) - U_m(\theta_{\Delta, n, 2}, 0^\circ); \quad (23.7)$$

3) attempting a mapping, find the number of the point on the middle of the core length $v = q$, considering $v = 0$ at the intersection of the pole axis with the yoke (in our example $q = 63$).

Then constant $C_{\Delta, n}$ will be determined thus:

$$C_{\Delta, n} \approx \frac{\varphi_1 q + \varphi_2 (N - q)}{N} \quad (3.8)$$

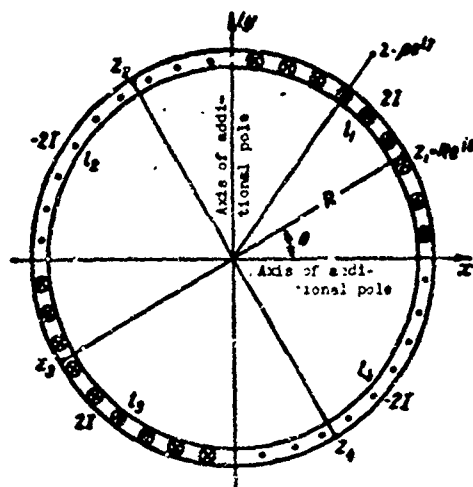


Fig. 35.

Check:

$$\varphi_1 = 0.018/W, \varphi_2 = 0.984/W, C_{a,n} = 0.347/W.$$

We determine constant $C_{a,n}$ for motor NE-409/840 with the armature winding of machine powered.

Let us assume that the current in the armature is distributed evenly on the surface of the armature in a thin film, the direction of the current being different on each quadrant of the circumference of armature. Distribution of current is shown in Fig. 35. Complex potential $d\Omega$ at point $z = qe^{i\varphi}$ from four filaments of current in symmetrically located points z_1, z_2, z_3, z_4 is

$$d\Omega = \frac{dl}{2\pi} \ln \frac{(z - z_1)(z - z_3)}{(z - z_2)(z - z_4)}. \quad (23.9)$$

Utilizing the condition of symmetry of distribution of current over the armature, integrating and eliminating the imaginary part from the expression for Ω , we obtain

$$U_n(q, \varphi) = -\frac{4I}{\pi^2} \sum_{n=1}^{\infty} \left(\frac{R}{q}\right)^{2n-1} \cdot \frac{\cos 2(2n-1)\varphi}{(2n-1)^2}, \quad (23.10)$$

on surface of armature $q = R$ and

$$U_n(R, \varphi) = -\frac{4I}{\pi^2} \sum_{n=1}^{\infty} \frac{\cos 2(2n-1)\varphi}{(2n-1)^2}, \quad (23.11)$$

Table 8.

No. of points	$\frac{U_m}{IW}$	No. of points	$\frac{U_m}{IW}$	No. of points	$-\frac{U_m}{IW}$	No. of points	$-\frac{U_m}{IW}$
1	0.445	5	0.355	9	0.241	13	0.171
2	0.44	6	0.326	10	0.225	14	0.1615
3	0.425	7	0.281	11	0.202	15	0.163
4	0.391	8	0.261	12	0.188	16	0.1613

where I is the number of ampere-turns occurring on the section of the armature between axes of neighboring - (main and auxiliary) - poles. The distribution of potential (23.11) on the developed circumference of the armature represents expansion into Fourier series of a periodic isosceles triangle.

Table 9.

No. of points	$\frac{U_m}{IW}$	No. of points	$\frac{U_m}{IW}$	No. of points	$-\frac{U_m}{IW}$	No. of points	$-\frac{U_m}{IW}$
1	0.5	5	0.25	9	0.138	13	0.157
2	0.45	6	-0.2435	10	0.1505	14	0.1588
3	0.4	7	-0.1476	11	0.1495	15	0.1596
4	0.35	8	-0.133	12	0.152	16	0.16

Results of calculation of values of potential at the same points of the contour as in the preceding example are given in Table 8 (contour of core of additional pole $J = 0$) and Table 9 (external contour of region $J = h$).

Curves of distribution of potential $U_{m1}(\tau)$, $U_{m1}(\tau + ih)$ and $U_{m1}(\tau + ih) - U_{m1}(\tau)$ are shown in Fig. 35, plotted along on the boundary of infinite band ($0 \leq \tau \leq N$).

We determine the constant $C_{\Pi.H.}$ from formula (14.30). Determining the area of curve $U_{m1}(\tau + ih) - U_{m1}(\tau)$ from the drawing on the interval ($0 \leq \tau \leq N$), we obtain $S = 25.61$ and, consequently,

$$C_{\Pi.H.} = \frac{S}{N} = \frac{25.61}{95.5} = 0.2681. \quad (23.12)$$

Replacing curve $U_{m1}(\tau + ih) - U_{m1}(\tau)$ by a rectangle of equivalent area, as it was shown by the dotted line in Fig. 35, it is easy to derive a simple rule for approximate determination of $C_{\Pi.H.}$ when the armature winding is fed. Indeed, as can be seen from Fig. 36, the width of the rectangle is equal to the number of

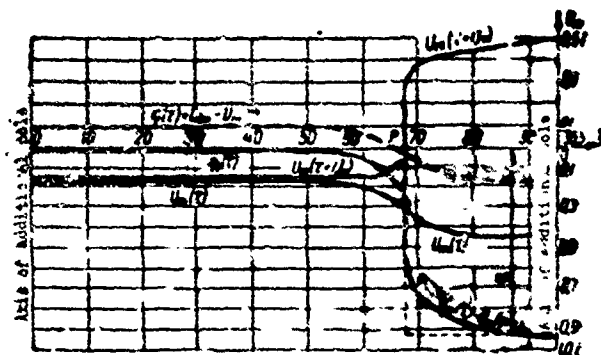


Fig. 36.

points occurring on the cross section of the contour of the model corresponding to the armature of the machine. The height of the rectangle is equal to the potential difference between the point on the base of the core of the auxiliary pole at a distance from its axis of $1/4$ of the base and corresponding to its point on the armature. The given relationships are general for all designs, therefore, determination of $C_{A.N.}$ when feeding the armature winding of a quadripole dc machine may be made in the following way:

- 1) determine the potential difference between the armature and core at points removed from the axis of the additional pole by a distance of $1/4$ the base of the core of the additional pole:

$$\varphi_2 = U_{m1}(\tau_1 + ih) - U_{m1}(\tau_1) = \left[1 - U_n \left(R, \frac{\theta_1}{2} \right) \right] - U_n \left(\rho_{A.N.}, \frac{\theta_1}{2} \right). \quad (23.13)$$

where θ_1 is the angle between the axis and angular point of the base of the core of the additional pole;

- 2) attempting a mapping, find the number of the point of intersection of the axis of the main pole with the armature $v = p$, considering $v = 0$ at the intersection of the axis of the additional pole with the yoke (in our example $p = 67.5$). Then constant $C_{A.N.}$ will be determined thus:

$$C_{A.N.} \approx \frac{\varphi_2(N - p)}{N}. \quad (23.14)$$

Check: $\varphi_2 = 0.9151$, $C_{A.N.} = 0.26851$.

Knowing the limiting values of potential of the field of magnetization on the contour of the core of the additional pole, the component of induction normal

to the armature can be determined just as when calculation the field when feeding the windings of the main poles, i.e., to make four cuts along segments of the axes between the yoke and cores of the additional poles and to thereby, convert the six-connected region of the air interval of the machine into a two-connected one. With conformal mapping (Fig. 30) the section of the model contour corresponding to the line of cut will practically reduce to a point and the change of potential on it will lead to a jump. Values of potential $\varphi_1(\tau)$ on all points of the boundaries of the band will consequently be determined.

Knowing the value of $C_{д.п.}$ it is simply to derive simple approximate formulas for the magnitude of induction of the field of additional poles and reaction of the armature at points on the circumference of the armature of a quadripole machine having a gap between the cores of the additional poles and the yoke.

Field of additional poles. From Fig. 34 one may see that constant $C_{д.п.}$ displaces the curve of potential distribution on the core of the pole such that the potential difference on the axis of the pole between the tip and the armature decreases to a magnitude equal to $IW_{д.п.} - C_{д.п.}$ and remains almost constant on the entire surface of the tip lying opposite the armature (dotted curve in Fig. 34).

Taking, as was done in § 22 the potential of the armature equal to zero, for the induction of the field of additional poles at points of the circumference of the armature we obtain:

$$B(b_n)_{a.c} = -\frac{\mu_0}{k_{an}h} \left| \frac{\Delta u_N}{\Delta u_n} \right| \frac{IW_{д.п.} - C_{д.п.}}{e^{k(\rho+1-n)} + 1}, \quad (23.15)$$

where $C_{д.п.}$ is determined from expression (23.8).

Field of reaction of armature. From Fig. 36 one may see that the constant $C_{д.п.}$ displaces the curve of potential distribution on the core of pole such that the potential difference on the axis of the pole between the tip and armature decreases to a magnitude equal to $IW_{д.п.} - C_{д.п.}$ where the magnitude of potential on the entire surface of the tip opposite the armature is almost unchanged (dotted curve in Fig. 36), whereas, the potential on the armature decreases linearly.

Taking in the same way as was done in § 22, the potential of the stator to equal to zero, the potential of the armature at point b_n is proportional to the distance along the circumference of the armature from the axis of the main pole to point b_n and equal to

$$\varphi_a(b_n) = \frac{b_n}{b_N} W_{a, \text{max}} \quad (23.16)$$

and, finally, the potential of the tip of the additional pole equals $C_{д.п.}$. For the magnitude of induction of the field of reaction of the armature at points on the circumference of the armature we obtain:

$$B(b_n)_a = -\frac{\mu_0}{k_{an}h} \left| \frac{\Delta v_N}{\Delta u_a} \right| \left[W_{a, \text{max}} \frac{b_n}{b_N} - \frac{C_{д.п.}}{e^{N(p+1-n)} + 1} \right]. \quad (23.17)$$

where $C_{д.п.}$ is determined from expression (23.16). Here the designations are the same as in formulas (22.15)-(22.18).

CHAPTER IV

INTEGRATORS FOR CALCULATION OF FLAT FIELDS AND THEIR APPLICATION

§ 24. Electrointegrator for Simulation of Particular Solution of Poisson Equation

Calculation of the static field in an isotropic medium reduces solution of the boundary value problem for the equation

$$\Delta\varphi=f(x, y). \quad (24.1)$$

As a rule density of field sources $f(x, y)$ is different from zero only in a limited region. On the remaining plane $\varphi(x, y)$ is a harmonic function. The contour of the investigated region usually is the boundary between two distinct media and the boundary conditions are determined by their properties. In individual cases, for example when calculating the magnetic field in an air interval of an electrical machine or when calculating the strength of a twisted prismatic rod, the right side of equation (24.1) is known and calculation immediately reduces to a solution of the boundary value problem for the Poisson equation. In other cases, for instance when calculating the distribution of density of sinusoidal current in a cylindrical conductor or the magnetic field in steel component an electrical machine, $\varphi(x, y)$ satisfies a more complicated differential equation the right side of which can depend on the sought function and its derivatives. However, even here sometimes can be obtained result by means of solution of a series of boundary value problems for the Poisson equation [27].

It is well known that any function which is a solution of the boundary value problem for the Poisson equation can be presented in the form of sum of the harmonic functions $\varphi_1(x, y)$ determined in the given region by boundary conditions, and the function $\varphi_2(x, y)$ determined on the entire plane only by the distribution of sources $f(x, y)$. The function $\varphi_2(x, y)$ carries name of particular solution of the Poisson equation. Analytic solution of the boundary value problem for the Poisson equation in general is very complicated and requires great expenditure of calculating labor and, moreover, does not ensure the accuracy necessary in practice. Therefore it is of interest to develop devices which model a solution to the problem. However to prepare a universal model allowing a change in the contour of the region and boundary conditions on it and at the same time ensuring the necessary accuracy is impossible. The manufacture of a model for every concrete problem is very complicated and costly.

In this connection a solution of the boundary value problem by complex means combining analytic calculation with simulation of the most complicated individual labor consuming mathematical operations is rational.

Let us clarify what has been said with an example.

It is known that a solution of the Dirichlet problem for the Poisson equation can be obtained using the following mathematical operations:

1) considering the region unlimited, find potential function $\varphi_2(x, y)$ with a given distribution of density of sources $f(x, y)$ in the region, in other words, find a particular solution of the Poisson equation;

2) having determined value of $\varphi_2(t)$ on the contour of the region, subtract them from the given contour values

$$\varphi_1(t) = \varphi(t) - \varphi_2(t);$$

3) considering $\varphi_1(t)$ as boundary values of harmonic function $\varphi_1(x, y)$, find this function, i.e., solve the Dirichlet problem for the Laplace equation;

4) combining $\varphi_1(x, y)$ and $\varphi_2(x, y)$, obtain a solution to the problem

$$\varphi(x, y) = \varphi_1(x, y) + \varphi_2(x, y).$$

Analytic fulfillment of the first and third operations of the given algorithm, being very complicated and labor consuming, are expediently modeled. Remaining operations cause no difficulty. Let us consider a device which models the particular solution of the Poisson equation and will clarify on what the accuracy of simulation on it depends.

As is known potential function $\varphi_2(x, y)$, satisfying the Poisson equation on a plane is determined by the expression

$$\varphi_2(x, y) = \operatorname{Im} \left[\frac{-i}{2\pi} \iint_S f(x_0, y_0) \ln(z - z_0) dS \right], \quad (24.2)$$

where $z_0 = x_0 + iy_0$ is a complex coordinate of element dS in the region S , filled by sources of density $f(x, y)$, over whose area integration is performed $z = x + iy$.

Analogous expression will determine the potential of the dc field in an unlimited conducting sheet with constant unit-surface conductivity γ if to every point of section S of the sheet is applied a current of density $\delta = \gamma f(x, y)$. Consequently the sought function $\varphi_2(x, y)$ can be modeled by the potential of a field of current in a conducting sheet.

So that the potential of the field of current in the sheet yields a particular solution of the Poisson equation it is necessary:

- 1) that the sheet be uniform and infinitely large;
- 2) that the distribution of density of current applied to the sheet correspond to the $f(x, y)$, standing in the right side of the Poisson equation.

It is not possible to prepare a model satisfying these requirements. Dimensions of the model are limited and distribution of adjustable sources on it can only be discrete. Besides, at the place of connection of the source homogeneity of the sheet of model is disturbed. All this causes an error during modeling. Let us estimate the magnitude of error and clarify the possibility of reducing it.

Obviously the modeling error will depend not only on the dimensions and form of the sheet but also on those boundary conditions which we assign to its perimeter. If the region filled with sources can be combined with section in center sheet and in it predominate sources of one sign then it would be to select the model sheet in the form of a circle and its contour attach a contact bus of great conductivity using it to draw current from the model. Really, with such a distribution of sources on an unlimited plane, according to removal from sources the lines of equal potential will approach concentric circles and if along one of them is cut a sheet, ensuring the former value of potential on the line of cut, the field of current in the sheet will not be changed. Inasmuch as at a finite distance from sources the lines of equal potential in general

will differ from circles, on the bus induced charges appear and their field will introduce an error.

We will consider that the model is made from a uniform conducting sheet in the form of a circle of radius R , the central part of which (circle of radius r) is filled with adjustable sources of current connected to individual points of the sheet. On the circumference of the sheet is soldered a bus of incommensurably large conductivity with help of which current is removed. If sources of one sign evenly fill inner circle r the equipotential line will coincide with the boundary of circle R and there will be no distortion of the field on the model.

The biggest distortion of the field induced on the bus by charges will occur when the sources are equal in magnitude, have opposite signs and are concentrated at two diametrically opposite points on the circumference.

When solving problems in the majority case it is required to find not the actual function $\varphi(x, y)$, but its derivative — the gradient. It is considerably more difficult, to ensure the necessary accuracy of simulation of the gradient of a function than the same accuracy of function modeling. Therefore the error during simulation will be estimate from the ratio of moduli of gradients of field potential produced by charges induced on the bus, and the field of sources.

Let us assume there are two sources — positive τ at point $(r, 0)$ and negative τ at point $(-r, 0)$ (Fig. 37). The complex potential of the field of these sources on an unlimited plane was equal to

$$W(z) = -i \frac{\tau}{2\pi\gamma} \ln \frac{z-r}{z+r}, \quad (24.3)$$

but the charges induced on the bus equalize the electrical potential of the bus making it constant, and distort the field within circle R .

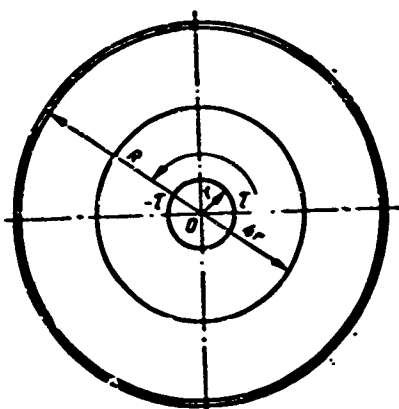


Fig. 37.

Applying the method of mirror images, we find the complex potential $W_1(z)$ of the resultant field. The field of charges induced on the bus of inside circle R is equivalent to the field of two imaginary charges $\pm\tau$, located at points $(-\frac{R^2}{r}, 0)$ and $(\frac{R^2}{r}, 0)$. Consequently

$$W_1(z) = -i \frac{\tau}{2\pi\gamma} \left[\ln \frac{z-r}{z+r} + \ln \frac{z + \frac{R^2}{r}}{z - \frac{R^2}{r}} \right]. \quad (24.4)$$

The potential of the distorting field of charges induced on the bus has the form

$$\Delta W(z) = W_1(z) - W(z) = -i \frac{\tau}{2\pi\gamma} \ln \frac{z + \frac{R^2}{r}}{z - \frac{R^2}{r}}. \quad (24.5)$$

The modulus of the gradient of this potential will be written thus:

$$|\text{grad } \Delta U| = |\Delta W'(z)| = -i \frac{\tau}{2\pi\gamma} \frac{R^2}{r^2} \left| \frac{2r}{z^2 - \frac{R^4}{r^2}} \right| \quad (24.6)$$

the modulus of the gradient of field potential of sources

$$|\text{grad } U| = |W'(z)| = -i \frac{\tau}{2\pi\gamma} \left| \frac{2r}{z^2 - r^2} \right|. \quad (24.7)$$

Magnitude of relative error ($z = qe^{i\psi}$)

$$\delta = \frac{|\text{grad } \Delta U|}{|\text{grad } U|} = \frac{R^2}{r^2} \left| \frac{z^2 - r^2}{z^2 - \frac{R^4}{r^2}} \right| = -\frac{q^2}{R^2} \sqrt{\frac{1 - 2\left(\frac{r}{q}\right)^2 \cos 2\psi + \left(\frac{r}{q}\right)^4}{1 - 2\left(\frac{rq}{R^2}\right)^2 \cos 2\psi + \left(\frac{rq}{R^2}\right)^4}}. \quad (24.8)$$

The quantity δ assumes maximum value on the circumference when $q = R$:

$$\delta_{\max} = 1 = 100\%.$$

In problems encountered in practice it is usually necessary to define the the function in a region whose dimensions exceed by 3-4 times the dimensions of the region occupied by the sources. Consequently it is possible to take $q < 4r$.

The biggest error in the considered region is determined by the expression

$$\delta_{\max} < \frac{16r^2}{R^2} \sqrt{\frac{1 - 2\left(\frac{1}{4}\right)^2 \cos 2\psi + \left(\frac{1}{4}\right)^4}{1 - 2\left(\frac{4r^2}{R^2}\right)^2 \cos 2\psi + \left(\frac{4r^2}{R^2}\right)^4}} \approx 16 \frac{r^2}{R^2} \quad (R > 4r). \quad (24.9)$$

So that the error does not exceed a permissible magnitude it is necessary to select an appropriate value of the ratio $\frac{r}{R}$. The radius of the section of the model filled by sources, from a consideration of convenience of simulation and measurement, will be taken equal to 15 cm. Taking the biggest permissible magnitude of error δ equal to 3%, we obtain

$$R = \frac{4r}{\sqrt{0.03}} = 23.1r = 346 \text{ cm},$$

i.e., the diameter of the sheet of the model must be made equal to 7 m.

It is natural that such dimensions of the model are totally unacceptable, and all the more so that the working part will be only the circle $q = 4r$.

The entire remaining part of the model — ring ($4r < q < 23r$) — serves to decrease the error in working circle.

Dimensions of the model may however be reduced to the dimensions of its working part if one were to replace the external nonworking ring ($4r < q < 23r$) with its conformal mapping realizing the function [11]

$$\zeta = \frac{(4r)^2}{z}. \quad (24.10)$$

As a result of mapping circumference $q = 4r$ (Fig. 37) will pass over to a circumference of the same radius

$$\zeta_1 = \frac{(4r)^2}{4re^{-i\theta}} = 4re^{i\theta}.$$

Circumference $q = R = 23r$ will also pass over into a circumference of radius $0.7r$

$$\zeta_2 = \frac{(4r)^2}{23re^{-i\theta}} = 0.7re^{i\theta}.$$

Consequently the external ring will be mapped also on a ring turned about the real axis by 180° since instead of z in formula (24.10) stand \bar{z} , the inner contour of the mapped ring passing over to the outer contour and conversely.

Let us imagine now that the mapped ring, as also the circle, is prepared from a conducting sheet. Let us put the ring under the circle and connect them electrically along circumference $q = 4r$. To the internal circumference of the ring we join a bus of infinite conductivity. The obtained model of a two-sheet surface with sources assigned in circle $q < 4r$ may be considered as region of existence of a complex potential $W_M(z)$ the current field equal in the circle $q < 4r$ to the complex potential $W_1(z)$ of the field in the initial great circle $q = R$ with just such a distribution of source in it.

Let us demonstrate this. Due to the electrical connection values of complex potential $W_M(z)$ on points of both circumferences $q = 4r$ of the ring and the circle will be equal and consequently $W_M(z)$ analytically will continue on the ring lying under the circle up to an internal circumference $q = 0.7r$ where its imaginary part — electrical potential U_M — will take on a constant value

$$U_M = \text{Im}[W_M(\zeta)] = \text{const.}$$

This is explained by the fact that there a bus of infinite conductivity is attached.

Let us map ring $0.7r < \rho < 4r$ with the help of inverse function

$$z = \frac{(4r)^2}{\xi} = \frac{(4r)^2}{\rho_1 e^{-i\varphi}} = \frac{(4r)^2}{\rho_1} e^{i\varphi} \quad (24.11)$$

onto an external ring $4r \leq \rho \leq R$. Here points of the internal circumference of the ring will remain coincident with points on the boundary of the circle. Values of complex potential at points of both rings corresponding to each other during conformal mapping are preserved, consequently, they are equal to the $W_M(4re^{i\varphi})$ on superimposed circumference $\rho=4r$ of the ring and circle. Hence complex potential of the current field in the external ring will be analytic continuation of the complex potential of current in the circle. On external circumference $\rho=R$ the imaginary part of $W_M(z)$ will be constant.

Comparing complex potentials $W_1(z)$ and $W_M(z)$ in the entire region — circle R , — we notice that each of them is completely determined by an identical distribution of sources in circle R and constant value of its imaginary part on the boundary of the region. Here, as follows from the theorem of uniqueness, $W_1(z)$ and $W_M(z)$ can differ only by a constant value which may be set equal to zero:

$$W_M(z) = W_1(z) + c.$$

Such a conclusion permits preparing a model for which, during modeling, the error caused by limited dimensions of the sheet will be arbitrarily small. For this it is sufficient to make the radius of the internal circumference of the ring, and hence the radius of the contact bus sufficiently small. We select the internal radius of the ring to equal to 2.5 cm. This corresponds to an outer circle circumference of $R = 1440$ cm. The greatest error ε_1 on the contour of the working circle of the model $\rho=4r=0.6$ m amounts to 0.17%.

The modeling circle and ring are prepared from a thin uniform metallic sheet (manganin of thickness 0.25-0.3 mm), then they are put one on the other and are welded along the circumference by contact spot welding. It necessary to ensure uniform and sufficiently frequent location of weld points along the circumference of the sheets. Between the sheets is laid a thin insulation. Connection of sources to the circle is accomplished through holes in the ring by contact screws of small diameter ($2 r_0 = 2$ mm). The sources of current are

made in the form of long rheostats of small diameter and are located in two rows along the circumference of the model. The supply unit is located under the model and consists of a stabilizer, 220/5 transformer and selenium rectifier. Total current in the sheet is 200 A.

§ 25. Modeling Errors

Influence of discrete distribution of sources. An assigned, continuous distribution of sources on the model is replaced by discrete supply of current to separate sections of the sheet. Sources of current are joined to the central circle r of the upper sheet of the model by means of brass contact screws of small diameter ($2r_0$), passing through holes in the sheet located in node of a square grid with sides d . The grid contains 400 contact screws. When solving a concrete problem the region occupied by the sources is put on a circle with contact screws and to those screws which fall in the region a current is supplied. The remaining screws are de-energized. The field in the model will obviously be distorted as compared to the one sought first due to discrete supply of current, second due to nonuniformities of the sheet by caused by the switching on of contact screws whose conductivity may be taken infinitely large. Let us estimate the magnitude of error caused by discrete feed of current to the model.

Distortion of the field in the model will have two causes: the discrete structure of all the totality of sources filling the assigned region; distribution of sources near point of measurement differing from that assigned.

Let us clarify the influence on magnitude of error of each of these causes.

We divide the entire region filled by sources into squares of side d and replace each square with a circular source of radius r_0 . The complex potential of the field of a source with magnitude τ , distributed evenly in a square with side d is expressed, outside the square, by the formula [24].

$$W(z) = -i \frac{\tau}{2\pi\gamma} \left[\ln z - \sum_{n=1}^{\infty} \frac{(-1)^n}{2n(2n+1)(4n+1)2^{2n+1}} \left(\frac{d}{z} \right)^{4n} \right] \quad (25.1)$$

(origin of coordinates $z = 0$ at the center of the square). The complex potential of a circular source r_0 of the same magnitude τ equals

$$W_1(z) = -i \frac{\tau}{2\pi\gamma} \ln z. \quad (25.2)$$

The difference in potentials is written thus:

$$\Delta W = W(z) - W_1(z) = \frac{i\tau}{2\pi\gamma} \sum_{n=1}^{\infty} \frac{(-1)^n}{2n(2n+1)(4n+1)2^{2n+1}} \left(\frac{d}{z}\right)^{4n}. \quad (25.3)$$

The component of the modulus of intensity brought about by this difference has the form

$$|\text{grad } \Delta U| = |\Delta W'(z)| = \frac{\tau}{2\pi\gamma} \left| \sum_{n=1}^{\infty} \frac{(-1)^n}{(2n+1)(4n+1)2^{2n}} \left(\frac{d}{z}\right)^{4n} \right| < \frac{\tau}{2\pi\gamma} \cdot \frac{1}{60|z|} \left(\frac{d}{|z|}\right)^4. \quad (25.4)$$

The modulus of field strength of the circular source is expressed by formula

$$|\text{grad } U_1| = |W'_1(z)| = \frac{\tau}{2\pi\gamma} \cdot \frac{1}{|z|}, \quad (25.5)$$

and relation of the moduli of intensity

$$\delta = \frac{|\text{grad } \Delta U|}{|\text{grad } U|} < \frac{1}{60} \left(\frac{d}{|z|}\right)^4. \quad (25.6)$$

For $|z| > d$ this quantity is less than 2% and drops rapidly with an increase in $|z|$. Consequently beyond the limits of a circle of radius d distortion of the field as a result of replacement of the source, continuously distributed in a square of side d , with a circular source r_0 cannot be taken into account. All the more so it is not possible to consider distortion of the field beyond the borders of the region caused by the discrete structure of the entire set of sources filling it. Distortion of the field inside the region will be caused only by those circular sources which are located alongside the considered point. Let us estimate the error caused by this distortion when measuring potential and intensity. We make the appraisal for the case when the entire circle r is filled with sources of constant density σ . Potential outside circle r is equal

$$U(q) = -\frac{\sigma r^2}{2\gamma} \ln q + c. \quad (25.7)$$

Let us take potential of contact bus on circumference R equal to zero, then

$$c = \frac{\sigma r^2}{2\gamma} \ln R \quad (25.8)$$

and

$$U(q) = \frac{\sigma r^2}{2\gamma} \ln \frac{R}{q} \quad (q > r).$$

Potential inside circle r equals

$$U^+(q) = -\frac{\sigma q^2}{4\gamma} + c_1.$$

On circumference $\rho = r$ the potential is continuous, hence

$$c_1 = \frac{\sigma r_1^2}{2\gamma} \left(\ln \frac{R}{r} + \frac{1}{2} \right)$$

and

$$U^+(q) = -\frac{\sigma q^2}{4\gamma} + \frac{\sigma r^2}{2\gamma} \left(\ln \frac{R}{r} + \frac{1}{2} \right). \quad (25.9)$$

With a decrease in radius of the contact screw r_0 its potential will increase and at the same time, distortion of the field near the screw will increase. Let us find the magnitude of the ratio $\frac{r_0}{d}$, at which the error caused by this distortion will be less than permissible. To simplify calculations we will consider that every circular source (screw) replaces a source continuously distributed in a circle R_1 of area d^2 . Besides, determination of the potential of source r_0 we will consider that all the remaining sources are continuously and evenly distributed in circle r .

Let us assume that the center of the considered source r_0 is at a distance m from the center of circle r . Since source r_0 replaces itself by sources evenly distributed within limits of circle R_1 , then its potential may be presented in the form of a sum of two components: the first, caused by all the remaining sources continuously distributed outside circle R_1 and the second caused by source r_0 . The first component of potential we calculate impressing on potential U of the field of positive sources evenly filling circle r , a potential of a field U_n of negative sources of the same density evenly filling a small circle R_1 displaced a distance m from the center of circle. Applying method of mirror images we find that outside of circle R_1

$$U_n^-(q) \approx \frac{\sigma R_1^2}{2\gamma} \ln \frac{\rho_1}{\rho_2} + c_n.$$

Here ρ_1 and ρ_2 — distance from point of determination of potential to point m and its mirror image R^2/m on circumference R respectively.

On the contact bus (when $\rho_1 = R - m$, $\rho_2 = \frac{R^2 - m^2}{m}$) the potential equals zero. Thus

$$c_n = -\frac{\sigma R_1^2}{2\gamma} \ln \frac{m}{R + m}, \quad (25.10)$$

$$U_n^-(q) = \frac{\sigma R_1^2}{2\gamma} \ln \frac{\rho_1 (R + m)}{\rho_2 m}.$$

Inside circle R_1

$$U_n^+(q_1) = \frac{\sigma q_1^2}{4\gamma} + c_{n1}.$$

On boundary $(q_1 = R, q_2 = \frac{R^2}{m} - m - R)$ the potential is continuous

$$\begin{aligned} \frac{\sigma R_1^2}{4\gamma} + c_{n1} &= \frac{\sigma R_1^2}{2\gamma} \ln \frac{R_1(R+m)}{R^2 - m^2 - R_1 m}; \\ U_n^+(q_1) &= \frac{\sigma q_1^2}{4\gamma} - \frac{\sigma R_1^2}{2\gamma} \left[\ln \frac{R^2 - m^2 - m R_1}{R_1(R+m)} + \frac{1}{2} \right]. \end{aligned} \quad (25.11)$$

Consequently the first component of potential at point m will be determined thus:

$$\begin{aligned} U_I(m) &= U^+(m) + U_n(0) = \\ &= -\frac{\sigma m^2}{4\gamma} + \frac{\sigma r^2}{2\gamma} \left(\ln \frac{R}{r} + \frac{1}{2} \right) - \frac{\sigma R_1^2}{2\gamma} \left[\ln \frac{R^2 - m^2 - m R_1}{R_1(R+m)} + \frac{1}{2} \right]. \end{aligned} \quad (25.12)$$

The second component of potential at point m caused by circular source r_0 equals

$$U_{II}(q_1) = -\frac{\sigma R_1^2}{2\gamma} \ln \frac{q_1(R+m)}{q_2 m}. \quad (25.13)$$

On circumference $\rho_1 = r_0$, and consequently, at point m

$$U_{II}(r_0) = -\frac{\sigma R_1^2}{2\gamma} \ln \frac{r_0(R+m)}{R^2 - m^2} = -\frac{\sigma R_1^2}{2\gamma} \ln \frac{r_0}{R-m}. \quad (25.14)$$

Resultant potential $U_{\Sigma} = U_I + U_{II}$ at point m is

$$U_{\Sigma}(m) = -\frac{\sigma m^2}{4\gamma} + \frac{\sigma r^2}{2\gamma} \left(\ln \frac{R}{r} + \frac{1}{2} \right) - \frac{\sigma R_1^2}{2\gamma} \left[\ln \frac{r_0(R^2 - m^2 - m R_1)}{R_1(R^2 - m^2)} + \frac{1}{2} \right]. \quad (25.15)$$

The absolute error at point m equals

$$\begin{aligned} U_{\Sigma}(m) - U^+(m) &= -\frac{\sigma R_1^2}{2\gamma} \left[\ln \frac{r_0}{R_1} \left(1 - \frac{m R_1}{R^2 - m^2} \right) + \frac{1}{2} \right] \approx \\ &\approx -\frac{\sigma R_1^2}{2\gamma} \left(\ln \frac{r_0}{R_1} + \frac{1}{2} \right). \end{aligned} \quad (25.16)$$

The relative error at point m (with respect to voltage between the center of the model and a circumference of radius r) is

$$\delta = \frac{U_{\Sigma}(m) - U^+(m)}{U^+(0) - U^+(r)} \approx -\frac{2R_1^2 \left(\ln \frac{r_0}{R_1} + \frac{1}{2} \right)}{r^2}. \quad (25.17)$$

Hence one may see that under the condition $\ln \frac{r_0}{R_1} = -\frac{1}{2}$ or $\frac{r_0}{R_1} = 0.606$ the

relative error δ equals zero. However during derivation we did not consider distortion of the field in the model due to nonuniformity of the sheet caused by attaching contact screws of radius r_0 . This distortion will be less smaller the ratio $\frac{r_0}{R_1}$, therefore we are assigned a permissible magnitude δ_m and from this condition we determine the minimum value of $\frac{r_0}{R_1}$

$$\delta_m^2 \leq -2R_1 \ln \frac{r_0}{R_1} - R_1^2. \quad (25.18)$$

In circle r is placed N sources, consequently $\pi r^2 = N a^2$, whence $r = d \sqrt{\frac{N}{\pi}}$. Considering what $\pi R_1^2 = d^2$, we obtain $r = R_1 \sqrt{N}$

Placing this value in expression (25.18) we have

$$\ln \frac{R_1}{r_0} \leq \frac{\delta_m N + 1}{2}, \quad (25.19)$$

whence $\frac{r_0}{d} > \frac{1}{\sqrt{\pi e^{\delta_m N + 1}}}$; for $r = 150$ mm, $\delta_m = 0.01$ and $N = 400$ we obtain $r_0 > 0.615$ mm.

Let us take $r_0 = 1$ mm, $d = 15$ mm and contact screws we select with dimension M2.

Let us now turn to an appraisal of error for intensity. Measurement of field strength on the model is made with a double probe with rigidly clamped needles, the distance between whose centers equals d . Actually the potential difference between two points at a distance d is measured, therefore the appraisal of error will determine for this difference.

The potential difference between points $(\varrho = m \pm \frac{d}{2})$ with continuous filling of circle r by sources of constant density σ should equal

$$\Delta U(m) = \frac{\sigma \left(m + \frac{d}{2}\right)^2}{4\gamma} - \frac{\sigma \left(m - \frac{d}{2}\right)^2}{4\gamma} = \frac{\sigma m d}{2\gamma}. \quad (25.20)$$

Let us find the voltage between those points with a discrete distribution of sources r_0 in circle r . All sources located beyond the limits of a circle of radius $R_2 = \frac{3}{2}d$ with center at point m (Fig. 38), will be replaced by continuously distributed sources. The voltage between the probe needles can now be calculated, determining the field in circle R_2 from sources continuously distributed outside the circle and from nine sources r_0 falling within the circle R_2 .

If during measurements the center of the probe coincides with the center of the contact screw, then due to symmetry of the field of nine sources r_0 both needles fall on the same equipotential line of the field of these sources and

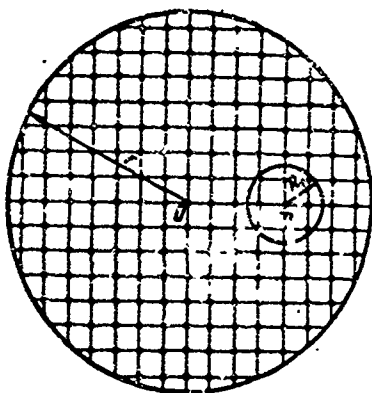


Fig. 38.

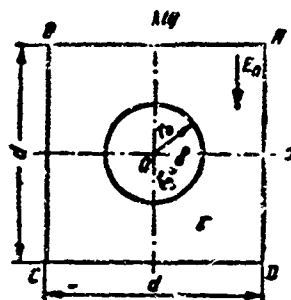


Fig. 39.

the voltage between the needles will be determined only by sources not falling within circle R_2 . Potential of the field of sources distributed outside the circle R_2 equals

$$U^+(q) + U_-(q) = -\frac{\sigma q^2}{4\gamma} + \frac{\sigma q_1^2}{4\gamma} + \sigma.$$

Voltage between points $\left(p = m \pm \frac{d}{2}, q_1 = \pm \frac{d}{2}\right)$

$$\Delta U_{\pm}(m) = \frac{\sigma \left(m + \frac{d}{2}\right)^2}{4\gamma} - \frac{\sigma \left(m - \frac{d}{2}\right)^2}{4\gamma} - \frac{\sigma \left(\frac{d}{2}\right)^2}{4\gamma} + \frac{\sigma \left(\frac{d}{2}\right)^2}{4\gamma} = \frac{\sigma m d}{2\gamma}, \quad (25.21)$$

i.e., equals the sought voltage

$$\Delta U_{\pm}(m) = \Delta U(m). \quad (25.22)$$

Displacement of the center of the probe from the center of source r_0 has little effect on the accuracy of measurement. Thus with displacement of the centers by $\frac{d}{4}$ the relative error will total $0.01 \frac{d}{m}$.

Thus during measurement of potential and average field strength in the model, both in the region occupied by sources and also outside it the error from their discrete distribution need not be considered in view of its smallness.

Influence of sheet nonuniformity. Let us estimate the error caused by connecting contact screws in the upper circle of the model. The conductivity of a unit surface of cross section of a contact screw is incommensurably larger than the conductivity of a unit surface γ , therefore the cross section of the

screw will be considered as a superconducting circle of radius r_0 . Under the influence of neighboring sources in every such circle charges will be displaced and will create their own field distorting the field of sources in the entire model. At separate points of every square with side d containing a contact screw, due to distortion the field strength may differ considerably from the intensity of the sought field of sources, however on an average its value measured with a double probe, local oscillations have little influence. This permits, during appraisal of error, to replace the nonuniform section of the sheet with screws by a uniform section of constant conductivity γ_1 equal to the conductivity of a square with side d in the center of which is connected a superconducting circle r_0 .

With our earlier selected magnitude of relation $\frac{d}{r_0} = 15$ the influence of displaced charges of one cylinder on the displacement of charges in the other is insignificant and during calculation this influence it need not be considered. Under this condition conductivity of a square d with a superconducting circle r_0 connected to it can be approximately found.

Let us consider a conducting cylinder placed in a uniform field (Fig. 39). The expression for complex potential of the resultant field in this case has the form

$$W(z) = J(x, y) + iU(x, y) = E_0 \left(z + \frac{r_0^2}{z} \right), \quad (25.23)$$

where E_0 — intensity of a uniform field

$$U(x, y) = E_0 \left(1 - \frac{r_0^2}{x^2 + y^2} \right) y, \quad J(x, y) = E_0 \left(1 + \frac{r_0^2}{x^2 + y^2} \right) x. \quad (25.24)$$

Conductivity of square d we find taking the ratio of mean value of difference of stream functions on the sides of the square AD and BC to the mean value of potential difference in sides AB and CD

$$\gamma_1 = \gamma g \approx \gamma \frac{\Delta J_{cp}}{\Delta U_{cp}}, \quad (25.25)$$

$$\Delta J_{cp} = \frac{1}{d} \int_{-\frac{d}{2}}^{\frac{d}{2}} \left[J\left(\frac{d}{2}, y\right) - J\left(-\frac{d}{2}, y\right) \right] dy = E_0 d \left(1 + \frac{\pi r_0^2}{d^2} \right). \quad (25.26)$$

$$\Delta U_{\text{ep}} = \frac{1}{d} \int_{-\frac{d}{2}}^{\frac{d}{2}} \left[U\left(x, \frac{d}{2}\right) - U\left(x, -\frac{d}{2}\right) \right] dx = E_0 d \left(1 - \frac{\pi r_0^2}{d^2} \right), \quad (25.27)$$

hence

$$\gamma_1 = \gamma g \approx \gamma \frac{1 + \frac{\pi r_0^2}{d^2}}{1 - \frac{\pi r_0^2}{d^2}} \approx \gamma \left(1 + 2 \frac{\pi r_0^2}{d^2} \right). \quad (25.28)$$

For $d = 15r_0$ we obtain

$$\gamma_1 \approx 1.03\gamma. \quad (25.29)$$

Let us now turn to an appraisal of the error. For this it is sufficient to solve the following problem: inside a circle of radius r and conductivity γ_1 is assigned the distribution of sources (giving rise to the biggest error). Conductivity of the remaining plane is γ . Find the field inside and outside circle r and compare it with a field of the same distribution of sources on a uniform plane with conductivity γ .

Let us find complex potential $W_1(z)$ of the field of source τ located at point z_1 of circle r (Fig. 40). Using the conclusions of Sirl [41] we will consider that the field inside circle r coincides with a field created by source τ at point z_1 and source $\tau_1 = \tau \frac{\gamma_1 - \gamma}{\gamma_1 + \gamma}$ at point $z_2 = \frac{r^2}{z_1}$, with the assumption that the entire plane has conductivity γ_1 , the field outside circle r coincides with a field created by source $\tau_2 = \tau \frac{2\gamma}{\gamma + \gamma_1}$ at point z_1 and source $\tau_3 = \tau_1$ at point $z = 0$, with the assumption that the entire plane has a conductivity γ .

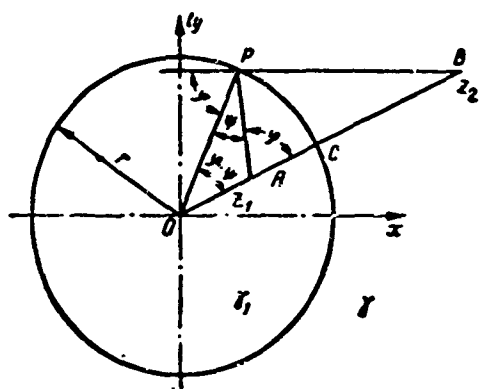


Fig. 40.

In accordance with this the complex potential of the field inside circle r has the form

$$W_1^+(z) = -i \frac{\tau}{2\pi\gamma_1} \left[\ln(z - z_1) + \frac{\gamma_1 - \gamma}{\gamma_1 + \gamma} \ln\left(z - \frac{r^2}{z_1}\right) \right]; \quad (25.30)$$

complex potential of the field outside the circle

$$W_1^-(z) = -i \frac{\tau}{2\pi\gamma} \left[\frac{\gamma_1 - \gamma}{\gamma_1 + \gamma} \ln z + \frac{2\gamma}{\gamma_1 + \gamma} \ln(z - z_1) \right]; \quad (25.31)$$

complex potential of the field of the same source in uniform medium with conductivity γ

$$W(z) = -i \frac{\tau}{2\pi\gamma} \ln(z - z_1). \quad (25.32)$$

The absolute error of potential inside the circle will be recorded thus:

$$\Delta W^+(z) = W_i^+(z) - W(z) = -i \frac{\tau}{2\pi\gamma_1} (\gamma_1 - \gamma) \left[\frac{1}{\gamma_1 + \gamma} \ln \left(z - \frac{r^2}{z_1} \right) - \frac{1}{\gamma} \ln(z - z_1) \right]; \quad (25.33)$$

absolute error outside the circle

$$\Delta W^-(z) = W_i^-(z) - W(z) = -i \frac{\tau}{2\pi\gamma} \cdot \frac{\gamma_1 - \gamma}{\gamma_1 + \gamma} \ln \left(1 - \frac{z_1}{z} \right); \quad (25.34)$$

error of intensity inside the circle

$$|\Delta W^+(z)| = -i \frac{\tau}{2\pi\gamma_1} (\gamma_1 - \gamma) \left[\frac{1}{(\gamma_1 + \gamma) \left(z - \frac{r^2}{z_1} \right)} - \frac{1}{\gamma(z - z_1)} \right], \quad (25.35)$$

$$|W'(z)| = -i \frac{\tau}{2\pi\gamma} \cdot \frac{1}{z - z_1}, \quad (25.36)$$

$$\delta^+ = \frac{|\Delta W^+(z)|}{|W'(z)|} = \frac{\gamma_1 - \gamma}{\gamma_1} \left| \frac{\gamma}{\gamma_1 + \gamma} \cdot \frac{z - z_1}{z - \frac{r^2}{z_1}} - 1 \right| =$$

$$= \frac{g - 1}{g} \left| \frac{1}{g + 1} \cdot \frac{z - z_1}{z - \frac{r^2}{z_1}} - 1 \right|. \quad (25.37)$$

Considering that g differs little from unity we may write

$$\delta^+ < (g - 1) \left| \frac{z - z_1}{2 \left(z - \frac{r^2}{z_1} \right)} - 1 \right| = \frac{g - 1}{2} \left| \frac{r^2 - |z_1|^2}{r^2 - z\bar{z}_1} + 1 \right|. \quad (25.38)$$

Let us set $|z_1| = ar$, $|z| = cr$, where $a \leq 1$ and $c \leq 1$, since $|z_1| < r$ and $z < r$, then, considering that the least value of the denominator $|r^2 - z\bar{z}_1|$ will occur under the condition $\arg z = \arg z_1$ we obtain

$$\left| \frac{r^2 - |z_1|^2}{r^2 - z\bar{z}_1} + 1 \right| < \left| \frac{1 - a^2}{1 - ac} + 1 \right|. \quad (25.39)$$

The biggest value of the right side of this inequality, equal to two, will occur under the condition $a = c$, i.e., when $z = z_1$ and the point of measurement coincides with the source. The relative error at this point is

$$\delta_{\text{max}}^+ < \frac{g-1}{2} 2 = g-1 \approx 2 \frac{\pi r_0^2}{d^2} = 0.03 = 3\%. \quad (25.40)$$

Hence it also follows that with any other distribution of sources in the circle the relative error δ^+ will be less than δ_{max}^+ .

The error of intensity outside the circle is written

$$|\Delta W'(z)| = i \frac{\tau}{2\pi\gamma} \cdot \frac{\gamma_1 - \gamma}{\gamma_1 + \gamma} \cdot \frac{z_1}{z(z - z_1)}, \quad (25.41)$$

$$\delta^- = \frac{|\Delta W'(z)|}{|W'(z)|} = \frac{\gamma_1 - \gamma}{\gamma_1 + \gamma} \left| \frac{z_1}{z} \right| = \frac{g-1}{g+1} \left| \frac{z_1}{z} \right|; \quad |z_1| < |z|, \quad r < |z|. \quad (25.42)$$

The maximum error δ_{max}^- will occur when $|z| = |z_1|$, i.e., when the source and point of measurement are on the boundary of the circle,

$$\delta_{\text{max}}^- = \frac{g-1}{g+1} \approx \frac{\pi r_0^2}{d^2} = 0.015 = 1.5\%. \quad (25.43)$$

For any other distribution of sources the relative error δ^- will be less than δ_{max}^- .

The analysis carried out leads to the conclusion that when solving concrete problems the resultant error of modeling the derivative of the sought function will not exceed 3% of the real magnitude at the measurement point. The error simulation of the function will be even less.

An electrointegrator permits determining not only the sought function but also its conjugate in that region where it exists. For instance, during calculation of the magnetic field in the air gap of an electrical machine it is necessary to know the distribution of the scalar magnetic potential along the contour of the steel parts for assigned distribution of current density in the cross section of the windings. The electrical potential of the field of current in the model can serve as an analog of only the vector magnetic potential which outside the cross section of the windings is a harmonic function, the conjugate of the scalar magnetic potential. Arranging the double probe in such a manner so that on every section of the contour of length d the needles of probe fall on the normal to the middle of the cross section on both sides at a distance $\frac{d}{2}$ from the contour, we can measure the increase in scalar magnetic potential on every section and thereby find the distribution of potential

along the contour.

§ 26. Electrointegrator for Solution of the Dirichlet and Neumann Problems

Let us now pursue the question of the simulation of the third mathematical operation of § 24, i.e., simulation of a solution to the Dirichlet problem for the Laplace equation. Immediately we note that the Neumann problem leads directly to the Dirichlet problem for the conjugate harmonic function. The usual method of simulation has essential deficiencies. Let us consider, for instance, the possibility of a solution to the Neumann and Dirichlet problems by means of simulation of the sought function by an electrical field of current in a conducting sheet.

As was shown in Chapter I any simply connected or two-connected region can be conformally mapped onto an infinite band. In Chapter III we considered in detail simulation of conformal mapping onto a band of the complex potential of a field of current in a conducting sheet. Modeling permits experimentally determining the corresponding points of any simply connected or two-connected region and an infinite band. Knowing the correspondence of points it is possible to transfer a solution to the Dirichlet or Neumann problem on to an infinite band where it is known in the form of a Poisson integral. However, even on a band numerical reduction of a solution is connected with a great expenditure of labor. In connection with this a modeling device was developed and prepared, an electrointegrator which permits fast and sufficiently accurate solution of the Dirichlet problem on an infinite band [36].

The electrointegrator is intended mainly for finding, on the boundary of the band the normal derivative of the harmonic function defined by its boundary values. It is based on the scheme for simulation of the harmonic field of the current function considered above (Fig. 12). The electrointegrator is shown schematically in Fig. 41. The basic element of the electrointegrator is a segment of band 1 in the form of a rectangle made from a sheet of 0.7 mm stainless steel measuring 250×2000 mm.

One side of the rectangle is intended for assignment of boundary values of the current function and is divided into 100 sections on each of which an adjustment of current is made with the help of rheostats 2. The current in each rheostat is set equal to the product of the increase in current function

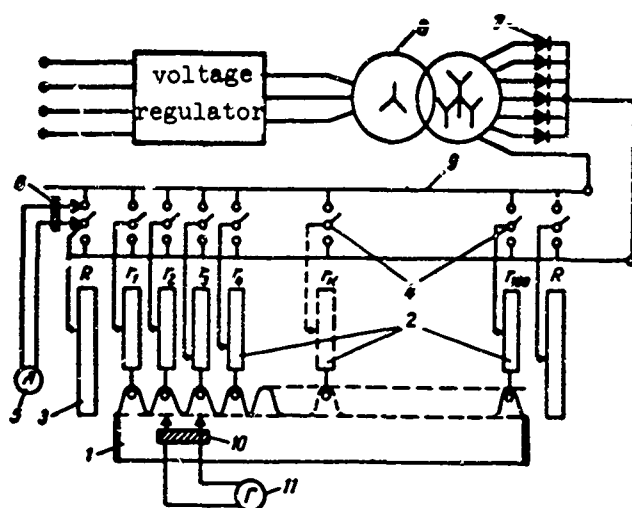


Fig. 41.

on the section of the boundary to which the rheostat is connected times the conductivity of a unit surface of the band. The sections constitute teeth whose form and dimensions are selected from conditions of uniform spreading of current in them. To the ends of the rectangle current is brought in through massive brass plates. Rheostats connected to teeth of the band permit setting currents from 0.025 to 2.5 A, and the end rheostats 3 — from 1 to 25 A. It is possible to change the direction of current in the rheostats with switches 4. Control of the current adjustment is performed with a multirange magnetoelectric ammeter 5 which with the help of special fork 6 is connected in turn in the circuit of each rheostat. The electrointegrator is powered by a single-phase 220 V line. A type [SN-250] (CH-250) fo. voltage stabilizer is incorporated a dc voltage is taken from the output of an [SV-100] (CB-100) selenium rectifier (7). The transformer of rectifier 8 has three different coefficients of transformation which permits obtaining 8, 10 and 12 V rectified voltage (unloaded). The dc voltage is supplied through buses 9 to which are connected the adjusting rheostats.

This simulation scheme ensures practically independent assignment of boundary values of the sought current function in the teeth of the band and at the same time permits obtaining values of potential gradient U sufficiently large for measurement. Measurement of the normal derivative of the current function on the contour of the region leads, as was shown above, to measurement of the voltage drop along the boundary over a section $\Delta\tau$, i.e., to a measurement of

mean value of electric current field strength over this section. Measurement is made with a probe with two contact needles 10 separated by a distance which equal to the tooth width. As studies have indicated, when measuring the mean value of intensity on a section of teeth division the magnitude of error appearing as a result of noncoincidence of values of the function of current at the base of the tooth with values of the sought function on the boundary is considerably reduced. For measurements is used a sensitive magnetoelectric galvanometer 11.

Simulation on a band permits instead of simultaneous assignment of limiting values of function on both boundaries of band to twice assign the function on one boundary ensuring every time on the other boundary a zero value of it. In the beginning, with the help of rheostats connected to the teeth values of the current function are values given which are proportional to the sought function on the upper boundary of the band and all necessary measurements are made. Then, considering the boundary with teeth the lower boundary of the band, values of the current function equal to values of the searched function on the lower edge are assigned to it and all measurements are also made. Summing values at points with coordinates x, y and $x, (h - y)$, the sought value is obtained. It is obvious that the boundary without teeth is everywhere a line of current, therefore J along the boundary is constant and may be set $J = 0$.

This permitted a twofold reduction in the number of adjusting rheostats. The superpositioning method makes it possible to increase the accuracy of problem solution due to the singling out of the constant component of threshold distribution of the function. The normal derivative $\frac{\partial \varphi}{\partial n}$ for a constant value of φ on the boundary can easily be calculated analytically. As investigation has shown, the influence of boundary values of functions removed from the considered point by a distance greater than double the width of the band are negligible. This permits on a rectangle, with a ratio of sides $l:h = 10:1$, to model the problem just as on an infinite band, boundary values of function on the entire length l of the rectangle being measured and the derivative on the middle part of it retreating from the edge $2h$ being measured. Thus on the rectangle a solution to the problem can be obtained from any section of an infinite band performing simulation along its sections. The possibility of solution of the problem by parts is the great advantage of simulation on the band since it permits a sharp reduction in the number of adjusting rheostats without a decrease in accuracy.

The normal derivative of hamonic function φ on the boundary of region D is expressed by formula

$$\left. \frac{\partial \varphi}{\partial n} \right|_r = \left. \frac{\partial \varphi_1}{\partial v} \right|_r \cdot \left| \frac{d\tau}{dt} \right|, \quad (26.1)$$

where $\left. \frac{\partial \varphi_1}{\partial v} \right|_r$ - normal derivative of sought function on the boundary of the band:

$\left| \frac{d\tau}{dt} \right|$ - modulus of derivative mapping the function;

dt - element of length of contour of region D corresponding to element of length $d\tau$ of the boundary of the band during conformal mapping.

During simulation of the conformally mapping function we obtain

$$\left| \frac{d\tau}{dt} \right| \approx \frac{\Delta\tau}{\Delta t} = \frac{\Delta\tau}{\Delta t_1} m, \quad (26.2)$$

where $\Delta\tau$ - width of band tooth;

Δt_1 - length of section of model of region D, corresponding to one tooth;

m - coefficient showing how many times the dimension of the region model are greater than dimensions of the actual region.

During simulation of the sought function φ_1 onto a band with the current function J we have

$$\frac{\partial \varphi_1}{\partial v} = k\gamma' \frac{\partial J}{\partial v} = k\gamma' \frac{\partial U}{\partial \tau} \approx k\gamma' \frac{\Delta U}{\Delta \tau}. \quad (26.3)$$

Here ΔU -- voltage drop on the section of a tooth;

γ' - conductivity surface of the band ($\gamma' = 8.04 \cdot 10^8 \frac{1}{\text{ohm}}$);

$k = \frac{\varphi_{\text{max}}}{\gamma J_{\text{max}}}$ - number of units of the sought function corresponding to a unit of current in the model (coefficient of simulation).

Substituting (26.2) and (26.3) in equation (26.1) we obtain

$$\left. \frac{\partial \varphi}{\partial n} \right|_r \approx mk\gamma' \frac{\Delta U}{\Delta t_1}. \quad (26.4)$$

Expression (26.4) can serve for calculation of the normal derivative of function φ . In Appendix 1 is given an example of calculation of the magnetic field of a dc machine.

Appendix 1

Example of calculation of radial components of magnetic induction of the field of main poles of dc machine HN-300.

Statement of problem

The configuration of the region of the air interval of the machine and of the windings of the main poles is given (Fig. 42). Determine the radial component of magnetic induction on the armature of an unsaturated machine.

Magnetic induction in the machine can be represented in the form of two components

$$\vec{B} = \vec{B}_0 + \vec{B}_n,$$

where \vec{B}_0 — component of induction of vortex field of currents flowing in windings;

\vec{B}_n — component of induction of field of magnetization of steel parts of machine.

Component \vec{B}_0 is easily found analytically, its magnitude on the circumference of the armature in an unsaturated machine is many times less than \vec{B}_n .

The radial component of vector \vec{B}_H is

$$B_{nr} = -\mu_0 \frac{\partial \varphi}{\partial n},$$

where φ is the scalar magnetic potential.

In an unsaturated machine it is possible to take $\mu = \infty$ and under this condition to calculate the boundary values of the scalar magnetic potential on the contour of the air interval. Thus the problem reduces to finding the normal derivative of potential on the circumference of the armature from its values on the boundary of the air interval.

Determination boundary values

Scalar magnetic potential was calculated at 19 points on the contour of the air interval of the machine graphoanalytically by the formula

$$\varphi(N) = \frac{IW}{2\pi n} \sum_{k=1}^s \alpha_k \arg(z_k),$$

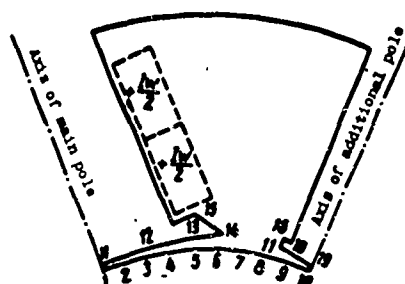
where IW — ampere-turns of one coil of the main pole;

n — number of the axes by which the cross section of the coil is replaced;

z_k — complex coordinate of the axis with current;

z_v — complex coordinate of the point in which is determined the scalar magnetic potential;

s — number of axes with current;



$\alpha_k = \pm 1$ depending upon direction of current in axis.

The cross section of the coil of the main pole is replaced by two axes with current (possibility of such replacement is shown earlier in § 4). Quadripole machine; $s = 16$.

Fig. 42
Values of $(z_k - z_N)$ were measured on the drawing with an accuracy of $15'$. Results of calculations are given in Table 10.

Table 10.

No. of point	$\frac{\Phi}{IW}$	No. of point	$\frac{\Phi}{IW}$	No. of point	$\frac{\Phi}{IW}$	No. of point	$\frac{\Phi}{IW}$
Armature circuit				Stator circuit			
1	-0.191	6	-0.078	11	0.800	16	0.028
2	-0.185	7	-0.055	12	0.822	17	-0.024
3	-0.170	8	-0.034	13	0.878	18	-0.025
4	-0.145	9	-0.016	14	0.911	19	0.000
5	-0.113	10	0.000	15	0.869		

Conformal mapping of region of air interval onto a band

The correspondence of points of the contour of region of air interval of machine to points of boundary of band during conformal mapping was found experimentally. A model of the region of the air interval was prepared from 0.25 mm dynamo steel in scale $m = 3:1$. The investigated section of region of air interval between axes of the main and additional poles is depicted on a rectangle with ratio of sides

$$\frac{l}{h} = \frac{R_m}{r} = 23.3,$$

where R_m — dc electrical resistance between contacts of model.

r — resistance of square prepared from material of model (r is conveniently calculated by measuring the resistance of a long rectangular strip).

During conformal mapping onto a band of width 250 mm the length of the band is found equal to 5.830 m and with a tooth width of 20 mm contains 290 teeth. Calculated values of magnetic potential on the contour of the air interval are translated to the corresponding points of boundary of band. Distribution curves for Φ along the lower and upper boundary of the band are shown in Fig. 43.

Solution of problem on electronintegrator

Assignment of threshold function. Since the investigated part of region is mapped onto a rectangle with ratio of sides 23.3:1, while the analog device permits assigning boundary values only on a section of a band, the problem was solved by parts. Dimensions of section of the band were selected in such a way as to ensure the largest possible accuracy of assignment of boundary

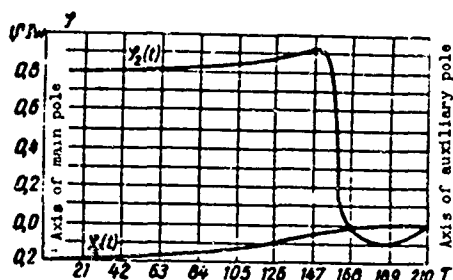


Fig. 43.

values and measurement of the normal derivative to the sought function. The constant component of boundary distribution $\varphi(t)$ was separated on each section.

Setting of currents in the rheostats was performed in turn it being assumed that the voltage on the rheostats under

operating conditions will equal half the source voltage (see diagram, Fig. 41). Voltage drop in the band leads to a redistribution of voltages on the adjusting rheostats which leads to a distortion of boundary values of the current function. However the analysis made showed that the distortion does not exceed 1%.

Finding the radial component of magnetic induction. Calculation of induction of the magnetization field was performed by the formula

$$B_{\text{an}} = \mu_0 m k \gamma' \frac{1}{k_z} \frac{\Delta U}{\Delta t_1},$$

where $\mu_0 = 4\pi \cdot 10^{-7}$ H/m;

k_z - coefficient taking into account toothed nature of armature,

$$m = 3, \quad k = 5.73;$$

ΔU - voltage drop in section of band tooth

$$\gamma' = 8.04 \cdot 10^2 \text{ l/ohm};$$

Δt_1 - length of section on boundary of air interval corresponding to one tooth of the band.

Substituting numerical values we obtain

$$B_{\text{an}} = 1.76 \cdot 10^{-3} \frac{\Delta U}{k_z \Delta t_1}.$$

Induction was calculated at twenty points evenly located on the circumference of the armature between the axes of the main and additional poles.

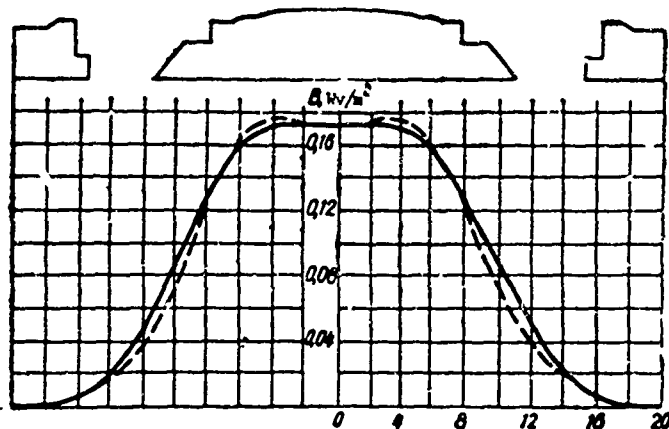


Fig. 44.

Values of ΔU were measured with a magnetoelectric galvanometer with a sensitivity of $S_H = 10^{-5}$ V/div.

Values of Δt_1 were determined by simulation of conformal mapping of region of the air interval onto a band.

The vortex component of induction B_{bn} under poles was calculated by the formula

$$B_{bn} \approx \mu_0 \frac{\Phi_{cr} - \Phi_a}{\sigma},$$

where σ — magnitude of air gap, but in the interval between the main and additional poles

$$B_{bn} \approx \mu_0 \frac{\varphi(M) - \varphi_a}{\sigma'},$$

where $\varphi(M)$ — potential of point M taken at a sufficiently small distance σ' from the considered point on armature along the radial direction.

Magnitude of B_{bn} nowhere on the armature exceeds 0.6% $B_{n \text{ max}}$.

In Table 11 are given computed values of $B_n = B_{nn} + B_{bn}$ and experimental data. Curves plotted from these data are shown in Fig. 44.

Table 11.

No. of point	B_n estimated	B_n experimental	No. of point	B_n estimated	B_n experimental
0	0.171	0.173	10	0.090	0.098
1	0.173	0.173	11	0.072	0.079
2	0.173	0.173	12	0.050	0.056
3	0.173	0.173	13	0.028	0.037
4	0.173	0.173	14	0.016	0.025
5	0.169	0.170	15	0.009	0.015
6	0.159	0.162	16	0.006	0.007
7	0.141	0.149	17	0	0.004
8	0.123	0.134	18	0	0.002
9	0.108	0.118	19	0	0.002
			20	0	0.002

§ 27. Electrointegrator Resolution

The basic element of the electrointegrator is a segment of thin steel tape in the form of a rectangle with ratio of sides 1:10. To the large side of the tape with the help of teeth of special form cut on it and regulating rheostats a direct current is applied to each tooth proportional to an assigned increase in current function on a section of the boundary of the band equal to the width of a tooth. To ends of the segment of tape are soldered massive brass contacts to which also is applied a current (Fig. 45).

The degree of homogeneity of stainless steel tape is very high. Measurements of the magnitude of conductivity of a unit surface of tape γ made by us showed that its deviation is less than 0.5% γ_{cp} .

Therefore the error due to nonuniformity of the tape will be disregarded.

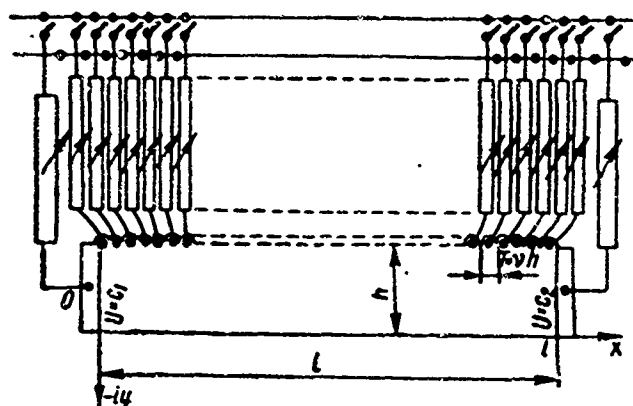


Fig. 45.

Sources of error of simulation of the sought function on the integrator are obviously;

- 1) distinction of form of tape, on which is modelled the sought function, from an infinite band;
- 2) deviation of fixed values of stream function at the base of every tooth from assigned values of the sought function;
- 3) redistribution of current applied to the teeth due to voltage drop in the tape.

Let us estimate the error of measurement of the normal derivative of the sought searched function introduced by each source separately [31].

Influence of lateral contacts. To ends of the tape along lines $x = 0$ and $x = l$ (Fig. 45) are soldered brass contacts responsible for a constant values

of potential $U = c_1$ and $U = c_2$ on these lines. Consequently the conducting tape will be a rectangle and not an infinite band. The boundary conditions on the rectangle will be mixed since on individual sections of the contour of the rectangle ($y = 0$ and $y = h$) values of stream function $J(x) = 0$ and $J(x, h)$, are assigned, on the other ($x = 0, x = l$) - values of potential $U = c_1$ and $U = c_2$.

Let us consider the line of contact $x = l$, on which we take $U = c_2 = 0$.

Potential of field of current U and the derivative normal to it $\frac{\partial U}{\partial n}$ are continuous as this line is approached and the values of potential on it are equal to zero. Consequently, the complex potential - analytic function $\Omega = U + iJ$ - is also continuous as the line $x = l$ is approached and on it takes the pure imaginary values $\Omega = iJ$. As follows from the Riemann-Schwarz principle of symmetry these conditions ensure symmetric continuation of function $\Omega(z)$ through the line of contact $x = l$ on the adjacent section of the band - a rectangle with boundaries $x = l$ and $x = 2l$, and consequently, also ensure equal values of current function $J(x, h)$ at points on the boundary symmetric with respect to the line of contact $x = l$, i.e., $J(x, h) = J(2l - x, h)$ [16]. Applying similar reasoning to the other line of contact $x = 0$ and to all lines $x = kl$ (k - integer) we conclude that mixed boundary values $U = c_1$ on $x = 0$, $U = c_2$ on $x = l$, $J = J(x, h)$ on $y = h$ and $J = 0$ on $y = 0$ are equivalent (for section of band $0 \leq x \leq l$) values of $J(x, h)$ periodically repeated on the boundary of the infinite band, even with respect to lines $x = kl$ and with value $J = 0$ on boundary $y = 0$ (Fig. 45).

Let us estimate the error, introduced by the contacts, in the magnitude of the normal derivative $\frac{\partial J}{\partial y}$ at boundary point of band x, h . In Fig. 46 the solid line represents limiting values of functions J on the boundary of an infinite band necessary according to conditions of the problem; the dotted line shows values equivalent to constraint assigned constant potentials $U = c_1$ and $U = c_2$ on the lines of contact. Obviously, the error in magnitude of the normal derivative $\frac{\partial J}{\partial y}$ will be determined by the difference of boundary values $J(x, h) - J(2l - x, h)$ beyond the lines of contacts $x = l$ and $x = 0$. For simplicity we consider the influence of the difference of limiting values J at distances greater than $2h$ from the considered point to be insignificant.

The magnitude of the normal derivative $\frac{\partial J}{\partial y}$ at point (x, h) , of the boundary of an infinite band, with an assigned distribution $J = J(x, h)$ on the upper boundary and $J = 0$ on the lower boundary of the band, must equal

$$\begin{aligned} \lim_{y \rightarrow h} \frac{\partial J}{\partial y} &= \frac{J(x, h)}{h} + \frac{k}{2h} \int_{-\infty}^0 \frac{J(\tau) - J(x, h)}{\operatorname{ch} k(\tau - x) - 1} d\tau + \\ &+ \frac{k}{2h} \int_0^l \frac{J(\tau) - J(x, h)}{\operatorname{ch} k(\tau - x) - 1} d\tau + \frac{k}{2h} \int_l^{\infty} \frac{J(\tau) - J(x, h)}{\operatorname{ch} k(\tau - x) - 1} d\tau \end{aligned} \quad (27.1)$$

$$\left(k = \frac{\pi}{h}\right).$$

In reality, due to the fact that the band is replaced by a rectangle with contacts along lines $x = 0$ and $x = l$, we have

$$\begin{aligned} \lim_{y \rightarrow h} \left(\frac{\partial J}{\partial y}\right)_1 &= \frac{J(x, h)}{h} + \frac{k}{2h} \int_{-\infty}^0 \frac{J(-\tau) - J(x, h)}{\operatorname{ch} k(\tau - x) - 1} d\tau + \\ &+ \frac{k}{2h} \int_0^l \frac{J(\tau) - J(x, h)}{\operatorname{ch} k(\tau - x) - 1} d\tau + \frac{k}{2h} \int_l^{\infty} \frac{J(2l - \tau) - J(x, h)}{\operatorname{ch} k(\tau - x) - 1} d\tau. \end{aligned} \quad (27.2)$$

Absolute error, consequently, is written

$$\begin{aligned} \Delta \frac{\partial J}{\partial y} \Big|_{y=h} &= \lim_{y \rightarrow h} \frac{\partial J}{\partial y} - \lim_{y \rightarrow h} \left(\frac{\partial J}{\partial y}\right)_1 = \\ &= \frac{k}{2h} \int_{-\infty}^0 \frac{J(\tau) - J(-\tau)}{\operatorname{ch} k(\tau - x) - 1} d\tau + \frac{k}{2h} \int_l^{\infty} \frac{J(\tau) - J(2l - \tau)}{\operatorname{ch} k(\tau - x) - 1} d\tau. \end{aligned} \quad (27.3)$$

Let us assume that point (x, h) is removed from the contact $x = l$ by a distance equal to double the width of the band, i.e., $x = 8h$ ($l = 10h$). We obtain the maximum error possible if we take the differences $J(\tau) - J(-\tau)$ and $J(\tau) - J(2l - \tau)$ equal to their maximum value M in the interval $l \leq \tau \leq l + h$ or $-h \leq \tau \leq 0$ (we assume that $J(\tau)$ is limited on the entire upper boundary of the infinite band and beyond the borders of the indicated interval $J(\tau) < 26M$). The value $J(\tau) = 26M$ for $\tau > l + h$ affects the value of $\Delta \frac{\partial J}{\partial y}$ at point $x = 8h$ less than the value of $J(\tau) = M$ within the limits of interval $l \leq \tau \leq l + h$

$$\begin{aligned} \Delta \frac{\partial J}{\partial y} \Big|_{y=h} &< \frac{kM}{2h} \int_{-\infty}^0 \frac{d\tau}{\operatorname{ch} k(\tau - 8h) - 1} + \frac{kM}{2h} \int_{10h}^{\infty} \frac{d\tau}{\operatorname{ch} k(\tau - 8h) - 1} = \\ &= \frac{M}{2h} \left[\int_{-\infty}^{-\pi} \frac{da}{\operatorname{ch} a - 1} + \int_{2\pi}^{\infty} \frac{da}{\operatorname{ch} a - 1} \right] = \frac{M}{2h} (\operatorname{cth} 4\pi + \operatorname{cth} \pi - 2) \approx \\ &\approx \frac{3.67 \cdot 10^{-3}}{2} \frac{M}{h} < 2 \cdot 10^{-3} \frac{M}{h}. \end{aligned} \quad (27.4)$$

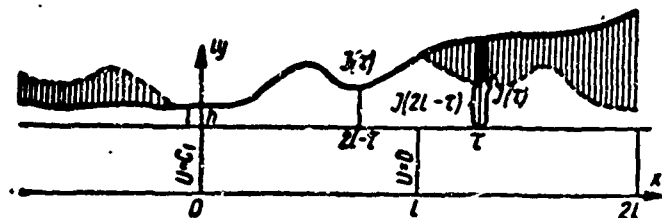


Fig. 46.

Consequently, at distances from contacts greater than twice the width of the band the error, introduced by contacts, in the magnitude of the normal derivative of the modelling function may be disregarded. Analogously it may be demonstrated that the error, introduced by contacts, in the magnitude of the modelling function J (and its conjugate), at distances from the contacts greater than twice the width of the band, is just as small.

Thus the middle part of a tape of length $10h - 4h = 6h$ will be the working section. The modelling function J on it (and also its conjugate U), if boundary values of $J(x, h)$ are fixed on the entire upper boundary on the tape will be very close to the sought function.

Influence of divergence of limiting values. Modelling current function J is established on the boundary of the band with the help of a rheostat connected to each tooth. To the tooth is applied a current proportional the increase of the sought function on the section of the boundary equivalent to the tooth width. The normal component of the vector of current density on the boundary of the band $y = h$ will be proportional to the tangent to the derivative of the current function

$$\delta_n = \gamma E_n = -\gamma \frac{\partial U}{\partial y} = \gamma \frac{\partial J}{\partial x}. \quad (27.5)$$

The distribution of current density δ_n on the boundary within the limits of a tooth width is determined by the form of tooth, the position of the contact on it, the magnitudes of currents in the neighboring of the teeth and the magnitude of current through the cross section of the tape, i.e., the magnitude of the current function at the base of the tooth. In general the distribution of current density does not coincide with the assigned distribution of the tangential to the derivative of the sought function. Therefore the value of current function J on the boundary $y = h$ will coincide with assigned values only between teeth at points of tangency of the line $y = h$ with the contour of the teeth. Even on

those sections of the boundary where assigned values of current function are constant, constant values of current function J cannot be assured due to current flow from the band into the tooth.

Divergence of boundary values of the current function with those assigned will be less the greater $v = \frac{h}{T}$ (h — width of band, T — width of tooth) and the greater the smoothly assigned values of function J on the boundary change. These factors determine the magnitude of error of the electrointegrator and its resolving power.

In order to find the normal derivative of the searched function it is necessary to measure the tangential component of intensity E_x on boundary $y = 0$ or $y = h$ of the band of the integrator. It is impossible to measure the value of intensity in any point of the band. Therefore the mean value of intensity is measured on a sufficiently small section of the boundary. Measurement is made a probe having two contact needles the distance between which is rigidly fixed.

Let us find the magnitude of error of such measurement obtained as a result of divergence of boundary values of the current function with assigned values of the sought function.

Let $J_1(x)$ be given according to the conditions of the problem of distribution of the current function on the boundary of the band, $J(x)$ — distribution fixed on the boundary of the conducting band of the electrointegrator by means of applying a current to the teeth proportional to increases on corresponding sections. The difference of these values $\Delta J(x) = J_1(x) - J(x)$ on the boundary yields an error when measuring of mean value of the normal derivative $\frac{\partial J}{\partial y}$.

Let us take the distance between probe needles equal to m . Then

$$\left. \frac{\partial \Delta J}{\partial y} \right|_{cp} = \frac{1}{m} \int_x^{x+m} \frac{\partial \Delta J}{\partial y} dx = \frac{1}{m} \int_x^{x+m} \frac{\partial \Delta U}{\partial x} dx = \frac{\Delta U}{m}, \quad (27.6)$$

where ΔU — corresponding potential difference between needles of probe caused by divergence of boundary values of the current function with assigned values of the sought function.

On the boundary of the band at point (x, h) the error has the form

$$\begin{aligned}
\frac{\partial \Delta J}{\partial y} \Big|_{y=h} &= \left[\frac{\partial J_1}{\partial y} - \frac{\partial J}{\partial y} \right]_{y=h} = \frac{J_1(x) - J(x)}{h} + \\
&+ \frac{k}{2h} \int_{-\infty}^{\infty} \frac{J_1(\tau) - J(\tau) - J_1(x) + J(x)}{\operatorname{ch} k(\tau - x) - 1} d\tau = \frac{\Delta J(x)}{h} + \\
&+ \frac{k}{2h} \int_0^{\infty} \frac{\Delta J(x + \alpha) + \Delta J(x - \alpha) - 2\Delta J(x)}{\operatorname{ch} k\alpha - 1} d\alpha.
\end{aligned} \quad (27.7)$$

The potential difference ΔU , caused by error $\frac{\partial \Delta J}{\partial y}$, at point x and $x + m$ on the boundary of a conducting band between needles of the probe will be (Appendix 1, § 27)

$$\begin{aligned}
\Delta U(x) &= \int_x^{x+m} \frac{\partial \Delta J}{\partial y} dx = \int_x^{x+m} \frac{\Delta J(x)}{h} dx + \\
&+ \frac{k}{2h} \int_x^{x+m} dx \int_0^{\infty} \frac{\Delta J(x + \alpha) + \Delta J(x - \alpha) - 2\Delta J(x)}{\operatorname{ch} k\alpha - 1} d\alpha = \\
&= \frac{1}{h} \int_x^{x+m} \Delta J(x) dx + \frac{k}{2h} \int_0^{\infty} \frac{\int_x^{x+m} [\Delta J(x + \alpha) + \Delta J(x - \alpha) - 2\Delta J(x)] dx}{\operatorname{ch} k\alpha - 1} d\alpha.
\end{aligned} \quad (27.8)$$

From this expression one may see what if on the boundary of band $\Delta J(x)$ there is a periodic function with a period to equal to m , then ΔU takes a minimum value

$$\Delta U_{\min} = \frac{1}{h} \int_x^{x+m} \Delta J(x) dx. \quad (27.9)$$

Since on the boundary of the band values of $J(x)$ coincide with values of $J_1(x)$ only at points between the teeth then the difference of these values $\Delta J(x)$ must be either a periodic function with period to equal to the tooth width T (when values of function $J_1(x)$ on the considered section are constant) or, as we will see later, can be represented in the form of a product of the periodic function of the same period times another function dependent on $J_1(x)$ (when $J_1(x)$ is changed). Therefore for increase of accuracy of measurements it is necessary that the distance m between needles of the probe be made equal to the width of the tooth T . Here formula (27.8) takes the form

$$\Delta U(x) = \frac{1}{h} \int_x^{x+T} \Delta J(x) dx + \frac{k}{2h} \int_0^{\infty} \frac{\int_x^{x+T} [\Delta J(x + \alpha) + \Delta J(x - \alpha) - 2\Delta J(x)] dx}{\operatorname{ch} k\alpha - 1} d\alpha. \quad (27.10)$$

Let us apply formula (27.10) for appraisal of the error in measurement of the mean value of the normal derivative of the sought function $J_1(x, y)$ on the boundary of band $y = h$ with different forms of behavior of the maximum values $J_1(x, h)$ near the point of measurement (x, h) .

1. Let us assume that on both sides of the measurement point x values of the given function are constant: $J_1(x, h) = \text{const} = c$. On the electrointegrator this signifies that to teeth on the left and right of this point current is not applied. Values of the current function J on the upper contour of the tape will also equal c but on the line $y = h$ due to flow of current in the teeth, values of current function $J(x, h)$ will differ from $J_1 = c$.

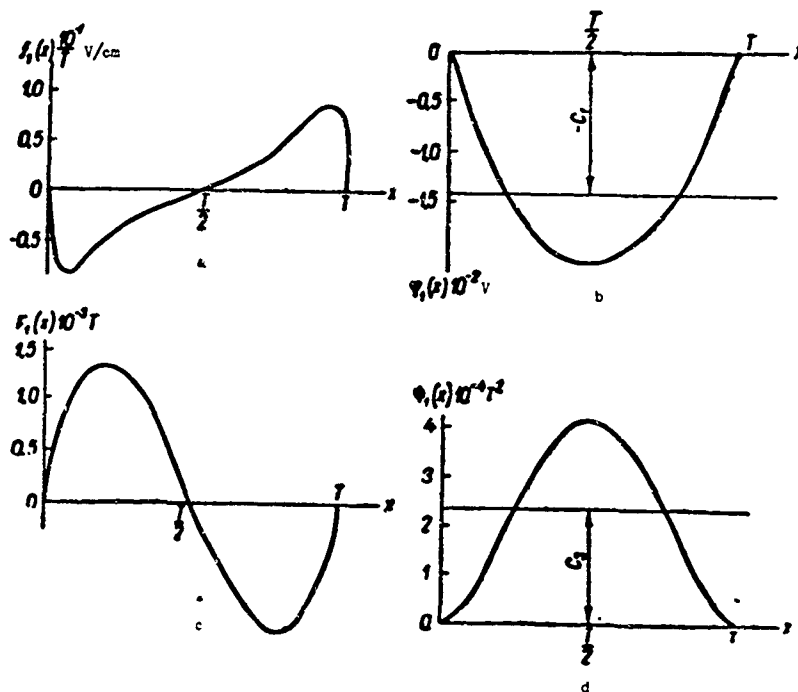


Fig. 47.

In Fig. 47, a is given the distribution of current density $\frac{1}{y} \delta_n = f_1(x)$ in the base of a tooth obtained experimentally. At the point of contact of line $y = h$ with contour of the tape $J = J_1 = c$, due to flow of current in the tooth the magnitude of $J(x, h)$ drops further attaining a minimum on the axis of the tooth. Then as a result of the flow of current from the tooth the magnitude $J(x, h)$ again increases and attains a maximum $J = J_1 = c$ between teeth.

On the line $y = h$ the value of the current function will equal (Fig. 47b)

$$J(x, h) = J_1 - \int_0^x J'(x) dx. \quad (27.11)$$

The difference of these values

$$\Delta J(x) = J_1 - J(x, h) = \int_0^x J'(x) dx \quad (27.12)$$

will obviously be a periodic function with period T . The error in measurement of average intensity ΔU is expressed thus:

$$\Delta U = \frac{1}{h} \int_x^{x+T} \Delta J(x) dx. \quad (27.13)$$

Let us demonstrate that this error can be predetermined and eliminated.

The mean value of $J(x, h)$ equals

$$\begin{aligned} J_{cp} &= \frac{1}{T} \int_x^{x+T} J(x, h) dx = \frac{1}{T} \int_x^{x+T} [J_1 - \Delta J(x)] dx = J_1 - \\ &\quad - \frac{1}{T} \int_x^{x+T} \Delta J(x) dx. \end{aligned} \quad (27.14)$$

From a comparison of formulas (27.13) and (27.14) we find

$$\Delta U = \frac{1}{h} \int_x^{x+T} \Delta J(x) dx = \frac{T}{h} (J_1 - J_{cp}). \quad (27.15)$$

In order to clarify the meaning of expression (27.15) we show that conductivity $g = \frac{h}{T} = v$ of a rectangle bounded by lines $x = 0$, $y = 0$, $x = T$ and $y = h$, is equal to the ratio of the difference in mean values of the current function ΔJ_{cp} on sides $y = h$ and $y = 0$ to the difference of mean values of potential ΔU_{cp} on sides $x = T$ and $x = 0$. Indeed

$$\begin{aligned} \Delta J_{cp} &= J_{cp}(x, h) - J_{cp}(x, 0) = \frac{1}{T} \int_0^T [J(x, h) - J(x, 0)] dx = \\ &= \frac{1}{T} \int_0^T dx \int_0^h \frac{\partial J}{\partial y} dy. \end{aligned} \quad (27.16)$$

$$\begin{aligned}\Delta U_{cp} &= U_{cp}(T, y) - U_{cp}(0, y) = \frac{1}{h} \int_0^h [U(T, y) - U(0, y)] dy = \\ &= \frac{1}{h} \int_0^h dy \int_0^T \frac{\partial U}{\partial x} dx.\end{aligned}\quad (27.17)$$

Function $J(x, y)$ is harmonic in the rectangle, including its contour, therefore

$$\begin{aligned}\Delta J_{cp} &= \frac{1}{T} \int_0^T dx \int_0^h \frac{\partial J}{\partial y} dy = \frac{1}{T} \int_0^T dx \int_0^h \frac{\partial U}{\partial x} dy = \\ &= \frac{1}{T} \int_0^h dy \int_0^T \frac{\partial U}{\partial x} dx = \frac{h}{T} \Delta U_{cp} = g \Delta U_{cp},\end{aligned}\quad (27.18)$$

whence

$$g = \frac{h}{T} = \frac{\Delta J_{cp}}{\Delta U_{cp}}. \quad (27.19)$$

Let us consider a section of tape with a tooth between line x and $x + T$ (Fig. 48a). If the current function on the upper contour of the tape is constant, then due to symmetry of the tooth lines x and $x + T$ will coincide with lines of equal potential $U = U_1$ and $U = U_2$. The conductivity of this section g_1 will consequently equal

$$g_1 = \frac{J_1}{U_2 - U_1} = \frac{h_m}{T}.$$

Here $h_m > h$ — height of rectangle on which the considered section of tape with tooth can be depicted if the width of this rectangle is taken equal to T . Conductivity of the rectangular part of the considered section of tape with tooth, bounded from above by the line $y = h$, has the form

$$g_2 = \frac{h}{T} = \frac{J_{cp}}{U_2 - U_1} = \frac{1}{U_2 - U_1} \left[J_1 - \frac{1}{T} \int_x^{x+T} \Delta J(x) dx \right], \quad (27.20)$$

and difference in conductivities

$$g_1 - g_2 = \frac{J_1 - J_{cp}}{U_2 - U_1}. \quad (27.21)$$

From formula (27.15) $J_1 - J_{sp} = \frac{h}{T} \Delta U$, formula (27.19)

$$U_2 - U_1 = \frac{T}{h_m} J_1.$$

Placing these values in expression (27.21), we obtain

$$\varepsilon_1 - \varepsilon_2 = \frac{h_1 h_m \Delta U}{T^2 J_1} = \frac{h_m - h_1}{T}. \quad (27.22)$$

Hence we obtain a measurement error for the average voltage, using a double probe with distance between needles equal to T , on the boundary of the band $y = h$

$$\Delta U = \frac{T}{h} \left(1 - \frac{h}{h_m} \right) J_1 = a J_1, \quad (27.23)$$

where $a = \frac{T}{h} \left(1 - \frac{h}{h_m} \right)$ - constant which can be determined experimentally, measuring

$$\varepsilon_1 = \frac{h_m}{T} = \frac{I_1}{\gamma(U_2 - U_1)} \quad (27.24)$$

on a model from conducting sheet with a conductivity of a unit surface γ in the form of the considered section of the tape with a tooth. In formula (27.24)

I_1 is the current through the model, $U_2 - U_1$ - the voltage between contacts of the model along lines x and $x + T$. Potentials on contacts must be constants.

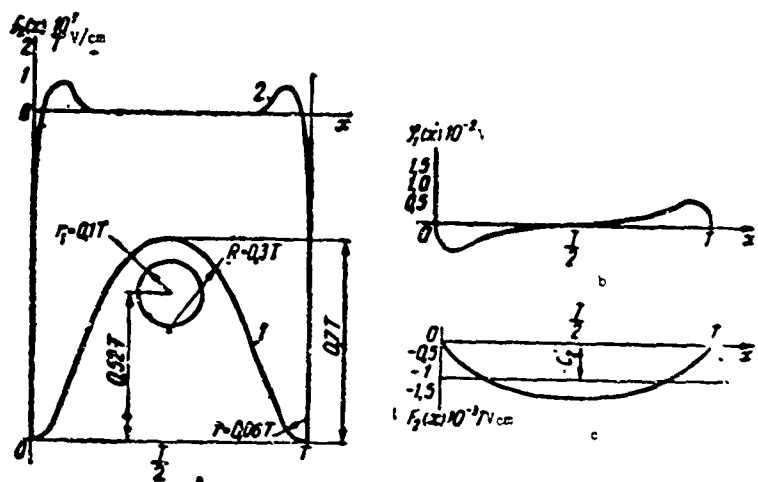


Fig. 48.

Thus, on those sections of the band boundary where the given function takes constant values the measuring error of mean value of the normal derivative of the assigned function on a section boundary of width T can be calculated beforehand.

The mean value of the normal derivative $\frac{\partial J}{\partial y}$ on section $(x, x + T)$ of the boundary $y = h$ will be recorded

$$\left. \frac{\partial J}{\partial y} \right|_{cp} = \frac{U(x+T) - U(x)}{T} + \frac{\Delta U}{T} = \frac{U(x+T) - U(x)}{T} + \frac{a}{T} J_1. \quad (27.25)$$

Noticing that for $J = J_1$

$$\frac{U(x+T) - U(x)}{T} = \frac{U_2 - U_1}{T} = \frac{J_1}{h_m} \quad (27.26)$$

and

$$\frac{a}{T} J_1 = \left(\frac{1}{h} - \frac{1}{h_m} \right) J_1. \quad (27.27)$$

we conclude that the influence of error ΔU on measurement of the normal derivative of the sought function on the boundary of the band is equivalent to an increase in width of the band from h to h_m . Considering the width of the band onto which the assigned region, equal to h_m (and not h) is mapped, completely eliminates the error ΔU .

2. Let us assume that both sides of the measurement x the assigned limiting values of the sought function $J_1(x, h)$ change linearly. We take as the origin for reading x the left edge of the tooth on which measurements are taken. Then the law of change of $J_1(x, h)$ will be:

$$J_1(x, h) = px + c. \quad (27.28)$$

On the electrointegrator this will signify that to teeth on the left and right of the point x an identical current is applied. The least divergence between $J_1(x)$ and $J(x)$, and consequently the least magnitude of error ΔU would occur, obviously, when the density of applied current δ_n at the base of the tooth ($y = h$) is constant. The divergence would then be determined only by the influx of current to the tooth from the band. Such a tooth form (Fig. 48a) was found experimentally in the base of which the density of applied current during free influx of current from the tooth differs little from its mean value and has the form shown in Fig. 48a.

The increase of the current function with an increase in x leads to an increase in current flowing into the teeth. Besides this, near the tooth is applied a current which does not succeed in being evenly distributed over the entire cross section of the tape and the influx of current in neighboring teeth increases

as a consequence. Considering all this, the error of assignment of the boundary values of density of current we write thus:

$$\frac{1}{Y}(\delta_{n1} - \delta_n) = \rho x f_1(x) + c f_1(x) + \rho [f_2(x) + f_3(x)]. \quad (27.29)$$

Here $f_1(x) = f_1(x + kT)$ is a periodic function conditioned by the flow of current into the teeth (Fig. 47a); $f_2(x) = f_2(x + kT)$ - a periodic function dependent on the divergence of density of current applied to the tooth with an assigned value of current density (Fig. 48a); $f_3(x) = f_3(x + kT)$ - a periodic function appearing due to an increase of influx into the tooth of current applied in neighboring teeth (Fig. 49a).

Let us consider the influence of every member of expression (27.29) on the magnitude of error $\Delta U(x)$.

As can be seen from the graphs (Fig. 48a and 49a) $f_2(x)$ and $f_3(x)$ - are even function with respect to the axis of the tooth. Consequently their antiderivatives

$$\Delta J_2(x) = \rho \varphi_2(x) = \rho \int f_2(x) dx$$

and

$$\Delta J_3(x) = \rho \varphi_3(x) = \rho \int f_3(x) dx$$

will be odd periodic functions whose constant components equal zero. Therefore

$$\Delta U_2 + \Delta U_3 = \frac{1}{h} \int_x^{x+T} [\Delta J_2(x) + \Delta J_3(x)] dx = 0. \quad (27.30)$$

Let us find the magnitude of error from $\rho x f_1(x)$. We designate

$$\int f_1(x) dx = \varphi_1(x) = \varphi_{11}(x) + \frac{1}{T} \int_0^T \varphi_1(x) dx = \varphi_{11}(x) + c_1. \quad (27.31)$$

$$\int \varphi_{11}(x) dx = F_1(x) = F_{11}(x) + \frac{1}{T} \int_0^T F_1(x) dx = F_{11}(x) + c_2. \quad (27.32)$$

Here $\varphi_{11}(x)$ and $F_{11}(x)$ are periodic functions whose constant components equal zero (Fig. 47b, c):

$$\int_0^T \varphi_{11}(x) dx = 0, \quad \int_0^T F_{11}(x) dx = 0. \quad (27.33)$$

We have

$$\begin{aligned}\Delta J_1(x) &= \rho \int_0^x f_1(x) dx = \rho [x \varphi_1(x) - \int \varphi_1(x) dx] = \\ &= \rho [\varphi_{11}(x) - F_{11}(x) + c_2].\end{aligned}\quad (27.34)$$

Placing the value of $\Delta J_1(x)$ in formula (27.10) we obtain

$$\Delta U_1(x) = \frac{\rho T}{h} \left[F_{11}(x) - c_2 + \frac{k}{2} \int_0^{\infty} \frac{F_{11}(x+\alpha) + F_{11}(x-\alpha) - 2F_{11}(x)}{\operatorname{ch} k\alpha - 1} d\alpha \right]. \quad (27.35)$$

As can be seen from the graphs (Fig. 47c) $c_2 = 0$, $F_1(x) = F_{11}(x)$ and in the middle of the bases of the tooth $F_{11}\left(\frac{T}{2}\right) = 0$; $F_{11}\left(\frac{T}{2} + \alpha\right) = -F_{11}\left(\frac{T}{2} - \alpha\right)$

Hence placing the needles of the probe during measurement at the middle of the bases of neighboring teeth $\left(x = \frac{T}{2}\right)$, it is possible to eliminate error $\Delta U_1(x)$:

$$\Delta U_1\left(\frac{T}{2}\right) = 0. \quad (27.36)$$

Thus in this case the error will be caused only by the component of current density proportional to $\varphi f_1(x)$. But $\varphi f_1(x)$ would be the current density flowing into the teeth if values of the current function on the upper boundary of the

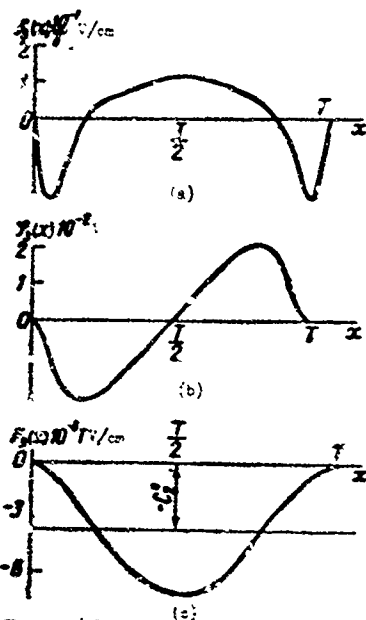


Fig. 49.

band were constants and equal to its value at the origin of the tooth (for $x = 0$ $J_1(0) = c$). Consequently taking the width of the band onto which is mapped the assigned region equal to h_m , we can completely eliminate the error in this case also.

3. Let us assume that on both sides the measurement point x the given limiting values of the sought function $J_1(x, h)$ are measured along the parabola

$$J_1(x) = qx^2 + px + c. \quad (27.37)$$

On the electrointegrator this indicates that to teeth on the left and right of x there is applied a linearly increasing current. In this case an error will arise due to the noncoincidence of density of the supplied current with the assigned values,

the flow of passing current in the tooth, and the nonuniform distribution of current over the cross section of the tape and the associated increase of influx to the neighboring teeth. With an increase in x the current function will increase proportional to x^2 , and the current supplied to the teeth proportional to x . Therefore the error of assignment of current density on boundary $y = h$ may be written:

$$\frac{1}{\gamma} (\delta_{n1} - \delta_n) = qx^2 f_1(x) + px f_1(x) + c f_1(x) + 2qx [f_2(x) + f_3(x)] + p [f_2(x) + f_3(x)]. \quad (27.38)$$

The error from components

$$px f_1(x) + c f_1(x) + p [f_2(x) + f_3(x)]$$

was determined in the preceding case.

Error caused by components of current density proportional to

$$qx^2 f_1(x) + 2qx [f_2(x) + f_3(x)],$$

can be estimated thus (Appendix 2, § 27):

$$\Delta U \left(\frac{T}{2} \right) < 4\pi q (c_3 + |c'_2| + |c'_2|). \quad (27.39)$$

Let us clarify the meaning of the obtained expression. On both sides of point of measurement x the assigned limiting values of the sought function $J_1(x, h)$ vary along the parabola

$$J_1(x) = qx^2 + px + c.$$

The difference of currents supplied to two neighboring teeth is here expressed by the formula

$$\begin{aligned} \Delta i = i_1 - i_2 &= \gamma \int_{\frac{\tau}{2}}^{\frac{\pi}{2}} J_1(x) dx - \gamma \int_0^{\frac{\tau}{2}} J_1(x) dx = \\ &= \gamma (qx^2 + px) \Big|_{\frac{\tau}{2}}^{\frac{\pi}{2}} - \gamma (qx^2 + px) \Big|_0^{\frac{\tau}{2}} = 2\gamma T^2 q, \end{aligned} \quad (27.40)$$

whence

$$q = \frac{\Delta i}{2\gamma T^2} = \frac{i_1 - i_2}{2\gamma T^2}, \quad (27.41)$$

and consequently

$$\Delta U \left(\frac{T}{2} \right) < \frac{2\pi}{T^2} (c_3 + |c'_2| + |c''_2|) \frac{l_1 - l_2}{\gamma}. \quad (27.42)$$

Thus in this case the measurement error of the normal derivative $\left. \frac{\partial J}{\partial y} \right|_{y=h}$ for an assigned ratio of band width h to width of tooth T is determined only by the magnitude of the difference of currents supplied to the two neighboring teeth. The relationship $\nu = \frac{h}{T}$ does not enter directly into the expression for error of ΔU however the quantities c_3 , c'_2 and c''_2 , determining error (27.42) depend on ν . Indeed, for a constant current density in the tooth, with a decrease of width of tooth T the form of functions $f_1(x)$, $f_2(x)$ and $f_3(x)$ will not change however their integrals $\varphi(x)$, $F(x)$ and $\psi(x)$, and consequently constants c_3 , c'_2 and c''_2 will decrease inversely proportional to ν in a degree equal to the multiplicity of integration. Thus the decrease in c_3 will be proportional to $1/\nu^3$, the decrease in c'_2 and c''_2 -- proportional to $1/\nu^2$. Considering that $|c'_2| + |c''_2| \gg c_3$, we conclude that the measurement error of the normal derivative of the sought function on the boundary of the band with a decrease in width of tooth (i.e., with an increase in ν) will decrease somewhat faster than $1/\nu^2$.

4. Let us assume that on both sides of the point of measurement x the assigned limiting values of sought function $J_1(x, h)$ are vary according to cubic parabola

$$J_1(x) = sx^3 + qx^2 + px + c. \quad (27.43)$$

On the electrointegrator this signifies what to the teeth on the left and right of x a current is supplied which increases according to law quadratic parabola law. With an increase in x the current function will increase proportional to x^3 and the current supplied to the teeth is proportional to x^2 . Therefore the error of current density on boundary $y = h$ may be written:

$$\begin{aligned} \frac{1}{\gamma} (\delta_{n1} - \delta_n) = & sx^2 f_1(x) + qx^2 f_1(x) + px f_1(x) + c f_1(x) + \\ & + 3sx^2 [f_2(x) + f_3(x)] + 2qx [f_2(x) + f_3(x)] + p [f_2(x) + f_3(x)]. \end{aligned} \quad (27.44)$$

Error from components

$$qx^2 f_1(x) + px f_1(x) + c f_1(x) + 2qx [f_2(x) + f_3(x)] + p [f_2(x) + f_3(x)]$$

was determined in the preceding case. The error caused by components of current density proportional to

$$sx^2 f_1(x) + 3sx^2 [f_2(x) + f_3(x)], \quad (27.45)$$

can be estimated as in the preceding case

$$\Delta U \left(\frac{T}{2} \right) < 12\pi T (c_3 + |c'_2| + |c'_2|)s. \quad (27.46)$$

The total error in this case will be determined thus:

$$\Delta U_x \left(\frac{T}{2} \right) < 4\pi (q + 3Ts) (c_3 + |c'_2| + |c'_2|). \quad (27.47)$$

Let us clarify meaning of the obtained expression. The difference of currents supplied to the tooth with point measurement x and its neighbor on the right equals

$$\begin{aligned} \Delta i_1 = i_1 - i_2 &= \gamma \int_0^T J'_1(x) dx - \gamma \int_0^T J'_1(x) dx = \\ &= \gamma (sx^3 + qx^2 + px) \Big|_0^T - \gamma (sx^3 + qx^2 + px) \Big|_0^T = (6sT^3 + 2qT^2) \gamma \end{aligned} \quad (27.48)$$

Difference of currents supplied to the tooth with point of measurement x and its neighbor on the left has the form

$$\Delta i_2 = i_2 - i_3 = \gamma \int_0^T J'_1(x) dx - \gamma \int_{-T}^0 J'_1(x) dx = 2qT^2 \gamma. \quad (27.49)$$

The change in difference of currents supplied to the teeth is

$$\Delta \Delta i = \Delta i_1 - \Delta i_2 = 6\gamma T^3 s,$$

hence

$$s = \frac{\Delta i_1 - \Delta i_2}{6T^3 \gamma}, \quad q = \frac{\Delta i_2}{2T^2 \gamma}. \quad (27.50)$$

Let us substitute into the expression for error (27.47) values q and s , expressed in terms of differences in currents supplied to the teeth

$$\Delta U_x \left(\frac{T}{2} \right) < \frac{2\pi}{T^2} (c_3 + |c'_2| + |c'_2|) \frac{\Delta i_1}{\gamma}, \quad (27.51)$$

or

$$\Delta U_x \left(\frac{T}{2} \right) < \frac{2\pi}{T^2} (c_3 + |c'_2| + |c'_2|) \frac{i_1 - i_2}{\gamma}. \quad (27.52)$$

Here i_2 - current in tooth on which the point of measurement x , lies, i_1 is the current in the tooth to the right of point x . The expression for error (27.52)

is the same as in the preceding case when limiting values of the function varied according to the quadratic parabola law (27.42). For $i_1 = i_2$ and $i_1 = i_2 = 0$, when the limiting values vary according to a linear law or remain constants, the error obviously will equal zero if the band width is taken equal to h_m .

From formulas (27.42) and (27.52) one may see that the measurement error for the mean value of the normal derivative of the sought function on width of tooth T is proportional to the difference of the increments of the threshold function $J_1(x)$ over the width of two teeth, i.e., is proportional to the mean value of the second derivative to this function over section $2T$.

Let us show that both for any other continuous law of change of limiting values of sought function $J_1(x)$ and its derivative $J_1'(x)$ the error must be determined by the values of current in two neighboring teeth to which the needles of the measuring probe are attached. From formula (27.39d) (see appendix) it is clear that the magnitude of error ΔU is basically determined by the magnitude of integral

$$k \int_0^T \frac{1 - \cos \omega a}{\operatorname{ch} ka - 1} da \approx 2\pi v - 1, \quad (27.53)$$

taking into account the influence of divergence of boundary values of the function of the entire upper boundary of the band. The portion of error caused by divergence of boundary values on the width of two teeth in the interval $-T \leq a \leq T$ obviously will be proportional to

$$\begin{aligned} k \int_0^T \frac{1 - \cos \omega a}{\operatorname{ch} ka - 1} da &= \left[(\cos \omega a - 1) \operatorname{cth} \frac{ka}{2} - \cos \omega a \right]_0^T - \\ &- 2\omega \sum_{n=1}^{\infty} \frac{n k \sin \omega a + \omega \cos \omega a}{e^{-\pi n} (n^2 k^2 + \omega^2)} \Big|_0^T = \sum_{n=1}^{\infty} \frac{2\omega^2}{n^2 k^2 + \omega^2} - \\ &- \sum_{n=1}^{\infty} \frac{2\omega^2 e^{-n\pi T}}{n^2 k^2 + \omega^2} = 8v^2 \sum_{n=1}^{\infty} \frac{1}{n^2 + 4v^2} - 2 \sum_{n=1}^{\infty} \frac{e^{-\pi \frac{n}{v}}}{1 + \frac{4v^2}{n^2}} > 2\pi v - \\ &- 1 - 2 \sum_{n=1}^{\infty} e^{-\pi \frac{n}{v}} = 2\pi v + 1 - \frac{2}{1 - e^{-\frac{\pi}{v}}} > 2v \left(\pi - \frac{1}{\pi} \right). \end{aligned} \quad (27.54)$$

Consequently the portion of error caused by divergence of boundary values on the entire remaining boundary of the band for $v = 10$ will be less than

$$\frac{2\pi\nu - 1 - 2\nu \left(\pi - \frac{1}{\pi} \right)}{2\pi\nu - 1} \cdot 100 = 8,8\%$$

of the total error and hence the error ΔU will depend very little on the character of change of the boundary values of the sought function beyond the limits of the two teeth.

Let us estimate the magnitude of the ΔU error. From the curves in Figs. 47d, 48c and 49c we find

$$c_3 = 0,05 \cdot 10^{-2}, |c'_2| = 0,16 \cdot 10^{-2}, |c'_2| = 0,55 \cdot 10^{-2}. \quad (27.55)$$

Thus

$$\begin{aligned} \Delta U_z \left(\frac{T}{2} \right) &< \frac{2\pi}{1,5} (0,05 + 0,16 + 0,55) \cdot 10^{-2} \frac{i_1 - i_2}{\gamma} = \\ &= 2,13 \cdot 10^{-2} \frac{i_1 - i_2}{\gamma}. \end{aligned} \quad (27.56)$$

The biggest value this quantity will be attained for $i_2 = -i_1 = i_{\text{max}}$. Rheostats connected to the teeth of the band permit regulating the current in them from 0.025 to 2.5 A, rheostats on the lateral contacts of the band — from 1 to 25 A.

$$i_{\text{max}} = 2,5 \text{ A}, I_m = 25 \text{ A}, \gamma = 8,04 \cdot 10^2 \frac{1}{\text{ohm}}.$$

The maximum value of absolute error of change in mean value of the normal derivative of the sought function equals

$$\frac{\Delta U_{\text{max}}}{T} = \frac{2,13 \cdot 10^{-2}}{2} \cdot \frac{5 \cdot 10^{-2}}{8,04} = 6,62 \cdot 10^{-5} \text{ V} \quad (27.57)$$

With a constant value of threshold function $J_1(x) = J_c = \text{const}$ it is easily possible to calculate the normal derivative

$$\frac{\partial J}{\partial y} = \frac{J_c}{h} = \frac{J_c}{\gamma h}. \quad (27.58)$$

Therefore for an increase in accuracy of problem solution on the integrator it is advisable to subtract from the ordinates of the curve of the boundary function constant equal to the initial ordinate J_1 (Fig. 50) of curve $J_1(x)$ at the origin of the considered section of the boundary of the band $l = 10h_m$, and to alter the scale of the remaining ordinates of the curve in such a manner

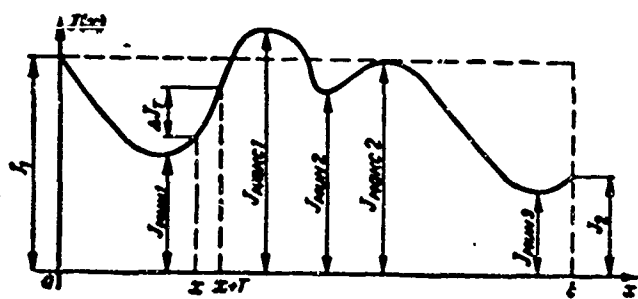


Fig. 50.

J_1 and J_2 - values of ordinates at the origin and end of the interval $l = 10h_m$, n and m - the number of maxima and minima of curve $J_1(x)$ respectively. The greatest relative error of the integrator (with respect to $\frac{l_m}{\gamma h}$) is expressed by the formula

$$\delta_{\max} = \frac{\Delta U_{\max}}{T} \cdot \frac{\gamma h}{I_m} = \frac{2,13 \cdot 10^{-2} i_{\max} \gamma v T}{\gamma T I_m} = 4,26 \cdot 10^{-2} = 4.26\%. \quad (27.60)$$

This value will correct only when the threshold function satisfies definite conditions for which its assignment on the integrator is possible namely:

1) after fulfillment of relationship (27.59) the increase of the boundary function on a section of the boundary of the band equal to the tooth width T , should nowhere in the interval $0 \leq x \leq l$ exceed $\frac{i_{\max}}{\gamma} = \frac{l_m}{10\gamma}$

$$\Delta J_1 = J_1(x + T) - J_1(x) \leq \frac{i_{\max}}{\gamma}; \quad (27.61)$$

2) the distance between any immediate extremal points of the function should be not less than $2T$.

From formula (27.60) it is easy to determine the additional conditions which must be satisfied by boundary function $J_1(x)$, so that the relative error does not exceed a given value, for instance one percent,

$$\delta = \frac{\Delta U_{\gamma} \gamma h}{T I_m} = \frac{2,13 \cdot 10^{-2} v (i_1 - i_2)}{I_m} = 0,01, \quad (27.62)$$

whence

$$i_1 - i_2 \leq \frac{l_m}{2,13v}. \quad (27.63)$$

so as to satisfy the relationship

$$\sum_{k=1}^n J_{\max k} - \sum_{k=1}^m J_{\min k} + (J_2 - J_1) = \frac{l_m}{\gamma} \quad (27.59)$$

Here $J_{\max k}$ and $J_{\min k}$ - are extreme ordinates of the curve $J_1(x)$,

i.e., the difference in current supplied to any two neighboring teeth need not exceed $I_m/2.13v$.

Error of problem solution on the integrator was determined under the condition that the threshold function and its derivative are continuous. We shall now demonstrate using the superposition principle with the integrator it is possible to solve the problem with the same accuracy as when threshold function and its derivative have discontinuity of the first kind.

Let us consider this with an example (Fig. 51). Assume that

$$J(x) = \begin{cases} J_I(x), & -\infty < x < x_1, \\ J_{II}(x), & x_1 < x < \infty, \end{cases}$$

where

$$J_{II}(x_1 + 0) - J_I(x_1 - 0) = c \neq 0, \quad J'_I(x_1 - 0) = q_1 \neq J'_{II}(x_1 + 0) = q_2.$$

We draw tangents to $J(x)$ to the left and right at point x_1 . Equations of the tangents are written:

$$\begin{aligned} J_1(x) &= q_1(x - x_1) + J_I(x_1), \\ J_2(x) &= q_2(x - x_1) + J_I(x_1) + c. \end{aligned} \quad (27.64)$$

We designate

$$\begin{aligned} J_I(x) - J_1(x) &= \xi_1(x), \\ J_{II}(x) - J_2(x) &= \xi_2(x). \end{aligned}$$

Now the assigned boundary function may be written: for $-\infty < x < x_1$

$$J(x) = J_I(x) = \xi_1(x) + q_1(x - x_1) + J_I(x_1), \quad (27.65)$$

for $x_1 < x < \infty$

$$J(x) = J_{II}(x) = \xi_2(x) + q_2(x - x_1) + J_I(x_1) + c.$$

Boundary function $\xi(x)$ is continuous together with own derivative and the component of the normal derivative conditioned by $\xi(x)$, can be found with the

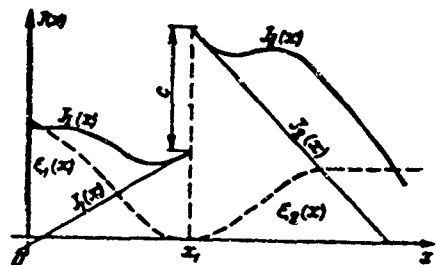


Fig. 51.

integrator. The component of the normal derivative conditioned by threshold function $J(x) = J_1(x)$ for $x < x_1$ and $J(x) = J_2(x)$ when $x > x_1$ it can be exactly calculated. Using formula (27.7) and substituting into it $\Delta J(x)$ on $J(x)$, after simple transformations we obtain:

on the upper boundary of the band ($y = h$)

$$\left. \frac{\partial J}{\partial y} \right|_{y=h} = \frac{J(x)}{h} + \frac{q_1 - q_2}{\pi} \ln(1 - e^{-\kappa(x-x_1)}) + \frac{a}{h(1 - e^{-\kappa(x_1-x)})}; \quad (27.66)$$

on the lower boundary of the band ($y = 0$)

$$\left. \frac{\partial J}{\partial y} \right|_{y=0} = \frac{J(x)}{h} - \frac{q_1 - q_2}{\pi} \ln(1 + e^{-\kappa(x-x_1)}) + \frac{a}{h(1 + e^{-\kappa(x_1-x)})} \quad (27.67)$$

In formulas (27.66) and (27.67) $J(x) = J_1(x)$ for $x < x_1$ and $J(x) = J_2(x) - c$ for $x > x_1$. Summing values of normal derivative calculated from formulas (27.66) and (27.67) with those measured on the integrator and stipulated by boundary function $\xi(x)$, we obtain a solution to the problem in this case also.

Influence of voltage drop in the tape. The voltage between buses fed from the rectifier and tape equals ± 5 V. If a current flows through the tape due to the voltage drop in it the potential difference U between the bus and different points on the tape will change and will differ from 5 V. This leads to a change of currents supplied to teeth of the tape and consequently to an error of assignment of boundary values of the searched function. Let us calculate the possible magnitude of this error.

The biggest voltage drop in the tape will be, if along the entire tape is passed a maximum current $I_{\text{max}} = 25$ A, is:

$$U_{\text{max}} = \frac{I_{\text{max}} l}{\gamma h} = \frac{25 \cdot 10}{8,04 \cdot 10^2} = 0,311 \text{ V.} \quad (27.68)$$

Hence the possible distortion of potential difference between the bus and different teeth of the tape, and means the possible relative error of assignment of boundary values of $J_1(x)$, will be

$$\delta_{1 \text{ max}} = \frac{U_{\text{max}}}{U} = \frac{0,311}{5} = 6,22 \cdot 10^{-2} = 6,22\% \quad (27.69)$$

This error is easily eliminated if, without disconnecting currents, we measure the current in every tooth and reduce it to the required magnitude. After the first such correction the error obviously will be less than

$$\delta_{2 \text{ max}} < \delta_{1 \text{ max}}^2 = 6,22^2 \cdot 10^{-4} < 0,4\%. \quad (27.70)$$

and may be neglected.

The connection between normal derivatives of the harmonic function on the boundary of the band and on the contour of the region in which the problem is solved, is known, is expressed in terms of the contour value of the derivative of the conformal mapping function

$$\frac{\partial J_1}{\partial n} = \left| \frac{d\tau}{dt} \right| \frac{\partial J}{\partial y} \bigg|_{y=h} \approx \left| \frac{\Delta\tau}{\Delta t} \right| \frac{\partial J}{\partial y} \bigg|_{y=h} \quad (27.71)$$

Here Δt — element of length of contour of the considered region; $\Delta\tau$ — its corresponding (during conformal mapping) element of length of the boundary of band or magnitude, proportional to the voltage drop on section Δt of the model contour during electrosimulation of conformal mapping.

If simulation of conformal mapping is performed on a model of thin metal sheet (electrical steel) the error of measurement of $\frac{\Delta\tau}{\Delta t}$ with a double probe with fixed distance Δt between needles connected to a galvanometer will differ little from the galvanometer error. This permits affirming that the electrointegrator in totality with simulation of conformal mapping make possible sufficiently accurate solution to the problem of determination of the normal derivative of the boundary function according to its limiting values on the contour of the considered region.

Appendix 1

Derivation of formula (27.8) for error $\Delta U(x)$

It is possible to alter the order integration in formula (27.8) by proving that the improper integral

$$\int_0^\infty \frac{\Delta J(x+a) + \Delta J(x-a) - 2\Delta J(x)}{\operatorname{ch} ka - 1} da$$

converges uniformly.

This integral has singular points $a = 0$ and $a = \infty$. At point $a = \infty$ uniform convergence is evidently due to a fast increase in the denominator. For uniform convergence when $a = 0$ it is necessary to introduce the following limitation: function $\Delta J(x)$ must be discontinuous and have a continuous first derivative. For $\Delta J(x)$ this is satisfied if we consider only continuously differentiable boundary conditions. The derivative here is limited:

$$\Delta J''(x) = \lim_{a \rightarrow 0} \frac{\Delta J(x+a) + \Delta J(x-a) - 2\Delta J(x)}{a^2} < c,$$

where c — some constant suitable for all x . Therefore for sufficiently small a

$$\Delta J(x+a) + \Delta J(x-a) - 2\Delta J(x) \leq ca^2.$$

Considering that

$$\operatorname{ch} k\alpha - 1 = \frac{k^2 \alpha^2}{2!} + \frac{k^4 \alpha^4}{4!} + \dots = \frac{k^2}{2} \alpha^2 \left(1 + \frac{2k^2 \alpha^2}{4!} + \dots \right)$$

decreases as $\alpha \rightarrow 0$ no faster than α^2 , we conclude that the integrand in the environment of zero and at zero is limited and, consequently integral (27.7) for all values x is finite. This permits integrating integral (27.7) according to parameter x within finite limits and to change the order of integration when deriving formula (27.8).

Appendix 2

Determination of the error caused by the component of current density, is proportional to $qx^2 f_1(x) + 2qx[f_2(x) + f_3(x)]$

Let us designate, as before (expressions (27.31) and (27.32))

$$\int_0^x f_1(x) dx = \varphi_1(x) = \varphi_{11}(x) + c_1, \quad \int_0^x \varphi_{11}(x) dx = F_1(x) = F_{11}(x) + c_2,$$

$$\int_0^x F_{11}(x) dx = \Psi_1(x) = \Psi_{11}(x) + c_3, \quad c_3 = \frac{1}{T} \int_0^T \Psi_1(x) dx,$$

$$\int_0^x f_2(x) dx = \varphi_2(x) = \varphi_{21}(x) + c'_1, \quad \int_0^x \varphi_{21}(x) dx = F_2(x) = F_{21}(x) + c'_2,$$

$$\int_0^x f_3(x) dx = \varphi_3(x) = \varphi_{31}(x) + c'_1, \quad \int_0^x \varphi_{31}(x) dx = F_3(x) = F_{31}(x) + c'_2,$$

$$c'_2 = \frac{1}{T} \int_0^T F_2(x) dx, \quad c'_2 = \frac{1}{T} \int_0^T F_3(x) dx, \quad \int_x^{x+T} \varphi_{21}(x) dx = 0,$$

$$\int_x^{x+T} \varphi_{31}(x) dx = 0, \quad \int_x^{x+T} F_{21}(x) dx = 0, \quad \int_x^{x+T} F_{31}(x) dx = 0, \quad \int_x^{x+T} \Psi_{11}(x) dx = 0.$$

Graphs of functions $f(x)$, $\varphi(x)$, $F(x)$, $\Psi(x)$ are shown in Figs. 47, 48 and 49. Divergence $\Delta J_1(x)$ from term $qx^2 f_1(x)$ will equal

$$\begin{aligned}\Delta J_1(x) &= q \int_0^x x^2 f_1(x) dx = qx^2 \varphi_{11}(x) - 2q \int_0^x x \varphi_{11}(x) dx = \\ &= q[x^2 \Psi_{11}(x) - 2xF_{11}(x) + 2\Psi_{11}(x) + 2c_3].\end{aligned}$$

Error $\Delta U(x)$, caused by divergence $\Delta J_1(x)$, has the form.

$$\begin{aligned}\Delta U(x) &= \frac{1}{h} \int_x^{x+T} \Delta J_1(x) dx + \\ &+ \frac{k}{2h} \int_0^{\infty} \frac{\int_x^{x+T} [\Delta J_1(x+a) + \Delta J_1(x-a) - 2\Delta J_1(x)] dx}{\operatorname{ch} ka - 1} da.\end{aligned}$$

We find each term separately

$$\begin{aligned}\frac{1}{h} \int_x^{x+T} \Delta J_1(x) dx &= \frac{q}{h} \int_x^{x+T} x^2 \varphi_{11}(x) dx - \frac{2q}{h} \int_x^{x+T} x F_{11}(x) dx + \\ &+ \frac{2q}{h} \int_x^{x+T} \Psi_{11}(x) dx + \frac{2qc_3 T}{h} = \frac{q}{h} x^2 F_{11}(x) \Big|_x^{x+T} - \frac{4q}{h} \int_x^{x+T} x F_{11}(x) dx + \\ &+ \frac{2qc_3 T}{h} = \frac{2qT}{h} \left[\left(x + \frac{T}{2} \right) F_{11}(x) - 2\Psi_{11}(x) + c_3 \right]; \\ \frac{1}{h} \int_x^{x+T} [\Delta J_1(x+a) + \Delta J_1(x-a) - 2\Delta J_1(x)] dx &= \\ &= \frac{2qT}{h} \left[\left(x + a + \frac{T}{2} \right) F_{11}(x+a) - 2\Psi_{11}(x+a) + \right. \\ &+ \left. \left(x - a + \frac{T}{2} \right) F_{11}(x-a) - 2\Psi_{11}(x-a) - \right. \\ &\quad \left. - 2 \left(x + \frac{T}{2} \right) F_{11}(x) + 4\Psi_{11}(x) \right].\end{aligned}$$

If the needles of the probe are connected to the middles of the teeth bases, i.e., for $x = \frac{T}{2}$

$$\begin{aligned}F_{11}\left(\frac{T}{2}\right) &= 0, F_{11}\left(\frac{T}{2} + a\right) = -F_{11}\left(\frac{T}{2} - a\right); \Psi_{11}\left(\frac{T}{2} + a\right) = \\ &= \Psi_{11}\left(\frac{T}{2} - a\right).\end{aligned}$$

Consequently

$$\Delta U\left(\frac{T}{2}\right) = \frac{2qT}{h} \left[c_2 - 2\Psi_{11}\left(\frac{T}{2}\right) + \right. \\ \left. + 2k \int_0^{\frac{T}{2}} \frac{\Psi_{11}\left(\frac{T}{2}\right) - \Psi_{11}\left(\frac{T}{2} + \alpha\right)}{\operatorname{ch} k\alpha - 1} d\alpha + k \int_0^{\frac{T}{2}} \frac{\alpha F_{11}\left(\frac{T}{2} + \alpha\right)}{\operatorname{ch} k\alpha - 1} d\alpha \right]. \quad (27.39a)$$

The error caused by components of current density proportional to $2qxf_2(x)$ and $2qxf_3(x)$, we find from formula (27.35) replacing in it p for $2q$, and $F_{11}(x)$ for $F_{21}(x)$ and $F_{31}(x)$ respectively. For $x = \frac{T}{2}$ we have

$$F_{21}\left(\frac{T}{2} + \alpha\right) = F_{21}\left(\frac{T}{2} - \alpha\right), \quad F_{31}\left(\frac{T}{2} + \alpha\right) = F_{31}\left(\frac{T}{2} - \alpha\right)$$

and consequently,

$$\Delta U_2\left(\frac{T}{2}\right) = \frac{2qT}{h} \left[F_{21}\left(\frac{T}{2}\right) - c'_2 + k \int_0^{\frac{T}{2}} \frac{F_{21}\left(\frac{T}{2} + \alpha\right) - F_{21}\left(\frac{T}{2}\right)}{\operatorname{ch} k\alpha - 1} d\alpha \right], \quad (27.39b)$$

$$\Delta U_3\left(\frac{T}{2}\right) = \frac{2qT}{h} \left[F_{31}\left(\frac{T}{2}\right) - c'_2 + k \int_0^{\frac{T}{2}} \frac{F_{31}\left(\frac{T}{2} + \alpha\right) - F_{31}\left(\frac{T}{2}\right)}{\operatorname{ch} k\alpha - 1} d\alpha \right]. \quad (27.39c)$$

In order to estimate the error we replace periodic curves $\Psi_{11}\left(\frac{T}{2} + \alpha\right)$, $F_{21}\left(\frac{T}{2} + \alpha\right)$ and $F_{31}\left(\frac{T}{2} + \alpha\right)$ amplitude of large with cosine curves with period T and angular $\omega = \frac{2\pi}{T}$. We take

$$\Psi_{11}\left(\frac{T}{2} + \alpha\right) = c_2 \cos \omega\alpha, \quad F_{21}\left(\frac{T}{2} + \alpha\right) = c'_2 \cos \omega\alpha, \\ F_{31}\left(\frac{T}{2} + \alpha\right) = c'_2 \cos \omega\alpha, \quad \Psi_{11}\left(\frac{T}{2}\right) = c_2, \quad F_{21}\left(\frac{T}{2}\right) = c'_2, \quad F_{31}\left(\frac{T}{2}\right) = c'_2, \\ F_{11}\left(\frac{T}{2} + \alpha\right) = \Psi'_{11}\left(\frac{T}{2} + \alpha\right) = -\omega c_2 \sin \omega\alpha.$$

Here we obtain a resultant error

$$\Delta U \left(\frac{T}{2} \right) = \Delta U_1 + \Delta U_2 + \Delta U_3 = \quad (27.39d)$$

$$= \frac{2qT}{h} \left[-c_2 + (2c_2 - c_2' - c_2'')k \int_0^{\infty} \frac{1 - \cos \omega a}{\operatorname{ch} ka - 1} da - c_3 k \int_0^{\infty} \frac{\omega a \sin \omega a}{\operatorname{ch} ka - 1} da \right].$$

Taking into account that

$$\operatorname{cth} \frac{ka}{2} = 1 + 2 \sum_{n=1}^{\infty} \frac{1}{e^{nka}}, \quad \frac{\omega}{k} = 2v,$$

we calculate the integrals entering into formula (27.39d)

$$\begin{aligned} k \int_0^{\infty} \frac{1 - \cos \omega a}{\operatorname{ch} ka - 1} da &= \left[(\cos \omega a - 1) \operatorname{cth} \frac{ka}{2} - \cos \omega a \right]_0^{\infty} - \\ &- 2\omega \int_0^{\infty} \sum_{n=1}^{\infty} \frac{\sin \omega a}{e^{nka}} da = -2\omega \sum_{n=1}^{\infty} \frac{nk \sin \omega a + \omega \cos \omega a}{e^{nka} (n^2 k^2 + \omega^2)} \Big|_0^{\infty} = \quad (27.39e) \\ &= 2 \frac{\omega^2}{k^2} \sum_{n=1}^{\infty} \frac{1}{n^2 + \frac{\omega^2}{k^2}} = 8v^2 \sum_{n=1}^{\infty} \frac{1}{n^2 + 4v^2}; \\ k \int_0^{\infty} \frac{\omega a \sin \omega a}{\operatorname{ch} ka - 1} da &= \omega a \left(1 - \operatorname{cth} \frac{ka}{2} \right) \sin \omega a \Big|_0^{\infty} + \\ &+ 2\omega \sum_{n=1}^{\infty} \int_0^{\infty} \frac{\sin \omega a}{e^{nka}} da + 2\omega \sum_{n=1}^{\infty} \int_0^{\infty} \frac{\omega a \cos \omega a}{e^{nka}} da = \quad (27.39f) \\ &= \omega a \left(1 - \operatorname{cth} \frac{ka}{2} \right) \sin \omega a \Big|_0^{\infty} + 2 \sum_{n=1}^{\infty} \frac{\omega a (\omega \sin \omega a - nk \cos \omega a)}{e^{nka} (n^2 k^2 + \omega^2)} \Big|_0^{\infty} + \\ &+ 2\omega \sum_{n=1}^{\infty} \frac{nk (\omega^2 - n^2 k^2) \sin \omega a - 2\omega n^2 k^2 \cos \omega a}{e^{nka} (n^2 k^2 + \omega^2)^2} \Big|_0^{\infty} = \\ &= 2\omega \sum_{n=1}^{\infty} \frac{2\omega n^2 k^2}{(n^2 k^2 + \omega^2)^2} = 4 \frac{\omega^2}{k^2} \sum_{n=1}^{\infty} \frac{n^2}{\left(n^2 + \frac{\omega^2}{k^2} \right)^2} = 16v^2 \sum_{n=1}^{\infty} \frac{n^2}{(n^2 + 4v^2)^2}. \end{aligned}$$

The magnitude of each sum we estimate by the integral

$$8v^2 \int_0^{\infty} \frac{dz}{z^2 + 4v^2} > 8v^2 \sum_{n=1}^{\infty} \frac{1}{n^2 + 4v^2} > 8v^2 \int_0^{\infty} \frac{dz}{(z+1)^2 + 4v^2},$$

or

$$2\pi v > k \int_0^{\infty} \frac{1 - \cos \omega \alpha}{\operatorname{ch} k \alpha - 1} d\alpha > 2\pi v - 4v \operatorname{arctg} \frac{1}{2v}. \quad (27.39g)$$

$$16v^2 \int_0^{\infty} \frac{z^2 dz}{(z^2 + 4v^2)^2} > 16v^2 \sum_{n=1}^{\infty} \frac{n^2}{(n^2 + 4v^2)^2} > 16v^2 \int_0^{\infty} \frac{(z+1)^2 dz}{[(z+1)^2 + 4v^2]^2}.$$

or

$$2\pi v > k \int_0^{\infty} \frac{\omega \alpha \sin \omega \alpha}{\operatorname{ch} k \alpha - 1} d\alpha > 2\pi v - 4v \operatorname{arctg} \frac{1}{2v} + \frac{16v^2}{2 + 8v^2}. \quad (27.39h)$$

Taking large values of integrals and substituting in the expression for error ΔU , we obtain

$$\begin{aligned} \Delta U \left(\frac{T}{2} \right) &< \frac{2qT}{h} [-c_3 + (2c_2 - c_2' - c_2'') 2\pi v - c_3 2\pi v] < \\ &< 4\pi q (c_3 + |c_2'| + |c_2''|). \end{aligned} \quad (27.39)$$

§ 28. Calculation of the Magnetic Field in the Gap of a Saturated Magnetic System

Different electrical devices contain, as one of the main sections, a magnetic system intended for producing a magnetic field of defined form and intensity in given volume. Below are considered dc magnetic systems for which a magnetic

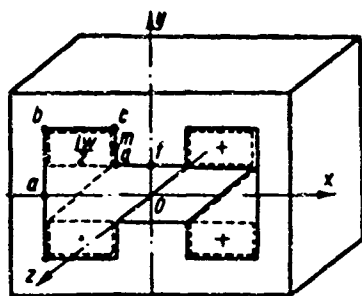


Fig. 52.

circuit of ferromagnetic material has the form shown in Fig. 52. Interest in such magnetic systems arises in connection with the development of new types of energy converters. Characteristic for such arrangements are high values of induction (higher than 2 Wb/m^2) in large air gaps between poles and, as a result, deep saturation of the magnetic circuit.

In § 21 and 22 was considered calculation of magnetic systems of electrical machines without taking into account the saturation of steel. If one were to set the permeability of steel equal to infinity than the boundary values of magnetization field potential on the surface of the steel can easily be determined and the problem of calculation of the field in air will reduce to solution of the Dirichlet problem for the Laplace equation. At saturation the permeability drops sharply and there appears a drop in magnetic potential $\Delta\varphi_m$ in the steel parts of the magnetic circuit. In principle calculation of saturation might be made if there were some method to determine the tangential component of intensity of the resultant field on the surface of steel parts of the magnetic circuit for actual values of permeability steel $\mu = \mu(B)$.

Then, integrating equality

$$H_{\text{at}} = H_t - H_{\text{at}} \quad (28.1)$$

over the contour of the core of the magnetic circuit, we obtain

$$\varphi_m(l) = \Delta\varphi_m(l) - U_m(l) + c. \quad (28.2)$$

However, in order to find tangential component of intensity H_t on the contour and, consequently, the distribution of potential $\Delta\varphi_m$, it is necessary, as will be shown below, to have values of the normal component of resultant induction B_n on the contour, in other words, to know in advance what it is necessary to determine.

Therefore calculation of the field of magnetization of a magnetic system with deep saturation is possible only by the method of successive approximations where as the initial approximation it is advantageous to take with the appropriate form the corrected results of calculation of the field for the condition $\mu = \infty$, i.e., with the assumption that the magnetic system is unsaturated.

Calculation of the field may be made according to the following scheme.

1. Determine the potential of the vortex field of currents flowing in the windings.
2. For the condition $\mu = \infty$ to find the distribution over the contour of the steel core of the potential of the field of magnetization $\varphi_1(t)$.
3. Solve the Dirichlet problem for region of air interval and find the normal component of induction of magnetization field B_{nn} on the contour.
4. Integrating values of induction B_{nn} over the contour of the magnetic circuit, find the distribution of the function of flux along the contour. If the differential equation which satisfies the function of flux in steel is known then solving the Dirichlet problem for this equation, we find the distribution of the function of flux in the magnetic circuit. Differentiating it with respect to the normal to the contour and dividing by the magnitude of permeability we find H_t on the contour of the magnetic circuit and consequently new, more precise values of distribution of potential of field of magnetization on the contour

$$\varphi_2(t) = \varphi_1(t) + \Delta\varphi_1(t).$$

5. From values of $\varphi_2(t)$ solve the new Dirichlet problem for the air interval and so forth as until $\Delta\varphi_k$ is equal with a given degree of accuracy, to $\Delta\varphi_{k-1}$.

How was demonstrated by Ye. M. Sinel'nikov, if we approximate the permeability of steel with the formula

$$\mu = \frac{a}{\sqrt{b^2 + H^2}}. \quad (28.3)$$

where a and b are constants selected for the type of steel then the field in the steel can be described by a scalar potential satisfying the equation of minimum surface

$$\frac{\partial^2 \varphi'}{\partial x^2} \left[1 + \left(\frac{\partial \varphi'}{\partial y} \right)^2 \right] - 2 \frac{\partial^2 \varphi'}{\partial x \partial y} \frac{\partial \varphi'}{\partial x} \frac{\partial \varphi'}{\partial y} + \frac{\partial^2 \varphi'}{\partial y^2} \left[1 + \left(\frac{\partial \varphi'}{\partial x} \right)^2 \right] = 0. \quad (28.4)$$

where $\Psi' = \frac{\Psi}{b}$.

Function Ψ , to the orthogonal potential, (function of flux) satisfies such an equation:

$$\begin{aligned} \frac{\partial^2 \Psi'}{\partial x^2} \left[1 - \left(\frac{\partial \Psi'}{\partial y} \right)^2 \right] + 2 \frac{\partial^2 \Psi'}{\partial x \partial y} \cdot \frac{\partial \Psi'}{\partial x} \cdot \frac{\partial \Psi'}{\partial y} + \\ + \frac{\partial^2 \Psi'}{\partial y^2} \left[1 - \left(\frac{\partial \Psi'}{\partial x} \right)^2 \right] = 0, \quad \Psi' = \frac{\Psi}{a}. \end{aligned} \quad (28.5)$$

The Dirichlet problem for equation (28.5) can be solved, for instance, by the method of grids on a computer. In order for the process of successive approximations to lead to a solution it is necessary, after determination of H_{tk} , to check whether the law of total current is satisfied

$$I\mathcal{W} = \oint H_{tk} dt. \quad (28.6)$$

If equation (28.6) is not satisfied it is necessary to proportionally alter the distribution of B_{tk} on the contour of the air interval and to repeat everything in Paragraph 4.

To facilitate calculation it is expedient in first approximations to calculate the field in steel by the usual methods of calculation taking into account scattering of magnetic flux in the air interval of the magnetic circuits. Here the magnetic circuit is divided into a series of sections 1, 2, 3, etc. (Fig. 53). From a solution of the problem in Paragraph 3 we find the magnitude of magnetic flux of the field of magnetization, Φ_{m1} , passing through sections of the magnetic circuit limiting the selected sections. Fluxes Φ_{m1} in sections of the ferromagnetic part of the magnetic circuit are equal to fluxes Φ_{m1} , passing through sections of the internal contour of the air interval limited on the one side by the point located on the axis of the pole and on the other by a point belonging to the given section. When solving the problem on an integrator for solution of the Dirichlet and Neumann problems fluxes Φ_{m1} are found by simple measurement with a voltmeter.

It is convenient to take the flux in one of the cross sections as basic. For instance in the cross section of a magnetic circuit coinciding with the working

surface of pole ($\Phi_{n,n}$), and all remaining fluxes Φ_m refer to the basic value, i.e.,

$$K_o = \frac{\Phi_{n,n}}{\Phi_{m,n}}. \quad (28.7)$$

Coefficient K_o takes into account scattering of flux by lateral surfaces of the magnetic circuit and bulging of the flux from the air gap between the poles.

In selected cross sections of the magnetic circuit fluxes of the vortex field Φ_m are determined. For a given current of excitation fluxes Φ_m are determined by the formula

$$\Phi_m = -\frac{\mu_0}{2\pi} \sum_{k=1}^n \pm I_k \ln \left| \frac{z_p - z_k}{z_q - z_k} \right|, \quad (28.8)$$

where I_k - current in cross section of winding by replacement by the axis;

z_q and z_p - complex coordinates of points limiting the cross section on the internal and, correspondingly, external circuit of the magnetic circuit;

z_k - complex coordinate of the axis with current.

For a rectangular form of the cross section of the windings of excitation it is possible to use more exact formula for $\Phi_{s,c}$, which is obtained by integration of expression (28.8) over the area of the cross section of the excitation winding.

For determination of $\Delta\varphi(t)$ calculation is made of the magnetic circuit. For this, setting the ratio of flux of the magnetization field to flux of the vortex field passing through working surface of pole,

$$\lambda = \frac{\Phi_{n,n}}{\Phi_{s,n}}. \quad (28.9)$$

find resultant flux in sections Φ_s by the formula

$$\Phi_s = \Phi_{s,c} + K_o \lambda \Phi_{s,n}. \quad (28.10)$$

Assuming in cross sections of the magnetic circuit the induction to be evenly distributed, find the mean value of induction

$$B_s = \frac{\Phi_s}{S}. \quad (28.11)$$

Further on the magnetization curve for a given sort of steel find the average intensity in the selected cross sections H_s and then the average field strength on the cross section of the magnetic circuit

$$H_{cpk} = \frac{H_{sk} + H_{s(k+1)}}{2}. \quad (28.12)$$

The magnetic intensity on the k-th section is found thus

$$\Delta\varphi_k(\tau) = H_{cpk} \Delta l_k.$$

where Δl_k - average length of section of magnetic circuit. After determining all $\Delta\varphi_k(\tau)$ it is necessary to verify fulfillment of the law of total current

$$IW = \sum_{k=1}^n \Delta\varphi_k(\tau). \quad (28.13)$$

If equality (28.13) is not satisfied one should assign a new value for λ and repeat the calculation.

Appendix 1

Example of calculation of magnetic induction of air gap between poles¹

Given: form and dimensions of magnetic circuit and windings of excitation (Fig. 53) ampere-turns of the excitation winding comprise $IW = 500\,000$ A the

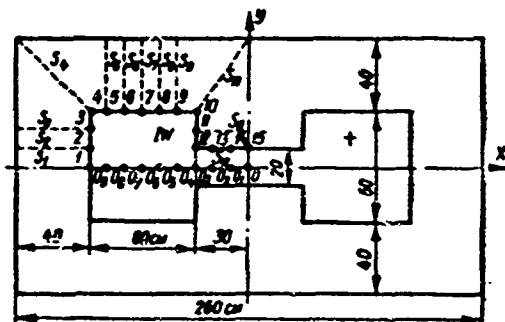


Fig. 53.

material of the magnetic circuit is grade [E2A] (32A) steel. Current density in the cross section of excitation windings is taken uniformly distributed and equal to $\delta = 1.4$ A/mm².

Determine the magnetic induction B_y on the neutral of the air gap between poles, taking the field to be plane-parallel.

¹Engineer V. F. Kuzovkov developed the method, derived the formulas and carried out the calculation.

The magnetic system has two axes of symmetry x and y therefore we will perform calculation for the region located in the second quadrant of the coordinate plane.

Magnetic induction B_y is in the form of the sum of components of the vortex field B_{xy} and magnetization field B_{my} . B_{my} was calculated for ten points located on the neutral (ox).

Results of calculation are given in Table 12.

Table 12

N_{point}	B_x	B_y	B	N_{point}	B_x	B_y	B
0	0.328	2.820	3.148	O_4	0.138	0.658	0.796
O_1	0.335	2.820	3.155	O_5	0.083	0.470	0.553
O_2	0.356	2.820	3.176	O_6	0.030	0.344	0.374
O_3	0.377	2.350	2.727	O_7	-0.149	0.282	0.133
O_4	0.320	1.160	1.480	O_8	-0.220	0.220	0

Calculation of B_{my} was accomplished with the help of simulation of the magnetization field by a dc field in a conducting sheet on an electrointegrator

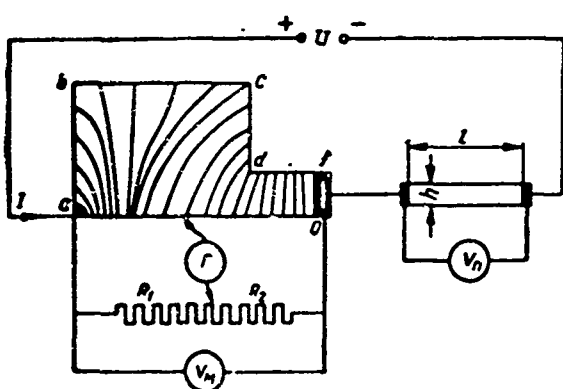


Fig. 54.

for solution of the Dirichlet and Neumann problems by the method presented in § 26 and 27.

Conformity of points of the internal contour of the region of the air interval to points on the boundary of the integrator band during conformal mapping took place on a model cut from 0.35 mm dynamo steels in a 1:3.33 scale.

The investigated section of the air interval region (region included in the second quadrant of the coordinate plane) is depicted on a rectangle with a ratio of sides 6.8 (Fig. 54).

In first iteration the system is summed unsaturated, i.e., $\Delta\varphi(\tau) = 0$, and values of $\varphi_n(\tau)_i$ were taken equal to $-\varphi_n(\tau)$.

The potential of the vortex field $\varphi_*(\tau)$ was calculated at 15 points on the internal contour (Fig. 53) with an interval between points of 10 cm, by the formula for two conductors of rectangular cross section:

$$\begin{aligned} \varphi_*(\tau) = & -\frac{\delta}{2\pi} \left\{ (y+b) \left[(x+a) \operatorname{arctg} \frac{y+b}{x+a} + (x-a) \operatorname{arctg} \frac{y+b}{x-a} - \right. \right. \\ & \left. \left. - (x+c) \operatorname{arctg} \frac{y+b}{x+c} - (x-c) \operatorname{arctg} \frac{y+b}{x-c} \right] - \right. \\ & \left. - (y-b) \left[(x+a) \operatorname{arctg} \frac{y-b}{x+a} + (x-a) \operatorname{arctg} \frac{y-b}{x-a} - \right. \right. \\ & \left. \left. - (x+c) \operatorname{arctg} \frac{y-b}{x+c} - (x-c) \operatorname{arctg} \frac{y-b}{x-c} \right] + \right. \\ & + \frac{1}{4} \left[(x+a)^2 \ln \frac{(x+a)^2 + (y-b)^2}{(x+a)^2 + (y+b)^2} + \right. \\ & + (x-a)^2 \ln \frac{(x-a)^2 + (y-b)^2}{(x-a)^2 + (y+b)^2} + (x+c)^2 \ln \frac{(x+c)^2 + (y+b)^2}{(x+c)^2 + (y-b)^2} + \\ & \left. \left. + (x-c)^2 \ln \frac{(x-c)^2 + (y+b)^2}{(x-c)^2 + (y-b)^2} \right] + \right. \\ & + \frac{1}{4} (y+b)^2 \left[\ln \frac{(x+a)^2 + (y+b)^2}{(x+c)^2 + (y+b)^2} + \ln \frac{(x-a)^2 + (y+b)^2}{(x-c)^2 + (y+b)^2} \right] + \\ & \left. + \frac{1}{4} (y-b)^2 \left[\ln \frac{(x+c)^2 + (y-b)^2}{(x+a)^2 + (y-b)^2} + \ln \frac{(x-c)^2 + (y-b)^2}{(x-a)^2 + (y-b)^2} \right] \right\}. \end{aligned} \quad (28.14)$$

Results of calculations of $\varphi_*(\tau)$ are given in Table 13.

Table 13

№ point	$\frac{\varphi_*(\tau)}{IW}$	№ point	$\frac{\varphi_*(\tau)}{IW}$	№ point	$\frac{\varphi_*(\tau)}{IW}$
1	0	6	0.1766	11	0.3750
2	0.0337	7	0.2115	12	0.4400
3	0.0687	8	0.2500	13	0.4310
4	0.0937	9	0.2800	14	0.4300
5	0.1262	10	0.3250	15	0.4275

Boundary values of $\varphi_*(\tau)$ were transferred to corresponding points of the upper boundary of the integrator band and were modelled with a current proportional to the increment $\Delta\varphi_*(\tau)$ on 86 sections of the upper boundary of the band.

Values of B_z and B calculated in the first approximation of the solution to the problem are given in Table 12.

For calculation of $\Delta\varphi(\tau)$ the magnetic circuit was divided into 12 sections (Fig. 53) from which eleven fell on the ferromagnetic part of the magnetic circuit.

The component of magnetic flux from the vortex field in cross sections bounding sections of the magnetic circuit was calculated by an exact formula in terms of the functions of flux

$$\Phi_{ss} = \mu_0 (\Psi_q - \Psi_p),$$

where Ψ_q and Ψ_p are functions of flux at points with coordinates (x_q, y_q) and (x_p, y_p) limiting the cross section on the internal and external contours of the magnetic circuit respectively. The formula for Ψ can be obtained by integration of the expression for the function of flux of complex potential created by the axis with current over the area of the cross section of the excitation winding. For the considered case when the cross section of the excitation winding comprises two rectangles the formula has the form:

$$\begin{aligned} \Psi(x, y) = & \frac{\delta}{4\pi} \left\{ (y+b) [(x+c) \ln((x+c)^2 + (y+b)^2) + (x-c) \times \right. \\ & \times \ln((x-c)^2 + (y+b)^2) - (x+a) \ln((x+a)^2 + (y+b)^2) - \\ & - (x-a) \ln((x-a)^2 + (y+b)^2)] - (y-b) [(x+c) \ln((x+c)^2 + (y-b)^2) + \\ & + (x-c) \ln((x-c)^2 + (y-b)^2) - (x+a) \ln((x+a)^2 + (y-b)^2) - \\ & - (x-a) \ln((x-a)^2 + (y-b)^2)] + \\ & + (y+b)^2 \left[\operatorname{arctg} \frac{x+c}{y+b} + \operatorname{arctg} \frac{x-c}{y+b} - \operatorname{arctg} \frac{x+a}{y+b} - \operatorname{arctg} \frac{x-a}{y+b} \right] - \\ & - (y-b)^2 \left[\operatorname{arctg} \frac{x+c}{y-b} + \operatorname{arctg} \frac{x-c}{y-b} - \operatorname{arctg} \frac{x+a}{y-b} - \operatorname{arctg} \frac{x-a}{y-b} \right] + \\ & + (x+c)^2 \left[\operatorname{arctg} \frac{y+b}{x+c} - \operatorname{arctg} \frac{y-b}{x+c} \right] + (x-c)^2 \left[\operatorname{arctg} \frac{y+b}{x-c} - \right. \\ & - \left. \operatorname{arctg} \frac{y-b}{x-c} \right] - (x+a)^2 \left[\operatorname{arctg} \frac{y+b}{x+a} - \operatorname{arctg} \frac{y-b}{x+a} \right] - \\ & - (x-a)^2 \left[\operatorname{arctg} \frac{y+b}{x-a} - \operatorname{arctg} \frac{y-b}{x-a} \right] + c. \end{aligned} \quad (28.15)$$

Computed data using formula (28.15), are given in Table 14.

Table 14

No section	Φ_{as}	K_{σ_1}	K_{σ_2}	K_{σ_3}	No section	Φ_{as}	K_{σ_1}	K_{σ_2}	K_{σ_3}
1	0.0615	1.380	1.430	1.432	8	0.067	1.290	1.287	1.290
2	0.059	1.385	1.437	1.435	9	0.0546	1.260	1.245	1.241
3	0.047	1.390	1.437	1.436	10	0.07	1.255	1.223	1.220
4	0.045	1.400	1.435	1.437	11	0.0975	1.219	1.200	1.1955
5	0.0615	1.390	1.425	1.435	12	0.103	1	1	1
6	0.07	1.360	1.405	1.403	13	0.116	0.855	0.920	0.920
7	0.073	1.341	1.350	1.350					

The component of flux of the magnetization field in the same sections was measured on the integrator and its values in relative units (in the form of coefficient K_{σ}) are given in Table 14. According to data from this table the magnetic circuit calculated in accordance with the method presented in the above mentioned calculation scheme for $\lambda = 5.125$, determined values of $\Delta\Phi(\tau)$ and found boundary values of potential of magnetization field $\Phi_H(\tau)_2$, necessary for solution of the Dirichlet problem in second approximation.

Boundary conditions and solution of the Dirichlet problem in the form of coefficients K_{σ_1} in second duration are given in Tables 14 and 15.

Table 15

No point	$\Phi_H(\tau)_2$	$\Phi_H(\tau)_3$	No point	$\Phi_H(\tau)_2$	$\Phi_H(\tau)_3$
1	0	0	9	114063	111700
2	15150	13300	10	135613	133220
3	29085	25450	11	122713	121750
4	40770	36050	12	131342	129075
5	45780	46585	13	128338	126075
6	63338	62460	14	126338	124075
7	82248	80305	15	125088	122825
8	100338	98135			

Then, analogously, according to the given K_{σ_1} were calculated potentials $\Phi_H(\tau)_3$ for the third iteration with $\lambda = 5.225$ and the problem of determining the magnetization field was solved. Values of $\Phi_H(\tau)_3$ and K_{σ_2} are also given in Tables 14 and 15. Comparing coefficients K_{σ_1} and K_{σ_2} , we notice that the maximum divergence between them in the same cross sections amounts to less than 0.15%. Being limited by an such accuracy we at this point terminate solution

Point	B_{H3}	B_3
0	1.69	2.011
O_1	1.69	2.025
O_2	1.74	2.096
O_3	1.5	1.877
O_4	0.78	1.1
O_5	0.51	0.648
O_6	0.396	0.479
O_7	0.281	0.311
O_8	0.209	0.06
O_9	0.22	0

I Table 10 are given values of induction of magnetization field and the resultant induction on the neutral between poles obtained after three iterations.

§ 29. On Electromodeling of a Magnetic Field
and on the Possibility of Computer
Calculation of Static Fields
in Nonlinear Media

176

field in the machine. Existing methods of calculation of this field in machine are based on the use of the circuit concept and therefore can give only approximate results the accuracy of which often does not satisfy technical requirements. This circumstance calls for a more strict approach to the problem of calculation of the magnetic field in machines. The complexity of solution of this problem is determined not only by the complexity of the configuration of the contour of the machine components but also by the fact that at great field intensity saturation of the steel parts of the machine occurs and their magnetic properties are changed. In this paragraph a mathematical formulation is given for the problem of calculating the magnetic field in an electrical machine and the possibility of its solution by electrosimulation and automatic digital computer is considered.

Simulation of magnetic field by a dc field in a conducting sheet. Statement of problem [2]. Let the form and location of cross sections of windings with current and the distribution of current in them be given; a form and location of steel machine components and their magnetic characteristics, represented by magnetization curves.

It is required to determine the magnetic induction in the air interval of the machine with the following assumptions: the medium is considered isotropic with respect to its magnetic properties; the magnetic field in machine is taken to be plane-parallel.

In order to use the method of superposition when determining of fields in steel parts we take into account the nonlinearity of the magnetic characteristic of steel with elementary currents of density c , distributed over the cross section and framework of current, with linear density τ , distributed over the contour of the cross section of the steel machine components. After that we will assume that the entire medium is uniform with permeability μ equal to the permeability of free space, μ_0 [21].

The magnetic field in the machine may now be represented as formed by three sources: current by density c in the cross section of the machine windings; elementary currents with density c in the cross section of the steel machine components; framework of current with density τ on the contour of the cross section of steel parts.

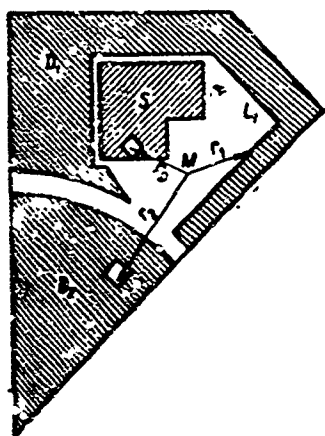
In accordance with this the vector potential of the magnetic field has the form

$$A = A_0 - \frac{\mu_0}{2\pi} \oint_L \tau \ln r_1 dl - \frac{\mu_0}{2\pi} \int_S \sigma \ln r_2 dS, \quad (29.1)$$

where

$$A_0 = - \frac{\mu_0}{2\pi} \int_S \delta \ln r_3 dS. \quad (29.2)$$

Function A_0 is known since the distribution of δ over the cross section of the windings of the machine is given (Fig. 56). In equation (29.1) integration



must be performed over cross sections of all steel bodies and their contours.

In order for equation (29.1) to yield the form of an integral equation we express σ and τ in terms of the sought quantity A . First we determine τ .

We delineate a section of the steel component of length dt and enclose it in a rectangle $abcd$. Applying the law of total current to contour $abcd$, we obtain

Fig. 56.

$$\oint_{abcd} \vec{B} d\vec{l} = \oint_{abcd} B_t di = \mu_0 di. \quad (29.3)$$

where di — current through surface bounded by contour $abcd$.

Infinitely approaching sections ab and cd in such a manner so that element dt remains continually between them, at the limit we obtain

$$\oint_{abcd} B_t^- dl = (B_t^- - B_t) dt = \mu_0 di, \quad (29.4)$$

where B^- and B — are induction in air and in steel respectively.

Taking into account the equality of components of intensity on the contour we obtain

$$\mu_0 \frac{dl}{dt} = \mu_0 \tau = B_t^- - B_t = - \left(\frac{\mu}{\mu_0} - 1 \right) \mu_0 H_t = - \left(\frac{\mu}{\mu_0} - 1 \right) B_t^-. \quad (29.5)$$

Since

$$B_t^- = - \frac{\partial A^-}{\partial n}, \quad (29.6)$$

where n - direction of external normal to contour L , then, designating $\frac{\mu}{\mu_0} = \mu$, for the framework of current τ , we have

$$\mu_0 \tau = (\mu - 1) \frac{\partial A^-}{\partial n}. \quad (29.7)$$

Let us turn to determination of σ . In accordance with Maxwell's first equation, in the cross section of a steel part we have

$$\mu_0 \vec{\sigma} = \text{rot} \vec{B}, \quad (29.8)$$

where

$$\text{rot} \vec{H} = 0 \text{ and } \vec{B} = \mu \vec{H}. \quad (29.9)$$

Substituting (29.9) into (29.8) we obtain

$$\mu_0 \vec{\sigma} = \text{rot} \mu \vec{H} = \mu \text{rot} \vec{H} + \text{grad} \mu \times \vec{H} = \text{grad} \mu \times \vec{H}. \quad (29.10)$$

For a flat field this relationship takes the form

$$\mu_0 \sigma = \frac{\partial \mu}{\partial x} H_y - \frac{\partial \mu}{\partial y} H_x = \frac{1}{\mu} \frac{d\mu}{dB} \left(\frac{\partial B}{\partial x} B_y - \frac{\partial B}{\partial y} B_x \right) \quad (29.11)$$

Since $\mu = \frac{B}{H}$, for $\frac{d\mu}{dB}$ we obtain

$$\frac{d\mu}{dB} = \frac{1}{H} - \frac{B}{H^2} \frac{dH}{dB} = \frac{1}{H} \left(1 - \mu \frac{dB}{dH} \right). \quad (29.12)$$

But $\frac{dB}{dH}$ is the dynamic permeability μ_d . Designating $\frac{\mu}{\mu_d} = \mu'$ and substituting

in (29.12), we obtain

$$\frac{1}{\mu} \frac{d\mu}{dB} = - \frac{\mu' - 1}{B}, \quad (29.13)$$

Considering what

$$B = \sqrt{B_x^2 + B_y^2}, \quad (29.14)$$

have

$$\frac{\partial B}{\partial x} = \frac{\partial B_x}{\partial x} \frac{B_x}{B} + \frac{\partial B_y}{\partial x} \frac{B_y}{B}, \quad \frac{\partial B}{\partial y} = \frac{\partial B_x}{\partial y} \frac{B_x}{B} + \frac{\partial B_y}{\partial y} \frac{B_y}{B}. \quad (29.15)$$

Substituting (29.13) and (29.15) in (29.11) and considering that

$$\operatorname{div} \vec{B} = \frac{\partial B_x}{\partial x} + \frac{\partial B_y}{\partial y} = 0, \quad (29.16)$$

we obtain

$$\mu_0 \sigma = \frac{(\mu' - 1)}{B^2} \left[B_x^2 \frac{\partial B_x}{\partial y} - B_y^2 \frac{\partial B_y}{\partial x} - 2 B_x B_y \frac{\partial B_z}{\partial x} \right]. \quad (29.17)$$

Substituting here

$$\begin{aligned} B_x &= \frac{\partial A}{\partial y} = A_y', & B_y &= -\frac{\partial A}{\partial x} = -A_x', & \frac{\partial B_x}{\partial y} &= \frac{\partial^2 A}{\partial y^2} = A_{yy}'', \\ \frac{\partial B_y}{\partial x} &= -\frac{\partial^2 A}{\partial x^2} = -A_{xx}'', & \frac{\partial B_z}{\partial x} &= \frac{\partial^2 A}{\partial x \partial y} = A_{xy}'', & B^2 &= A_x'^2 + A_y'^2. \end{aligned} \quad (29.18)$$

we express σ in terms of the vector magnetic potential

$$\mu_0 \sigma = (\mu' - 1) \frac{A_x'^2 A_{xx}'' + A_y'^2 A_{yy}'' + 2 A_x' A_y' A_{xy}''}{A_x'^2 + A_y'^2}. \quad (29.19)$$

Substituting expressions for τ and σ into initial equation (29.1) we obtain an integral equation for the vector magnetic potential of the field in the machine

$$\begin{aligned} A &= A_0 - \frac{1}{2\pi} \oint_L (\mu' - 1) \frac{\partial A}{\partial n} \ln r_1 dl - \\ &- \frac{1}{2\pi} \int_D (\mu' - 1) \frac{A_x'^2 A_{xx}'' + 2 A_x' A_y' A_{xy}'' + A_y'^2 A_{yy}''}{A_x'^2 + A_y'^2} \ln r_2 dS. \end{aligned} \quad (29.20)$$

Equation (20.20) can be solved by the usual method of solving similar integral equations, i.e., sequentially substituting under the radical integral values $A_0, A_1, \dots, A_k, A_{k+1}$, where

$$A_1 = A_0 - \frac{1}{2\pi} \oint_L (\mu_i - 1) \frac{\partial A_0}{\partial n} \ln r_1 di \quad (20.21)$$

$$- \frac{1}{2\pi} \int_D (\mu_i - 1) \frac{A_0^2 A_{0x} + 2A_{0x} A_{0y} A_{0x} + A_0^2 A_{0y}}{A_0^2 + A_0^2} \ln r_2 d\Omega$$

etc., as long as A_{k+1} differs from A_k by a value smaller than the permitted error.

Obviously this solution scheme has meaning only if the process of successive approximations is convergent. In the present work questions associated with convergence of the process are not considered inasmuch as they require special investigation. But even under the condition of convergence of the process analytical solution of equation (29.20) is very complicated and laborious. Therefore it is proposed that equation (29.20) be solved by simulation.

Before proceeding to an account of this question we will convert equation (20.29) into a more convenient form. Let us rewrite equation (20.11), substituting equation (29.13) into it

$$\mu_0 \sigma = \frac{i}{\mu} \frac{d\mu}{dB} \left(\frac{\partial B}{\partial x} B_x - \frac{\partial B}{\partial y} B_y \right) = (\mu_i - 1) \left(\frac{\partial B}{\partial y} \frac{B_x}{B} - \frac{\partial B}{\partial x} \frac{B_y}{B} \right) \quad (20.22)$$

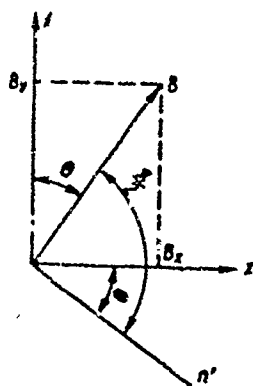
But from the other side

$$-\frac{B_x}{B} = \sin \theta = \frac{\partial y}{\partial n'}, \quad \frac{B_y}{B} = \cos \theta = \frac{\partial x}{\partial n'} \quad (20.23)$$

where n' is the direction, normal to vector \vec{E} (Fig. 57), obtained during turning. Consequently

$$\mu_0 \sigma = -(\mu_i - 1) \times$$

$$\times \left[\frac{\partial B}{\partial y} \frac{\partial y}{\partial n'} + \frac{\partial B}{\partial x} \frac{\partial x}{\partial n'} \right] = -(\mu_i - 1) \frac{\partial B}{\partial n'} \quad (20.24)$$



Equation (29.20) will be converted now thus:

$$A = A_0 + \frac{1}{2\pi} \oint_L (\mu_r - 1) B_r \ln r_i di + \frac{1}{2\pi} \int_S (\mu_r - 1) \frac{\partial B}{\partial n} \ln r^2 dS. \quad (29.25)$$

Fig. 57.

Let us show what vector potential \bar{A} , satisfying equation (29.20) or (29.25) can, by means of successive approximations, be simulated by the electrical potential of a dc field in a conducting sheet.

We take the model of an unlimited plane — an electrointegrator for simulation of particular solution of the Poisson equation (§ 24). Potential of the current of density δ_1 applied to the model on section S_1 is determined by formula (16.13).

Comparing it with (29.1) and (29.2) we notice that if cross section of conductor S and density of current in it δ in a magnetic field are equal to surface S_1 and density of current supplied to it δ_1 on the model, then the vector potential of magnetic field \bar{A} will be numerically equal to the electrical potential on the model U multiplied by $\mu_0 \gamma$

$$A = \mu_0 \gamma U. \quad (29.26)$$

Equipotential lines $U = \text{const}$ on the model will correspond to magnetic lines $A = \text{const}$, magnetic induction \bar{B} will be determined from relationship

$$B = -\frac{\partial A}{\partial n} = -\mu_0 \gamma \frac{\partial U}{\partial n}, \quad (29.27)$$

where n is the direction of the external normal to the magnetic line (line $U = \text{const}$ on the model). Finally the magnetic flux through any cylindrical surface between two points M_1 and M_2 will be defined as a magnitude proportional to the voltage U_{12} between these points on model

$$\Phi = (A_1 - A_2)h = \mu_0 \gamma h (U_1 - U_2) = \mu_0 \gamma h U_{12}. \quad (29.28)$$

where h is the dimension of the surface in the direction of the axis of conductors with current.

To model a continuous distribution of current on section of surface model S_1 by the indicated is obviously possible since we cannot at every point connect a conductor with current. However it is possible to divide region S into separate, sufficiently small sections and, assuming within the limits of each section a constant density of current, with the help of thin conductors supply to every section the appropriate current. It is expedient to split the entire region into equal squares and to apply a current to the center of each such square. Then the actual value of potential at any point will differ from the value calculated from formula (16.13) by a magnitude of error obtained by replacement the integral with a finite sum.

Let us consider how it is possible to model a magnetic field in a ferromagnetic medium. Obviously this problem reduces to detecting that distribution of elementary currents σ and τ for which integral equation (29.20) or (29.25) is satisfied.

We split the region occupied by steel into squares of equal size ΔS and the contour region into sections of equal length Δl . At the center of each square and also to each section of the contour Δl by means of a thin plate we connect the conductors. The algorithm of simulation of vector potential A is similar to the algorithm of analytic solution of equation (29.20) or (29.25) and contains the following operations.

1. On the section of the model corresponding to the cross section of the winding with current we assign a distribution of current in the conducting wires $\delta = \mu_0 \gamma \delta$, corresponding to the distribution of current in the winding of machine and thereby model the field of vector potential A_0 .

2. With a probe connected to a zero galvanometer we plot the family of equipotential lines $U_0 = \text{const}$ corresponding to lines $A_0 = \text{const}$.

3. With a double probe with distance d between needles connected to an ordinary galvanometer we measure the magnitude of induction \vec{B} at internal points of the region occupied with steel. For this purpose we place the probe perpendicular to line $U = \text{const}$.

4. From the found value of B from the magnetization curve we find μ' . From Fig. 58 it is clear μ' is determined from the magnetization curve

And computer calculation of static fields in nonlinear media. As is known, the static magnetic or electrical field in any isotropic medium is described by the following system of equations (hereinafter the presentation will be conducted for a magnetic field although all results are directly applicable to an electrical field also):

$$\begin{aligned}\operatorname{div} \bar{B} &= 0, \\ \operatorname{rot} \bar{H} &= \delta, \\ \bar{B} &= \mu \bar{H}.\end{aligned}\tag{29.29}$$

We assume here a permeability depending on the modulus of field strength

$H: \mu = \mu(H)$, i.e., it is nonlinear.

Usually the field sources - macroscopic currents - are situated in a linear medium. In a nonlinear medium the field satisfies the system of equations

$$\begin{aligned}\operatorname{div} \bar{B} &= 0, \\ \operatorname{rot} \bar{H} &= 0, \\ \bar{B} &= \mu \bar{H}.\end{aligned}\tag{29.30}$$

The second equation of system (29.30) permits introducing a scalar function - potential φ - from the relationship

$$\begin{aligned}\bar{H} &= -\operatorname{grad} \varphi, \\ H &= \sqrt{\varphi_x^2 + \varphi_y^2 + \varphi_z^2}\end{aligned}\tag{29.31}$$

and to reduce system of equations (29.30) to one differential equation for potential φ

$$\operatorname{div} (\mu \operatorname{grad} \varphi) = 0\tag{29.32}$$

or

$$\frac{\partial}{\partial x}(\mu \varphi_x) + \frac{\partial}{\partial y}(\mu \varphi_y) + \frac{\partial}{\partial z}(\mu \varphi_z) = 0.$$

On boundary of separation of media following boundary conditions hold:

$$\begin{aligned}\varphi^+(l) &= \varphi^-(l), \\ \mu^+ \frac{\partial \varphi^+}{\partial n} &= \mu^- \frac{\partial \varphi^-}{\partial n}.\end{aligned}\tag{29.33}$$

the + and - signs designating potential and permeability on opposite sides of the boundary.

Thus in the entire space outside the sources calculation the field reduces to a solution of the boundary value problem for equation (29.32) with boundary conditions (29.33).

With defined, sufficiently weak limitations imposed on the form of the boundary of the media and their magnetic characteristics, there is a basis to assume that a solution of this problem can be obtained by means of a solution of a series of simpler boundary value problems of first and second kind in each of the media separately. However nonlinearity of permeability leads to equation (29.32) becoming nonlinear and the solution of even these simpler problems turns out to be exceptionally complicated where for every form of nonlinearity it is necessary to a special method of solution.

At the same time another approach to the problem of calculation of the field permits constructing very general method of solution which depends not only on the form of nonlinearity of the medium but also on the dimension of region. Let us show that the boundary value problem of first or second kind for equation (29.32) can be replaced by the variational problem of finding the minimum of a certain functional. Let us consider the functional

$$J(\varphi) = \iiint_D F(\varphi, \varphi_x, \varphi_y, \varphi_z, x, y, z) dx, dy, dz, \quad (29.34)$$

where D — region in which the potential satisfies equation (29.32); F — some function.

So that the extremal of functional (29.34) be potential φ satisfying equation (29.32) and the given boundary values it is necessary and sufficiently that equation (29.32) be the Euler equation for functional (29.34) [22]. In general form the Euler equation for functional (29.34) is written:

$$F_\varphi - \frac{\partial}{\partial x} F_{\varphi_x} - \frac{\partial}{\partial y} F_{\varphi_y} - \frac{\partial}{\partial z} F_{\varphi_z} = 0. \quad (29.35)$$

If we consider that F is a function only of $\varphi_x, \varphi_y, \varphi_z$, then equation (29.35) takes the form:

$$\frac{\partial}{\partial x} F_{\varphi_x} + \frac{\partial}{\partial y} F_{\varphi_y} + \frac{\partial}{\partial z} F_{\varphi_z} = 0. \quad (29.36)$$

Here the total differential dF has the form

$$dF = F_{\varphi_x} d\varphi_x + F_{\varphi_y} d\varphi_y + F_{\varphi_z} d\varphi_z. \quad (29.37)$$

Comparing equations (29.32) and (29.36) we note that if the following conditions are satisfied

$$\begin{aligned} \frac{\partial}{\partial \varphi_y} (\mu \varphi_x) &= \frac{\partial}{\partial \varphi_x} (\mu \varphi_y), \\ \frac{\partial}{\partial \varphi_z} (\mu \varphi_y) &= \frac{\partial}{\partial \varphi_y} (\mu \varphi_z), \\ \frac{\partial}{\partial \varphi_x} (\mu \varphi_z) &= \frac{\partial}{\partial \varphi_z} (\mu \varphi_x), \end{aligned} \quad (29.38)$$

that it is possible to set

$$\mu \varphi_x = F_{\varphi_x}, \quad \mu \varphi_y = F_{\varphi_y}, \quad \mu \varphi_z = F_{\varphi_z}, \quad (29.39)$$

i.e., to present $\mu \varphi_x$, $\mu \varphi_y$, $\mu \varphi_z$ in the form of partial derivatives of integrand F .

We have

$$\frac{\partial}{\partial \varphi_y} (\mu \varphi_x) = \frac{\partial \mu}{\partial \varphi_y} \varphi_x = \frac{d\mu}{dH} \frac{\partial H}{\partial \varphi_y} \varphi_x = \frac{\mu'}{H} \varphi_y \varphi_x = \frac{\partial}{\partial \varphi_x} (\mu \varphi_y). \quad (29.40)$$

Analogously it is possible to show that the other two of conditions (29.38) are satisfied. Consequently

$$\begin{aligned} dF &= \mu \varphi_x d\varphi_x + \mu \varphi_y d\varphi_y + \mu \varphi_z d\varphi_z = \frac{\mu}{2} d(\varphi_x^2 + \varphi_y^2 + \varphi_z^2) = \\ &= \mu \cdot \sqrt{\varphi_x^2 + \varphi_y^2 + \varphi_z^2} \cdot d(\sqrt{\varphi_x^2 + \varphi_y^2 + \varphi_z^2}) = \mu(H) \cdot H dH. \end{aligned} \quad (29.41)$$

Integrating dF from 0 to $H = \sqrt{\varphi_x^2 + \varphi_y^2 + \varphi_z^2}$, we obtain the sought function F

$$\begin{aligned} F(H) &= \int_0^H \mu(H) H dH = \int_0^{\sqrt{\varphi_x^2 + \varphi_y^2 + \varphi_z^2}} \mu \sqrt{\varphi_x^2 + \varphi_y^2 + \varphi_z^2} \times \\ &\quad \times d(\sqrt{\varphi_x^2 + \varphi_y^2 + \varphi_z^2}). \end{aligned} \quad (29.42)$$

or more concisely

$$F(H) = \int_0^H B dH. \quad (29.43)$$

Let us check if partial derivatives F satisfy equation (29.39).

We have

$$F_{\varphi_x} = \frac{dF}{dH} \cdot \frac{\partial H}{\partial \varphi_x} = \mu H \cdot \frac{\varphi_x}{H} = \mu \varphi_x,$$

and likewise

$$F_{\varphi_y} = \mu \varphi_y, \quad F_{\varphi_z} = \mu \varphi_z.$$

Consequently functional (29.34) has the form

$$J(\varphi) = \iiint_D \left[\int_0^{\sqrt{\varphi_x^2 + \varphi_y^2 + \varphi_z^2}} \mu \sqrt{\varphi_x^2 + \varphi_y^2 + \varphi_z^2} d(\sqrt{\varphi_x^2 + \varphi_y^2 + \varphi_z^2}) \right] dx dy dz. \quad (29.44)$$

or more concisely

$$J(\varphi) = \iiint_D \left[\int_0^H \mu(H) \cdot H dH \right] dV = \iiint_D \left[\int_0^H B dH \right] dV. \quad (29.45)$$

Functional (29.44) possesses the property that it attains a minimum for that φ , which satisfies the sought field equations (29.30) or their equivalent equation (29.32). If medium is linear, i.e., μ does not depend on intensity H , then this functional expresses the field energy in volume D . Indeed, in this case

$$F = \int_0^H \mu H dH = \frac{\mu H^2}{2} \quad (29.46)$$

and the functional takes on the form

$$J(\varphi) = \iiint_D \frac{\mu H^2}{2} dV = W. \quad (29.47)$$

Its minimum determines the field in a linear medium.

As Chaplygin demonstrated his book "On Gas Streams" if one were to set

$$\mu = \frac{i}{\sqrt{1 + \varphi_x^2 + \varphi_y^2}}, \quad (29.48)$$

that in a flat field equation (29.30) will be converted into the equation of minimum surface. If one were to take $\varphi = z$, functional (29.44) for this value of μ will express the area S of the surface bounded by the space contour L whose projection onto plane XoY limits the region D . In this case

$$F = \frac{1}{2} \int_0^H \frac{d(H^2)}{\sqrt{1 + H^2}} = \sqrt{1 + H^2} - 1 = \sqrt{1 + \varphi_x^2 + \varphi_y^2} - 1,$$

and functional (29.44) has the form (we neglect the one).

$$J(\varphi) = \iint_D \sqrt{1 + \varphi_x^2 + \varphi_y^2} dx dy = \iint_D \sqrt{1 + z_x^2 + z_y^2} dx dy = S. \quad (29.49)$$

The minimum of the functional will determine the minimum surface drawn over space contour L .

If expression $J(\varphi)$ is known it is not difficult to replace the boundary value problem of calculation of a field in a linear or nonlinear isotropic medium with the problem of detecting the relative minimum of the corresponding functional. For instance, solution of the first boundary value problem for equation (29.32) is equivalent to detecting the minimum of functional $J(\varphi)$ for boundary condition $\varphi(t) = f_1(t)$ (where t - point on boundary of region and $f_1(t)$ - given function). This condition may be written:

$$Q_1(\varphi) = \oint_S (f_1(t) - \varphi(t))^2 dS = 0. \quad (29.50)$$

Here S - boundary of region D .

Really, if we find the potential φ at which simultaneously condition $Q(\varphi) = 0$ is satisfied and functional $J(\varphi)$ has a minimum that we thereby obtain a solution to the first boundary value problem.

If $\mu(H)$ is a single-valued function satisfying to inequalities $\mu > 0$ and $\frac{dB}{dH} > 0$, then function $F(H)$, expressing the area of the magnetization curve (Fig. 58) the function of derivatives of potential φ will be convex, i.e., there will be a single minimum obtainable under the condition $H = 0$. Here functional $J(\varphi)$ will also have a single minimum for $H = 0$ or, what is the same, when $\varphi = \text{const}$, at all points of region D. Actually the function $\Phi(x, y, \dots, \omega)$, is by definition convex if it satisfies the condition

$$\Phi\left(\frac{x_1+x_2}{2}, \dots, \frac{\omega_1+\omega_2}{2}\right) \leq \frac{\Phi(x_1, \dots, \omega_1) + \Phi(x_2, \dots, \omega_2)}{2}$$

for any $x_1, x_2, \dots, \omega_1, \omega_2$. The sum of any number of convex functions is also a convex function.

For every three values x, y, z of the coordinates of the element of volume $dV = dx dy dz$ of region D, $F(H)$ will be a convex function of derivatives of φ . Integration with respect to x, y, z constitutes a summation of convex functions over the entire volume of D. Consequently integral $J(\varphi)$ is a convex function of derivatives of φ , i.e., has a single minimum obtainable during the condition $\varphi(x, y, z) = \text{const}$.

Potential $\varphi(x, y, z)$ is an extremal of functional $J(\varphi)$ at assigned boundary conditions differing from condition $\varphi = \text{const}$ and can be found approximately by the method of fast descent. We will look for an expression for potential φ in the form of the first n members of any full family of functions $\psi_k(x, y, z)$

$$\varphi(x, y, z) \approx \sum_{k=1}^n a_k \psi_k(x, y, z) = P(x, y, z). \quad (29.51)$$

as is done in the Ritz method. In the expression for P n unknown parameters $\{a_k\}$ will enter. Here solution of our boundary value problem will lead to detecting n parameters of $\{a_k\}$, at which functional $J(\varphi)$ attains a minimum and boundary condition (29.50) is satisfied.

We replace potential φ by its approximate value P from (29.51) and substitute in expression for functional $J(\varphi)$ the boundary condition. Since for a finite number of n members of expression (29.51) it is impossible bring parbitrarily P close to φ then the right side of boundary condition (29.50) should be set

equal to $\epsilon > 0$. The magnitude of ϵ is smaller the higher the number n : it characterizes the accuracy of satisfaction of boundary conditions.

After replacement of φ through P functional $J(P)$ and boundary condition $Q(P) = \epsilon$ can be considered as functions only n unknown parameters $\{a_k\}$. In order to facilitate construction of algorithm of fast descent for the finding of potential $\varphi \approx P$, at which functional $J(P)$ attains a relative minimum, we use a geometric interpretation as is done in functional analysis. We will consider parameters $\{a_k\}$ as independent coordinates of n -dimensional Euclidean space analogous to coordinates x, y, z of ordinary three-dimensional space. Then boundary condition $Q(P) = \epsilon$ may be considered as the equation of a hypersurface of the second order in n -dimensional space of parameter $\{a_k\}$, and functional $J(P)$ as a simple convex function of these parameters. From the geometric point of view our problem consists of the fact that in order to find the point $P_0(a_1^{(0)}, a_2^{(0)}, \dots, a_n^{(0)})$ on the surface $Q(P) = \epsilon$, at which functional $J(P)$ takes a least value.

Surface $Q(P) = \epsilon$ is a hypersurface of the second order — n -dimensional ellipsoid — this smooth analytic surface is without singular points and ribs. On the other hand since functional $J(P)$ has a single minimum at the origin of coordinates (for $\{a_k\} = 0$), surfaces of level $J(P) = \text{const}$ will be closed smooth analytic surfaces embracing one another. The relative minimum of functional $J(P)$ will be attained at the point of contact $P_0(a_1^{(0)}, a_2^{(0)}, \dots, a_n^{(0)})$ of one of the surfaces level $J(P) = \text{const}$ with surface $Q(P) = \epsilon$ (Fig. 59). Since both surfaces

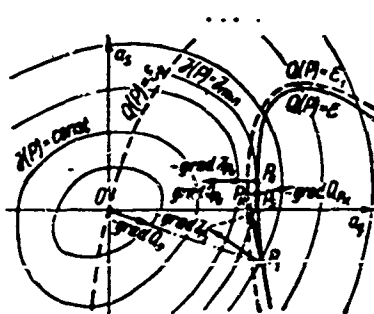


Fig. 59.

are smooth and surface $Q(P) = \epsilon$ does not pass through the origin of coordinates (the trivial case $\oint [f(t) - c]^2 dS = 0$ we do not consider) the normal drawn to the point of contact to one of the surfaces coincides with the normal to the other surface.

In order to construct a normal at any point $P(a_1, a_2, \dots, a_n)$ to a surface of level $J(P) = \text{const}$ or to surface $Q(P) = \epsilon$ it is sufficient to find J_p and $\text{grad } Q_p$ in this point. The equation of the tangent plane to the surface $Q(P) = \epsilon$ at point P_1 will be

$$\text{grad } Q_{P_i}(P - P_i) = 0.$$

Consequently our problem consists of finding such a point P_0 on surface $Q(P) = \epsilon$ at which the projection of J_{P_0} onto the tangential plane to the surface $Q(P) = \epsilon$ is equal to zero.

Let us consider now how to construct the algorithm of fast descent for finding point P_0 on surface $Q(P) = \epsilon$. The direction of fastest descent to the minimum point of functional $J(P)$ coincides with the direction of its antigradient. This direction can rapidly lead away from surface $Q(P) = \epsilon$, we have to find the point lying on the surface. The tangent plane in a small environment of the point of tangency in first approximation constitutes an element of surface. We move to the sought point P_0 in the direction of projection of antigradient $J(P)$ on the tangent plane. With such motion we also will depart from surface $Q(P) = \epsilon$, however considerably less than if we moved in the direction of the antigradient. Let us anticipate a return to the surface $Q(P) = \epsilon$ after every step. If the step is small then its final point P_k falls on surface $Q(P) = \epsilon_1$ close to surface $Q(P) = \epsilon$. Equation of surface $Q(P) = \epsilon_1$ differs from equation $Q(P) = \epsilon$ only with the right side $\epsilon_1 \neq \epsilon$. Therefore a return to the surface $Q(P) = \epsilon$ is advisably made in the direction of the normal at point P_k to surface $Q(P) = \epsilon_1$ (Fig. 59). For this it is sufficient to plot a straight line coinciding with $\text{grad } Q$ at point P_k , and to find the point of intersection of this line with the surface of boundary conditions $Q(P) = \epsilon$. As an appraisal of the sufficiency of approximation of point P_2 to the sought point P_0 of minimum of $J(P)$ can serve the length of projection of gradient $J(P)$ on the tangent plane to surface $Q(P) = \epsilon$. At the sought point of minimum P_0 length of projection of gradient $J(P)$ is equal to zero.

Point P_1 from which one should start the descent to minimum can be obtained thus: at point 0 (at the origin of coordinates) find the direction of $\text{grad } Q_0$, to plot a straight line coinciding with this direction and find the point of intersection of this line with surface $Q(P) = \epsilon$. This point if it exists, may be taken as initial point $P_1(a_1^{(1)}, a_2^{(1)}, \dots, a_n^{(1)})$. As can be seen from Fig. 59, it lies near the sought point of minimum P_0 .

§ 30. Electrosimulation of Distribution of Sinusoidal Current in Current Carriers

The growth in power of electrical generators and different electrical installations led to the appearance of high-power transmission lines with polyphase currents of great force. In connection with this there appeared the problem of calculation of parameters of polyphase lines under conditions when simplifications lying at the base of conception of the circuit, are impermissible. Polyphase lines for energy transfer with current of great force constitute system current carriers of large cross section consisting of buses or pipes of different profile. Sinusoidal current flowing along a given line is distributed nonuniformly over the cross section of the current carrier. A skin effect and effect of proximity arise. Due to this calculation of the line becomes very complicated.

In order to calculate parameters of the line, i.e., to find its resistance and reactance it is sufficient, establishing the external voltage of source \dot{E}_0 occurring per unit length of each current carrier of the line, to find the magnitude of the resistive I_a and reactive I_p components of current in each current carrier. It is possible to find the only by calculating the distribution of current density in the cross section of the current carrier. The problem of determination of the field of sinusoidal current in the current carriers is formulated in the form of an integral equation. However the formulation known in literature [1] is inconvenient for calculation and modeling, therefore we give it here in modified form. We will proceed from Kirchhoff's laws. Let us consider an m-phase system of current carriers. The cross section of the k-th current carrier we designate D_k . All together we have m current carriers. Let us take the filament of current passing through point Q_v normal to the plane of the figure in the cross section of the v-th current carrier (Fig. 60). In accordance with Kirchhoff's second law for a unit length of filament we can write

$$\dot{E}_e(Q_v) = \frac{\dot{\delta}(Q_v)}{\gamma_v} + \frac{d\dot{\Phi}(Q_v)}{dt} = \dot{E}(Q_v) + i\omega\dot{\Phi}(Q_v). \quad (30.1)$$

Here $\dot{\delta}$ — complex of current density;

\dot{E} — complex of internal electric field strength in current carrier;

$\dot{\Phi}$ — complex of magnetic flux linked with a filament of current at point Q_v ;

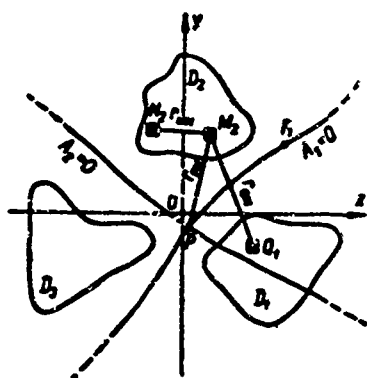


Fig. 60.

ω - angular frequency of current;

γ - conductivity of current carrier material

$$i = \sqrt{-1}.$$

At the same time, as a result of continuity of current or Kirchhoff's first law for any cross section of the line the following condition should be satisfied:

$$\sum_{k=1}^n i_k - \sum_{k=1}^n \gamma_k \int_{D_k} \vec{E}(Q_k) dQ_k = 0 \quad (30.2)$$

Let us consider the magnetic field embracing the line to the plane-parallel. From condition (30.2) it follows that magnetic flux linked with every current carrier of the line is limited. Let us clarify how it is possible to express flux $\Phi(Q_v)$ in terms of internal field strength in the current carrier. Let us assume first that along the current carriers there flows a single-phase current. Flux $\Phi(Q_v)$, linked with filament of current at point Q_v can be defined as the difference of vector magnetic potentials \vec{A} at point Q_v and at any other point P_1 , lying on a magnetic line of force differentiating the flux linked with a current carrier with a forward current from the flux linked with a current carrier with reverse current. If the current carriers do not envelope one another then this delineating line of force passing between cross sections of current carriers D_k , departs further into infinity. Flux on one side of the differentiating line during its change cuts only current carriers with forward current, on the other side - only current carriers with reverse current.

Any polyphase regime of current flow can be represented as the result of superposition of two single-phase regimes. The first regime consists of the set of real components I_a of currents in phases of the line, the second - the set of imaginary components I_p . Each regime, considered separately, will determine its own dividing magnetic line. These lines will intersect in at least one point P. Let us take the value of the vector potentials on various lines in both regimes equal to zero. Vector potential \vec{A} at point Q_v has the form

$$\vec{A}(Q_v) = -\frac{\mu}{2\pi} \sum_{k=1}^n \gamma_k \int_{D_k} \vec{E}(M_k) \ln r_{Q_v M_k} dM_k + \vec{c}_A \quad (30.3)$$

Constant \dot{c}_A will be determined from condition $A(P) = 0$, i.e.,

$$\dot{c}_A = \frac{\mu}{2\pi} \sum_{k=1}^m \gamma_k \int_{D_k} \dot{E}(M_k) \ln r_{PM_k} dM_k. \quad (30.4)$$

Consequently, flux linked with filament of current at point Q_v under polyphase conditions is equal to the vector potential at that same point:

$$\Phi(Q_v) = \dot{A}(Q_v) - \dot{A}(P) = \dot{A}(Q_v) = -\frac{\mu}{2\pi} \sum_{k=1}^m \gamma_k \int_{D_k} \dot{E}(M_k) \ln \frac{r_{Q_v M_k}}{r_{PM_k}} dM_k. \quad (30.5)$$

Let us assume that the electrical conductivity γ of all current carriers of the line are identical and their permeability is equal to the permeability of the surrounding medium μ_C . Placing the expressed for flux in equation (30.1) and designating $\lambda = \mu_C \gamma \frac{\omega}{2\pi}$, we obtain

$$\dot{E}_A(Q_v) = \dot{E}(Q_v) - i\lambda \sum_{k=1}^m \int_{D_k} \dot{E}(M_k) \ln \frac{r_{Q_v M_k}}{r_{PM_k}} dM_k. \quad (30.6)$$

Thus the problem of defining the field of a polyphase sinusoidal current in the cross section of current carriers of a transmission line reduced to the solution of a Fredholm integral equation of second kind. However formulation of the problem in such a form is indefinite. Indeed the nucleus of equation (30.6) $\ln r_{Q_v M_k} / r_{PM_k}$ depends on the position of point P crossing of differentiating magnetic lines which can be found only after solution of the problem. In spite of this, condition (30.2) permits unambiguous formulation of the problem. Let us write equation (30.6) thus:

$$\dot{E}_A(Q_v) = \dot{E}(Q_v) - i\lambda \sum_{k=1}^m \int_{D_k} \dot{E}(M_k) \ln r_{Q_v M_k} dM_k + \dot{C}. \quad (30.7)$$

Here

$$\dot{C} = i\lambda \sum_{k=1}^m \int_{D_k} \dot{E}(M_k) \ln r_{PM_k} dM_k \quad (30.8)$$

does not depend on point Q_v and consequently is a constant. At the same time the magnitude of \dot{C} depends on the total distribution of \dot{E} in the cross section of the current carries of the line and can be determined from condition (30.2).

Let us take the integral over all of D_k from both parts of equation (30.7). For brevity henceforth \int_D we will designate $\sum_{k=1}^m \int_{D_k}$, the area of cross section of all current carriers $\sum_{k=1}^m D_k$ we will designate D :

$$\int_D \dot{E}_0(Q) dQ = \int_D \dot{E}(Q) dQ - i\lambda \int_D \left[\int_D \dot{E}(M) \ln r_{QM} dM \right] dQ + D\dot{C}. \quad (30.9)$$

Hence we obtain

$$\dot{C} = i\lambda \int_D \dot{E}(M) \left[\frac{1}{D} \int_D \ln r_{QM} dQ \right] dM + \frac{1}{D} \int_D \dot{E}_0(Q) dQ. \quad (30.10)$$

We place this value of \dot{C} in equation (30.7)

$$\begin{aligned} \dot{E}_0(Q) - \frac{1}{D} \int_D \dot{E}_0(Q) dQ &= \dot{E}(Q) - i\lambda \int_D \dot{E}(M) \left(\ln r_{QM} - \right. \\ &\quad \left. - \frac{1}{D} \int_D \ln r_{QM} dQ \right) dM. \end{aligned} \quad (30.11)$$

Equation (30.11) formulates our problem. Let us show that for any distribution of \dot{E}_0 the solution of equation (30.11) uniquely satisfied condition (30.2).

We take the integral over cross section D from both parts of equation (30.11)

$$\begin{aligned} \int_D \dot{E}(Q) dQ - i\lambda \int_D \left[\int_D \dot{E}(M) \left(\ln r_{QM} - \frac{1}{D} \int_D \ln r_{QM} dQ \right) dM \right] dQ &= \\ = \int_D \dot{E}(Q) dQ - i\lambda \int_D \dot{E}(M) \left[\int_D \ln r_{QM} dQ - \frac{D}{D} \int_D \ln r_{QM} dQ \right] dM &= \\ = \int_D \dot{E}(Q) dQ = 0. \end{aligned}$$

We designate

$$\int_b \dot{E}(M) \left(\ln r_{QM} - \frac{1}{D} \int_b \ln r_{QM} dQ \right) dM = T\dot{E}, \quad (30.12)$$

$$\dot{E}_0(Q) - \frac{1}{D} \int_b \dot{E}_0(Q) dQ = f_0(Q) \quad (30.13)$$

and write equation (30.11) thus:

$$\dot{E}(Q) - i\lambda T\dot{E} = [\mathcal{E} - i\lambda T]\dot{E} = A_0\dot{E} = f_0(Q), \quad (30.14)$$

where \mathcal{E} - identity operator.

Obviously operator A_0 translates any element \dot{E} of subspace H^* , defined by condition (30.2) in an element of the same subspace, i.e., maps subspace H^* onto itself. Let us show now that operator T is self adjugate, i.e., the following equality holds:

$$(Tx, z) = (x, Tz), \quad x, z \in H^*$$

(parenthesis here designate the scalar product). Indeed:

$$\begin{aligned} (Tx, z) &= \int_b \left[\int_b x(M) \left(\ln r_{QM} - \frac{1}{D} \int_b \ln r_{QM} dQ \right) dM \right] z(Q) dQ = \\ &= \int_b x(M) \left[\int_b z(Q) \ln r_{QM} dQ \right] dM - \frac{1}{D} \int_b x(M) \left[\int_b \ln r_{QM} dQ \right] dM \times \\ &\times \int_b z(Q) dQ = \int_b x(M) \left[\int_b z(Q) \ln r_{QM} dQ \right] dM - \frac{1}{D} \int_b z(Q) \times \\ &\times \left[\int_b \ln r_{QM} dM \right] dQ = \int_b x(M) dM = \int_b x(M) \left[\int_b z(Q) \left(\ln r_{QM} - \right. \right. \\ &\left. \left. - \frac{1}{D} \int_b \ln r_{QM} dM \right) dQ \right] dM = (x, Tz). \end{aligned}$$

This signifies that eigenvalues of operator T are real and homogeneous equation

$$Tx(Q) - i\lambda Tx = 0$$

has only a trivial zero solution. Hence solution of equation (30.11) is unique.

Will apply the conjugate operator to equation (30.14)

$$\begin{aligned} A_0^* &= [\mathcal{E} + i\lambda T], \\ A_0^* A_0 \dot{E} &= [\mathcal{E} + i\lambda T][\mathcal{E} - i\lambda T] \dot{E} = \dot{E} + \lambda^2 T^2 \dot{E} = \dot{f}_0 + i\lambda T \dot{f}_0. \end{aligned} \quad (30.15)$$

Separating the real and imaginary part in equation (30.15) we obtain two independent equations relative to the sought real E_a and imaginary E_p components of internal intensity

$$\begin{aligned} E_a(Q) + \lambda^2 T^2 E_a &= f_{0a}(Q) - \lambda T f_{0p} = f_a, \\ E_p(Q) + \lambda^2 T^2 E_p &= f_{0p}(Q) + \lambda T f_{0a} = f_p. \end{aligned} \quad (30.16)$$

The second of equations (30.16) is equivalent to:

$$E_p = f_{0p} + \lambda T E_a. \quad (30.17)$$

Here

$$\begin{aligned} T^2 E &= KE = \int_D E(N) K(Q, N) dN, \\ K(Q, N) &= \int_D \left(\ln r_{QM} - \frac{1}{D} \int_D \ln r_{QM} dQ \right) \left(\ln r_{MN} - \frac{1}{D} \int_D \ln r_{MN} dM \right) dM. \end{aligned}$$

All quantities entering into equations (30.16) are real, operator $A = A_0^* A_0 = [\mathcal{E} + \lambda^2 T^2]$ is positively definite. Let us consider how to obtain a solution of our problem by modeling.

As is known, potential U of a dc electrical field in an unlimited conducting sheet with constant conductivity of unit surface γ_a is determined by the expression

$$U(Q) = -\frac{1}{2\pi\gamma_a} \int_D \delta_a(M) \ln r_{QM} dM + c. \quad (30.18)$$

Here $\delta_a(M)$ — density of current supplied to point M of the sheet, D — the section of the sheet to whose points current is supplied. If the total current supplied to the sheet is equal to zero, i.e.,

$$\int_D \delta_a(M) dM = 0,$$

then the equipotential line dividing sections of the sheet with supplied and removed current and extending to infinity will coincide with a differentiating magnetic line also extending to infinity. Assuming on this line a potential U equal to zero, we obtain an expression for the constant in formula (30.18)

$$c = \frac{1}{2\pi\gamma_a} \int_D \delta_a(M) \ln r_{PM} dM.$$

The potential difference between points Q and P are defined thus

$$U = U(Q) = - \frac{1}{2\pi\gamma_a} \int_D \delta_a(M) \ln \frac{r_{QM}}{r_{PM}} dM. \quad (30.19)$$

From a comparison of expressions (30.6) and (30.19) one may see that potential U can be used as an analog of components of internal intensity E in current carriers. Instead of unlimited conducting sheet can be used its model — the electrointegrator for simulation of a particular solution to the Poisson equation (see § 24).

The center of the lower circle of the modelling element of the integrator corresponds to a point at infinity. Since the differentiating magnetic line passes through this point can always be taken as the unknown point P and all measurements of potential U can be made on the model with respect to the center of the lower circle.

As we have seen, equation (30.6) together with condition (30.2) is equivalent to equation (30.11) and, consequently, equations (30.16) containing only real quantities modelled by a direct current in the electrointegrator [33].

Application of operator $T^2 = K$ to element F is equivalent to the following operations on the electrointegrator:

- 1) establish current in sources connected to points of region D of the upper circle of the model proportional to $2\pi\gamma_n E$;
- 2) measure potential U at the same points with respect to a point at infinity;
- 3) establish new values of current in the sources proportional to $2\pi\gamma_n U$.

After this the potential U of the field of current in the model will be proportional to the result of operation $T^2 E = KE$, n-fold application of operator K to element E obviously is equivalent to n-fold repetition of this sequence of actions on the model.

Consequently, for simulation on an electrointegrator of the field of a sinusoidal current in the cross section of conductors solution of equations (30.16) must be presented in the form of a convergent sequence of operations $K^n E_0$. The method of successive approximations under certain conditions leads to a sequence known the Neumann series [14].

The nucleus of equations (30.16) $K(Q, N)$ satisfies the conditions

$$\begin{aligned} \int_D |K(Q, N)|^2 dN &< \infty, \\ \int_D \int_D |K(Q, N)|^2 dQ dN &= B^2 < \infty. \end{aligned} \quad (30.20)$$

As is known [14], during fulfillment of these conditions the Neumann series for equations (30.16) absolutely and evenly converges to a solution at Γ if the following inequality is satisfied:

$$\lambda^2 \|K\| = \lambda^2 B < 1. \quad (30.21)$$

Thus, if inequality

$$\lambda^2 < \frac{1}{\sqrt{\int_D \int_D |K(Q, N)|^2 dQ dN}}, \quad (30.22)$$

is not satisfied then the Neumann series cannot converge.

The left part of inequality (30.22) is determined by the properties of the current carrier and surrounding medium and also the frequency of current, the right part on the location and dimensions of cross sections of the current

carriers. In practice the necessity of calculation of current carriers appears when the dimensions of the cross section exceed the depth of penetration of the electromagnetic wave. In this case inequality (30.22) is not only not satisfied, it is replaced by the reverse inequality.

We will demonstrate this on an example of calculation of two current carriers of circular cross section with diameter d , distance between centers of which equals $3d$. Let us estimate from below the magnitude of B . From the symmetry of the cross sections of the current carriers and distribution of density of current in them, it follows that the dividing magnetic line coincides with the axis of ordinates. Let us combine point P with the origin of coordinates, point O . Then, considering that $\vec{E}(M) = -E(M')$, $OM = OM'$, equation (30.6) we will convert thus:

$$\vec{E}_0(Q) = \vec{E}(Q) - i\lambda \int_{D_1} \vec{E}(M) \ln \frac{r_{QM}}{r_{QM'}} dM, \quad (30.23)$$

or, performing a transformation analogous to that which yielded equation (30.16)

$$E_0(Q) = E_s(Q) + \lambda^2 \int_{D_1} E_s(N) K(Q, N) dN, \quad (30.24)$$

where

$$K(Q, N) = \int_{D_1} \ln \frac{r_{QM}}{r_{QM'}} \ln \frac{r_{MN}}{r_{M'N}} dM.$$

For appraisal of magnitude B it is sufficient to estimate from below the norm of operator $T^2 = K$

$$\|K\| = \sup \frac{\|KE_s\|}{\|E_s\|} \geq \frac{\|KC\|}{\|C\|} = \left\| \int_{D_1} \int_{D_1} \ln \frac{r_{QM}}{r_{QM'}} \ln \frac{r_{MN}}{r_{M'N}} dM dN \right\|. \quad (30.25)$$

The following inequalities are evident

$$\left| \ln \frac{r_{QM}}{r_{QM'}} \right| > \left| \ln \frac{d}{2d} \right| = \ln 2, \quad \left| \ln \frac{r_{MN}}{r_{M'N}} \right| > \ln 2.$$

Placing them in (30.25) we strengthen inequality

$$\|K\| > \left\| \int_{b_1} \int_{b_1} (\ln 2)^2 dM dN \right\| = \left(\frac{\pi d^2}{4} \right)^2 (\ln 2)^2.$$

Consequently

$$\lambda B > \lambda \frac{\pi d^2}{4} \ln 2.$$

Will find the magnitude diameter d_0 for which the right side of this inequality is equal to one:

$$d_0 = \frac{2}{\sqrt{\lambda \pi \ln 2}} = \frac{1,35}{\sqrt{\lambda}}.$$

For aluminum at 40°C

$$\gamma = 30 \cdot 10^8 \frac{1}{\Omega \cdot \text{cm}}, \quad \mu = \mu_0 = 4\pi \cdot 10^{-7} \frac{\Omega \cdot \text{s}}{\text{cm}}, \quad \omega = 100\pi \frac{1}{\text{s}},$$

$$\lambda = \mu_0 \gamma \frac{\omega}{2\pi} = 1,885 \cdot 10^3 \frac{1}{\text{cm}^2}, \quad d_{0A} = 3,1 \text{ cm}.$$

For copper at 40°C

$$\gamma = 52,5 \cdot 10^8 \frac{1}{\Omega \cdot \text{cm}}, \quad \mu = \mu_0, \quad \lambda = 3,3 \cdot 10^3 \frac{1}{\text{cm}^2}, \quad d_{0M} = 2,35 \text{ cm}.$$

Consequently, if the dimensions of the cross sections of the current carriers exceed the magnitude of d_0 then we cannot use the method of successive approximations in usual form for construction of an algorithm of simulation of equations (30.16). However the methods of functional analysis permit presenting a solution to these equations in the form of a convergent sequence of combinations of operations $K^{\circ}E$ in the case when inequality (30.22) is not satisfied. Let us show how to obtain such a sequence.

Let us record equation (30.16) in the form:

$$AE = f. \quad (30.26)$$

We will designate μ_1 - eigenvalues of self adjoint operator T . Eigenvalues of operator $K = T^2$, equal to μ_1^2 , are real, positive and form a denumerable set with

point of concentration at zero

$$0 < \mu_i^2 < \mu_1^2.$$

Eigenvalues of operator A equal

$$\nu_i = 1 + \lambda^2 \mu_i^2.$$

We designate m and M the lower and upper bounds of the spectrum of operator A, respectively,

$$m = 1 < \nu_i < 1 + \lambda^2 \mu_1^2 = M \leq 1 + \lambda^2 \sqrt{\iint_{D^2} |K(Q, N)|^2 dQ dN}.$$

We replace equation (30.26) with

$$E = P_n(A)E + Q_n(A)f, \quad (30.27)$$

where $P_n(A)$ and $Q_n(A)$ are n order polynomials of the operator A. For equivalence of equations (30.26) and (30.27) it is necessary to satisfy certain conditions [8]. Let us find them. We have identity

$$AE - f = P_n(A)(AE - f),$$

or

$$AE = P_n(A)AE + [E - P_n(A)]f. \quad (30.28)$$

Under the condition $\|P_n(A)\| < 1$ solution of equation (30.28) coincides with solution of equations (30.26).

Applying the inverse operator to both parts of equation (30.28) we obtain

$$E = P_n(A)E + A^{-1}[E - P_n(A)]f. \quad (30.29)$$

From comparison of equations (30.27) and (30.29) we find

$$Q_n(A) = A^{-1}[E - P_n(A)].$$

Thus for equivalence of equations (30.27) and (30.26) it is necessary and sufficiently that the following conditions be satisfied:

$$\begin{aligned} \varepsilon Q_n(\varepsilon) &= 1 - P_n(\varepsilon), \\ P_n(0) &= 1 \text{ и } \|P_n(A)\| < 1, \end{aligned} \quad (30.30)$$

where ε is a parameter.

If conditions (30.30) are satisfied then equation (30.27) can be solved by the method of successive approximations and its solution coincides with the solution of initial equations (30.16). So that the process of successive approximations yields a solution as fast as possible it is necessary to select polynomial $P_n(\varepsilon)$ in such a manner so that the norm of operator $P_n(A)$ is as small as possible. This can be reached from the following considerations: if the interval of change of parameter ε includes the entire spectrum of operator A then the norm $P_n(A)$ will not exceed the biggest value of $P_n(\varepsilon)$ on this interval. Therefore for the construction of polynomial $P_n(\varepsilon)$ we use Chebyshev polynomials as was done in [9].

The Chebyshev polynomial deviating least from zero on segment $[-1, 1]$, has the form [10]

$$\begin{aligned} T_n(x) &= \frac{1}{2^{n-1}} (n \arccos x) = \\ &= \frac{(x + \sqrt{x^2 - 1})^n + (x - \sqrt{x^2 - 1})^n}{2^n} = x^n + a_{n-1}x^{n-1} + \dots + a_0. \end{aligned}$$

Converting segment $[-1, 1]$ to segment $[m, M]$, we find

$$x = ae + b = \frac{2}{M-m} z - \frac{M+m}{M-m}. \quad (30.31)$$

Passing in polynomial $T_n(x)$ to the new variable ε , we obtain

$$\begin{aligned} T_n(ae + b) &= a^n e^n + \dots + a_0 + b^n + a_{n-1}b^{n-1} + \dots + a_1b = \\ &= a^n e^n + \dots + T_n(b). \end{aligned}$$

In order to satisfy condition $P_n(0) = 1$, it is necessary to set

$$P_n(\varepsilon) = \frac{T_n(ae + b)}{T_n(b)}. \quad (30.32)$$

The biggest absolute value of $P_n(\varepsilon)$ on segment $[m, M]$ equals

$$\begin{aligned} \max_{\varepsilon \in [m, M]} |P_n(\varepsilon)| &= \frac{1}{|T_n(b)|} \max_{\varepsilon \in [m, M]} |T_n(a\varepsilon + b)| = \\ &= \frac{1}{|T_n(b)|} \max_{x \in [-1, 1]} |T_n(x)| = \frac{1}{2^{n-1} |T_n(b)|}. \end{aligned}$$

Consequently

$$\|P_n(A)\| \leq \frac{1}{2^{n-1} |T_n(b)|}. \quad (30.33)$$

We will show that $\|P_n(A)\| \leq 1$. We have

$$\begin{aligned} T_n(b) &= \frac{b^n}{2^n} \left[\left(1 + \frac{\sqrt{b^2 - 1}}{b} \right)^n + \left(1 - \frac{\sqrt{b^2 - 1}}{b} \right)^n \right] = \\ &= \frac{b^n}{2^{n-1}} \left[1 + \frac{n(n-1)}{2!} \cdot \frac{b^2 - 1}{b^2} + \dots \right] > \frac{b^n}{2^{n-1}}, \end{aligned}$$

hence

$$\|P_n(A)\| \leq \frac{1}{2^{n-1} |T_n(b)|} < \frac{1}{|b^n|} = \left(\frac{M-1}{M+1} \right)^n < 1. \quad (30.34)$$

Placing values for a and b in formula (30.32) we obtain an explicit expression for polynomial $P_n(\varepsilon)$:

$$P_n(\varepsilon) = \frac{[(M-\varepsilon) + (m-\varepsilon) + 2\sqrt{(M-\varepsilon)(m-\varepsilon)}]^n + [(M-\varepsilon) + (m-\varepsilon) - 2\sqrt{(M-\varepsilon)(m-\varepsilon)}]^n}{(M+m+2\sqrt{Mm})^n + (M+m-2\sqrt{Mm})^n}. \quad (30.35)$$

We will show that the iterative process conducted in accordance with algorithm

$$E^{(0)} = f, \quad E^{(m)} = P_n(A) E^{(m-1)} + Q_n(A) f, \quad (30.36)$$

absolutely and uniformly converges to a solution of equations (30.16).

For the $m-1$ -th iteration we obtain

$$E^{(m-1)} = P_n(A) E^{(m-2)} + Q_n(A) f.$$

The difference of two neighboring iterations has the form

$$E^{(m)} - E^{(m-1)} = P_n(A) (E^{(m-1)} - E^{(m-2)}) = [P_n(A)]^{m-1} (E^{(1)} - E^{(0)}).$$

Assuming $E^{(0)} = f$ we find

$$\begin{aligned} E^{(1)} - f &= P_n(A)f + Q_n(A)f - f = [E - AQ_n(A) + Q_n(A) - E]f = \\ &= Q_n(A)(E - A)f = -\lambda^2 K Q_n(A)f. \end{aligned}$$

Consequently,

$$\begin{aligned} |E^{(m)} - E^{(m-1)}| &= \lambda^2 \int_b |K(Q, N)| \cdot |[P_n(A)]^{m-1} \cdot Q_n(A)f| \cdot dN < \\ &< \lambda^2 \sqrt{\int_b |K(Q, N)|^2 dN} \cdot \sqrt{\int_b |[P_n(A)]^{m-1} \cdot Q_n(A)f|^2 dN} = \\ &= a_1^* \| [P_n(A)]^{m-1} Q_n(A)f \| < a^* \| P_n(A) \|^{m-1}. \end{aligned} \quad (30.37)$$

Here the constants are expressed by the formulas

$$a_1^* = \lambda^2 \sqrt{\int_b |K(Q, N)|^2 dN}, \quad a^* = a_1^* \| Q_n(A)f \|.$$

Considering that

$$\| P_n(A) \| = q < 1 \text{ и } |E^{(m)} - E^{(m-1)}| < a^* q^{m-1}.$$

We conclude that the series

$$E^{(0)} + (E^{(1)} - E^{(0)}) + \dots + (E^{(m)} - E^{(m-1)}) + \dots$$

converges absolutely and uniformly a solution of initial equations (30.16) not slower than the sum of members of a geometric progression with exponent $q < 1$.

Let us apply these results to a concrete problem. Let us consider a transmission line for energy of sinusoidal current consisting of two aluminum current carriers of rectangular cross section. Dimensions of the cross sections of the current carriers is $3 \times 10 \text{ cm}^2$, distance between them 3 cm. The integral equation for this case coincides with (30.24). By approximate calculation by means of replacement of the integral by a finite sum, we find

$$\begin{aligned} \|K\| &= \sqrt{\int_{b_1, b_2} \int_{b_1, b_2} |K(Q, N)|^2 dQ dN} < \\ &< \int_{b_1, b_2} \int_{b_1, b_2} \left| \ln \frac{r_{QM}}{r_{QN'}} \right|^2 dQ dM < 1.09 \cdot 10^{-5} \text{ м}^2. \end{aligned} \quad (30.38)$$

Dimensions of the current carrier cross sections D_1 exceed d_{0a} and inequality (30.22) is not satisfied

$$\lambda^2 = 3,55 \cdot 10^4 \gg \frac{1}{1,09 \cdot 10^{-5}} = 9,17 \cdot 10^4.$$

Therefore the usual process of successive approximations for solution of the equation will not apply.

Let us use the above mentioned method for obtaining a convergent process. Considering $n = 1$ in formulas (30.30) and (30.35) we have

$$P_1(s) = 1 - \frac{2s}{M+1}; \quad Q_1(s) = \frac{1 - P_1(s)}{s} = \frac{2}{M+1}. \quad (30.39)$$

Substituting these values in equation (30.27) we obtain

$$\begin{aligned} E &= P_1(A)E + Q_1(A)f = E - \frac{2}{M+1}(AE - f) = \\ &= a_1 KE + a_0 E + b_0 f, \end{aligned} \quad (30.40)$$

where

$$a_1 = -\frac{2\lambda^2}{M+1}, \quad a_0 = \frac{M-1}{M+1}, \quad b_0 = \frac{2}{M+1} \quad (30.41)$$

We write the norm of operator $P_1(A)$

$$\|P_1(A)\| = \frac{1}{|T_1(b)|} = \frac{1}{|b|} = \frac{M-1}{M+1} \approx 0,95.$$

Obviously, convergence will be slow and for production of a result with small error it is necessary to perform a large number of iterations.

Let us consider the iterative process when $n = 2$.

$$\begin{aligned} P_2(s) &= 1 + 8s \frac{s - M - m}{M^2 + 6Mm + m^2}; \\ Q_2(s) &= 8 \frac{M + m - s}{M^2 + 6Mm + m^2}. \end{aligned} \quad (30.42)$$

Substituting in equation (30.27) we find

$$E^{(m)} = E^{(m-1)} + \gamma [A(AC^{(m-1)} - f) - (M+1)(AE^{(m-1)} - f)],$$

where

$$\gamma = \frac{8}{M^2 + 6M + 1}.$$

Substituting here $AE = E + \lambda^2 KE$, we obtain

$$\begin{aligned} E^{(m)} &= \gamma \lambda^2 K^2 E^{(m-1)} - \gamma \lambda^2 (M-1) K E^{(m-1)} + (1 - \gamma M) E^{(m-1)} - \\ &- \gamma \lambda^2 K f + \gamma M f = a_2 K^2 E^{(m-1)} + a_1 K E^{(m-1)} + a_0 E^{(m-1)} + b_1 K f + b_0 f. \end{aligned} \quad (30.43)$$

We write the norm of operator $P_2(A)$

$$\|P_2(A)\| = \frac{1}{2|T_2(b)|} = \frac{1}{2\left(b^2 - \frac{1}{2}\right)} = \frac{1}{1 + \frac{8M}{(M-1)^2}} = 0,825,$$

i.e., $\|P_2(A)\| \approx \|P_1(A)\|^4$. Consequently to obtain a result with the same accuracy as for $n = 1$ we now require almost 4 times fewer iterations. However the duration of each iteration will be twice as great as for $n = 1$ since it will be necessary each time to model the term $K^2 E$.

It is conveniently to perform simulation on two identical models of an unlimited conducting sheet - electrointegrators with identical modelling element. Joining sources of current to points of the first model within the limits of sections D_1' and D_2' , corresponding to the sections of the current carriers D_1 and D_2 , the current in the sources is set proportional to $E_a^{(m-1)}$. The potential of the field of current in the model will here be proportional to

$$\int_{D_1} E_a^{(m-1)}(N) \ln \frac{r_{MN}}{r_{MN'}} dN.$$

Having measured the values of potential, a current proportional to them is established in the sources connected to the same points of sections D_1'' and D_2'' on the second model. The potential on the second model will be proportional to $KE_a^{(m-1)}$. To obtain the term $K^2 E_a^{(m-1)} = K[KE_a^{(m-1)}]$ it is necessary to repeat

the operations on models. Measurement of potential on the model should be made with respect to a point at infinity, i.e., with respect to the center of the lower sheet. Only in this case will the total flux $\Phi(Q)$, linked with the filament of current at point Q be taken into account. The sum of currents in the current carriers of the line is always equal to zero. Therefore the voltage between any point of the model and a point at infinity is limited.

Simulation is carried out until we obtain

$$E_i^{(n)} \approx E_i^{(n-1)}.$$

After termination of the process of simulation on models it is easy to measure not only values of E_a and E_p but also all the remaining quantities of interest when designing a current carrier. Supplying each cross section of a system of current carriers on electrointegrator from its own cross section of buses, it is possible to measure the integral magnitudes characterizing the resistance and conductivity of the system of current carriers. Simulation can be performed on a single electrointegrator. Here it is necessary to record at every point of sections D_1 and D_2 all intermediate values of results of measurements of potential.

§ 31. Computer Calculation of Parameters of a Three-Phase System of Current Carrier

The thickness of the wall of industrial current carriers usually does not exceed the depth of penetration of the electromagnetic wave and varies from 1 to 2 cm. This circumstance facilitates application of a numerical method of calculation of the field of current in the cross section of current carriers allowing application of the algorithm presented in § 30 for calculation on an electronic computer. Integration over the cross-sectional current carriers may here be replaced by summation over the contour of the center line of the cross section. For practical calculations with replacement of the integral by a sum it is convenient as the element of area ΔS to take a square with side equal to the thickness of the wall of the current carrier. Distribution of density of current along the direction of the normal to the external contour of the cross section of the current carrier can be approximately taken the same as

during penetration of a plane wave in a flat conducting wall. With computer solution of the problem time is saved and the necessity for a specialized modeling device is eliminated.

Current carriers of a three-phase transmission line usually are disposed symmetrically about the vertical axis either in one plane or so that their cross sections fall on the corners of an equilateral triangle. So as to reduce the volume of calculations and to economize the fast store of the machine during composition of the algorithm we will use symmetry. For this we shall divide the three-phase symmetric operating conditions of the line into two single-phase consisting of a set real components E_{0a} of emf E_0 in phases of the line (I regime) and from a totality of imaginary components E_{0p} (II regime). Let us take emf E_0 in the second phase equal to one [3]:

$$\text{I regime: } E_{0a1} = -\frac{1}{2}, \quad E_{0a2} = 1, \quad E_{0a3} = -\frac{1}{2}, \quad (31.1)$$

$$\text{II regime: } E_{0p1} = i\frac{\sqrt{3}}{2}, \quad E_{0p2} = 0, \quad E_{0p3} = -i\frac{\sqrt{3}}{2}. \quad (31.2)$$

Equations (30.16) are altered thus:

$$\text{I regime: } \begin{cases} E_{a1}(Q) + \lambda^2 T^2 E_{a1} = E_{0a}(Q), \\ E_{p1}(Q) = \lambda T E_{a1} \end{cases} \quad (31.3)$$

$$\text{II regime: } \begin{cases} E_{p2}(Q) + \lambda^2 T^2 E_{p2} = E_{0p}(Q), \\ E_{a2}(Q) = -\lambda T E_{p2}. \end{cases} \quad (31.4)$$

All quantities entering into these equations are symmetric relative to the vertical axis. Will designate quantities on the left side of the axis of symmetry by the sign "*", on the right we leave the designations unchanged: D^* and D_n — areas of cross sections current carriers to the left and right of the axis of symmetry respectively (Fig. 61)

We have

$$\int_{D^*} \ln r_{Q^*M^*} dQ^* = \int_{D_n} \ln r_{QM} dQ; \quad \int_{D^*} \ln r_{Q^*N} dQ^* = \int_{D_n} \ln r_{QN} dQ. \quad (31.5)$$

$$\text{For I regime } E(M^*) = E(M); \quad (31.6)$$

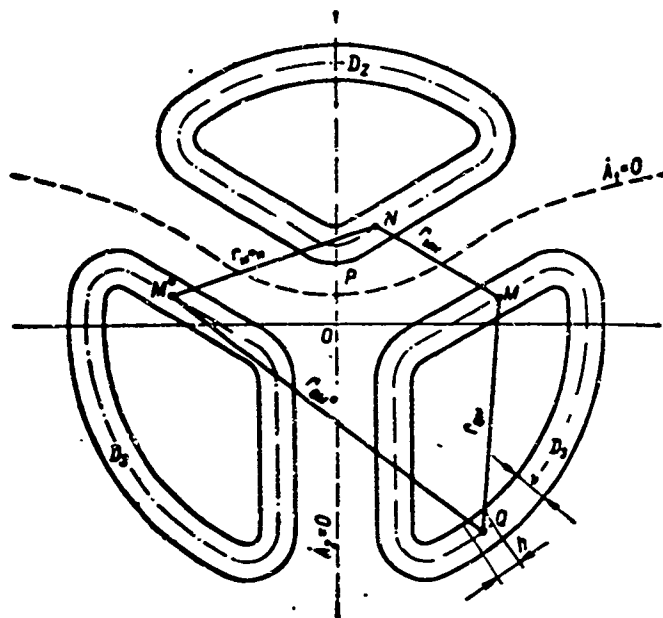


Fig. 61.

$$\text{for II regime } E(M^*) = -E(M). \quad (31.7)$$

Let us convert the expressions for operators T and T^2 taking into account these conditions of symmetry:

for I regime

$$\begin{aligned} T_1 E &= \int_D E(M) \left(\ln r_{QM} - \frac{1}{D} \int_D \ln r_{QM} dQ \right) dM = \\ &= \int_{D^*} E(M^*) \left(\ln r_{QM^*} - \frac{1}{D} \int_{D^*} \ln r_{QM^*} dQ^* - \frac{1}{D} \int_{D_n} \ln r_{QM^*} dQ \right) dM^* + \\ &+ \int_{D_n} E(M) \left(\ln r_{QM} - \frac{1}{D} \int_{D^*} \ln r_{QM} dQ^* - \frac{1}{D} \int_{D_n} \ln r_{QM} dQ \right) dM = \\ &= \int_{D_n} E(M) \left(\ln r_{QM} r_{QM^*} - \frac{1}{D_n} \int_{D_n} \ln r_{QM} r_{QM^*} dQ \right) dM, \end{aligned} \quad (31.8)$$

$$\begin{aligned} T_1^2 E &= K_1 E = \int_{D_n} E(N) K_1(Q, N) dN, \\ K_1(Q, N) &= \int_{D_n} \left(\ln r_{MN} r_{M^*N} - \frac{1}{D_n} \int_{D_n} \ln r_{MN} r_{M^*N} dM \right) \times \\ &\times \left(\ln r_{QM} r_{QM^*} - \frac{1}{D_n} \int_{D_n} \ln r_{QM} r_{QM^*} dQ \right) dM; \end{aligned} \quad (31.9)$$

for II regime

$$T_2 E = \int_{b_n} E(M) \ln \frac{r_{MQ}}{r_{QM^*}} dM, \quad (31.10)$$

$$T_2^2 E = K_2 E = \int_{b_n} E(N) K_2(Q, N) dN, \quad (31.11)$$

$$K_2(Q, N) = \int_{b_n} \ln \frac{r_{QM}}{r_{QM^*}} \ln \frac{r_{MN}}{r_{M^*N}} dM.$$

In these expressions it is assumed that during integration with respect to M in D_n symmetric element of area M^* passes the entire cross section D^* . Let us replace equations (31.3) and (31.4) by their equivalents as was done in (30.27). During computer calculations the number of iterations may be allowed to be very large, therefore as polynomial $P_n(A)$ we select a polynomial of first degree. Equivalent equations have the form:

$$E_{(p2)}^{(1)}(Q) = \frac{M-1}{M+1} E_{(p2)}^{(1)}(Q) - \frac{2}{M+1} \lambda^2 T_{(1)}^2 E_{(p2)}^{(1)} +$$

$$+ \frac{2}{M+1} E_{(op)}^{(0)}(Q), \quad (31.12)$$

$$E_{(p2)}^{(1)}(Q) = (\pm) \lambda T_{(1)} E_{(p2)}^{(1)}.$$

Subscripts in parentheses above pertain to the first regime, below - to the second.

The algorithm of solution of equations (31.12) will be such:

$$E_{(p2)}^{(0)}(Q) = E_{(op)}^{(0)}(Q),$$

$$E_{(p2)}^{(m)}(Q) = \frac{M-1}{M+1} E_{(p2)}^{(m-1)}(Q) - \frac{2}{M+1} \lambda^2 T_{(1)}^2 E_{(p2)}^{(m-1)} +$$

$$+ \frac{2}{M+1} E_{(op)}^{(0)}(Q). \quad (31.13)$$

For determination of the upper boundary $M_{(1)}^{(1)}$ of the spectrum of operator A we use inequality

$$M_{(1)}^{(1)} \leq 1 + \lambda^2 \sqrt{\int_{b_n} \int_{b_n} |K_{(1)}^{(1)}(Q, N)|^2 dQ dN}. \quad (31.14)$$

Summing components E_a and E_p of both regimes we obtain the cross-sectional distribution over cross sections of the current compressing the intensity E_x of the symmetric three-phase regime, E_{ax} - coinciding in phase with external voltage \dot{E}_{a2} , applied to the second phase and E_{px} - leading E_{ax} by $\frac{\pi}{2}$.

Integrating E_{ax} and E_{px} over the cross section of second phase, we find the active and reactive components of current in second phase

$$\begin{aligned} I_{a2} &= \int_{D_1} \gamma E_{ax} dS, \\ I_{p2} &= \int_{D_1} \gamma E_{px} dS. \end{aligned} \quad (31.15)$$

If cross sections of the current carriers are located symmetrically in the corners of an equilateral triangle then the active and reactive conductance of a unit length of current carrier of one phase, for instance the second, are defined thus:

$$g_{a2} = \frac{I_{a2}}{E_{a2}} = I_{a2}, \quad b_{a2} = \frac{I_{p2}}{E_{a2}} = I_{p2}. \quad (31.16)$$

The total conductivity of a unit length of current carrier of second phase is

$$y_{a2} = \sqrt{g_{a2}^2 + b_{a2}^2} = \sqrt{I_{a2}^2 + I_{p2}^2} = I_r. \quad (31.17)$$

The resistance of unit length of current carrier of second phase

$$r_{a2} = \frac{I_{a2}}{I_{a2}^2 + I_{p2}^2}, \quad x_{a2} = \frac{I_{p2}}{I_{a2}^2 + I_{p2}^2}, \quad z_{a2} = \frac{1}{\sqrt{I_{a2}^2 + I_{p2}^2}}. \quad (31.18)$$

Algorithm of solution (31.13) was computer programmed. The program, intended for use of only the fast store of the machine, consists of five main parts each of which executes an independent function: leading part, calculation of norm, calculation of $K_1(Q, N)$ and $E(Q)$ for I regime, calculation of $K_2(Q, N)$ and $E(Q)$ for II regime and calculation of parameters. Leading part of program introduces initial data and controls count. Initial data are:

- a) coordinates of points x and y of center line of cross section of wall of current carrier selected at identical intervals;
- b) parameter $\lambda = \mu \gamma f$, depending on frequency of current and properties of material of current carrier;
- c) external voltage \dot{E}_0 , per unit length of current carrier of each phase;
- d) ν - thickness of wall current carrier;
- e) accuracy of calculations ε , achievement of which terminates iterative process.

For calculation of norm and $K(Q, N)$ it is necessary to calculate a series of integrals of the form

$$\begin{aligned} \int_{D_n} \left| \ln \frac{r_{QM}}{r_{QM^*}} \right|^2 dM; \quad \int_{D_n} \ln \frac{r_{QM}}{r_{QM^*}} dM; \quad \int_{D_n} \ln \frac{r_{QM}}{r_{QM^*}} \ln \frac{r_{MN}}{r_{MN^*}} dM; \\ \int_{D_n} \left(\ln r_{QM} \cdot r_{QM^*} - \frac{1}{D_n} \int_{D_n} \ln r_{QM} \cdot r_{QM^*} dQ \right) \left(\ln r_{MN} \cdot r_{MN^*} - \right. \\ \left. - \frac{1}{D_n} \int_{D_n} \ln r_{MN} \cdot r_{MN^*} dM \right) dM. \end{aligned} \quad (31.19)$$

where r - distance between points of different cross sections. Let us present the first of integrals (31.19) in the form of a sum of two integrals

$$\int_{D_n} \left| \ln \frac{r_{QM}}{r_{QM^*}} \right|^2 dM = \int_{D_n - \Delta D} \left| \ln \frac{r_{QM}}{r_{QM^*}} \right|^2 dM + \int_{\Delta D} \left| \ln \frac{r_{QM}}{r_{QM^*}} \right|^2 dM,$$

where $\Delta D = \Delta D_1 + 2\Delta D_2$ - element of area in which points M and Q coincide (Fig. 62).

We will replace $\int_{\Delta D} \left| \ln \frac{r_{QM}}{r_{QM^*}} \right|^2 dM$ with a finite sum and $\int_{\Delta D} \left| \ln \frac{r_{QM}}{r_{QM^*}} \right|^2 dM$ we calculate in the following way:

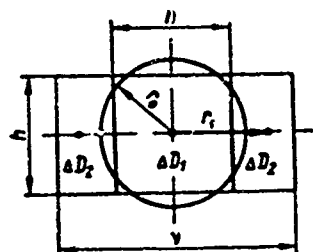


Fig. 62.

$$\begin{aligned}
 \int_{\Delta D} \left| \ln \frac{r_{QM}}{r_{QM^*}} \right|^2 dM &= \int_{\Delta D} \left| \ln \frac{r_{QM}}{r_{QM^*}} \right|^2 dM + 2 \int_{\Delta D_1} \left| \ln \frac{r_{QM}}{r_{QM^*}} \right|^2 dM \approx \\
 &\approx 2\pi \int_0^{\sqrt{\frac{h^2}{\pi}}} r \left(\ln \frac{r_{QM^*}}{r} \right)^2 dr + \\
 &+ h(v-h) \left(\ln \frac{r_{QM^*}}{r_1} \right)^2 = \\
 &= \frac{h^2}{4} \left\{ [2 \ln \sqrt{(x_{M^*} - x_Q)^2 + (y_{M^*} - y_Q)^2}]^2 + \left(\ln \frac{h^2}{\pi} \right)^2 - \right. \\
 &- 2 \left(\ln \frac{h^2}{\pi} - 1 \right) - 4 \ln \sqrt{(x_{M^*} - x_Q)^2 + (y_{M^*} - y_Q)^2} \cdot \left(\ln \frac{h^2}{\pi} - 1 \right) \Big\} + \quad (31.20) \\
 &+ (v-h) h \ln^2 \frac{4 \sqrt{(x_{M^*} - x_Q)^2 + (y_{M^*} - y_Q)^2}}{v+h}.
 \end{aligned}$$

Here square ΔD_1 is replaced by a circle of the same area. Consequently the integral can be written:

$$\begin{aligned}
 \int_{\Delta D} \left| \ln \frac{r_{QM}}{r_{QM^*}} \right|^2 dM &\approx \sum_{i=1}^{n-1} \left(\ln \frac{r_{QM_i}}{r_{QM^*}} \right)^2 v h + \frac{h^2}{4} \left\{ \left(\ln \frac{h^2}{\pi} \right)^2 - \right. \\
 &- 2 \left(\ln \frac{h^2}{\pi} - 1 \right) - 4 \ln \sqrt{(x_{M^*} - x_Q)^2 + (y_{M^*} - y_Q)^2} \left(\ln \frac{h^2}{\pi} - 1 \right) + \\
 &+ 4 \left[\ln \sqrt{(x_{M^*} - x_Q)^2 + (y_{M^*} - y_Q)^2} \right]^2 \Big\} + \quad (31.21) \\
 &+ (v-h) h \ln^2 \frac{4 \sqrt{(x_{M^*} - x_Q)^2 + (y_{M^*} - y_Q)^2}}{v+h}.
 \end{aligned}$$

The remaining integrals (31.19) are calculated analogously.

The operational scheme of the program has the form

P_{21} -- determine if inequality

$$|E_{s1}^{(m)}(Q) - E_{s1}^{(m-1)}(Q)| < \varepsilon$$

L_{22} - calculate $E_{p1}(Q)$ of I regime;

L₂₃ - calculate $E_{ax}(Q)$, $E_{px}(Q)$, I_a , I_p , $|\dot{E}(Q)|$, $\arg \dot{E}(Q)$, r_0 , x_0 , z_0 .

\mathcal{A}_{14} - stop operator

$$\dot{u}_{k0} = \dot{E}_{k1} - \dot{E}_{00} \quad (k = 1, 2, \dots, m-1). \quad (31.22)$$
[illegible]
$$\begin{aligned} \dot{u}_{10} &= \dot{l}_1 z_{11} + \dot{l}_2 z_{12}, & \dot{u}_{10} &= \dot{l}_1 z_{11} + \dot{l}_2 z_{12}, \\ \dot{u}_{20} &= \dot{l}_1 z_{21} + \dot{l}_2 z_{22}, & \dot{u}_{20} &= \dot{l}_1 z_{21} + \dot{l}_2 z_{22}. \end{aligned} \quad (31.24)$$

Solving this system with respect to unknowns z_{jk} , we find them.

CHAPTER V

MODEL FOR INVESTIGATION OF VOLUMETRIC FIELDS

§ 32. Difficulties of Modeling

The most effective means of determination of a volumetric static field is its modeling in an electrolytic bath or in a volumetric grid with a dc field. However during modeling there appear defined difficulties connected with nonuniform field intensity. For solution of one or other technical problem usually it is sufficient to know the field in a small volume, in that part of it which determines characteristics and properties of the electromagnetic arrangement being designed. But then in this volume quantities characterizing the intensity of the field have to be determined with sufficient accuracy. This means that the scale of modeling must be relatively large.

The field of the object spreads out without limit, occupying all of the surrounding space. In order to model only a part of it, it is necessary on the boundary of the model to carry out the same threshold conditions which take place in the actual field of the object on the imagined boundary of the volume of the modelled part. To find values of quantities characterizing field intensity on some surface is just as difficult at any other place. Therefore it is necessary to model large volumes of the field trying to approach the natural boundary conditions, i.e., to ensure in the model disappearance of the field at its boundaries. Dimensions of the model are always limited and the modeling scale must be selected very small. In this case the model the section of the field which is of interest also becomes small, the accuracy of modeling and the accuracy of measurements on the model drop sharply.

In separate cases it is necessary to model the field in a relatively large

scale in a region of such large dimensions that it becomes immediately impracticable to construct a model the entire field. It is necessary to model the field in sections. Here the problem of preliminary detecting of boundary conditions on the boundaries of the sections again arises.

Let us define an element of unlimited space as a mentally a region of finite dimensions delimited within it. The element can constitute a volume, a section of surface or, finally, a segment of a line. Difficulties with guarantee of conditions on the boundary of the model would disappear of themselves if the volume of the model (or at least its part) possessed properties of an element of unlimited space similar to it. In distinction from the mental boundary of an element, the boundary of the model is always the physical interface of two different media. The field of sources in the model is reflected from its boundary, the reflected field falls on basic field and the resultant turns out to be different from the field of the same sources in a similar element of unlimited space. Thus the boundary of the model (wall of electrolytic bath or boundary of a grid) introduces a distortion in the modelled field. It is of great interest to construct a model for modeling a field whose volume would possess the properties of the corresponding element of unlimited space. No attempts have been made to construct a model in which the field of sources would not be distorted by mapping. The original work of Bogolyubov and Shamayev [5, 6] containing a description of the models — an electrolytic bath with semiconducting walls — and L. V. Nitsetskiy [17] on grid attenuators for baths are well known. However all earlier constructions are technically difficult to realize or costly to manufacture and, most important, are not universal since their properties depend on the location of sources in the modelled field.

Below are expounded the principles of construction of electrolytic baths — models of elements of unlimited space. The mapped field in such models in a defined region of their volume is small for any distributions of sources of the modelled field and properties of the medium filling the model. The following problem is posed and solved: find the form of the surface of walls of the model and their structure ensuring an expedient minimum of distortions of the modelled field in given region D , independent of the location of the field sources and properties of the medium in which it must be modelled. As will be evident from what follows, such a formulation of the problem is correct and problem has a

unique solution if a metric is selected in which distortion is minimized.

Before going on to a solution of this problem let us present a derivation of the necessary relationships.

§ 33. Green's Theorem

The theorem of Gauss can be formulated in such form:

$$\oint_S E_n dS = \int_V \operatorname{div} \vec{E} dV. \quad (33.1)$$

Here V — volume bounded by closed surface S ; E_n — normal component of vector E on surface S .

We set $\vec{E} = \psi \operatorname{grad} \varphi$, where ψ and φ are arbitrary scalar functions. We have

$$\operatorname{div} \psi \operatorname{grad} \varphi = \operatorname{grad} \psi \operatorname{grad} \varphi + \psi \Delta \varphi,$$

$$[\psi \operatorname{grad} \varphi]_n = \psi \frac{\partial \varphi}{\partial n},$$

placing these values in the formula of Gauss we obtain

$$\oint_S \psi \frac{\partial \varphi}{\partial n} dS = \int_V \operatorname{grad} \psi \operatorname{grad} \varphi dV + \int_V \psi \Delta \varphi dV. \quad (33.2)$$

Substituting now $\vec{E} = \varphi \operatorname{grad} \psi$. We have

$$\operatorname{div} \varphi \operatorname{grad} \psi = \operatorname{grad} \varphi \operatorname{grad} \psi + \varphi \Delta \psi,$$

$$[\varphi \operatorname{grad} \psi]_n = \varphi \frac{\partial \psi}{\partial n},$$

$$\oint_S \varphi \frac{\partial \psi}{\partial n} dS = \int_V \operatorname{grad} \varphi \operatorname{grad} \psi dV + \int_V \varphi \Delta \psi dV. \quad (33.3)$$

Subtracting equation (33.3) from (33.2) we obtain

$$\oint_S \left[\psi \frac{\partial \varphi}{\partial n} - \varphi \frac{\partial \psi}{\partial n} \right] dS = \int_V [\psi \Delta \varphi - \varphi \Delta \psi] dV. \quad (33.4)$$

Instead of ψ we take a centrally symmetric solution of the Laplace equation — function $1/r$, where

$$r = \sqrt{(x - x_0)^2 + (y - y_0)^2 + (z - z_0)^2}.$$

At $r = 0$ it undergoes a break, therefore in order to apply formula (33.4), we separate point (x, y, z) where $r = 0$, surrounding it with a sphere of small radius r_1 .

$$\int_{V-\Delta V} \left[\frac{\Delta \varphi}{r} - \varphi \Delta \left(\frac{1}{r} \right) \right] dV = \oint_S \left[\frac{1}{r} \frac{\partial \varphi}{\partial n} - \varphi \frac{\partial}{\partial n} \left(\frac{1}{r} \right) \right] dS + \\ + \oint_{\Delta S} \left[\frac{1}{r_1} \frac{\partial \varphi}{\partial n} - \varphi \frac{\partial}{\partial n} \left(\frac{1}{r} \right) \right] dS.$$

On small sphere ΔS of radius r_1

$$\frac{\partial \varphi}{\partial n} = -\frac{\partial \varphi}{\partial r}, \quad \frac{\partial}{\partial n} \left(\frac{1}{r} \right) = -\frac{1}{r_1^2}.$$

Therefore with contraction of surface ΔS to point (x, y, z) in the limit we obtain

$$\lim_{r_1 \rightarrow 0} \oint_{\Delta S} \frac{1}{r_1} \frac{\partial \varphi}{\partial n} dS = \lim_{r_1 \rightarrow 0} \left[-\frac{1}{r_1} \oint_{\Delta S} \frac{\partial \varphi}{\partial r} dS \right] = \lim_{r_1 \rightarrow 0} \left[-\frac{\partial \bar{\varphi}}{\partial r} 4\pi r_1^2 \right] = 0, \\ \lim_{r_1 \rightarrow 0} \oint_{\Delta S} \varphi \frac{\partial}{\partial n} \left(\frac{1}{r} \right) dS = \lim_{r_1 \rightarrow 0} \left[\frac{1}{r_1^2} \oint_{\Delta S} \varphi dS \right] = \lim_{r_1 \rightarrow 0} \frac{1}{r_1^2} \bar{\varphi} \cdot 4\pi r_1^2 = 4\pi \varphi(x, y, z).$$

Here $\partial \bar{\varphi} / \partial r$ and $\bar{\varphi}$ are mean values on surface ΔS of $\partial \varphi / \partial r$ and φ .

Considering that $\Delta(1/r) = 0$ and substituting values of limits in formula (33.4), we obtain the well known Green formula [22]

$$\varphi(x, y, z) = -\frac{1}{4\pi} \int_V \frac{\Delta \varphi}{r} dV + \frac{1}{4\pi} \oint_S \left[\frac{1}{r} \frac{\partial \varphi}{\partial n} - \varphi \frac{\partial}{\partial n} \left(\frac{1}{r} \right) \right] dS. \quad (33.5)$$

If point (x, y, z) lies outside of volume V then the left side of this formula becomes zero. Green's theorem (33.5) shows that potential φ (function having continuous second derivatives inside closed surface S) is fully defined at every point of the space limited by this surface if we know:

- 1) density of field sources φ ($\Delta \varphi = -\frac{\rho}{\epsilon}$) at every point of volume V ; here ρ — volumetric charge density;
- 2) value of function φ at every point on surface S ;
- 3) value of derivative with respect to normal $\partial \varphi / \partial n$ at every point of surface S .

In order to clarify the meaning of integrals in formula (33.5) we will consider the field of a system of two equal charges q of opposite sign located at distance l from each other. Vector $\vec{p} = q\vec{l}$ is called the electrical moment of such a system, vector \vec{l} is considered directed from charge $-q$ to $+q$. If without limit we bring the charges together, preserving a constant moment \vec{p} , then at the

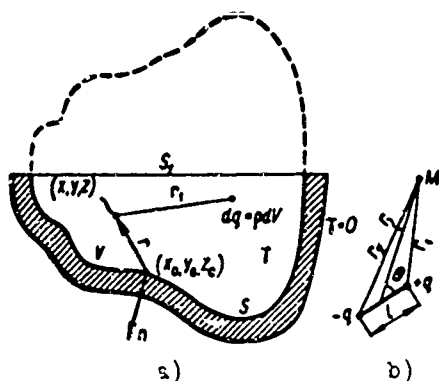


Fig. 63.

limit we obtain a dipole. The potential of a dipole at arbitrary point M equals:

$$\begin{aligned}\varphi(M) &= \lim_{\substack{l \rightarrow 0 \\ q \rightarrow \infty}} \frac{q}{4\pi\epsilon} \left(\frac{1}{r_1} - \frac{1}{r_2} \right) = \\ &= \lim_{\substack{l \rightarrow 0 \\ q \rightarrow \infty}} \frac{q}{4\pi\epsilon} \frac{r_2 - r_1}{r_1 r_2}.\end{aligned}$$

But as can be seen from Fig. 63b

$$\lim_{l \rightarrow 0} (r_2 - r_1) = l \cos \theta, \quad \lim_{l \rightarrow 0} r_1 r_2 = r^2,$$

consequently

$$\varphi(M) = \frac{q}{4\pi\epsilon} \cdot \frac{l \cos \theta}{r^2} = \frac{p \cos \theta}{4\pi\epsilon r^2} = \frac{p \cos(\widehat{r, \vec{l}})}{4\pi\epsilon r^2}.$$

We return to the Green formula (33.5). We have

$$\frac{\partial}{\partial n} \left(\frac{1}{r} \right) = \frac{\partial}{\partial r} \left(\frac{1}{r} \right) \frac{\partial r}{\partial n} = -\frac{1}{r^2} \frac{\partial r}{\partial n}. \quad (33.6)$$

From Fig. 63a it is evident that

$$\frac{\partial r}{\partial n} = \lim_{\Delta n \rightarrow 0} \frac{\Delta r}{\Delta n} = -\cos \theta = -\cos(\widehat{r, \vec{n}}).$$

Consequently

$$\frac{\partial}{\partial n} \left(\frac{1}{r} \right) = \frac{\cos(\widehat{r, \vec{n}})}{r^2}.$$

Potential φ in general satisfies the Poisson equation

$$\Delta \varphi = -\frac{\rho}{\epsilon}.$$

Considering this, formula (33.5) can be altered thus:

$$\varphi(x, y, z) = \frac{1}{4\pi\epsilon} \int_V \frac{\rho dV}{r} + \frac{1}{4\pi\epsilon} \oint_S \frac{1}{r} \epsilon \frac{\partial \varphi}{\partial n} dS - \frac{1}{4\pi\epsilon} \oint_S \frac{\epsilon \varphi \cos(\widehat{n, \vec{r}})}{r^2} dS \quad (33.7)$$

Let us assume that S is the surface of the conductor ($\epsilon_S = \infty$), then on it

$\varphi = c = \text{const}$

$$\begin{aligned}\frac{1}{4\pi} \oint_S \varphi \frac{\partial}{\partial n} \left(\frac{1}{r} \right) dS &= \frac{c}{4\pi} \oint_S \frac{\partial}{\partial n} \left(\frac{1}{r} \right) dS = \\ &= \lim_{r_1 \rightarrow 0} \frac{c}{4\pi} \left[\oint_{S+\Delta S} \frac{\partial}{\partial n} \left(\frac{1}{r} \right) dS - \oint_{\Delta S} \frac{\partial}{\partial r} \left(\frac{1}{r} \right)_{r=r_1} dS \right] = \frac{c}{4\pi} (0 + 4\pi) = c.\end{aligned}$$

Here ΔS is a sphere of small radius r_1 with center at point (x, y, z) where $r = 0$.

On the surface of the conductor $\epsilon \frac{\partial \varphi}{\partial n} = \sigma$ (σ - surface charge density).

Consequently in this case

$$\varphi(x, y, z) = \frac{1}{4\pi\epsilon} \int_V \frac{\rho dV}{r} + \frac{1}{4\pi\epsilon} \oint_S \frac{\sigma dS}{r} + c, \quad (33.8)$$

potential φ consists of potential φ_1 field of charges by density ρ distributed in volume V

$$\varphi_1 = \frac{1}{4\pi\epsilon} \int_V \frac{\rho dV}{r}, \quad (33.9)$$

and potential φ_2 of field of charges of surface density σ induced on conducting surface S

$$\varphi_2 = \frac{1}{4\pi\epsilon} \oint_S \frac{\sigma dS}{r} + c. \quad (33.10)$$

Potential φ_2 is called the potential of a simple layer of charges.

Let us assume now that S will be the surface of an ideal dielectric with $\epsilon = 0$, then on it $\partial\varphi/\partial n = 0$ and

$$\varphi(x, y, z) = \frac{1}{4\pi\epsilon} \int_V \frac{\rho dV}{r} - \frac{1}{4\pi\epsilon} \oint_S \frac{\epsilon\varphi \cos(\hat{r}, \hat{n})}{r^2} dS. \quad (33.11)$$

Magnitude $\epsilon\varphi dS$ may be regarded as the electrical moment of a dipole at a point on the surface S . Then the integral over S will constitute the potential of a double layer of induced dipoles on the boundary of a dielectric. Moments of the dipoles are directed normal to surface S .

If S is the interface of two dielectrics with different permeabilities $\epsilon_1 \neq \epsilon_2$, $0 < \epsilon < \infty$, then it will exist both a single and a double layer of charges.

§ 34. Formulation of the Problem of Construction of a Model Element of Unlimited Space

We return now to the problem stated in § 32. Let us apply the analogy of a dc field in a conducting medium to an electrostatic field in a dielectric and following presentation we will conduct in electrostatic terms [34].

Let us consider a bath with insulating walls filled with a medium of specific conductivity γ . To different points in the medium are supplied currents or, as we have stipulated, in the medium are distributed sources with density ρ . The conductivity of the bath walls is zero, therefore using formula (33.11) we can write an expression for potential φ at any point (x, y, z) of volume V of

bath of limited surface area S of its walls:

$$\varphi(x, y, z) = \frac{1}{4\pi\gamma} \int \frac{\rho dV}{r} + \frac{1}{4\pi} \oint_S \varphi \frac{1}{r^2} \frac{\partial r}{\partial n} dS. \quad (34.1)$$

Here \vec{n} — vector of external normal to surface S

$$r = \sqrt{(x-x_0)^2 + (y-y_0)^2 + (z-z_0)^2}.$$

If in the bath there is a free surface of electrolyte S_1 , then during integration should understand S to be the surface of the walls of the bath plus its mirror image in free surface S_1 and V to be the volume limited by the surface of the walls and its mirror image (Fig. 63a).

From formula (34.1) it is evident that no simple layer of charges appears on the insulating walls of the bath and the field in the bath is distorted only by the double layer of induced dipole. Our objective is to decrease the potential of distortion introduced by the walls and to achieve a potential φ which differs as little as possible from the potential of the field of sources ρ . Noting that the second integrand in formula (34.1) is proportional to the value of potential $\varphi(x_0, y_0, z_0)$ on the walls of the bath, we will try to compensate the second integral with potential of an artificially created simple layer of charges on the walls. This can be done as follows: over the insulating walls a metallic housing is placed on the bath and in the walls are drilled small holes. Each hole, after being filled with the conducting medium poured into the bath will connect the internal volume of the bath with the metallic housing and play the role of a surface charge Δq since to it lines of flux will converge. Let us take the potential of the housing equal to zero. Then the magnitude of such a charge will also be proportional to potential $\varphi(x_0, y_0, z_0)$ and equal to

$$\Delta q = -\varphi(x_0, y_0, z_0) g_0.$$

where g_0 — conductivity of column of medium filling the hole.

If holes in the walls are made sufficiently frequent then their action is as close as to the desired action of a simple layer of charges with surface density

$$\sigma_1 = -\varphi g_1 = -\varphi g_0.$$

where g_1 — conductivity of holes present on a unit surface of the wall. Potential $\varphi_0(x, y, z)$ caused by the influence of holes has the form

$$\varphi_0(x, y, z) = \frac{1}{4\pi} \oint_S \frac{\sigma_1}{\gamma r} dS = -\frac{1}{4\pi} \oint_S \varphi \frac{g}{r} dS. \quad (34.2)$$

The resultant potential now will be:

$$\varphi(x, y, z) = \frac{1}{4\pi\gamma} \int_V \frac{\rho}{r} dV + \frac{1}{4\pi} \oint_S \frac{\varphi}{r} \left(\frac{1}{r} \frac{\partial r}{\partial n} - g \right) dS = \varphi_1 + \varphi_2. \quad (34.3)$$

Here

$$\varphi_1 = \frac{1}{4\pi\gamma} \int_V \frac{\rho dV}{r}. \quad (34.4)$$

φ_1 - potential of undistorted field of sources

$$\varphi_2 = \frac{1}{4\pi} \oint_S \frac{\varphi}{r} \left(\frac{1}{r} \frac{\partial r}{\partial n} - g \right) dS. \quad (34.5)$$

φ_2 - potential of distortion introduced by walls taking into account the influence of holes in them. Conductivity of holes g can always be selected such that at a given point (x, y, z) the potential φ_2 becomes zero. Our objective is to make φ_2 as small as possible in all points of the given region D .

The integrand in formula (34.5) constitutes the product of potential

$\varphi(x_0, y_0, z_0)$ and a purely geometric quantity $\frac{1}{r} \left(\frac{1}{r} \frac{\partial r}{\partial n} - g \right)$.

Potential $\varphi(x_0, y_0, z_0)$ is determined by the sources and we can have no effect on it. However we can change the magnitude $\frac{1}{r} \left(\frac{1}{r} \frac{\partial r}{\partial n} - g \right)$ and thereby effect the potential of distortion φ_2 . It is possible to decrease φ_2 by increasing r , however this is inexpedient since it will lead to an increase of dimensions of the bath. There remains on possibility to reduce φ_2 at the expense of expression $\left(\frac{1}{r} \frac{\partial r}{\partial n} - g \right)$, depending at a fixed r on conductivity g and direction of normal \bar{n} .

The direction of the vector in space is fully defined by the two angles which it forms with the coordinate axes. Consequently it is possible to decrease potential φ_2 , influencing on three magnitudes: conductivity g and the two angles of determining the direction of normal \bar{n} .

Depending upon the character of the solved problems during modeling of a field in the bath we will select a suitable form of region D - element of unlimited space - and metrics in which it is expedient to look for minimum.

distribution of φ_2 in this region. Then minimizing the functional (norm of quantity $\left(\frac{1}{r} \frac{\partial r}{\partial n} - g\right)$ in the selected metrics with respect to all three parameters at every point (x_0, y_0, z_0) we find the distribution of conductivity $g = g(x_0, y_0, z_0)$ and field of unit normals \vec{n}^0 which in turn determine the monoparametric family of surfaces S . Given by the dimensions of the bath, we select from this family a suitable surface of its walls and find on it the distribution of conductivity g .

Thus solution of our problem reduces to finding the minimum of a function depending on the magnitude of $\left(\frac{1}{r} \frac{\partial r}{\partial n} - g\right)$.

§ 35. Basic Geometric Presentations

We designate

$$\frac{1}{r} \frac{\partial r}{\partial n} = \varepsilon(x, y, z, x_0, y_0, z_0, \vec{n}^0) \quad (35.1)$$

and consider the geometry of the field of this magnitude. In the rectangular system of coordinates (Fig. 64) we have

$$r = \sqrt{(x-x_0)^2 + (y-y_0)^2 + (z-z_0)^2},$$

$$\frac{\partial r}{\partial n} = \frac{\partial r}{\partial x_0} \frac{\partial x_0}{\partial n} + \frac{\partial r}{\partial y_0} \frac{\partial y_0}{\partial n} + \frac{\partial r}{\partial z_0} \frac{\partial z_0}{\partial n},$$

but $\frac{\partial x_0}{\partial n} = \cos \alpha$, $\frac{\partial y_0}{\partial n} = \cos \beta$, $\frac{\partial z_0}{\partial n} = \cos \gamma$ - directional cosines of unit vector \vec{n}^0 , and $\frac{\partial r}{\partial x_0} = -\frac{x-x_0}{r}$; $\frac{\partial r}{\partial y_0} = -\frac{y-y_0}{r}$; $\frac{\partial r}{\partial z_0} = -\frac{z-z_0}{r}$. Placing these values in expression (35.1) we obtain

$$\varepsilon = \frac{1}{r} \frac{\partial r}{\partial n} = -\frac{(x-x_0)\cos\alpha + (y-y_0)\cos\beta + (z-z_0)\cos\gamma}{(x-x_0)^2 + (y-y_0)^2 + (z-z_0)^2}. \quad (35.2)$$

Will combine the origin of coordinates with point (x_0, y_0, z_0) and direct the axis oz along the axis of the dipole (along vector \vec{n}^0) then

$$x_0 = y_0 = z_0 = 0, \quad \cos \alpha = \cos \beta = 0, \quad \cos \gamma = -1.$$

Using the axial symmetry of field ε we will consider it only in the cross section

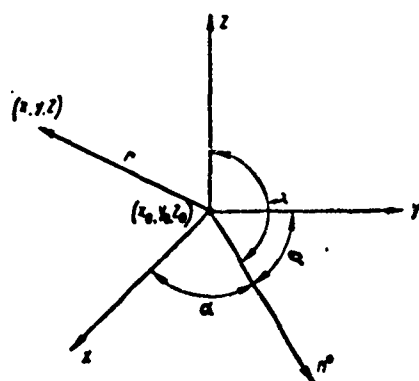


Fig. 64.

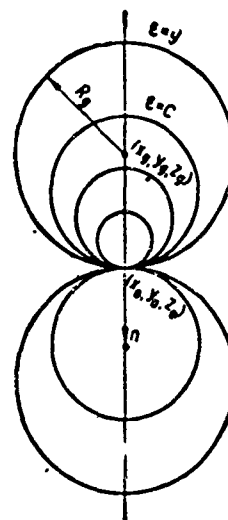


Fig. 65.

with plane $y = 0$. In this plane

$$\epsilon(x, z) = \frac{-z}{x^2 + z^2}.$$

Hence the equation of the line of constant values of ϵ will be

$$x^2 + \left(z - \frac{1}{2C}\right)^2 = \left(\frac{1}{2C}\right)^2. \quad (35.3)$$

This is the equation of a circle with center at point

$$x_u = y_u = 0, \quad z_u = \frac{1}{2C}$$

and radius

$$R_u = \frac{1}{2C}.$$

Consequently, in space of the surfaces of equal values of ϵ will be spheres encompassing one other and touching at point (x_0, y_0, z_0) (Fig. 65). Let us assume that now the dipole is located at point (x_0, y_0, z_0) and its axis (normal \vec{n}^0) will form with the axes coordinates the angles α , β and γ . Equation of surfaces of equal values of ϵ will be recorded thus:

$$\epsilon = - \frac{(x - x_0) \cos \alpha + (y - y_0) \cos \beta + (z - z_0) \cos \gamma}{(x - x_0)^2 + (y - y_0)^2 + (z - z_0)^2} = C, \quad (35.4)$$

or after elementary transformations

$$\left(x - x_0 + \frac{\cos \alpha}{2C}\right)^2 + \left(y - y_0 + \frac{\cos \beta}{2C}\right)^2 + \left(z - z_0 + \frac{\cos \gamma}{2C}\right)^2 = \left(\frac{1}{2C}\right)^2. \quad (35.5)$$

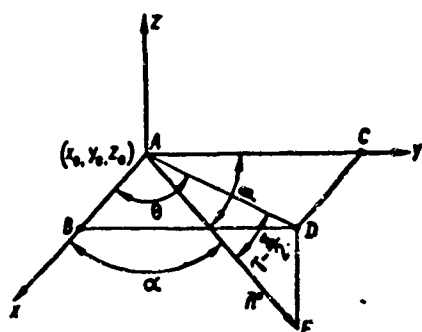


Fig. 66.

Hence it is clear that this is the equation of a sphere with radius

$$R_u = \frac{1}{2C} \quad (35.6)$$

and coordinates of center

$$x_u = x_0 - \frac{\cos \alpha}{2C}; \quad y_u = y_0 - \frac{\cos \beta}{2C}; \quad z_u = z_0 - \frac{\cos \gamma}{2C}. \quad (35.7)$$

Let us assume that normal \vec{n}^0 (axis of dipole) will form with the coordinate axes the angles α , β and γ . We extend through vector \vec{n}^0 a vertical plane and project segment AE coinciding with vector \vec{n}^0 onto the axes ox, oy and plane xoy (Fig. 66). We have $AB = AE \cos \alpha$, $AC = AE \cos \beta$,

$$AD = AE \cos\left(\gamma - \frac{\pi}{2}\right) = AE \sin \gamma,$$

on the other hand

$$AB = AD \cos \theta = AE \sin \gamma \cos \theta; \quad AC = AD \sin \theta = AE \sin \gamma \sin \theta.$$

From comparison of these segments we obtain

$$\cos \alpha = \sin \gamma \cos \theta, \quad \cos \beta = \sin \gamma \sin \theta. \quad (35.8)$$

Here θ — angle between plane xoz and vertical plane in which lies vector \vec{n}^0 .

Placing (35.8) in expression (35.2) we obtain

$$\varepsilon = - \frac{(x - x_0) \sin \gamma \cos \theta + (y - y_0) \sin \gamma \sin \theta + (z - z_0) \cos \gamma}{(x - x_0)^2 + (y - y_0)^2 + (z - z_0)^2}. \quad (35.9)$$

If in space we extend a plane it will intersect sphere $\varepsilon = \text{const}$ and the line of intersection will obviously be a circle. Thus for instance on the plane $z = 0$ the equation of lines of equal values of ε will be written:

$$\varepsilon = - \frac{(x - x_0) \sin \gamma \cos \theta + (y - y_0) \sin \gamma \sin \theta - z_0 \cos \gamma}{(x - x_0)^2 + (y - y_0)^2 + z_0^2} = C.$$

Hence after elementary conversion

$$\begin{aligned} \left(x - x_0 + \frac{\sin \gamma \cos \theta}{2C}\right)^2 + \left(y - y_0 + \frac{\sin \gamma \sin \theta}{2C}\right)^2 &= \\ &= \frac{1}{4C^2} - \left(z_0 - \frac{\cos \gamma}{2C}\right)^2. \end{aligned} \quad (35.10)$$

This is the equation of a circle of radius

$$R_c = \sqrt{\frac{1}{4C^2} - \left(z_0 - \frac{\cos \gamma}{2C}\right)^2} \quad (35.11)$$

and coordinates of its center

$$x_c = x_0 - \frac{\sin \gamma \cos \theta}{2C}; \quad y_c = y_0 - \frac{\sin \gamma \sin \theta}{2C}. \quad (35.12)$$

§ 36. Model with Minimum of Average Value of Absolute Magnitude of Potential of Distortion

Let us consider now how to set up an electrolytic bath ensuring in an assigned region D an expedient minimum mean absolute value of potential of the field reflected from its walls. In other words we will seek the form of the surface of the walls of the bath S and the distributions of conductivity of holes g on it ensuring the possible the minimum of integral

$$J = 4\pi \int_D |\varphi_2| dV_1 = \int_D \left| \oint_S \frac{\varphi}{r} \left(\frac{1}{r} \frac{\partial r}{\partial n} - g \right) dS \right| dV_1. \quad (36.1)$$

We have inequality

$$4\pi |\varphi_2| \leq \oint_S \left| \frac{\varphi}{r} \left| \frac{1}{r} \frac{\partial r}{\partial n} - g \right| \right| dS. \quad (36.2)$$

Consequently

$$J \leq J_1 = \int_D \left[\oint_S \left| \frac{\varphi}{r} \left| \frac{1}{r} \frac{\partial r}{\partial n} - g \right| \right| dS \right] dV. \quad (36.3)$$

If we will make J_1 small, then we thereby guarantee the smallness of J. Changing the order of integration in expression (36.3) we obtain

$$J_1 = \oint_S |\varphi| \left| \int_D \frac{1}{r} \left| \frac{1}{r} \frac{\partial r}{\partial n} - g \right| dV \right| dS. \quad (36.4)$$

It is possible to decrease integral J_1 if we decrease as far possible each of the components

$$dJ_1 = |\varphi| \left| \int_D \frac{1}{r} \left| \frac{1}{r} \frac{\partial r}{\partial n} - g \right| dV \right| dS.$$

Potential $|\varphi|$ depends on the location and magnitude of sources in the bath and we are not able to affect it. Therefore we will attempt to decrease dJ_1 only at the expense of a decrease of integral

$$J_2 = \int_D \frac{1}{r} \left| \frac{1}{r} \frac{\partial r}{\partial n} - g \right| dV. \quad (36.5)$$

which may be viewed as the value of potential at point (x_0, y_0, z_0) from fictitious charge Q distributed in region D with density

$$q_1 = \left| \frac{1}{r} \frac{\partial r}{\partial n} - g \right|.$$

It is possible either by decreasing to decrease potential J_2 the charge Q creating it or by increasing the distance r from charge Q to point (x_0, y_0, z_0) on the surface of the bath walls. As already was indicated an increase in r is technically impracticable, it leads to an increase in the dimensions of the bath. Therefore we will decrease charge Q , decreasing thereby potential J_2 . Actually, applying the mean value theorem to integral

$$J_2 = \int_D \frac{1}{r} \left| \frac{1}{r} \frac{\partial r}{\partial n} - g \right| dV = \frac{1}{r_{cp}} \int_D \left| \frac{1}{r} \frac{\partial r}{\partial n} - g \right| dV = \frac{1}{r_{cp}} Q. \quad (36.6)$$

we see that J_2 is proportional to the magnitude of integral Q . Here r_{cp} - distance from point (x_0, y_0, z_0) to one of the points of region D .

Thus the problem of detecting a practicable minimum of integral J has been reduced to the problem of detecting of minimum at every point (x_0, y_0, z_0) of the simpler integral

$$Q = \int_D \left| \frac{1}{r} \frac{\partial r}{\partial n} - g \right| dV = \int_D |\varepsilon - g| dV. \quad (36.7)$$

Magnitude of integral Q for a fixed value of r depends on the magnitude of conductivity g at point (x_0, y_0, z_0) and the direction of the normal \vec{n}^0 in it, i.e., on the magnitude of angles γ and φ . Let us try so to order these magnitudes so as to make Q minimum.

Let region D , in which is necessary to obtain the least distortion of field, in other words an element of unlimited space presented as a limited volume. Spheres $\varepsilon = \text{const}$ will intersect region D . Let us show that the integral of Q attains minimum at such value of g at which sphere $\varepsilon = g$ divides the volume of region D into two equal parts D_1 and $D - D_1$.

We will call D_1 that part of volume D in which difference $(\varepsilon - g)$ is positive in the remain volume $(D - D_1)$ the difference $(\varepsilon - g)$ is negative. Taking this into account, the magnitude of integral Q can be defined:

$$Q = \int_D |\varepsilon - g| dV = \int_{D_1} (\varepsilon - g) dV - \int_{D-D_1} (\varepsilon - g) dV. \quad (36.8)$$

We give g an increase $+\Delta g$, then volume D_1 in which the difference $(\epsilon - g)$ is positive will decrease by ΔV , volume $(D - D_1)$ in which the difference is negative will increase by the same magnitude. Integral Q takes the new value

$$\begin{aligned} Q_1 &= Q + \Delta Q_1 = \int_{D_1 - \Delta V} (\epsilon - g - \Delta g) dV - \int_{D - D_1 + \Delta V} (\epsilon - g - \Delta g) dV = \\ &= \int_{D_1} (\epsilon - g) dV - \int_{D - D_1} (\epsilon - g) dV - 2 \int_{\Delta V} (\epsilon - g) dV - \Delta g (D_1 - \Delta V) + \\ &+ \Delta g (D - D_1 + \Delta V) = Q + \Delta g (D - 2D_1) - 2 \int_{\Delta V} \epsilon dV + 2g\Delta V + 2\Delta g\Delta V. \end{aligned}$$

The increase is expressed by the formula

$$\Delta Q_1 = \Delta g (D - 2D_1) + 2g\Delta V - 2 \int_{\Delta V} \epsilon dV + 2\Delta g\Delta V. \quad (36.9)$$

Volume ΔV constitutes a layer limited by two spherical surfaces $\epsilon = g$ and $\epsilon = g + \Delta g$. The mean value of ϵ in volume ΔV with an accuracy of a higher than first order infinitesimal obviously equals:

$$\epsilon_{cp} \approx g + \frac{\Delta g}{2}.$$

Consequently, for small Δg we may set

$$2 \int_{\Delta V} \epsilon dV = 2\epsilon_{cp}\Delta V \approx 2g\Delta V + \Delta g\Delta V.$$

Substituting this value in expression (36.9) we obtain

$$\Delta Q_1 \approx \Delta g (D - 2D_1) + \Delta g\Delta V. \quad (36.10)$$

Will give g an increase $-\Delta g$, then volume D_1 will increased by ΔV , volume $(D - D_1)$ will decrease by ΔV . Integral Q will take a new value

$$\begin{aligned} Q_2 &= Q + \Delta Q_2 = \int_{D_1 + \Delta V} (\epsilon - g + \Delta g) dV - \int_{D - D_1 - \Delta V} (\epsilon - g + \Delta g) dV = \\ &= \int_{D_1} (\epsilon - g) dV - \int_{D - D_1} (\epsilon - g) dV + 2 \int_{\Delta V} (\epsilon - g) dV + \Delta g (D_1 + \Delta V) - \\ &- \Delta g (D - D_1 - \Delta V) = Q + \Delta g (2D_1 - D) - 2g\Delta V + \\ &+ 2 \int_{\Delta V} \epsilon dV + 2\Delta g\Delta V. \end{aligned}$$

The increase ΔQ_2 is written:

$$\Delta Q_2 = \Delta g (2D_1 - D) - 2g\Delta V + 2 \int_{\Delta V} \epsilon dV + 2\Delta g\Delta V. \quad (36.11)$$

Mean value of ϵ in volume ΔV in this case has the form

$$\varepsilon_{\infty} \approx g - \frac{\Delta g}{2}$$

and consequently for small Δg

$$2 \int_{\Delta V} \varepsilon dV \approx 2g\Delta V - \Delta g\Delta V.$$

Substituting this value in expression (36.11) we obtain

$$\Delta Q_1 \approx \Delta g(2D_1 - D) + \Delta g\Delta V. \quad (36.12)$$

Under the condition that $D = 2D_1$, in both cases, i.e., with a change in conductivity g by $\pm \Delta g$ we obtain the same positive increase of integral Q

$$\Delta Q = \Delta g\Delta V.$$

Consequently integral Q attains a minimum with that value of g which ε takes on a sphere dividing the volume of region D into two equal parts.

Knowing the equation of the surface limiting the volume of element D , always it is possible to express the magnitude of volume $D_1 = D/2$ in terms of radius R_g and coordinates x_g, y_g, z_g of the center of sphere $\varepsilon = g$ tangent to the surface of bath walls S at the point (x_0, y_0, z_0) . Considering in formulas (35.6) and (35.7) $C = g$, we obtain an expression for the radius and coordinates of the center of the sphere

$$R_g = \frac{1}{2g}, \quad (36.13)$$

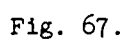
$$x_g = x_0 - \frac{\sin \gamma \cos \theta}{2g}, \quad y_g = y_0 - \frac{\sin \gamma \sin \theta}{2g}, \quad z_g = z_0 - \frac{\cos \gamma}{2g}.$$

As can be seen from these expressions the radius of the sphere and the coordinates of its center are functions of conductivity g . Expressing the volume of region $D_1 = D/2$ in these terms, we obtain an equation relative to g . Let us assume that it has the form:

$$D_1 = \frac{D}{2} = \Phi(g). \quad (36.14)$$

Solving this with respect to g we find the magnitude of conductivity at which Q reaches a minimum.

Precisely the same conclusions can be drawn in the case when element D constitutes a section of a plane of limited area. Spheres $\varepsilon = \text{const}$ intersect region D along circles. Integral Q attains a minimum at such a value of g at



Knowing the equation of the contour bounding the area of element D it is always possible to express the area $D_1 = D/2$ in terms through of the radius and coordinates of the center of circle $s = g$. Substituting $C = g$, in formulas (35.11) and (35.12) we obtain an expression for the radius and coordinates of the center of this circle:

Expressing the area of region $D_1 = D/2$ in these terms we obtain an equation with respect to ξ

If the form of the surface of the bath walls is given then the fixed direction of normal \vec{n}^0 at each point (x_0, y_0, z_0) and integral Q will thereby be a function of conductivity g only. In this case determination of g from equation (36.14) will be a solution to the problem posed. If, moreover, the problem of detecting of the form of the bath wall for which distortion of the field in element D will

be minimum is imposed, then it is necessary to seek the direction of normal \vec{n}^0 (dipole axis) at every point (x_0, y_0, z_0) at which integral Q attains a minimum. This can be done as follows.

On sphere $\varepsilon = g$ the difference $(\varepsilon - g)$ changes sign, therefore for Q we may write

$$Q = \int_b |\varepsilon - g| dV = \int_{b_1} (\varepsilon - g) dV - \int_{b-b_1} (\varepsilon - g) dV = 2 \int_{b_1} \varepsilon dV - \int_b \varepsilon dV - g(2D_1 - D) = 2 \int_{b_1} \varepsilon dV - \int_b \varepsilon dV. \quad (36.16)$$

Integral $\int_b \varepsilon dV$ is a function of parameters, angles γ and θ , integral $\int_{b_1} \varepsilon dV$ moreover is a function of the boundary of region D_1 a section of sphere $\varepsilon = g$ (or arc $\varepsilon = g$ when element D is a part of the plane) which in turn is a function of conductivity g . Considering g as a function of the parameters γ and θ found earlier (36.14), we can establish the equation for determination of values of γ and θ at which Q reaches a minimum

$$\begin{aligned} \frac{\partial Q}{\partial \gamma} &= 2 \frac{\partial}{\partial \gamma} \int_{b_1} \varepsilon dV - \frac{\partial}{\partial \gamma} \int_b \varepsilon dV = 2 \frac{d}{d\gamma} \int_{b_1} \varepsilon dV \cdot \frac{dV}{dg} \cdot \frac{\partial g}{\partial \gamma} - \frac{\partial}{\partial \gamma} \int_b \varepsilon dV = 0, \\ \frac{\partial Q}{\partial \theta} &= 2 \frac{\partial}{\partial \theta} \int_{b_1} \varepsilon dV - \frac{\partial}{\partial \theta} \int_b \varepsilon dV = 2 \frac{d}{d\theta} \int_{b_1} \varepsilon dV \cdot \frac{dV}{dg} \cdot \frac{\partial g}{\partial \theta} - \frac{\partial}{\partial \theta} \int_b \varepsilon dV = 0. \end{aligned} \quad (36.17)$$

But

$$\frac{d}{dV} \int_{b_1} \varepsilon dV = \lim_{\Delta V \rightarrow 0} \frac{\int_{b_1 + \Delta V} \varepsilon dV - \int_{b_1} \varepsilon dV}{\Delta V} = \lim_{\Delta V \rightarrow 0} \frac{\int_{\Delta V} \varepsilon dV}{\Delta V} = g. \quad (36.18)$$

From equation (36.14)

$$\frac{dV}{dg} = \frac{d\Phi}{dg}. \quad (36.19)$$

Substituting these values in system (36.17) and replacing ε by expression (35.9), we obtain

$$\begin{cases} 2g \frac{d\Phi}{dg} \cdot \frac{\partial g}{\partial \gamma} + \cos \gamma \cos \theta \int_b \frac{x - x_0}{r^2} dV + \cos \gamma \sin \theta \int_b \frac{y - y_0}{r^2} dV - \\ \quad - \sin \gamma \int_b \frac{z - z_0}{r^2} dV = 0, \\ 2g \frac{d\Phi}{dg} \frac{\partial g}{\partial \theta} - \sin \gamma \sin \theta \int_b \frac{x - x_0}{r^2} dV + \sin \gamma \cos \theta \int_b \frac{y - y_0}{r^2} dV = 0. \end{cases} \quad (36.20)$$

Such a system will take place when element D is a part of plane $z = 0$.

Solving system (36.20) relatively to α and β we find the direction of normal \vec{n}^0 at every point (x_0, y_0, z_0) at which Q is minimum. Thus determining the field of vectors \vec{n}^0 in space it is easy to compose differential equations of a family of surfaces orthogonal to them. As is known from differential geometry this system is:

$$\begin{aligned}\frac{\partial z_0}{\partial x_0} &= -\frac{\cos \alpha}{\cos \gamma} = -\operatorname{tg} \gamma \cos \theta, \\ \frac{\partial z_0}{\partial y_0} &= -\frac{\cos \beta}{\cos \gamma} = -\operatorname{tg} \gamma \sin \theta.\end{aligned}\quad (36.21)$$

Integrating this system we obtain the equation of a one-parameter family of surfaces

$$z_0 = j(x_0, y_0, C). \quad (36.22)$$

Parameter C will be defined if at least one point (x_0, y_0, z_0) is given through which it is desirable to conduct surface S of the bath walls.

Thus the problem and in this case can be completely solved.

§ 37. Model with Zero Mean Value of Potential of Distortion

For modeling of a field of stray currents in earth during calculation of electroprotection of underground installations from corrosion it is desirable to have a model of an element of unlimited space D in the form of a section of free surface of the conducting composition of the bath. Here it is important in region D to ensure first a zero mean value of potential of distortion φ_2 in every point of region D. As will be evident below, these two requirements almost never contradict each other and can be satisfied.

The first requirement determines the magnitude of conductivity g in every point (x_0, y_0, z_0) . It is formulated thus:

$$J = 4\pi \int_D \varphi_2 dS_1 = \int_D \left\{ \oint_S \frac{\varphi}{r} \left(\frac{1}{r} \frac{\partial r}{\partial n} - g \right) dS_1 \right\} dS = 0. \quad (37.1)$$

Change the order of integration we obtain

$$\oint_S \varphi \left\{ \int_D \frac{1}{r} \left(\frac{1}{r} \frac{\partial r}{\partial n} - g \right) dS_1 \right\} dS = 0. \quad (37.2)$$

This equality will be satisfied if at every point (x_0, y_0, z_0) the surface of the

bath walls S is ensured

$$\int_b \frac{1}{r} \left(\frac{1}{r} \frac{\partial r}{\partial n} - g \right) dS_1 = 0.$$

Hence we directly obtain

$$g(x_0, y_0, z_0) = \frac{\int_b \frac{1}{r^2} \frac{\partial r}{\partial n} dS_1}{\int_b \frac{dS_1}{r}} = \frac{\int_b \frac{e}{r} dS_1}{\int_b \frac{dS_1}{r}}. \quad (37.3)$$

The second requirement determines the form of the surface of the bath walls S. From expression (34.5) one may see that to decrease magnitude $|\varphi_2|$ without increasing the dimensions of the bath is possible at the expense of a decrease of magnitude $|\varepsilon - g|$. Applying mean value theorem to the integral standing in the numerator of the expression for conductivity (37.3), we obtain

$$g(x_0, y_0, z_0) = \frac{e(x_1, y_1, z_1)}{\int_b \frac{dS_1}{r}} \int_b \frac{dS_1}{r} = e(x_1, y_1, z_1),$$

where point (x_1, y_1, z_1) belongs to the region and consequently

$$\varepsilon_{\min} \leq g \leq \varepsilon_{\max}, \quad (37.4)$$

where ε_{\min} and ε_{\max} are minimum and maximum values of ε in region D respectively.

In order to minimize distribution of magnitude $|\varepsilon - g|$ in region D in the Chebyshev sense it is sufficient: 1) to find such distribution ε in D for which difference $\varepsilon_{\max} - \varepsilon_{\min}$ will be minimum; 2) to take the magnitude of conductivity g equal to $(\varepsilon_{\max} + \varepsilon_{\min})/2$. In our case the magnitude of g is already determined by (37.3) and we cannot obtain a minimum of the modulus of difference $|\varepsilon - g|$, although, as can be seen from inequality (37.4), conductivity g is close to

$$\frac{\varepsilon_{\max} + \varepsilon_{\min}}{2}.$$

Finding the distribution of ε in D for which difference $\varepsilon_{\max} - \varepsilon_{\min}$ is minimum, we will approach a minimum magnitude $|\varepsilon - g|$ and, consequently, $|\varphi_2|$. The problem consists of finding that direction of normal \vec{n} at each point of the surface of the bath walls (x_0, y_0, z_0) for which difference $\varepsilon_{\max} - \varepsilon_{\min}$ in region D will be minimum.

In the considered case region D is a part to the plane and constitutes a section of the free surface of the bath. Considering in formula (35.11) $R_c = 0$ we find

$$\epsilon_{\text{max}} = - \frac{1 - \cos \gamma}{2z_0}. \quad (37.5)$$

Substituting this value in formulas (35.12) we find the coordinates of the point of region D at which $\epsilon = \epsilon_{\text{max}}$:

$$x_m = x_0 + z_0 \frac{\sin \gamma \cos \theta}{1 - \cos \gamma}, \quad y_m = y_0 + z_0 \frac{\sin \gamma \sin \theta}{1 - \cos \gamma}. \quad (37.6)$$

The surface of the bath walls S rests on the free surface of conducting composition S_1 from below. Therefore $z_0 \leq 0$, $\gamma > \frac{\pi}{2}$ and from formulas (37.6) it may be concluded that if $|z_0|$ is less than half the diameter of free surface S_1 then point (x_m, y_m) will be internal for S_1 .

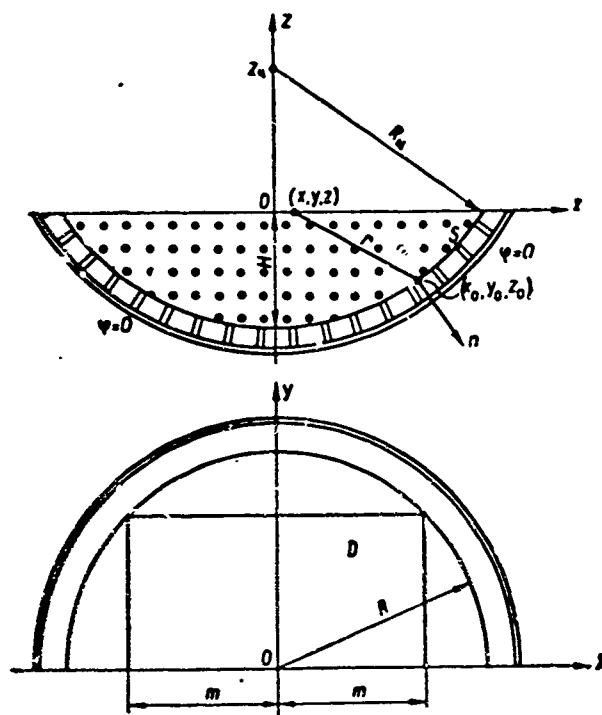


Fig. 68.

Let us assume that element D constitutes a circle of radius R (Fig. 68). Let us combine the coordinate origin with the center of the circle and direct axis oz normal to its plane. From the geometry of field ϵ one may see that it is

always possible to select such a direction of the normal \bar{n} at point (x_0, y_0, z_0) at which the trace of one of the spheres $\varepsilon = C$ on plane $z = 0$ will coincide with the circumference of circle R . Here the point at which ε takes a maximum value will be inside circle R and $\varepsilon = C$ on circle R obviously will be minimum. As follows from formula (35.6), it equals

$$\varepsilon_{\min} = \frac{1}{2R_u}. \quad (37.7)$$

Normal \bar{n}^0 obviously will lie in a vertical plane passing through the axis oz (i.e., angle $\theta = \arctg \frac{y_0}{x_0}$), and coincide with the direction of the radius of sphere $\varepsilon = C$. The center of the sphere is on axis oz at point z_u . Let us designate the distance from axis oz to arbitrary point (x, y) by ρ ($\rho^2 = x^2 + y^2$) and write the equation of the circle formed by the sphere $\varepsilon = C$ in the vertical plane passing through axis oz and normal \bar{n}

$$\rho^2 + (z - z_u)^2 = R_u^2. \quad (37.8)$$

Substituting in this equation the coordinates of points $(\pm R, 0)$ and (ρ_0, z_0) through which should pass the circle we find

$$R_u = \sqrt{R^2 + z_u^2}, \quad z_u = \frac{\rho_0^2 + z_0^2 - R^2}{2z_0}. \quad (37.9)$$

We write the equation of the straight line coinciding with direction of normal \bar{n}^0 at point (ρ_0, z_0) and radius of sphere $\varepsilon = C$

$$z = \frac{z_0 - z_u}{\rho_0} \rho + z_u = k\rho + z_u. \quad (37.10)$$

Consequently the tangent of the angle between normal \bar{n}^0 and axis oz has the form

$$\tg \gamma = \frac{1}{k} = \frac{\rho_0}{z_0 - z_u} = \frac{2z_0\rho_0}{R^2 + z_0^2 - \rho_0^2}. \quad (37.11)$$

We now show that in this case the direction of normal \bar{n}^0 , i.e., when

$$\theta = \arctg \frac{y_0}{x_0}, \quad \gamma = \gamma_1 = \arctg \frac{2z_0\rho_0}{R^2 + z_0^2 - \rho_0^2}$$

the difference $(\varepsilon_{\max} - \varepsilon_{\min})$ in a circle of radius R will be minimum. We proceed from the fact that the point at which $\varepsilon = \varepsilon_{\max}$ lies inside circle R , the point at which $\varepsilon = \varepsilon_{\min}$ — on the circumference of the circle. Converting to cylindrical coordinates in formula (35.9) and substituting

$$x = R \cos \psi, \quad y = R \sin \psi, \quad x_0 = \rho_0 \cos \psi_0, \quad y_0 = \rho_0 \sin \psi_0.$$

for the value of ε on circle R we obtain

$$\varepsilon = \frac{z_0 \cos \gamma - [R \cos(\psi - \theta) - \rho_0 \cos(\psi_0 - \theta)] \sin \gamma}{R^2 + \rho_0^2 - 2R\rho_0 \cos(\psi - \psi_0) + z_0^2}. \quad (37.12)$$

Since $\varepsilon_{\text{макс}}$ is independent of ψ , then setting the derivative of ε with respect to ψ equal to zero we find the values of ψ for which the difference $\varepsilon_{\text{макс}} - \varepsilon_{\text{мин}}$ has the extremum

$$\frac{\partial \varepsilon}{\partial \psi} = \frac{[R \sin(\psi - \theta_1) - \rho_0 \sin(\psi_0 - \theta_1)] \sin \gamma}{R^2 + \rho_0^2 - 2R\rho_0 \cos(\psi - \psi_0) + z_0^2} = 0.$$

For any ρ_0 this equality holds only if

$$\sin(\psi_0 - \theta_1) = \sin(\psi - \theta_1) = 0,$$

therefore either

$$\psi_0 - \theta_1 = \psi - \theta_1 = 0, \quad \theta_1 = \psi_0 = \psi, \quad (37.13)$$

or

$$\psi_0 - \theta_1 = \psi - \theta_1 + \pi = 0, \quad \theta_1 = \psi_0 = \psi + \pi.$$

From these relationships it follows that the vertical plane passing through normal \bar{n} should pass also through the axis oz , i.e.,

$$\theta_1 = \psi_c = \arctg \frac{y_0}{x_0}.$$

Substituting values of ψ and ψ in expression (37.12), we obtain

$$\begin{aligned} \varepsilon_1 &= \frac{z_0 \cos \gamma - (R - \rho_0) \sin \gamma}{R^2 + \rho_0^2 - 2R\rho_0 + z_0^2}, \\ \varepsilon_2 &= \frac{z_0 \cos \gamma + (R + \rho_0) \sin \gamma}{R^2 + \rho_0^2 + 2R\rho_0 + z_0^2}. \end{aligned} \quad (37.14)$$

Here ε_1 and ε_2 are, respectively, the minimum and maximum values of ε on the circle R.

Let us demonstrate that the difference $\varepsilon_{\text{макс}} - \varepsilon_{\text{мин}}$ will occur at a value $\gamma = \gamma_1$.

The maximum value of ε was found by us to be

$$\varepsilon_{\text{макс}} = - \frac{1 - \cos \gamma}{2z_0},$$

as $\varepsilon_{\text{мин}}$ we take the smaller of expressions (37.14) which are equal for $\gamma = \gamma_1$

$$\varepsilon_1(\gamma_1) = \varepsilon_2(\gamma_1) = \frac{1}{2R_u}.$$

Giving γ_1 an increase $\pm \Delta \gamma$, we obtain an increment of difference $\Delta(\varepsilon_{\text{макс}} - \varepsilon_{\text{мин}})$.

If it is positive for $\Delta \gamma$ of either sign then the difference $(\varepsilon_{\text{макс}} - \varepsilon_{\text{мин}})$ is

minimum. With an increase of γ_1 by $+\Delta\gamma_1$ and ε_2 take on increases of different sign

$$\begin{aligned}\Delta\varepsilon_1 &\cong \frac{\partial\varepsilon_1}{\partial\gamma}\bigg|_{\gamma=\gamma_1} \Delta\gamma = \frac{-z_0 \sin \gamma_1 - (R - \varrho_0) \cos \gamma_1}{(R - \varrho_0)^2 + z_0^2} \Delta\gamma = \\ &= \frac{(R - \varrho_0)(z_u - z_0) - z_0 \varrho_0}{R_u [(R - \varrho_0)^2 + z_0^2]} \Delta\gamma > 0, \\ \Delta\varepsilon_2 &\cong \frac{\partial\varepsilon_2}{\partial\gamma}\bigg|_{\gamma=\gamma_1} \Delta\gamma = \frac{-z_0 \sin \gamma_1 + (R + \varrho_0) \cos \gamma_1}{(R + \varrho_0)^2 + z_0^2} \Delta\gamma = \\ &= \frac{-(R + \varrho_0)(z_u - z_0) - z_0 \varrho_0}{R_u [(R + \varrho_0)^2 + z_0^2]} \Delta\gamma < 0.\end{aligned}$$

Consequently, for $+\Delta\gamma$ it is necessary to consider the increment of difference $(\varepsilon_{\text{макс}} - \varepsilon_{\text{мин}})$, for $-\Delta\gamma$, an increment of difference $(\varepsilon_{\text{макс}} - \varepsilon_1)$. For a positive increase of γ we obtain

$$\begin{aligned}\varepsilon_{\text{макс}}(\gamma_1 + \Delta\gamma) - \varepsilon_2(\gamma_1 + \Delta\gamma) &\cong \varepsilon_{\text{макс}}(\gamma_1) - \varepsilon_2(\gamma_1) + \\ &+ \left(\frac{\partial\varepsilon_{\text{макс}}}{\partial\gamma} - \frac{\partial\varepsilon_2}{\partial\gamma} \right)_{\gamma=\gamma_1} \Delta\gamma = \varepsilon_{\text{макс}}(\gamma_1) - \varepsilon_2(\gamma_1) + \left[\frac{\sin \gamma_1}{-2z_0} + \right. \\ &+ \left. \frac{(R + \varrho_0)(z_u - z_0) + z_0 \varrho_0}{R_u [(R + \varrho_0)^2 + z_0^2]} \right] \Delta\gamma = (\varepsilon_{\text{макс}} - \varepsilon_2)(\gamma_1) + \frac{R\Delta\gamma}{-2z_0 R_u}.\end{aligned}$$

Difference $(\varepsilon_{\text{макс}} - \varepsilon_{\text{мин}})$ undergoes a positive increase

$$\Delta(\varepsilon_{\text{макс}} - \varepsilon_{\text{мин}}) = \frac{R\Delta\gamma}{-2z_0 R_u}.$$

With a negative increase in γ we obtain

$$\begin{aligned}\varepsilon_{\text{макс}}(\gamma_1 - \Delta\gamma) - \varepsilon_1(\gamma_1 - \Delta\gamma) &= \varepsilon_{\text{макс}}(\gamma_1) - \varepsilon_1(\gamma_1) - \\ &- \left(\frac{\partial\varepsilon_{\text{макс}}}{\partial\gamma} - \frac{\partial\varepsilon_1}{\partial\gamma} \right)_{\gamma=\gamma_1} \Delta\gamma = (\varepsilon_{\text{макс}} - \varepsilon_1)(\gamma_1) - \left[\frac{\sin \delta_1}{-2z_0} - \right. \\ &- \left. \frac{(R - \varrho_0)(z_u - z_0) - z_0 \varrho_0}{R_u [(R - \varrho_0)^2 + z_0^2]} \right] \Delta\gamma = (\varepsilon_{\text{макс}} - \varepsilon_1)(\gamma_1) + \frac{R\Delta\gamma}{-2z_0 R_u}.\end{aligned}$$

Difference $(\varepsilon_{\text{макс}} - \varepsilon_{\text{мин}})$ in this case also takes on a positive increase

$$\Delta(\varepsilon_{\text{макс}} - \varepsilon_{\text{мин}}) = \frac{R\Delta\gamma}{-2z_0 R_u}.$$

This proves that for $\gamma = \gamma_1$ difference $(\varepsilon_{\text{макс}} - \varepsilon_{\text{мин}})$ has a minimum.

Let us go now to the construction of the surface of the bath walls S.

Considering that

$$\operatorname{tg} \gamma = -\frac{dz_0}{dQ_0}, \quad (37.15)$$

we write the differential equation of the trace of the sought surface in the vertical plane (poz)

$$\frac{dz_0}{dQ_0} = -\frac{2z_0Q_0}{R^2 + z_0^2 - Q_0^2}. \quad (37.16)$$

The general integral of the differential equation will be

$$z_0 - \frac{R^2 - Q_0^2}{z_0} = C, \quad (37.17)$$

whence

$$Q_0^2 + \left(z_0 - \frac{C}{2}\right)^2 = R^2 + \frac{C^2}{4}. \quad (37.18)$$

This is the equation of a circle with center on the oz axis at the point $z_c = C/2$

and radius $R_c = \sqrt{R^2 + \frac{C^2}{4}}$. Constant C will be determined by the maximum

depth of the bath H. Assuming $H = vR$ and substituting coordinates of the deepest point $(0, -vR)$ into equation (37.18) we find

$$C = \frac{1-v^2}{v} R, \quad (37.19)$$

and consequently the equation of the trace of the surface of the bath walls will be:

$$Q_0^2 + \left(z_0 - \frac{1-v^2}{2v} R\right)^2 = \left(R \frac{1+v^2}{2v}\right)^2. \quad (37.20)$$

Considering the axial symmetry of surface S we conclude that it will be spherical (Fig. 68) with its center on axis oz at the point

$$z_u = R \frac{1-v^2}{2v} \quad (37.21)$$

and with radius

$$R_u = R \frac{1+v^2}{2v}. \quad (37.22)$$

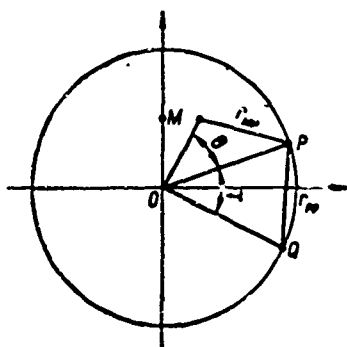
If region D differs from a circle then the form of the surface of the bath walls S also is expedient to select spherical, resting on a circumference the diameter of which is equal to the diameter of region D. In this case the values of the difference $(\epsilon_{V2KC} - \epsilon_{MH})$ for different points of spherical surface S will be only less or equal to values at points of the surface of the bath walls resting

on the contour of region D. The magnitude of conductivity g however must be determined from equation (37.3) by integrating over region D.

It is important to note that property of baths of designed and built by this method do not depend on the properties of the medium filling the bath. In particular they will be maintained even during modeling of the field in nonuniform and nonlinear media. In fact, if within the volume of the bath there were some nonuniform or nonlinear inclusions then when producing a field in the bath these inclusions will be equivalent to additional sources distributed over their boundaries and volume. Properties of the bath do not depend on distribution of field sources in it and consequently are maintained during modeling of the field in nonuniform and nonlinear media.

§ 38. On Accuracy of Modeling

Let us find the connection between the normal component of intensity $E_n(P)$ and potential $f(P)$ on a sphere of radius R in a uniform unbounded medium where



we will consider the field produced by a point source q located at point M inside the sphere. Potential $f(P)$ has the form (Fig. 69)

$$f(P) = \frac{q}{4\pi\gamma r_{MP}} = \frac{q}{4\pi\gamma \sqrt{R^2 + q^2 - 2Rq \cos \theta}}, \quad \theta = (\widehat{r_{OP}, r_{OM}}). \quad (38.1)$$

The normal component of intensity

$$E_n(P) = -\frac{\partial f}{\partial R} = \frac{q}{4\pi\gamma \sqrt{R^2 + q^2 - 2Rq \cos \theta}} \cdot \frac{R - q \cos \theta}{R^2 + q^2 - 2Rq \cos \theta} = f(P) \epsilon(P), \quad (38.2)$$

here

$$\epsilon(P) = \frac{R - q \cos \theta}{R^2 + q^2 - 2Rq \cos \theta} = \frac{NP}{r_{MP}^2} = \frac{\cos(r, n)}{r_{MP}}, \quad (38.3)$$

$\epsilon(P)$ — function playing role of proportionality factor between $f(P)$ and $\partial f / \partial n$ at every point of the sphere. In the model of an element of unlimited space in form of a sphere of radius R function ϵ we replace with a constant — conductivity of holes g connecting the internal volume of the model with the external metallic housing. Such a substitution will decrease the influence of the

boundary more the smaller the value of difference $(\varepsilon - g)$ in volume D.

The least and greatest values of ε respectively equal

$$\varepsilon_{\min} = \frac{1}{2R}, \quad \varepsilon_{\max} = \infty. \quad (37.7)$$

Let us find the mean value of ε the entire over volume D. Surface $\varepsilon = \varepsilon_0 = \text{const}$ is a sphere of radius

$$R_0 = \frac{1}{2\varepsilon_0}. \quad (35.6)$$

The volume of the sphere of bounded by this surface is

$$V_{\varepsilon} = \frac{4}{3} \pi R_0^3 = \frac{\pi}{6\varepsilon_0^3}. \quad (38.4)$$

The derivative of this volume with respect to ε_0 is

$$\left| \frac{dV}{d\varepsilon_0} \right| = \left| \frac{\pi}{2\varepsilon_0^4} \right|, \quad dV = \frac{\pi}{2\varepsilon_0^4} d\varepsilon_0. \quad (38.5)$$

The mean value of ε within the volume of a sphere of R can be written:

$$\begin{aligned} \varepsilon_{cp} &= \frac{1}{V} \int_V \varepsilon_0 dV = \frac{3}{4\pi R^3} \int_{\varepsilon_{\min}}^{\varepsilon_{\max}} \frac{\pi}{2\varepsilon_0^4} d\varepsilon_0 = \frac{3}{8R^3} \left(-\frac{1}{2\varepsilon_0^3} \right) \Big|_{\frac{1}{2R}}^{\infty} = \frac{3}{4R}, \\ \varepsilon_{cp} &= \frac{3}{2} \varepsilon_{\min}. \end{aligned} \quad (38.6)$$

It is also easy to find the mean square value within the volume of the sphere

$$\begin{aligned} \varepsilon_{cpl}^2 &= \frac{3}{4\pi R^3} \int_{\frac{1}{2R}}^{\infty} \varepsilon_0^2 \frac{\pi}{2\varepsilon_0^4} d\varepsilon_0 = \frac{3}{4R^3}, \\ \varepsilon_{cpl} &= \sqrt{3} \varepsilon_{\min}. \end{aligned} \quad (38.7)$$

As can be seen, ε_{cp} differs little from ε_{\min} , consequently function ε differs little from a constant. Ensuring in the model a conductivity of the boundary $g = \varepsilon_{cp}$, we thereby reduce the distortion introduced by the boundary in a definite sense to a minimum.

The exact calculation of error introduced by the boundary of model in the investigated field in general constitutes a very complicated problem. However for the most important case when element D constitutes a sphere and the boundary

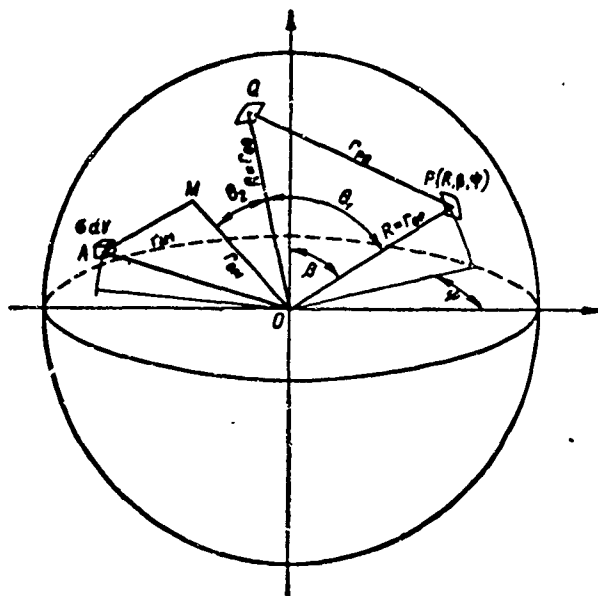


Fig. 70.

of the model its surface, we can be obtained an expression for the potential of distorting field for any distribution of sources in such a model in the form of a rapidly conveying series.

Let us consider a solution of the following problem: in a model whose boundary is a sphere of radius R with constant conductivity g of unit surface is given the distribution of volumetric density of charges $\sigma(x_0, y_0, z_0)$. Is required to find potential φ at any point $M(x, y, z)$ of the model (Fig. 70).

By the formula of Green, potential at point of the M model has the form

$$\varphi(M) = \frac{1}{4\pi\gamma} \int_V \frac{\sigma dV}{r_1} + \frac{1}{4\pi} \int_{S_R} \frac{\varphi(P)}{r_{PM}} \left[\frac{\cos(r, n)}{r_{PM}} - g \right] dS_P. \quad (38.8)$$

Converting point M to point Q lying on sphere S_R , within the limit we obtain

$$\varphi(Q) = \frac{1}{4\pi\gamma} \int_V \frac{\sigma dV}{r_1} + \frac{1}{4\pi} \oint_{S_R} \frac{\varphi(P)}{r_{PQ}} \left[\frac{\cos(r, n)}{r_{PQ}} - g \right] dS_P + \frac{1}{2} \varphi(Q),$$

or

$$\varphi(Q) = \frac{1}{2\pi\gamma} \int_V \frac{\sigma dV}{r_1} + \frac{1}{2\pi} \oint_{S_R} \frac{\varphi(P)}{r_{PQ}} \left[\frac{\cos(r, n)}{r_{PQ}} - g \right] dS_P. \quad (38.9)$$

On sphere S_R of radius R , the magnitude of $\cos(r, n)/r_{PQ}$ is constant and equal to

$$g = \frac{\cos(r, n)}{r_{PQ}} = \frac{1}{2R}.$$

Due to symmetry, conductivity g is constant. Let us take it equal to

$$g = \frac{\nu}{2R} = \epsilon_0. \quad (1 < \nu < 2). \quad (38.10)$$

Consequently

$$\frac{\cos(r, n)}{r_{PQ}} - g = \frac{1 - \nu}{2R} = \frac{\alpha}{2R}, \quad (|\alpha| < 1) \quad (38.6)$$

is also constant and the expression for potential φ takes the following form:

$$\varphi(Q) = 2f(Q) + \frac{\alpha}{4\pi R} \oint_{S_R} \frac{\varphi(P)}{r_{PQ}} dS_P = 2f(Q) + \alpha \lambda K\varphi. \quad (38.11)$$

Here

$$f(Q) = \int \frac{\sigma dV}{4\pi r_{PQ}}, \quad \lambda = \frac{1}{4\pi R}, \quad K\varphi = \oint_{S_R} \frac{\varphi(P)}{r_{PQ}} dS_P. \quad (38.12)$$

We will consider expression (38.11) as a Fredholm integral equation of second kind with respect to potential φ . Let us present a solution of equation (38.11) in the form of a Neumann series

$$\varphi(Q) = 2f(Q) + 2[\alpha\lambda Kf + \alpha^2\lambda^2 K^2f + \dots]. \quad (38.13)$$

Potential of distortion φ_2 will be recorded also in the form of series

$$\varphi_2(Q) = \varphi(Q) - f(Q) = f(Q) + 2[\alpha\lambda Kf + \alpha^2\lambda^2 K^2f + \dots]. \quad (38.14)$$

Let us show that this series converges rapidly. For this we will estimate the norm of operator K . We have

$$\begin{aligned} |K\varphi| &= \left| \oint_{S_R} \frac{\varphi(P)}{r_{PQ}} dS_P \right| < \oint_{S_R} |\varphi(P)| \left| \frac{1}{r_{PQ}} \right| dS_P < \max_{S_R} |\varphi| \oint_{S_R} \frac{dS_P}{r_{PQ}} = \\ &= \max_{S_R} |\varphi| \pi R \int_0^\pi \frac{\sin \gamma d\gamma}{\sin \frac{\gamma}{2}} = 4\pi R \max_{S_R} |\varphi|. \end{aligned} \quad (38.15)$$

Consequently

$$\|K\varphi\| = \max_{S_R} |\varphi| \max_{S_R} \left| \oint_{S_R} \frac{dS_P}{r_{PQ}} \right| = 4\pi R \max_{S_R} |\varphi|. \quad (38.16)$$

whence

$$\|K\| = \frac{\|K\varphi\|}{\|\varphi\|} = 4\pi R = \frac{1}{\lambda}. \quad (38.17)$$

Thus

$$\|\alpha\lambda K\| = |\alpha|. \quad (38.18)$$

If one were to take $g = 3/4R$, then $\alpha = -\frac{1}{2}$ and consequently series (38.14) converges rapidly.

The expression for potential $\varphi_2(M)$ in any internal point M gives Poisson integral

$$\varphi_2(M) = \frac{1}{4\pi R} \oint_{S_R} \frac{R^2 - r_{OM}^2}{(R^2 - 2Rr_{OM} \cos \theta_2 + r_{OM}^2)^{\frac{3}{2}}} \varphi_2(Q) dS_Q(\theta_2 = r_{OM}, r_{OQ}). \quad (38.19)$$

Substituting here instead of $\varphi_2(Q)$ its expression (38.14) and limiting ourselves to two or three members of the series we obtain an expression for distortion potential at any internal point of the model

$$\varphi_2(M) = \frac{1}{4\pi R} \oint_{S_R} \frac{f(Q) + 2\alpha\lambda Kf + 2\alpha^2\lambda^2 K^2f + \dots}{(R^2 - 2Rr_{OM} \cos \theta_2 + r_{OM}^2)^{\frac{3}{2}}} [R^2 - r_{OM}^2] dS_Q. \quad (38.20)$$

Definition of φ_2 in the model is equivalent to a solution of the following boundary value problem for a harmonic function.

Presenting the resultant potential φ in the form of sum f and φ_2 we obtain the boundary condition for φ_2

$$\left. \frac{\partial \varphi_2}{\partial n} \right|_{S_R} = \left. \frac{\partial f}{\partial n} \right|_{S_R} + g f \Big|_{S_R} + g \varphi_2 \Big|_{S_R} = F + g \varphi_2 \Big|_{S_R}. \quad (38.21)$$

Here F is the well known function:

$$F = \left. \frac{\partial f}{\partial n} \right|_{S_R} + g f \Big|_{S_R}. \quad (38.22)$$

The boundary value problem can be formulated thus: find the harmonic function φ_2 inside sphere if the following relationship between values of function φ_2 and its normal derivative on the sphere are given:

$$\left. \frac{\partial \varphi_2}{\partial n} \right|_{S_R} - g \varphi_2 \Big|_{S_R} = F. \quad (38.23)$$

For appraisal of influence of the boundary of the model on the accuracy of modeling the field in the following experiment was performed. An electrolytic bath was prepared in the form of rectangular. Conductivity g in the walls of the bath was replaced by conductivity of holes drilled normal to the walls at

distances of 2 cm from one another over the entire surface of the walls.

Internal dimensions of the bath are $1400 \times 700 \times 250$ mm.

On the surface of the electrolyte of the bath was mounted a spherical electrode of small radius having a point charge. The second electrode was connected to the external housing of the bath. A voltmeter was used to obtain a field pattern of current in the bath on the surface on the electrolyte and this was compared with calculations. Here it proved that noticeable distortions of the field pattern were observed only near the bath walls at distances of less than 5 cm. These distortions are apparently explained by the fact that continuous distribution of conductivity of boundaries is replaced by a discrete distribution of holes.

§ 35. Model of an Element of Unbounded Space Having the Form of a Rectangle

Let us consider how to find the conductivity g of the walls of the model of an element of unbounded space having the form of a rectangle D with sides m and $2m$ if the surface of the walls constitutes the surface of a rectangular parallelepiped whose upper margin is a rectangle. The depth of the conducting composition of the model is $H = km$ ($k \approx 0.2$). Conductivity g will be sought from the conditions of minimum of integral Q . As we clarified in § 36 integral Q attains a minimum at such value of g for which the circumference $\epsilon = g$ divides the area of region D into two equal parts D_1 and $D - D_1$. Using formulas (36.15) we derive equation (36.14).

Let us take as the origin of coordinates the center of rectangle D and direct the axis oz normally to its plane. Axes ox and oy we direct parallel to sides of length $2m$ and m . Equation (36.14) has different forms for different edges of the surface and even within limits of one edge its form changes depending upon the position of point (x_0, y_0, z_0) on it. Due to symmetry of region D relative to axes ox and oy it is sufficient to derive equation (36.14) for the two halves of the lateral faces and a quarter of the lower.

Derivation of equation (36.14) for lateral face of length $2m$ (Fig. 71).

On this face

$$\mu = \frac{\pi}{2}, \quad \gamma = \frac{\pi}{2}, \quad \theta = \frac{\pi}{2}. \quad (39.1)$$

Placing these values in formulas (36.15) we obtain

From Fig. 71 one may see that

$$\psi_1 = \arccos \frac{y_g + \frac{m}{2}}{R_g}, \quad \psi_2 = \arccos \frac{m - x_g}{R_g}.$$

Substituting values for ψ_1 and ψ_2 and replacing R_g , y_g with their expressions (39.2) we obtain three equations for the determination of conductivity g :

$$1) \quad \pi - \arccos \frac{m - \frac{1}{2g}}{\sqrt{\frac{1}{4g^2} - z_0^2}} = \frac{m^2 - \left(m - \frac{1}{2g}\right) \sqrt{\frac{m}{g} - m^2 - z_0^2}}{\frac{1}{4g^2} - z_0^2}; \quad (39.6)$$

$$2) \quad \pi - \arccos \frac{m - \frac{1}{2g}}{\sqrt{\frac{1}{4g^2} - z_0^2}} - \arccos \frac{m - x_0}{\sqrt{\frac{1}{4g^2} - z_0^2}} = \frac{m^2 - \left(m - \frac{1}{2g}\right) \sqrt{\frac{m}{g} - m^2 - z_0^2} - (m - x_0) \sqrt{\frac{1}{4g^2} - z_0^2 - (m - x_0)^2}}{\frac{1}{4g^2} - z_0^2}; \quad (39.7)$$

$$3) \quad \frac{3}{2} \pi - \arccos \frac{m - \frac{1}{2g}}{\sqrt{\frac{1}{4g^2} - z_0^2}} - \arccos \frac{m - x_0}{\sqrt{\frac{1}{4g^2} - z_0^2}} = \frac{2x_0 m + (m - x_0) \left[\frac{1}{g} - \sqrt{\frac{1}{4g^2} - z_0^2 - (m - x_0)^2} \right] - \left(m - \frac{1}{2g}\right) \sqrt{\frac{m}{g} - m^2 - z_0^2}}{\frac{1}{4g^2} - z_0^2}. \quad (39.8)$$

Let us find the boundaries of sections for which one should use one or the other formula: Setting $R_g = m - x_0$ and placing this value in formula (39.6) we find $x_0 = x_{01}$, starting from which one should use formula (39.7). From the condition $z_0 \pm H = 0.2$ m, disregarding member z_0^2 we obtain

$$R_g = \frac{1}{2g} = m - x_{01},$$

$$\pi - \arccos \frac{x_{01}}{m - x_{01}} = \frac{m^2 - x_{01} \sqrt{m^2 - 2mx_{01}}}{(m - x_{01})^2}. \quad (39.9)$$

The root of equation (39.9) will be $x_{01} = 0.4$ m. Setting

$$R_s = \frac{1}{2g} = \sqrt{(m - x_0)^2 + \left(y_s + \frac{m}{2}\right)^2} = \sqrt{(m - x_{01})^2 + \left(m - \frac{1}{2g}\right)^2}$$

we obtain

$$\frac{1}{2g} = \frac{(m - x_{01})^2 + m^2}{2m}.$$

Substituting this value in formula (39.7) and disregarding the term z_0^2 we find $x_0 = x_{01}$ starting from which one should use formula (39.8)

$$\begin{aligned} \pi - \arccos \frac{x_{01}(2m - x_{01})}{m^2 + (m - x_{01})^2} - \arccos \frac{2m(m - x_{01})}{m^2 + (m - x_{01})^2} = \\ m^2 - \frac{x_{01}}{2m} (2m - x_{01})(m - x_{01}) - (m - x_{01}) \times \\ \times \sqrt{\left[\frac{(m - x_{01})^2 + m^2}{2m} \right]^2 - (m - x_{01})^2} = \\ = \frac{\left[\frac{(m - x_{01})^2 + m^2}{2m} \right]^2}{\left[\frac{(m - x_{01})^2 + m^2}{2m} \right]^2}. \end{aligned}$$

The root of this equation will be $x_{02} = 0.49$ m, consequently for determination of conductivity g for $0 \leq x_0 \leq 0.4$ m one should use equation (39.6), for $0.4 \text{ m} \leq x_0 \leq 0.49$ m - equation (39.7) and for $0.49 \text{ m} \leq x_0 \leq m$ - equation (39.8).

Derivation of equation (36.14) for a lateral face of length m (Fig. 72).

On this face

$$\begin{aligned} x_0 = m, \quad y = \frac{\pi}{2}, \quad \theta = 0, \quad x_s = x_0 - \frac{1}{2g}, \\ y_s = y_0, \quad R_s = \sqrt{\frac{1}{4g^2} - x_0^2}. \end{aligned} \quad (39.10)$$

As can be seen from Fig. 72 circumference $\epsilon = g$ can occupy two different positions with respect to rectangle D. Each of these positions corresponds to a definite form of equation (36.14). We express area D_1 for each position of circumference $\epsilon = g$:

$$\begin{aligned} 1) \quad R_s \leq y_0 + \frac{m}{2}, \\ D_1 = \pi^2 = R_s^2(\pi - \psi_1) + \left(\frac{m}{2} - y_s\right) \sqrt{R_s^2 - \left(\frac{m}{2} - y_s\right)^2}; \end{aligned} \quad (39.11)$$

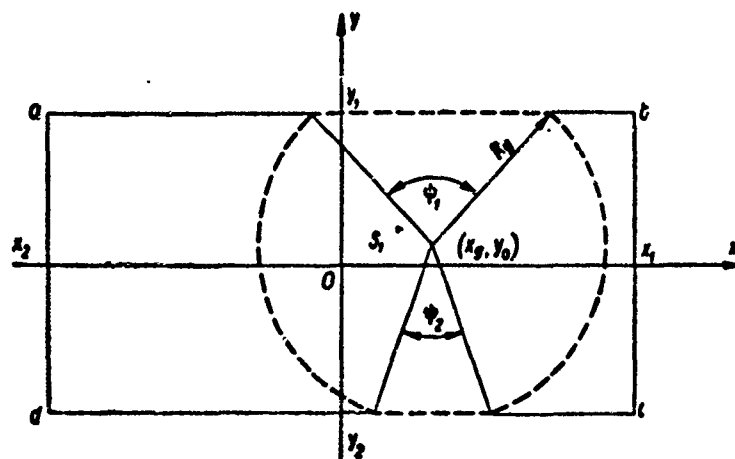


Fig. 72.

$$2) \quad R_g > y_0 + \frac{m}{2},$$

$$D_1 = m^2 = R_g^2 (\pi - \psi_1 - \psi_2) + \left(\frac{m}{2} - y_g \right) \sqrt{R_g^2 - \left(\frac{m}{2} - y_g \right)^2} + \left(y_g + \frac{m}{2} \right) \sqrt{R_g^2 - \left(y_g + \frac{m}{2} \right)^2}. \quad (39.12)$$

From Fig. 72 it is evident that

$$\psi_1 = \arccos \frac{\frac{m}{2} - y_g}{R_g}, \quad \psi_2 = \arccos \frac{y_g + \frac{m}{2}}{R_g}.$$

Substituting values for ψ_1 and ψ_2 , replacing R_g and y_g with their expressions (39.10), we obtain two equations for the determination of conductivity g

$$1) \quad \pi - \arccos \frac{\frac{m}{2} - y_0}{\sqrt{\frac{1}{4g^2} - z_0^2}} = \frac{m^2 - \left(\frac{m}{2} - y_0 \right) \sqrt{\frac{1}{4g^2} - z_0^2} - \left(\frac{m}{2} - y_0 \right)^2}{\frac{1}{4g^2} - z_0^2}, \quad (39.13)$$

$$\begin{aligned}
2) \quad & \pi - \arccos \frac{\frac{m}{2} - y_0}{\sqrt{\frac{1}{4g^2} - z_0^2}} - \arccos \frac{\frac{m}{2} + y_0}{\sqrt{\frac{1}{4g^2} - z_0^2}} = \\
& \frac{m^2 - \left(\frac{m}{2} - y_0\right) \sqrt{\frac{1}{4g^2} - z_0^2} - \left(\frac{m}{2} - y_0\right)^2 -}{- \left(\frac{m}{2} + y_0\right) \sqrt{\frac{1}{4g^2} - z_0^2} - \left(\frac{m}{2} + y_0\right)^2} = \\
& \frac{1}{4g^2 - z_0^2}.
\end{aligned} \tag{39.14}$$

Let us find boundaries of sections for which one should use one or another formula. Setting $R_g = \frac{m}{2} + y_0$ and substituting value in formula (39.13) we find the magnitude of $y_0 = y_{02}$, starting with which one should use formula (39.14). Disregarding form z_0^2 we obtain

$$\begin{aligned}
R_g = \frac{1}{2g} = \frac{m}{2} + y_{01}, \\
\pi - \arccos \frac{m - 2y_{01}}{m + 2y_{01}} = \frac{m^2 - \left(\frac{m}{2} - y_{01}\right) \sqrt{2y_{01}}}{\left(\frac{m}{2} + y_{01}\right)^2}.
\end{aligned}$$

The root of this equation will be $y_{01} = 0.095$ m, consequently for determination of conductivity g for $0 \leq y_0 \leq 0.095$ m one should use equation (39.14), for $0.095 \text{ m} \leq 0.5 \text{ m}$ - equation (39.13).

c) Derivation of equation (36.14) for the lower face of the model surface.

On this face

$$\gamma = \pi, \quad z_0 = -H, \quad x_g = x_0, \quad y_g = y_0, \quad R_g = \sqrt{\frac{H}{g} - H^2}. \tag{39.15}$$

As can be seen from Fig. 73 circumference $\varepsilon = g$ can occupy seven different positions relative rectangle D. Each of these positions corresponds to a defined form of equation (36.14). The area of application of each of the equations may be determined from a system of inequalities characterizing the position of circumference $\varepsilon = g$ in rectangle D. An approximate form of these regions is shown in Fig. 74. The digit on each region indicates the number of the equation. Below are presented inequalities characterizing the position of circumference

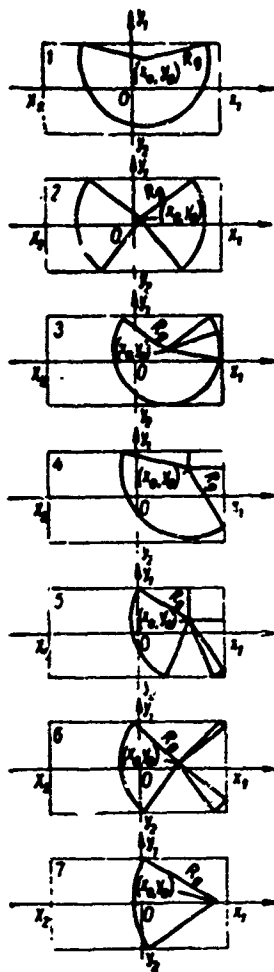


Fig. 73.

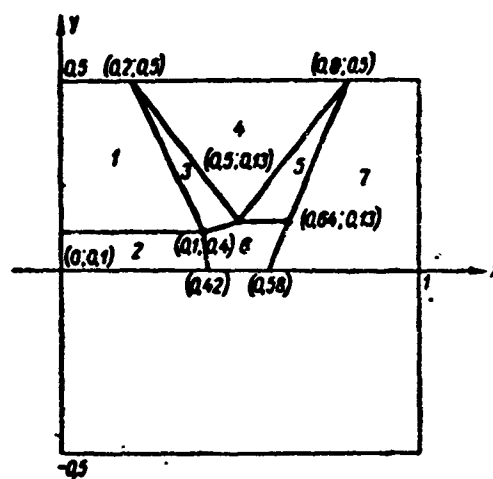


Fig. 74.

$\varepsilon = g$ and equations for each region of the fourth part of the lower face of the model

$$1) \quad R_g < m - x_0, \quad R_g < y_0 - \frac{m}{2}$$

$$m^2 = \left(\frac{H}{g} - H^2 \right) \left[\pi - \arctg \frac{\sqrt{\frac{H}{g} - H^2 - \left(\frac{m}{2} - y_0 \right)^2}}{\frac{m}{2} - y_0} \right] +$$

$$+ \left(\frac{m}{2} - y_0 \right) \sqrt{\frac{H}{g} - H^2 - \left(\frac{m}{2} - y_0 \right)^2}; \quad (39.16)$$

$$2) \quad y_0 + \frac{m}{2} < R_s < m - x_0$$

$$m^2 = \left(\frac{H}{g} - H^2 \right) \left[\pi - \operatorname{arctg} \frac{\sqrt{\frac{H}{g} - H^2 - \left(\frac{m}{2} - y_0 \right)^2}}{\frac{m}{2} - y_0} - \right. \\ \left. - \operatorname{arctg} \frac{\sqrt{\frac{H}{g} - H^2 - \left(\frac{m}{2} + y_0 \right)^2}}{\frac{m}{2} + y_0} \right] + \left(\frac{m}{2} - y_0 \right) \times \\ \times \sqrt{\frac{H}{g} - H^2 - \left(\frac{m}{2} - y_0 \right)^2} + \left(\frac{m}{2} + y_0 \right) \sqrt{\frac{H}{g} - H^2 - \left(\frac{m}{2} + y_0 \right)^2}; \quad (39.17)$$

$$3) \quad m - x_0 < R_s < y_0 + \frac{m}{2}, \quad R_s < \sqrt{(m - x_0)^2 + \left(\frac{m}{2} - y_0 \right)^2},$$

$$m^2 = \left(\frac{H}{g} - H^2 \right) \left[\pi - \operatorname{arctg} \frac{\sqrt{\frac{H}{g} - H^2 - \left(\frac{m}{2} - y_0 \right)^2}}{\frac{m}{2} - y_0} - \right. \\ \left. - \operatorname{arctg} \frac{\sqrt{\frac{H}{g} - H^2 - (m - x_0)^2}}{m - x_0} \right] + \\ + \left(\frac{m}{2} - y_0 \right) \sqrt{\frac{H}{g} - H^2 - \left(\frac{m}{2} - y_0 \right)^2} + \\ + (m - x_0) \sqrt{\frac{H}{g} - H^2 - (m - x_0)^2};$$

$$4) \quad (m - x_0)^2 + \left(\frac{m}{2} - y_0 \right)^2 < R_s^2 < \left(y_0 + \frac{m}{2} \right)^2$$

$$m^2 = \frac{1}{2} \left(\frac{H}{g} - H^2 \right) \left[\frac{3\pi}{2} - \operatorname{arctg} \frac{\sqrt{\frac{H}{g} - H^2 - (m - x_0)^2}}{m - x_0} - \right. \\ \left. - \operatorname{arctg} \frac{\sqrt{\frac{H}{g} - H^2 - \left(\frac{m}{2} - y_0 \right)^2}}{\frac{m}{2} - y_0} \right] + \\ + \frac{1}{2} \left(\frac{m}{2} - y_0 \right) \sqrt{\frac{H}{g} - H^2 - \left(\frac{m}{2} - y_0 \right)^2} + \\ + \frac{1}{2} (m - x_0) \sqrt{\frac{H}{g} - H^2 - (m - x_0)^2} + (m - x_0) \left(\frac{m}{2} - y_0 \right);$$

$$\begin{aligned}
5) \quad & (m-x_0)^2 + \left(\frac{m}{2} - y_0\right)^2 < R_z^2 < (m-x_0)^2 + \\
& + \left(y_0 + \frac{m}{2}\right)^2, \quad R_z > y_0 + \frac{m}{2}, \\
m^2 = & \frac{1}{2} \left(\frac{H}{g} - H^2\right) \left[\frac{3\pi}{2} - \operatorname{arctg} \frac{\sqrt{\frac{H}{g} - H^2 - \left(\frac{m}{2} - y_0\right)^2}}{\frac{m}{2} - y_0} - \right. \\
& - \operatorname{arctg} \frac{\sqrt{\frac{H}{g} - H^2 - (m-x_0)^2}}{m-x_0} - \\
& \left. - 2 \operatorname{arctg} \frac{\sqrt{\frac{H}{2} - H^2 - \left(\frac{m}{2} - y_0\right)^2}}{\frac{m}{2} + y_0} \right] + \\
& + \frac{1}{2} \left(\frac{m}{2} - y_0\right) \sqrt{\frac{H}{g} - H^2 - \left(\frac{m}{2} - y_0\right)^2} + \\
& + \frac{1}{2} (m-x_0) \sqrt{\frac{H}{2} - H^2 - (m-x_0)^2} + \\
& + \left(\frac{m}{2} + y_0\right) \sqrt{\frac{H}{g} - H^2 - \left(\frac{m}{2} + y_0\right)^2} + (m-x_0) \left(\frac{m}{2} - y_0\right);
\end{aligned}$$

$$\begin{aligned}
6) \quad & (m-x_0)^2 < R_z^2 < (m-x_0)^2 + \left(\frac{m}{2} - y_0\right)^2, \quad y_0 + \frac{m}{2} < R_z, \\
m^2 = & \left(\frac{H}{g} - H^2\right) \left[\pi - \operatorname{arctg} \frac{\sqrt{\frac{H}{g} - H^2 - \left(\frac{m}{2} - y_0\right)^2}}{\frac{m}{2} - y_0} - \right. \\
& - \operatorname{arctg} \frac{\sqrt{\frac{H}{g} - H^2 - \left(\frac{m}{2} + y_0\right)^2}}{\frac{m}{2} + y_0} - \\
& \left. - \operatorname{arctg} \frac{\sqrt{\frac{H}{g} - H^2 - (m-x_0)^2}}{m-x_0} \right] +
\end{aligned}$$

$$\begin{aligned}
& + \left(\frac{m}{2} - y_0 \right) \sqrt{\frac{H}{g} - H^2 - \left(\frac{m}{2} - y_0 \right)^2} + \\
& + \left(\frac{m}{2} + y_0 \right) \sqrt{\frac{H}{g} - H^2 - \left(\frac{m}{2} + y_0 \right)^2} + \\
& + (m - x_0) \sqrt{\frac{H}{g} - H^2 - (m - x_0)^2};
\end{aligned}$$

$$7) \quad (m - x_0)^2 + \left(y_0 + \frac{m}{2} \right)^2 < R_g^2$$

$$\begin{aligned}
m^2 = \frac{1}{2} \left(\frac{H}{g} - H^2 \right) & \left[\pi - \operatorname{arctg} \frac{\sqrt{\frac{H}{g} - H^2 - \left(\frac{m}{2} - y_0 \right)^2}}{\frac{m}{2} - y_0} - \right. \\
& \left. - \operatorname{arctg} \frac{\sqrt{\frac{H}{g} - H^2 - \left(\frac{m}{2} + y_0 \right)^2}}{\frac{m}{2} + y_0} \right] + \\
& + \left(\frac{m}{2} - y_0 \right) \sqrt{\frac{H}{g} - H^2 - \left(\frac{m}{2} - y_0 \right)^2} + \\
& + \left(\frac{m}{2} + y_0 \right) \sqrt{\frac{H}{g} - H^2 - \left(\frac{m}{2} + y_0 \right)^2} + m(m - x_0).
\end{aligned}$$

Calculation is carried out as follows: coordinates of point x_0, y_0 are and according to Fig. 74 determine the number of the equation which one should use; substitute in this equation the coordinates x_0, y_0 and find the value of g which satisfies it.

§ 40. Models for Calculation of Space Fields

Let us consider two models of element of unlimited space of simple form. Let us assume that the first element D constitutes a sphere of radius r . Let us

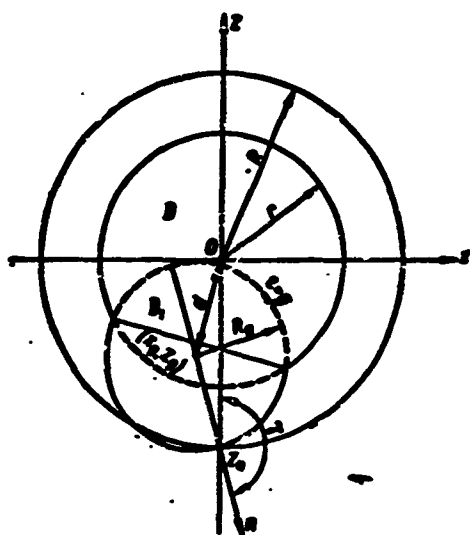


Fig. 75.

construct a model of element D ensuring in D an expedient minimum of mean value of modulus of potential of distortion φ_2 , in other words let us find the form of the border of model S and distribution of conductivity g on it from the condition of minimum of integral Q . From symmetry of region D it follows that conductivity g depends only on distance from point (x_0, y_0, z_0) to the center of the sphere. Let us place the origin of coordinates at the center of sphere D and direct axis oz in the direction of the segment connecting point (x_0, y_0, z_0) with the center of sphere D. Here $x_0 = y_0 = 0$. Let us

direct axis ox in such a manner that it passes through the projection of normal n onto plane xoy , i.e., we set angle θ equal to zero (Fig. 75). As follows from § 30, the minimum of integral Q with respect to parameter g will occur under the condition that sphere $\varepsilon = g$ divides the volume of sphere D into two equal parts D_1 and $D - D_1$. Let us compose equation (30.14), using this condition. In general $|z_0| > r$ and region D_1 constitutes two spherical segments having a common base (Fig. 75). Let us designate h_k and h_r the heights of the segments, q the distance between centers of sphere D and sphere $\varepsilon = g$ of radius $R_g = \frac{1}{2g}$. Let us express the volume of region D_1 , in terms of radii r and R_g and distance d . We have

$$q = \sqrt{R_g^2 - (r - h_r - d)^2} = \sqrt{r^2 - (r - h_r)^2},$$

hence

$$h_r = \frac{R_g^2 - (r - d)^2}{2d}, \quad h_r + R + r - d - h_r = \frac{r^2 - (R_g - d)^2}{2d}.$$

The volumes of the segments are

$$V_R = \frac{1}{3} \pi h^2 (3R_g - h_R) = \frac{\pi}{24d^3} (R_g^3 - r^3 + d^3 - 3R_g^2 r^2 + 3R_g^2 r^4 + 3r^4 d^2 - 3r^4 d^4 - 9R_g^2 d^2 - 9R_g^2 d^4 + 16R_g^2 d^3 + 6R_g^2 r^2 d^3); \quad (40.1)$$

$$V_r = \frac{1}{3} \pi h^2 (3r - h_r) = \frac{\pi}{24d^3} (r^3 - R_g^3 + d^3 - 3r^2 R_g^2 + 3r^2 R_g^4 + 3R_g^2 d^2 - 3R_g^2 d^4 - 9r^2 d^2 - 9r^2 d^4 + 16r^2 d^3 + 6r^2 R_g^2 d^3). \quad (40.2)$$

The volume of region D_1

$$V = V_R + V_r = \pi \left[\frac{d^3}{12} - \frac{(R_g^3 - r^3)}{4d} - \frac{d}{2} (R_g^2 + r^2) + \frac{2}{3} (R_g^3 + r^3) \right]. \quad (40.3)$$

Expressing distance d in terms of coordinates of the center of the sphere $\varepsilon = g$ and its radius

$$\begin{aligned} R_g &= \frac{1}{2g}, \quad x_g = -\frac{\sin \gamma}{2g} = -R_g \sin \gamma, \\ y_g &= 0, \quad z_g = z_0 - \frac{\cos \gamma}{2g} = z_0 - R_g \cos \gamma, \\ d &= \sqrt{z_g^2 + x_g^2} = \sqrt{z_0^2 - 2z_0 R_g \cos \gamma + R_g^2} \end{aligned}$$

and equating the volume of region D_1 to half the volume of sphere D , we obtain

$$\frac{2}{3} \pi r^3 = \pi \left[\frac{d^3}{12} - \frac{(R_g^3 - r^3)}{4d} - \frac{d}{2} (R_g^2 + r^2) + \frac{2}{3} (R_g^3 + r^3) \right]. \quad (40.4)$$

Substituting for d and R_g we obtain

$$\begin{aligned} Q(z_0, \gamma, g) &= \left(z_0^2 - \frac{2z_0}{g} \cos \gamma + \frac{1}{4g^2} \right)^3 - \\ &- 6 \left(z_0^2 - \frac{2z_0}{g} \cos \gamma + \frac{1}{4g^2} \right) \left(\frac{1}{4g^2} + r^2 \right) + \\ &+ \frac{1}{g^2} \sqrt{z_0^2 - \frac{2z_0}{g} \cos \gamma + \frac{1}{4g^2}} - 3 \left(\frac{1}{4g^2} - r^2 \right)^2 = 0. \end{aligned} \quad (40.5)$$

Let us show what the minimum of integral Q with respect to γ will be for $\gamma = \pi$.

For this it is sufficient to show that following are fulfilled conditions:

$$\left. \frac{\partial Q}{\partial \gamma} \right|_{\gamma=\pi} = 0, \quad \left. \frac{\partial^2 Q}{\partial \gamma^2} \right|_{\gamma=\pi} > 0. \quad (40.6)$$

Assuming $\gamma = \pi$ in Equation (40.5) and considering that here $d = -(z_0 + R_2)$, we obtain

$$\begin{aligned} \left(z_0 + \frac{1}{2g}\right)^4 - 6\left(z_0 + \frac{1}{2g}\right)^2 \left(\frac{1}{4g^2} + r^2\right) - \\ - \frac{1}{g^2} \left(\frac{1}{2g} + z_0\right) - 3\left(\frac{1}{4g^2} - r^2\right)^2 = 0, \end{aligned} \quad (40.7)$$

or after transformations

$$\alpha^4 - 2v\alpha^2 - 2v(3 - v^2)\alpha + 3 + 6v^2 - v^4 = 0. \quad (40.8)$$

Here is designated $\alpha = \frac{1}{gr}$ and $z_0 = -vr$ ($v > 1$). The sought value of α at which sphere $\epsilon = g$ divides sphere D into two equal parts falls in the interval

$$v + \frac{1}{2v} < \alpha < v + \frac{1}{2v} + \frac{1}{11v^3}. \quad (40.9)$$

Indeed, composing for equation (40.8) the series of Sturm functions

$$\begin{aligned} f(\alpha) &= \alpha^4 - 2v\alpha^2 - 2v(3 - v^2)\alpha + 3 + 6v^2 - v^4, \\ \frac{1}{2}f'(\alpha) &= 2\alpha^2 - 3v\alpha^2 - 3v + v^2, \\ f_1(\alpha) &= v^2\alpha^2 - 2(v^2 - 3)v\alpha - 4 - 7v^2 + v^4, \\ f_2(\alpha) &= v(v^2 - 5)\alpha - v^4 + 5v^2 + 3, \\ f_3(\alpha) &= v^4 - 6v^2 + 3, \end{aligned} \quad (40.10)$$

and substituting in it instead of α the values $\alpha_1 = v + \frac{1}{2v}$ and $\alpha_2 = v + \frac{1}{2v} + \frac{1}{11v^3}$, we are persuaded that in the interval $\left[v + \frac{1}{2v}, v + \frac{1}{2v} + \frac{1}{11v^3}\right]$ the number of sign changes in the series of Sturm functions is changed in units

$$\begin{aligned} f(\alpha_2) &= \left(v + \frac{1}{2v}\right)^4 - 2v\left(v + \frac{1}{2v}\right)^2 - 2v(3 - v^2)\left(v + \frac{1}{2v}\right) + 3 + 6v^2 - \\ &\quad - v^4 = \frac{1}{16v^4} + \frac{1}{4v^2} > 0, \\ \frac{1}{2}f'(\alpha_2) &= 2\left(v + \frac{1}{2v}\right)^2 - 3v\left(v + \frac{1}{2v}\right)^2 - 3v + v^2 = \\ &\quad = \frac{1}{4v^3} + \frac{3}{4v} - 3v < 0, \end{aligned}$$

$$f_1(a_1) = v^3 \left(v + \frac{1}{2v} \right)^2 - 2(v^2 - 3)v \left(v + \frac{1}{2v} \right) - \\ - 4 - 7v^2 + v^4 = -\frac{3}{4} - v^2 < 0.$$

$$f_2(a_1) = v(v^2 - 5) \left(v + \frac{1}{2v} \right) - v^4 + 5v^2 + 3 = \frac{v^3}{2} + \frac{1}{2} > 0.$$

$$f_3(a_1) = v^4 - 6v^2 + 3 < 0, \quad \text{if } v < 2.34, \text{ and } f_3(a_1) > 0, \\ \text{if } v > 2.34$$

(there are three changes of sign if $v < 2.34$, or two if $v > 2.34$);

$$f(a_2) = \left(v + \frac{1}{2v} + \frac{1}{11v^2} \right)^4 - 2v \left(v + \frac{1}{2v} + \frac{1}{11v^2} \right)^3 - \\ - 2v(3 - v^2) \left(v + \frac{1}{2v} + \frac{1}{11v^2} \right) + 3 + 6v^2 - v^4 = \\ = -\frac{13}{44v^2} + \frac{79}{352v^4} + \frac{17}{242v^6} + \frac{37}{2662v^8} + \frac{2}{11^2v^{10}} + \frac{1}{11^2v^{12}} > 0,$$

$$\frac{1}{2}f'(a_2) = 2 \left(v + \frac{1}{2v} + \frac{1}{11v^2} \right)^3 - 3v \left(v + \frac{1}{2v} + \frac{1}{11v^2} \right)^2 - \\ - 3v + v^3 = -3v + \frac{3}{4v} + \frac{23}{44v^3} + \frac{39}{42v^5} + \frac{1}{242v^7} + \frac{1}{11^2v^9} < 0,$$

$$f_1(a_2) = v^3 \left(v + \frac{1}{2v} + \frac{1}{11v^2} \right)^2 - 2v(v^2 - 3) \left(v + \frac{1}{2v} + \frac{1}{11v^2} \right) - \\ - 4 - 7v^2 + v^4 = -v^2 - \frac{3}{4} + \frac{7}{11v^2} + \frac{1}{121v^4} < 0,$$

$$f_2(a_2) = v(v^2 - 5) \left(v + \frac{1}{2v} + \frac{1}{11v^2} \right) - v^4 + 5v^2 + 3 = \\ = \frac{v^3}{2} + \frac{13}{22} - \frac{5}{11v^2} > 0,$$

$$f_3(a_2) = v^4 - 6v^2 + 3 < 0, \quad \text{if } v < 2.34, \text{ and } f_3(a_2) > 0, \\ \text{if } v > 2.34$$

(there are two changes of sign if $v < 2.34$, or one if $v > 2.34$).

Consequently, in interval $\left[v + \frac{1}{2v}, v + \frac{1}{2v} + \frac{1}{11v^2} \right]$ there is one root of equation (40.8).

Sitting in Equations (36.20) $\theta = 0$, $y = 0$, $y_0 = 0$, $x_0 = 0$, we find

$$\frac{\partial \Phi}{\partial v} = 2g \frac{\partial \Phi}{\partial g} \cdot \frac{\partial g}{\partial v} + \cos \gamma \int_b^x \frac{x}{r^2} dv - \sin \gamma \int_b^z \frac{z - z_0}{r^2} dv. \quad (40.11)$$

Considering that due to symmetry

$$\int_D \frac{x}{r^3} dv = 0 \quad (40.12)$$

for $\gamma = \pi$ we obtain

$$\left. \frac{\partial Q}{\partial \gamma} \right|_{\gamma=\pi} = 2g \left. \frac{\partial \Phi}{\partial g} \right|_{\gamma=\pi} \cdot \left. \frac{\partial g}{\partial \gamma} \right|_{\gamma=\pi}. \quad (40.13)$$

But

$$\frac{\partial g}{\partial \gamma} = -\frac{\Phi'_\gamma}{\Phi'_g} = -\frac{\frac{\partial \Phi}{\partial \gamma}}{\frac{\partial \Phi}{\partial g}} \quad \text{and} \quad \left. \frac{\partial g}{\partial \gamma} \right|_{\gamma=\pi} = 0. \quad (40.14)$$

since

$$\begin{aligned} \Phi'_\gamma|_{\gamma=\pi} = & \left[2 \left(z_0^2 - \frac{z_0}{g} \cos \gamma + \frac{1}{4g^2} \right) \frac{z_0}{g} \sin \gamma - 6 \left(\frac{1}{4g^2} + r^2 \right) \frac{z_0}{g} \sin \gamma + \right. \\ & \left. + \frac{z_0}{2g^2} \frac{\sin \gamma}{\sqrt{z_0^2 - \frac{z_0}{g} \cos \gamma + \frac{1}{4g^2}}} \right]_{\gamma=\pi} = 0. \end{aligned}$$

Consequently at $\gamma = \pi$ $\frac{\partial Q}{\partial \gamma} = 0$, i.e., integral Q attains an extremum.

Let us write the second derivative of Q with respect to γ

$$\begin{aligned} \frac{\partial^2 Q}{\partial \gamma^2} = & 2 \frac{\partial \Phi}{\partial g} \left(\frac{\partial g}{\partial \gamma} \right)^2 + 2g \left(\frac{\partial g}{\partial \gamma} \right)^2 \frac{\partial^2 \Phi}{\partial g^2} + \\ & + 2g \frac{\partial \Phi}{\partial g} \frac{\partial^2 g}{\partial \gamma^2} - \sin \gamma \int_D \frac{x}{r^3} dv - \cos \gamma \int_D \frac{z - z_0}{r^3} dv. \end{aligned} \quad (40.15)$$

Setting $\gamma = \pi$, we obtain

$$\left. \frac{\partial^2 Q}{\partial \gamma^2} \right|_{\gamma=\pi} = 2g \left. \frac{\partial \Phi}{\partial g} \right|_{\gamma=\pi} \left. \frac{\partial^2 g}{\partial \gamma^2} \right|_{\gamma=\pi} + \int_D \frac{z - z_0}{r^3} dv. \quad (40.16)$$

But

$$\left. \frac{\partial^2 g}{\partial \gamma^2} \right|_{\gamma=\pi} = \frac{2\Phi'_\gamma \Phi'_g \Phi''_{\gamma\gamma} - (\Phi'_g)^2 \Phi''_{\gamma\gamma} - (\Phi'_\gamma)^2 \Phi''_{gg}}{(\Phi'_g)^3} \Big|_{\gamma=\pi} = -\frac{\Phi''_{\gamma\gamma}}{\Phi'_g} \Big|_{\gamma=\pi} \quad (40.17)$$

and

$$\begin{aligned} \frac{\partial^2 Q}{\partial \gamma^2} \Big|_{\gamma=\pi} &= 2g \Phi_{\gamma} \left(-\frac{\Phi_{\gamma\gamma}}{\Phi_{\gamma}} \right) \Big|_{\gamma=\pi} + \\ &+ \int_b^{\pi} \frac{z-z_0}{r^2} dv = -2g \Phi_{\gamma\gamma} \Big|_{\gamma=\pi} + \int_b^{\pi} \frac{z-z_0}{r^2} dv. \end{aligned} \quad (40.18)$$

The value of derivative $\Phi_{\gamma\gamma}|_{\gamma=\pi}$ equals

$$\begin{aligned} \Phi_{\gamma\gamma}|_{\gamma=\pi} &= \left[2 \frac{z_0^2}{r^2} \sin^2 \gamma + 2 \left(z_0^2 - \frac{z_0}{g} \cos \gamma + \frac{1}{4g^2} \right) \frac{z_0}{g} \cos \gamma - \right. \\ &- 6 \left(\frac{1}{4g^2} + r^2 \right) \frac{z_0}{g} \cos \gamma + \frac{z_0}{2g^2} \frac{\cos \gamma}{\sqrt{z_0^2 - \frac{z_0}{g} \cos \gamma + \frac{1}{4g^2}}} - \\ &\left. - \frac{z_0^2}{4g^2} \left(z_0^2 - \frac{z_0}{g} \cos \gamma + \frac{1}{4g^2} \right)^{-\frac{3}{2}} \sin^2 \gamma \right]_{\gamma=\pi} = \\ &= -2 \frac{z_0}{g} \frac{2g^2 z_0 (z_0^2 - 3r^2) + 3g^2 (z_0^2 - r^2) - 1}{g^2 (2gz_0 + 1)} = \\ &= 2v \frac{r^2}{g} \frac{2v(3-v^2) + 3(v^2-1)a - a^2}{a-2v}. \end{aligned} \quad (40.19)$$

Putting here the value for α , we find

$$\Phi_{\gamma\gamma}|_{\gamma=\pi} < 0. \quad (40.20)$$

Considering that $\int_b^{\pi} \frac{z-z_0}{r^2} dv > 0$, we obtain

$$\frac{\partial^2 Q}{\partial \gamma^2} \Big|_{\gamma=\pi} > 0. \quad (40.21)$$

Consequently, at $\gamma = \pi$ integral Q attains a minimum. Thus the normal \bar{n} to border of model S at point $(0,0, z_0)$ is directed along the radius of sphere D . Inasmuch as point (x_0, y_0, z_0) was taken arbitrarily, surface S should have the form of a sphere concentrically enclosing sphere D . Conductivity g of sphere S is constant and equal to a smaller positive root of equation (40.8). Its value can be estimated from inequality (40.9)

$$v + \frac{1}{2v} < \frac{1}{gr} < v + \frac{1}{2v} + \frac{1}{11v^2}. \quad (40.22)$$

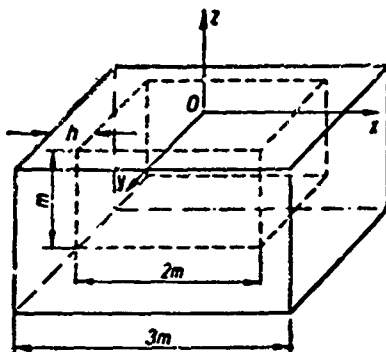


Fig. 76.

The radius of the sphere $S - R = |z_0| = vr$. Placing this value in (40.22), we find

$$\frac{1}{R\left(1 + \frac{1}{2v^2}\right)} > g > \frac{1}{R\left(1 + \frac{1}{2v^2} + \frac{1}{11v^4}\right)}. \quad (40.23)$$

Let us consider model of element D constituting a cube with side 2 m. In this case the problem of determination of the form of the border of model S from conditions of minimum of integral Q with respect to parameters γ and θ is extraordinarily complicated. Therefore, we will assign the form of border S selecting it in the form of the surface of a cube with faces removed from faces of cube D by a distance h. We will seek the distribution of conductivity g on surface S from the conditions of minimum of integral Q only with respect to parameter g. Each face of surface S is symmetric with respect to cube D and in turn has four axes of symmetry. It is therefore sufficient to calculate conductivity for any face on one eighths of its part inconcluded between two neighboring axes of symmetry (Fig. 76).

Let us combine the origin of coordinates with the center of the cube and direct the axes of coordinates parallel to its edges. Inasmuch as the form of border of model S was selected by us, then thereby are determined the angles between the normal to S at each point (x_0, y_0, z_0) and the coordinates axes. Therefore, conductivity g will be function only of coordinates (x_0, y_0, z_0) . As follows from § 36, the minimum of integral Q with respect to parameter g will occur under the condition that the sphere on which $\varepsilon = g$ divides volume of cube D into two equal parts. Using this condition it is possible to compose equation (36.14) for

determination of g at each point of the face of surface S . However in this case form of equation (36.14) becomes different for different sections of the surfaces of the face. For definitiveness we will examine the lower bound of surface S . Spheres $\epsilon = g$ touch on it in points (x_0, y_0, z_0) , radii of the spheres

$$R_\epsilon = \frac{1}{2g}.$$

Thus, calculation of conductivity g at point (x_0, y_0, z_0) leads to determination of the radius of a sphere tangent to the face of surface S in this point and evenly dividing the volume of the cube D .

Center of sphere $\epsilon = g$ of minimum radius obviously will lie on axis oz . Let us find the radius of this sphere. Let us assume that the sphere intersects only one lower bound of cube D . Volume D_1 , cut by it in cube D will constitute the volume of a sphere without segment by height h . Equating it to half the volume of the cube we obtain

$$V_{D_1} = V_D - V_\epsilon = \frac{4}{3} \pi R_\epsilon^3 - \frac{1}{3} \pi h^2 (3R_\epsilon - h) = 4m^3. \quad (40.24)$$

Let us take clearance h between cube faces D and bound of model S such:

$$h = \frac{m}{2}.$$

Equation (40.24) will take the form

$$R_\epsilon^3 - \frac{3}{16} m^2 R_\epsilon - \left(\frac{3}{8} - \frac{1}{32} \right) m^3 = 0. \quad (40.25)$$

Solving this equation we find that $R_\epsilon = 1.038 m > m$, i.e., sphere $\epsilon = g$ necessarily intersects the lateral faces of cube D also. Consequently, minimum radius $R_\epsilon > 1.038 m$ and sphere $\epsilon = g$ will intersect, besides lower, also at least two adjacent lateral faces of cube D . In general border of region D_1 will consist of sections of faces of cube D and part of sphere $\epsilon = g$ therefore, volume D_1 , equal to half the volume of the cube D , can be presented in the form of algebraic sum of spherical volumes bounded by sphere $\epsilon = g$, spherical segments and parts of spherical segments cut from the sphere by two or three mutually perpendicular planes. In Fig. 77 are represented diverse variants of intersection of sphere

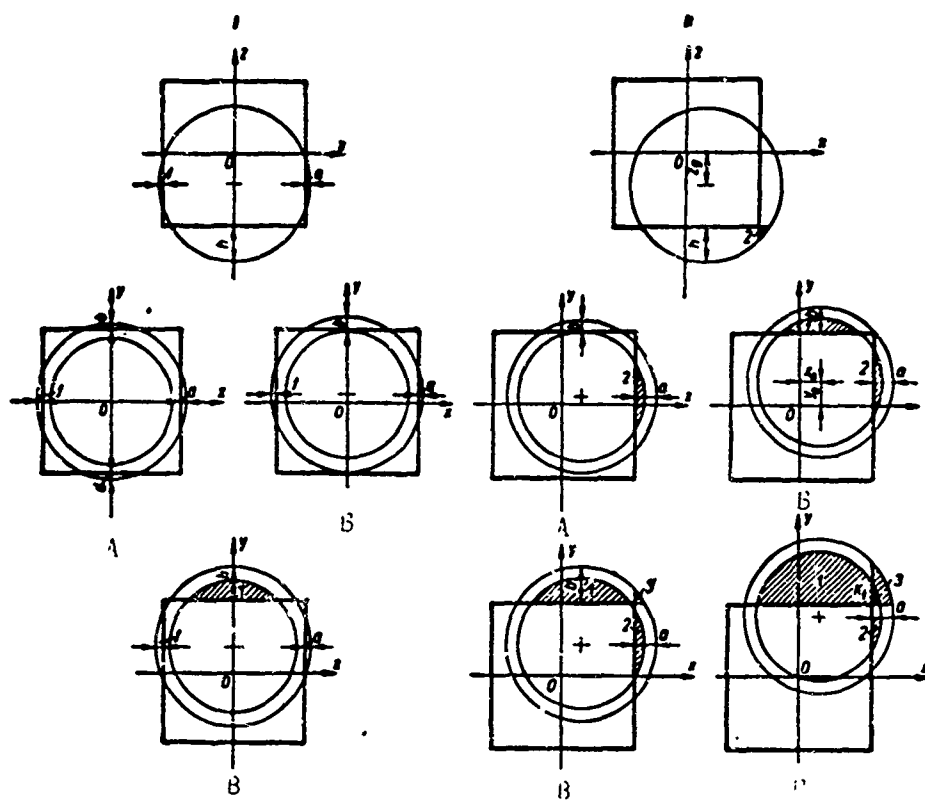


Fig. 77 (I-II).

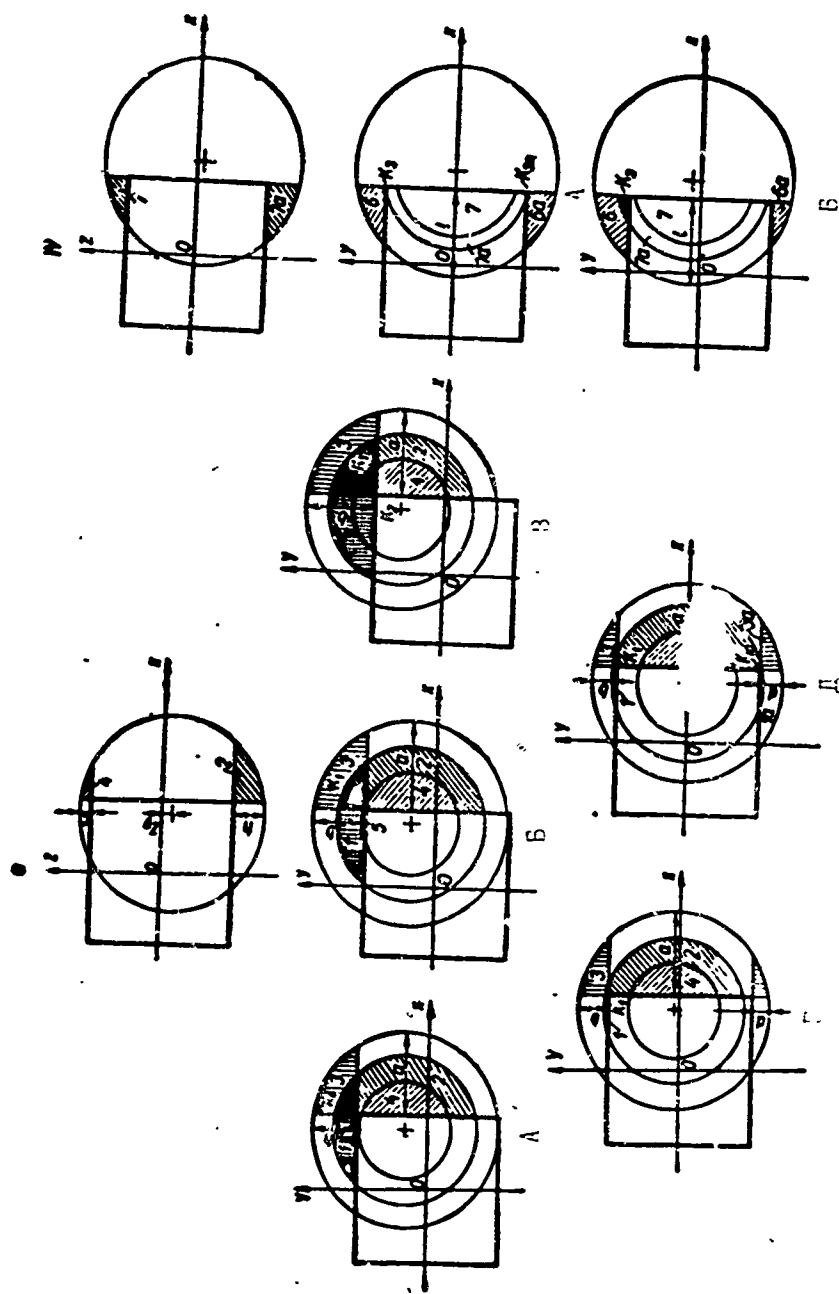


Fig. 77 (III-IV).

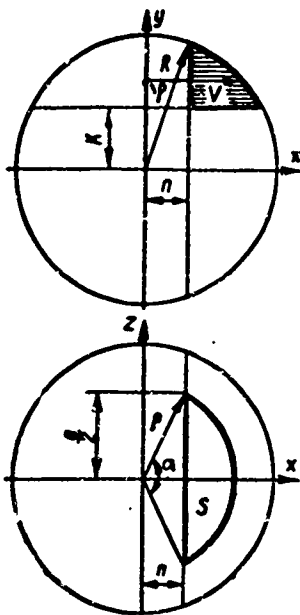


Fig. 78.

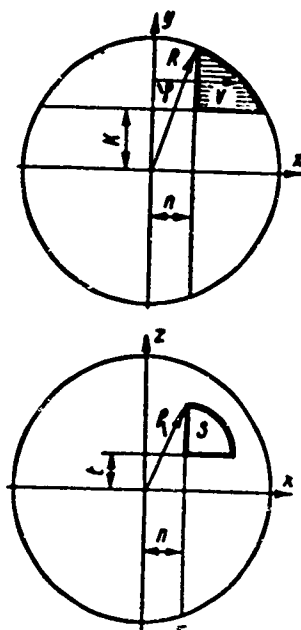


Fig. 79.

the radius of the sphere R_g . Analogously are composed equations for all the remaining variants. Each of volumes V_c , V_n and V_x can be expressed in terms of the radius R_g of the sphere, the length of a cube edge $2m$ and coordinates of the point of contact of the sphere with a face of surface S (x_0, y_0, z_0)

$$V_x = \frac{1}{3} \pi a^2 (3R_g - a). \quad (40.27)$$

For calculation of volumes of different segments in formula (40.27) one should substitute different values of height a in accordance with Table 17.

Table 17.

V_{ac}	$a = R_g - m + x_0$	V_{dc}	$a = R_g - m - y_0$
V_{hc}	$a = h = \frac{m}{2}$	V_{cc}	$a = 2R_g - 2.5m$
V_{ic}	$a = R_g - m - x_0$	V_{ec}	$a = R_g - x_0 - m$
V_{xc}	$a = R_g - m + y_0$		

Let us derive a formula for the volume of part of spherical segment II (Fig. 78). Volume V_{II} we present in the form of the sum of elementary volumes $S(y)dy$, included between two planes parallel to the base of the segment and passing through points with coordinates y and $y + dy$.

$$V_{II} = \int_k^{\sqrt{R_g^2 - n^2}} S(y) dy. \quad (40.28)$$

Here k and n are distances from the center of the sphere to cube faces

$$S(y) = \frac{q^2}{2} \alpha - n \sqrt{q^2 - n^2} = (R_g^2 - y^2) \operatorname{arctg} \sqrt{\frac{R_g^2 - y^2}{n^2}} - 1 - n \sqrt{R_g^2 - n^2 - y^2}. \quad (40.29)$$

Placing this value of $S(y)$ in formula (40.28) we obtain

$$\begin{aligned} V_{II} &= \int_k^{\sqrt{R_g^2 - n^2}} (R_g^2 - y^2) \operatorname{arctg} \sqrt{\frac{R_g^2 - y^2}{n^2}} - 1 dy \\ &\quad - n \int_k^{\sqrt{R_g^2 - n^2}} \sqrt{R_g^2 - y^2 - n^2} dy = \\ &= \left[y \left(R_g^2 - \frac{y^2}{3} \right) \operatorname{arctg} \frac{\sqrt{R_g^2 - n^2 - y^2}}{n} - \frac{2ny \sqrt{R_g^2 - n^2 - y^2}}{3} + \right. \\ &\quad \left. + \frac{2}{3} R_g^3 \operatorname{arctg} \frac{ny}{R_g \sqrt{R_g^2 - n^2 - y^2}} - \right. \\ &\quad \left. - n \left(R_g^2 - \frac{n^2}{3} \right) \arcsin \frac{y}{\sqrt{R_g^2 - n^2}} \right]_k^{\sqrt{R_g^2 - n^2}} = \\ &= \frac{2}{3} R_g^3 \operatorname{arctg} \frac{R_g \sqrt{R_g^2 - n^2 - k^2}}{nk} - \\ &\quad - k \left(R_g^2 - \frac{k^2}{3} \right) \operatorname{arctg} \frac{\sqrt{R_g^2 - k^2 - n^2}}{n} - \\ &\quad - n \left(R_g^2 - \frac{n^2}{3} \right) \operatorname{arctg} \frac{\sqrt{R_g^2 - n^2 - k^2}}{k} + \\ &\quad + \frac{2nk \sqrt{R_g^2 - n^2 - k^2}}{3}. \end{aligned} \quad (40.30)$$

Table 18.

K	t	k	n	\mathcal{N}	k	n	\mathcal{N}	k	n
K_1	$m - y_0$	$R_g - 0.5 m$	$m - x_0$	\mathcal{N}_9	$2.5 m - R_g$	$x_0 - m$	\mathcal{N}_9	$m - y_0$	$m - x_0$
K_2	$m - y_0$	$2.5 m - R_g$	$m - x_0$	\mathcal{N}_{10}	$R_g - 0.5 m$	$x_0 - m$	\mathcal{N}_{10}	$m + y_0$	$m - x_0$
K_3	$m - y_0$	$0.5 m$	$x_0 - m$	\mathcal{N}_8	$y_0 - m$	$x_0 - m$	\mathcal{N}_8	$2.5 m - R_g$	$m - x_0$
K_{3a}	$m + y_0$	$R_g - 0.5 m$	$x_0 - m$	\mathcal{N}_1	$R_g - 0.5 m$	$m - y_0$	\mathcal{N}_1	$2.5 m - R_g$	$m - y_0$
K_4	$m - y_0$	$2.5 m - R_g$	$x_0 - m$	\mathcal{N}_{11}	$R_g - 0.5 m$	$m + y_0$	\mathcal{N}_8	$m - y_0$	$x_0 - m$
K_{4a}	$m + y_0$	$2.5 m - R_g$	$x_0 - m$	\mathcal{N}_8	$R_g - 0.5 m$	$m - x_0$	\mathcal{N}_{10a}	$m + y_0$	$x_0 - m$

Analogously it is possible to derive a formula for the volume of K (Fig. 79).

It has the form

$$\begin{aligned}
 V_K = & \frac{R_g^3}{3} \left(\operatorname{arctg} \frac{R_g \sqrt{R_g^2 - n^2 - k^2}}{kn} + \operatorname{arctg} \frac{R_g \sqrt{R_g^2 - k^2 - t^2}}{tk} + \right. \\
 & \left. + \operatorname{arctg} \frac{R_g \sqrt{R_g^2 - t^2 - n^2}}{nt} - \pi \right) - \\
 & - \frac{t}{2} \left(R_g^2 - \frac{t^2}{3} \right) \left(\operatorname{arctg} \frac{\sqrt{R_g^2 - t^2 - k^2}}{k} + \operatorname{arctg} \frac{\sqrt{R_g^2 - t^2 - n^2}}{n} \right) - \\
 & - \frac{k}{2} \left(R_g^2 - \frac{k^2}{3} \right) \left(\operatorname{arctg} \frac{\sqrt{R_g^2 - k^2 - n^2}}{n} + \operatorname{arctg} \frac{\sqrt{R_g^2 - k^2 - t^2}}{t} \right) - \\
 & - \frac{n}{2} \left(R_g^2 - \frac{n^2}{3} \right) \left(\operatorname{arctg} \frac{\sqrt{R_g^2 - n^2 - t^2}}{t} + \operatorname{arctg} \frac{\sqrt{R_g^2 - n^2 - k^2}}{k} \right) + \\
 & + \frac{nk}{3} \sqrt{R_g^2 - n^2 - k^2} + \frac{tn}{3} \sqrt{R_g^2 - t^2 - n^2} + \\
 & + \frac{kt}{3} \sqrt{R_g^2 - k^2 - t^2} + \frac{\pi}{4} R_g^2 (t + k + n) - \frac{\pi}{12} (t^3 + k^3 + n^3). \quad (40.31)
 \end{aligned}$$

For calculation of volumes of different parts J and K in formulas (40.30) and (40.31) one should substitute different values of parameters t , k and n in accordance with Table 18.

It should be remembered that formulas (40.30) and (40.31) determine the smallest volumes J or K cut from the sphere by two or three orthogonal intersecting planes respectively. Below are given equations for different cases of intersection of cube D by sphere $\varepsilon = g$ with indication of conditions during fulfillment of which these equations have meaning. Numbers of the equations correspond to the numbers in Fig. 77. It is assumed that $x_0 > 0$ and $y_0 > 0$:

I

$$\begin{aligned}
 A \quad V_{\square} - V_{bc} - V_{ac} - V_{tc} - V_{bc} - V_{dc} &= 4m^3, \\
 m + x_0 < R_g, \quad \sqrt{(m - x_0)^2 + (R_g - 0.5m)^2} &> R_g, \\
 m + y_0 < R_g, \quad \sqrt{(m - y_0)^2 + (R_g - 0.5m)^2} &> R_g, \\
 2m + h &> 2R_g;
 \end{aligned} \quad (40.32)$$

$$\begin{aligned}
\text{B. } & V_w - V_{hc} - V_{ac} - V_{lc} - V_{bc} = 4m^2, \\
& m + x_0 < R_g, \quad \sqrt{(m - x_0)^2 + (R_g - 0,5m)^2} > R_g, \\
& m + y_0 > R_g, \quad \sqrt{(m - y_0)^2 + (R_g - 0,5m)^2} > R_g, \\
& m - y_0 < R_g, \\
& 2m + h > 2R_g;
\end{aligned} \tag{40.33}$$

$$\begin{aligned}
\text{B. } & V_w - V_{hc} - V_{ac} - V_{bc} - V_{lc} + V_{al} = 4m^2, \\
& m + x_0 < R_g, \quad \sqrt{(m - x_0)^2 + (R_g - 0,5m)^2} > R_g, \\
& m + y_0 > R_g, \quad \sqrt{(m - y_0)^2 + (R_g - 0,5m)^2} < R_g, \\
& 2m + h > 2R_g;
\end{aligned} \tag{40.34}$$

II

$$\begin{aligned}
\text{A. } & V_w - V_{hc} - V_{ac} - V_{bc} + V_{a2} = 4m^2, \\
& m + x_0 > R_g, \quad \sqrt{(m - x_0)^2 + (R_g - 0,5m)^2} < R_g, \\
& m + y_0 > R_g, \quad \sqrt{(m - y_0)^2 + (R_g - 0,5m)^2} > R_g, \\
& m - y_0 < R_g, \quad 2m + h > 2R_g;
\end{aligned} \tag{40.35}$$

$$\begin{aligned}
\text{B. } & V_w - V_{hc} - V_{ac} - V_{bc} + V_{a1} + V_{a2} = 4m^2, \\
& m + x_0 > R_g, \quad \sqrt{(m - x_0)^2 + (R_g - 0,5m)^2} < R_g, \\
& m + y_0 > R_g, \quad \sqrt{(m - y_0)^2 + (R_g - 0,5m)^2} < R_g, \\
& 2m + h > 2R_g, \quad \sqrt{(m - x_0)^2 + (m - y_0)^2} > R_g;
\end{aligned} \tag{40.36}$$

$$\begin{aligned}
\text{B. } & V_w - V_{hc} - V_{ac} - V_{bc} + V_{a1} + V_{a2} + V_{a3} = 4m^2, \\
& m + x_0 > R_g, \quad \sqrt{(m - x_0)^2 + (R_g - 0,5m)^2} < R_g, \quad 2m + h > 2R_g, \\
& m + y_0 > R_g, \quad \sqrt{(m - y_0)^2 + (R_g - 0,5m)^2} < R_g, \\
& \sqrt{(m - x_0)^2 + (m - y_0)^2} < R_g, \quad \sqrt{(m - x_0)^2 + (m - y_0)^2 + (R_g - 0,5m)^2} > R_g;
\end{aligned} \tag{40.37}$$

$$\begin{aligned}
\text{Г. } & V_w - V_{hc} - V_{ac} - V_{bc} + V_{a1} + V_{a2} + V_{a3} - V_{k1} = 4m^2, \\
& m + x_0 > R_g, \quad \sqrt{(m - x_0)^2 + (m - y_0)^2 + (R_g - 0,5m)^2} < R_g, \\
& m + y_0 > R_g, \quad 2m + h > 2R_g;
\end{aligned} \tag{40.38}$$

III

$$\begin{aligned}
\text{A. } & V_w - V_{hc} - V_{ac} - V_{bc} - V_{ac} + V_{a1} + V_{a2} + V_{a3} + V_{a4} - V_{k1} = 4m^2, \\
& m + x_0 > R_g, \quad \sqrt{(m - x_0)^2 + (2,5m - R_g)^2} < R_g, \\
& m + y_0 > R_g, \quad \sqrt{(m - y_0)^2 + (2,5m - R_g)^2} > R_g, \\
& 2m + h < 2R_g, \quad \sqrt{(m - x_0)^2 + (m - y_0)^2 + (R_g - 0,5m)^2} < R_g;
\end{aligned} \tag{40.39}$$

$$\begin{aligned} \text{B. } V_{\bar{u}} - V_{\bar{u}} - V_{\bar{u}} - V_{\bar{u}} - V_{\bar{u}} + V_{u1} + V_{u2} + V_{u3} + V_{u4} + V_{u5} - V_{u1} &= 4m^2, \\ m + x_0 > R_g, \quad m + y_0 > R_g, \quad \sqrt{(m-x_0)^2 + (m-y_0)^2 + (R_g - 0.5m)^2} < \\ < R_g, \end{aligned} \quad (40.40)$$

$$\begin{aligned} 2m + h < 2R_g, \quad \sqrt{(m-x_0)^2 + (m-y_0)^2 + (2.5m - R_g)^2} > R_g, \\ \sqrt{(m-x_0)^2 + (2.5m - R_g)^2} < R_g, \quad \sqrt{(m-y_0)^2 + (2.5m - R_g)^2} < R_g; \\ \text{B. } V_{\bar{u}} - V_{\bar{u}} - V_{\bar{u}} - V_{\bar{u}} - V_{\bar{u}} + V_{u1} + V_{u2} + V_{u3} + V_{u4} + V_{u5} - \\ - V_{u1} - V_{u3} = 4m^2, \end{aligned}$$

$$\begin{aligned} m + x_0 > R_g, \quad \sqrt{(m-x_0)^2 + (m-y_0)^2 + (R_g - 0.5m)^2} < R_g, \quad (40.41) \\ m + y_0 > R_g, \quad \sqrt{(m-x_0)^2 + (m-y_0)^2 + (2.5m - R_g)^2} < R_g, \\ 2m + h < 2R_g; \end{aligned}$$

$$\begin{aligned} \Gamma. V_{\bar{u}} - V_{\bar{u}} - V_{\bar{u}} - V_{\bar{u}} - V_{\bar{u}} + V_{u1} + V_{u2} + V_{u3} + V_{u4} - V_{u1} - \\ - V_{u3} + V_{u3} = 4m^2, \end{aligned}$$

$$\begin{aligned} \sqrt{(m-x_0)^2 + (2.5m - R_g)^2} < R_g, \quad \sqrt{(m-y_0)^2 + (2.5m - R_g)^2} > R_g, \\ m + x_0 > R_g, \quad \sqrt{(m-x_0)^2 + (m-y_0)^2 + (R_g - 0.5m)^2} < R_g; \\ 2m + h < 2R_g, \quad \sqrt{(m+y_0)^2 + (R_g - 0.5m)^2} < R_g; \end{aligned} \quad (40.42)$$

$$\begin{aligned} \Delta. V_{\bar{u}} - V_{\bar{u}} - V_{\bar{u}} - V_{\bar{u}} - V_{\bar{u}} - V_{\bar{u}} + V_{u1} + V_{u2} + V_{u3} + V_{u3a} + \\ + V_{u4} - V_{u1} - V_{u1a} = 4m^2, \end{aligned}$$

$$\begin{aligned} m + x_0 > R_g, \quad \sqrt{(m-x_0)^2 + (2.5m - R_g)^2} < R_g, \quad (40.43) \\ 2m + h < 2R_g, \quad \sqrt{(m-y_0)^2 + (2.5m - R_g)^2} > R_g, \\ \sqrt{(m-x_0)^2 + (m+y_0)^2 + (R_g - 0.5m)^2} < R_g; \end{aligned}$$

IV

$$\begin{aligned} \text{A. } V_{\bar{u}} - V_{\bar{u}} - V_{\bar{u}} - V_{\bar{u}} - V_{\bar{u}} + V_{u3} + V_{u3a} = 4m^2, \\ \sqrt{(x_0 - m)^2 + (2.5m - R_g)^2} < R_g, \quad \sqrt{(m-y_0)^2 + (2.5m - R_g)^2} > R_g, \\ 2m + h < 2R_g, \quad \sqrt{(x_0 - m)^2 + (m+y_0)^2 + (R_g - 0.5m)^2} < R_g; \end{aligned} \quad (40.44)$$

$$\begin{aligned} \text{B. } V_{\bar{u}} - V_{\bar{u}} - V_{\bar{u}} - V_{\bar{u}} - V_{\bar{u}} + V_{u3} = 4m^2, \\ \sqrt{(m+y_0)^2 + (R_g - 0.5m)^2} < R_g, \quad \sqrt{(x_0 - m)^2 + (2.5m - R_g)^2} < R_g, \\ \sqrt{(m-y_0)^2 + (2.5m - R_g)^2} > R_g, \quad \sqrt{(x_0 - m)^2 + (m+y_0)^2} < R_g, \\ \sqrt{(x_0 - m)^2 + (m+y_0)^2 + (R_g - 0.5m)^2} > R_g, \quad 2m + h < 2R_g, \quad (40.45) \\ \sqrt{(x_0 - m)^2 + (m-y_0)^2 + (R_g - 0.5m)^2} < R_g; \end{aligned}$$

$$A. \bar{V}_{ac} - \bar{V}_{as} - \bar{V}_{at} - \bar{V}_{ata} + V_{k1} + V_{k3} = 4m^3.$$

$$m + y_0 > R_g, \quad \sqrt{(x_0 - m)^2 + (m - y_0)^2 + (R_g - 0.5m)^2} < R_g, \quad (40.46)$$

$$2m + h < 2R_g, \quad \sqrt{(x_0 - m)^2 + (m - y_0)^2 + (2.5m - R_g)^2} < R_g;$$

$$B. \bar{V}_{ac} - \bar{V}_{as} - \bar{V}_{ata} - \bar{V}_{at} - \bar{V}_{ata} + V_{k1} + V_{k3} = 4m^3.$$

$$\sqrt{(x_0 - m)^2 + (y_0 + m)^2} < R_g, \quad \sqrt{(m + y_0)^2 + (R_g - 0.5m)^2} > R_g.$$

$$2m + h < 2R_g, \quad \sqrt{(x_0 - m)^2 + (m - y_0)^2 + (R_g - 0.5m)^2} < R_g.$$

$$\sqrt{(x_0 - m)^2 + (m - y_0)^2 + (2.5m - R_g)^2} < R_g, \quad (40.47)$$

$$B. \bar{V}_{as} - \bar{V}_{as} - \bar{V}_{as} = 4m^3, \quad \sqrt{(m + y_0)^2 + (2.5m - R_g)^2} > R_g;$$

$$2m + h < 2R_g, \quad \sqrt{(x_0 - m)^2 + (y_0 - m)^2 + (R - 0.5m)^2} < R_g.$$

$$\sqrt{(x_0 - m)^2 + (y_0 - m)^2 + (2.5m - R_g)^2} < R_g. \quad (40.48)$$

Calculation of conductivity g was done by the above mentioned formulas for 15 points on one eighth part of the area of the lower face of surface of model S. Results of calculation are given in Table 19 in which in scale are placed points on a fourth part of the lower face and the value of conductivity in them is shown. Near every point is shown the number of the equation which satisfies conductivity in it. Calculation was carried out on digital computer "Promin" as follows.

Table 19.

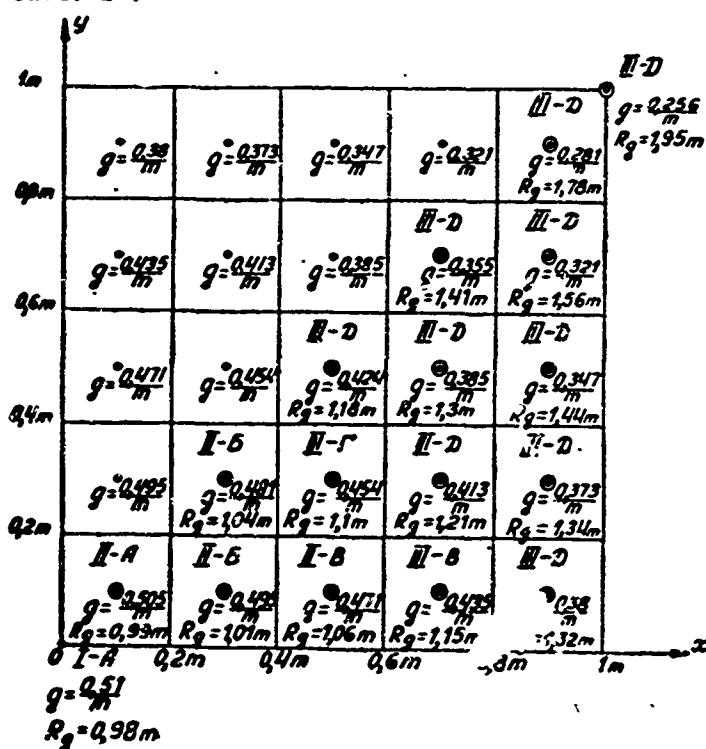
15m	$g = \frac{0.332}{m}$	$g = \frac{0.311}{m}$	$g = \frac{0.288}{m}$	$g = \frac{0.244}{m}$	$\bar{V}-B$ $g = \frac{0.215}{m}$
12m				$\bar{V}-B$ $g = \frac{0.272}{m}$	$\bar{V}-B$ $g = \frac{0.244}{m}$
9m	$g = \frac{0.364}{m}$	$g = \frac{0.347}{m}$	$g = \frac{0.312}{m}$	$R_g = 1.78m$	$R_g = 2.05m$
6m	$g = \frac{0.417}{m}$	$g = \frac{0.385}{m}$	$g = \frac{0.351}{m}$ $R_g = 1.435m$	$\bar{V}-A$ $g = \frac{0.312}{m}$ $R_g = 1.6m$	$\bar{V}-A$ $g = \frac{0.288}{m}$ $R_g = 1.8m$
3m	$g = \frac{0.447}{m}$	$g = \frac{0.414}{m}$ $R_g = 1.21m$	$g = \frac{0.385}{m}$ $R_g = 1.3m$	$g = \frac{0.347}{m}$ $R_g = 1.44$	$g = \frac{0.311}{m}$ $R_g = 1.62m$
0	$\bar{V}-5$ $g = \frac{0.472}{m}$ $R_g = 1.06m$	$\bar{V}-B$ $g = \frac{0.447}{m}$ $R_g = 1.12m$	$\bar{V}-r$ $g = \frac{0.417}{m}$ $R_g = 1.2m$	$\bar{V}-5$ $g = \frac{0.364}{m}$ $R_g = 1.375m$	$\bar{V}-5$ $g = \frac{0.332}{m}$ $R_g = 1.51m$
	$g = \frac{0.481}{m}$ $R_g = 1.04m$	0.3m	0.6m	0.9m	1.2m
					1.5m

An equation for conductivity g at the given point was selected randomly. Part of the members of the equation was transferred to the right part so that they took the form

$$f_1(g) = f_2(g).$$

Then, substituting different values of g , the left $f_1(g)$ and the right $f_2(g)$ parts of the equation were calculated, curves were plotted according to calculations and their point of intersection found. Coordinate g of the point of intersection of the curves were checked according to conditions for the given equation. If the found value of g did not satisfy these conditions another equation was selected and calculations carried out in this way until an equation for which the found value of g satisfies all conditions is found.

Table 20.



Here the obtained results are directly applicable to the construction of attenuators of space grid models. In this case instead of conductivity of holes to nodes of the grid on its border it is necessary to join electrical conductivities

proportional to those shown in the table. Short-circuited ends of all conductivities will serve as an analog of a point at infinity. In Table 20 are given results of calculation of distribution of conductivity g over surface S of a model. Region D is a cube with side 2 m, surface S coincides with the surface of cube D .

Knowing g at point (x_0, y_0, z_0) of the model border it is easy to find the diameter of hole d in this point if is selected the distance a between holes and thickness l of boundary S

$$g = \frac{\pi d^2}{4la^2}, \quad d = \sqrt{\frac{4gla^2}{\pi}}, \quad (40.49)$$

or the distance a between holes if their diameter is selected

$$a = \sqrt{\frac{\pi d^2}{4lg}}. \quad (40.50)$$

§ 41. Simulation of Field of Stray Currents in the Networks of Electrified Railroads and Underground Pipelines

Insulating coverings of pipes of underground constructions do not ensure full protection of them from corrosion and destruction. Stray currents of electrified railroads redouble the processes of destruction and rapidly lead to unfitness of large sections of pipelines. For protection of metallic underground constructions from corrosion and dissolution by stray currents are developed effective protective means namely cathode and drainage protection. However to this time no method has been found for the calculation of safety devices with the help of which it would have been possible to determine their number, form and place of location in a network of pipes.

Designing of devices of cathode and drainage shielding reduces to calculation of a field of protective and stray currents in the ground surrounding the entire network of underground construction. Mathematical formulation of this problem was done by V. N. Ostapenko [19] but no analytic solution to it in general has yet been found. Let us give mathematical expression to the problem.

Let us introduce the following designations:

U — electrical potential of field of current; $\gamma_1, \gamma_2, \gamma_3, \gamma_4, \gamma_5$ — conductivity

of pipeline, roadbed, insulating covering of pipes, insulation of rail, and ground respectively.

The entire network of pipelines is placed in half-space $x < 0$ in parallel to surface $x=0$ (surface of earth) at a depth m from it. On surface $x=0$ lies the network of electrified railroads. The potential in the lower half-space satisfies the equation

$$\frac{\partial}{\partial x} \left(\gamma \frac{\partial U}{\partial x} \right) + \frac{\partial}{\partial y} \left(\gamma \frac{\partial U}{\partial y} \right) + \frac{\partial}{\partial z} \left(\gamma \frac{\partial U}{\partial z} \right) = 0, \quad (41.1)$$

$$\gamma = \begin{cases} \gamma_1 & \text{— in wall of pipes,} \\ \gamma_2 & \text{— in rails of railroad.} \\ \gamma_3 & \text{— in insulation of pipes,} \\ \gamma_4 & \text{— in insulation of rail,} \\ \gamma_5 & \text{— in ground} \end{cases}$$

everywhere, besides the fixed points of connection of poles of sources of current to the pipeline (with cathodic protection) and moving points of contact of a trolley with rails (during travel of electric locomotives), in which potential has peculiarities. On surface $x = 0$

$$\frac{\partial U}{\partial n} = 0 \quad (41.2)$$

everywhere with the exception of ground points of poles of sources of current (with cathodely shielding) and line of railroad. The intensity of processes of corrosion and dissolution of metal of pipes is determined by difference potentials of the pipeline and earth, in other words, by the voltage on the insulating covering of the pipe. From the essence of cathodic protection it follows that this voltage should be not less than a certain definite value and at the same time, from technical considerations, should not be too large. The problem consists in detecting such a distribution of cathode shielding devices and drainage cables for which the change of voltage on the insulation of the pipes over the entire extent of the network will be limited by the assigned limits. The number of safety devices besides should be as small as possible.

The complexity and variety of forms of pipeline networks and railroad lines so hamper analytic solution of the problem that it becomes practically impossible even with the use of digital computers. However, solution of the problem nevertheless can be obtained with the help of a model used to find voltage on insulating covering of pipes of network. Sequentially modelling diverse variants of location of safety

devices, it is possible to find an optimum.

The extent of networks of gas conduits is measured in tens, hundreds and even thousands of kilometers. At the same time the value of diameters of the pipes does not exceed one meter and the thickness of their insulation - one centimeter. Such a ratio of dimensions gives rise to great difficulties when simulating the field of stray and protective currents in a network of gas conduits. Actually the dimensions of the model are desirably limited to a value of 2-3 m and at the same time in model it is necessary to retain the actual ratio of length of network to diameter of pipes and thickness of insulation on them. Even if the extent of the gas conduit model reaches several kilometers, the diameter of pipes on the model will be measured in hundredth parts of a millimeter and the thickness of insulation in microns. To prepare such a model and to make the necessary measurements on it is technically impracticable. This circumstance compels abandoning attempts at straight simulation of the field and switching to a more complicated model using characteristic peculiarities of the structure of the field investigated.

Let us consider a long rectilinear pipeline of radius R covered with a thin layer of imperfect insulation and located at a depth m from the surface of the Earth ($x=0$). Let us join one pole of the source of electromotive force to the pipeline, the other pole we will ground at a great distance from it. Disregarding potential drop along the pipe and considering the surface of the insulation equipotential and the grounded pole infinitely remote, we find the field of current in ground near the pipe.

Applying method of mirror images, we replace the investigated field by the field of two parallel pipes of identical potential in a uniform medium (ground). The overall potential of the sought field is expressed thus [7]:

$$W(\Omega) = \frac{I_0}{2\pi\gamma} \ln \frac{\Theta_1\left(i \frac{\Omega - \Omega_0}{2h}, i \frac{a}{h}\right)}{\Theta_1\left(i \frac{\Omega - \bar{\Omega}_0}{2h}, i \frac{a}{h}\right)}. \quad (41.3)$$

Here I_0 is the current flowing through surface of pipe per unit length; γ is the conductivity of ground

$$\Omega(z) = \frac{-ih}{\ln \frac{m - \sqrt{m^2 - R^2}}{m + \sqrt{m^2 - R^2}}} \ln \frac{z - \sqrt{m^2 - R^2}}{z + \sqrt{m^2 - R^2}} + i \frac{h}{2} = u + iv. \quad (41.4)$$

$\Omega(z)$ is the function infinite-sheetly conformally mapping the entire plane with the exception of circular sections of pipes, onto an infinite band of width h and translating the circuit of the upper pipe to upper limit of band $v = h$, the circuit of the lower pipe to the lower bound of band $v = 0$. Here the point at infinity passes onto the band in a series of equidistant points with coordinates

$$\Omega_k = 2ak + \frac{ih}{2} \quad (k - \text{any integer})$$

$$a = \frac{2\pi h}{\ln \frac{m + \sqrt{m^2 - R^2}}{m - \sqrt{m^2 - R^2}}}; \quad \Omega_0 = i \frac{h}{2}; \quad \bar{\Omega}_0 = -i \frac{h}{2}. \quad (41.5)$$

Presenting function Θ_1 in the form of a series we obtain

$$\Theta_1(\xi_1) = 2[q^{\frac{1}{4}} \sin \pi \xi_1 - q^{\frac{9}{4}} \sin 3\pi \xi_1 + q^{\frac{25}{4}} \sin 5\pi \xi_1 - \dots] \quad (41.6)$$

$$q = e^{-\frac{\pi^2}{h}} = e^{-\frac{2\pi^2}{\ln \frac{m + \sqrt{m^2 - R^2}}{m - \sqrt{m^2 - R^2}}}}$$

$$\xi_1 = i \frac{\Omega - \Omega_0}{2h} = \frac{\ln \frac{z - \sqrt{m^2 - R^2}}{z + \sqrt{m^2 - R^2}}}{2 \ln \frac{m - \sqrt{m^2 - R^2}}{m + \sqrt{m^2 - R^2}}};$$

$$\xi_1 = i \frac{\Omega - \bar{\Omega}_0}{2h} = \frac{\ln \frac{z - \sqrt{m^2 - R^2}}{z + \sqrt{m^2 - R^2}}}{2 \ln \frac{m - \sqrt{m^2 - R^2}}{m + \sqrt{m^2 - R^2}}} - \frac{1}{2} = \xi_1 - \frac{1}{2};$$

$$\Theta_1(\xi) = \Theta_1\left(\xi_1 - \frac{1}{2}\right) = -\Theta_1(\xi_1) =$$

$$= -2[q^{\frac{1}{4}} \cos \pi \xi_1 + q^{\frac{9}{4}} \cos 3\pi \xi_1 + q^{\frac{25}{4}} \cos 5\pi \xi_1 + \dots]. \quad (41.7)$$

Placing these values in formal (41.3), we have

$$\begin{aligned} W(z) &= \frac{I_0}{2\pi\gamma} \ln \frac{\Theta_1\left(\xi_1, i \frac{a}{h}\right)}{\Theta_2\left(\xi_1, i \frac{a}{h}\right)} + i \frac{I_0}{2\gamma} = \\ &= \frac{I_0}{2\pi\gamma} \left[\ln \frac{\sin \pi \xi_1 - q^2 \sin 3\pi \xi_1 + q^8 \sin 5\pi \xi_1 - q^{12} \sin 7\pi \xi_1 + \dots}{\cos \pi \xi_1 + q^2 \cos 3\pi \xi_1 + q^8 \cos 5\pi \xi_1 + q^{12} \cos 7\pi \xi_1 + \dots} + \right. \\ &\quad \left. + \pi i \right] = \frac{I_0}{2\pi\gamma} \ln \frac{\sum_{n=1}^{\infty} (-1)^n q^{\frac{(2n-1)^2-1}{4}} \sin(2n-1)\pi \xi_1}{\sum_{n=1}^{\infty} q^{\frac{(2n-1)^2-1}{4}} \cos(2n-1)\pi \xi_1}. \end{aligned} \quad (41.8)$$

Considering values of m and R close to real ($m \approx 4R, R \approx 0.5h$), we estimate the value of q

$$q = e^{\frac{-2\pi^2}{\ln \frac{m+\sqrt{m^2-R^2}}{m-\sqrt{m^2-R^2}}}} = e^{\frac{-2\pi^2}{\ln \frac{1+\sqrt{15}}{1-\sqrt{15}}}} = e^{-4.81} \approx \frac{1}{123}; \quad q^2 \approx 10^{-4}. \quad (41.9)$$

Consequently, all members besides the first in expressions of sums, standing under the sign of the logarithm, without loss of accuracy, may be disregarded

$$W(z) = \frac{I_0}{2\pi\gamma} (\ln \operatorname{tg} \pi \xi_1 + \pi i). \quad (41.10)$$

Let us designate $b = \sqrt{m^2 - R^2}$, then

$$\begin{aligned} \pi \xi_1 &= \frac{a}{4h} \ln \frac{z+b}{z-b} = \frac{a}{4h} \left[\ln \sqrt{\frac{(x+b)^2+y^2}{(x-b)^2+y^2}} - \right. \\ &\quad \left. - i \operatorname{arctg} \frac{2by}{x^2+y^2-b^2} \right] = c - id, \\ c &= \frac{a}{8h} \ln \frac{(x+b)^2+y^2}{(x-b)^2+y^2}; \quad d = \frac{a}{4h} \operatorname{arctg} \frac{2by}{x^2+y^2-b^2}; \\ \operatorname{tg} \pi \xi_1 &= \operatorname{tg}(c - id) = \frac{\sin 2c - i \operatorname{sh} 2d}{\cos 2c + \operatorname{ch} 2d} = \\ &= \sqrt{\frac{\operatorname{ch} 2d - \cos 2c}{\operatorname{ch} 2d + \cos 2c}} e^{-i \operatorname{arctg} \frac{\operatorname{sh} 2d}{\sin 2c}}. \end{aligned} \quad (41.11)$$

Placing these expressions in formula (41.10) we obtain

$$\begin{aligned} W(z) &= \frac{I_0}{2\pi\gamma} \left(\ln \sqrt{\frac{\operatorname{ch} 2d - \cos 2c}{\operatorname{ch} 2d + \cos 2c}} + k_0 + \pi i - \right. \\ &\quad \left. - i \operatorname{arctg} \frac{\operatorname{sh} 2d}{\sin 2c} \right) = U(x, y) + i \Psi(x, y). \end{aligned} \quad (41.12)$$

Consequently, the electrical potential equals:

$$U(x, y) = \frac{I_0}{4\pi\gamma} \ln \frac{\operatorname{ch} 2d - \cos 2c}{\operatorname{ch} 2d + \cos 2c} + k_0. \quad (41.13)$$

Let us set potential at point $(0, 0)$ equal to zero. We have

$$d(0, 0) = \frac{a}{4h} \operatorname{arctg} \frac{0}{-b^2} = \frac{a\pi}{4h}; \quad c(0, 0) = \frac{a}{8h} \ln 1 = 0.$$

$$U(0,0) = \frac{I_0}{4\pi\gamma} \ln \frac{\operatorname{ch} \frac{a\pi}{2h} - 1}{\operatorname{ch} \frac{a\pi}{2h} + 1} + k_0 = 0, \quad (41.14)$$

$$k_0 = \frac{I_0}{4\pi\gamma} \ln \frac{\operatorname{ch} \frac{a\pi}{2h} + 1}{\operatorname{ch} \frac{a\pi}{2h} - 1}.$$

Placing this value of the constant in formula (41.13), we obtain

$$U(x,y) = \frac{I_0}{4\pi\gamma} \ln \frac{(\operatorname{ch} 2d - \cos 2c) \left(\operatorname{ch} \frac{a\pi}{2h} + 1 \right)}{(\operatorname{ch} 2d + \cos 2c) \left(\operatorname{ch} \frac{a\pi}{2h} - 1 \right)}. \quad (41.15)$$

We write the equation of the line of equal potential

$$\ln \frac{\operatorname{ch} 2d - \cos 2c}{\operatorname{ch} 2d + \cos 2c} = \text{const.} \quad (41.16)$$

According to the removal from the pipes, the form of lines of equal potential approaches a circle. Indeed, considering $z \gg R$ and $z \gg m$, from formula (41.10) we obtain

$$\begin{aligned} \ln \operatorname{tg} \pi \xi_1 &= \ln \left(\operatorname{tg} \frac{a}{4h} \ln \frac{z+b}{z-b} \right) = \\ &= \ln \left(\operatorname{tg} \frac{a}{4h} \ln \frac{1 + \frac{b}{z}}{1 - \frac{b}{z}} \right) \approx \ln \operatorname{tg} \frac{ab}{2hz} \approx \ln \frac{ab}{2hz} = \\ &= \ln \frac{ab}{2h} - \ln r - i\gamma. \end{aligned}$$

Here

$$r = \sqrt{x^2 + y^2}, \quad \gamma = \operatorname{arctg} \frac{y}{x}.$$

More exactly the equation of equipotentials $z \gg R$ and $z \gg m$ can be derived replacing the pipe by parallel charged axes with charges on them of $+I_0/2$ and distance between them $2n$

$$U_1(x,y) = \frac{I_0}{4\pi\gamma} \ln \sqrt{(x^2 + y^2 + n^2 - 2nx)(x^2 + y^2 + n^2 + 2nx)} + k_1.$$

Considering $U_1(0, 0) = 0$, we find

$$U_1(0, 0) = -\frac{I_0}{4\pi\gamma} \ln n^2 + k_1 = 0. \quad k_1 = \frac{I_0}{8\pi\gamma} \ln n^2.$$

$$U_1(x, y) = \frac{I_0}{8\pi\gamma} \ln \frac{n^2}{(x^2 + y^2 + n^2 - 2nx)(x^2 + y^2 + n^2 + 2nx)}. \quad (41.17)$$

Let us derive the equation of equipotential line passing through point $(0, y_1)$. Potential at this point, calculated by the formula (41.15), we designate U_1 :

$$U_1 = U(0, y_1) = \frac{I_0}{4\pi\gamma} \ln \frac{\left(\operatorname{ch} \frac{a}{2h} \operatorname{arctg} \frac{2by_1}{y_1^2 - b^2} - 1 \right) \left(\operatorname{ch} \frac{a}{2h} + 1 \right)}{\left(\operatorname{ch} \frac{a}{2h} \operatorname{arctg} \frac{2by_1}{y_1^2 - b^2} + 1 \right) \left(\operatorname{ch} \frac{a}{2h} - 1 \right)}.$$

We have

$$U_1 = \frac{I_0}{8\pi\gamma} \ln \frac{n^2}{(x^2 + y^2 + n^2 - 2nx)(x^2 + y^2 + n^2 + 2nx)}.$$

We set

$$\frac{I_0}{4\pi\gamma} = 1,$$

then

$$\frac{n^2}{(x^2 + y^2 + n^2 - 2nx)(x^2 + y^2 + n^2 + 2nx)} = e^{2U_1}.$$

$$(x^2 + y^2 + n^2 - 2nx)(x^2 + y^2 + n^2 + 2nx) = n^2 e^{-2U_1} = c_1.$$

We set $x = vn$, $y^2 = z$, then

$$z^2 + 2n^2(v^2 + 1)z + n^4(v^2 - 1)^2 - c_1 = 0.$$

Hence

$$z = \sqrt{4v^2n^4 + c_1} - n^2(v^2 + 1),$$

$$y = \sqrt{z} = \pm n \sqrt{\sqrt{4v^2 + e^{-2U_1}} - v^2 - 1}. \quad (41.18)$$

Considering $x = 0$ ($v = 0$), we find

$$y_1 = n \sqrt{e^{-U_1} - 1}.$$

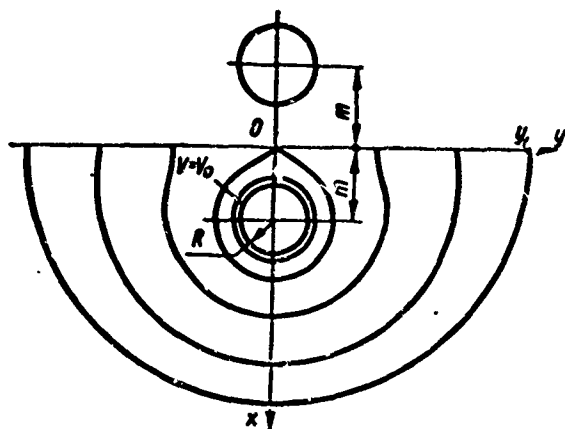


Fig. 80.

hence

$$n = \frac{y_1}{\sqrt{e^{-U_1} - 1}}, \quad v = \frac{x}{n} = \frac{x \sqrt{e^{-U_1} - 1}}{y_1}. \quad (41.19)$$

Placing this value of v in the equation of the equipotential line (41.18), we obtain

$$y = \pm \frac{y_1}{\sqrt{e^{-U_1} - 1}} \sqrt{\frac{4x^2(e^{-U_1} - 1)}{y_1^2 + e^{-2U_1}} - \frac{x^2(e^{-U_1} - 1)}{y_1^2} - 1}. \quad (41.20)$$

As can be seen from Fig. 80 the line of equal potential for $y_1 \geq 20R$ differs very little from a semicircle with its center on the surface of the ground.

Let us take the assumption made during derivation of formula (41.15) and apply conditions which take place in reality, i.e., we will consider that travel along the pipe the potential slowly changes, the grounded pole is located at a finite but sufficiently great distance from the pipe and the pipeline consists of separate rectilinear sections connected to one another at different angles. Here the picture of the field near the pipe in a cross section normal to its axis is almost unchanged although the value of potential at identical points of different sections will be different. The picture of the field of various sections will be similar to each other. Only the field near the points of break and branching of the pipeline will be changed, however, even at these places the form of the field will be practically independent of position of remote poles and can be determined beforehand.

This characteristic peculiarity — independence of form of field near the pipe from position of remote sources — is used for construction of a model [35].

Let us divide the investigated field into two parts including: 1) pipeline, insulation and nearby layer of ground bounded by a surface which is formed by the family of lines of equal potential equally remote from the axis of the pipe: 2) the whole remaining ground. For each of these parts of the field we construct own model, but, both models are combined in such a way as to immediately obtain a solution to the problem. The final object of simulation is determination of voltage on the insulation of the pipeline, in other words determination of potential difference between two equipotential lines in every cross section of the pipeline. From this point of view the distribution of field intensity along lines of equal potential are not of interest, therefore, considering constancy of form of field near the pipe, it is possible to regard it as two-dimensional in coordinates counted off along the axis of pipe (in units of length) and along any flow line (in units of potential).

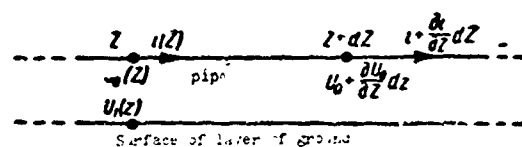


Fig. 81.

Let us find the connection between potential on the surface of the pipe U_0 and potential on the surface of a separated layer of ground U_1 (Fig. 81). Considering the portion of current flowing along the insulation and ground along the axis of the pipe equal to zero, which is very close to the actual case, we obtain

$$\begin{aligned} U_0 - \left(U_0 + \frac{dU_0}{dz} dz \right) &= r_0 i dz, \\ i - \left(i + \frac{di}{dz} dz \right) &= g_0 (U_0 - U_1) dz. \end{aligned} \quad (41.21)$$

Hence after differentiation and elimination of current i we obtain

$$\frac{d^2 U_0}{dz^2} = r_0 g_0 (U_0 - U_1). \quad (41.22)$$

Here r_0 is the resistance of unit length of pipe; g_0 is the conductivity of

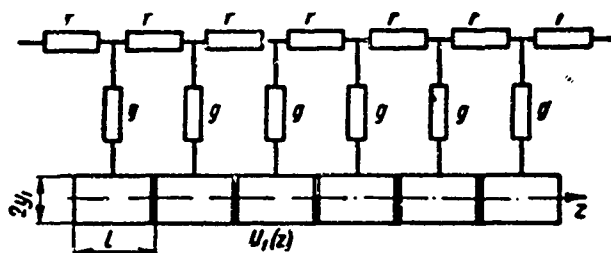


Fig. 82.

insulation and separated layer of ground happening per unit length of pipe.

Precisely the same, with the same assumptions, will be the equation connecting potential on rails of railroad with potential on surface of separated layer of ground. Here by r_0 one should understand the resistance of a unit length of rail, by g_0 — the conductivity of the separated layer of ground happening per unit length of rail.

Equation (41.22) is similar to the equation of a long line and potentials entering it can be modelled by the distribution of voltages in a recurrent circuit containing the longitudinal resistances and transverse conductivities g .

In the remaining part of the ground the field is essentially a three-dimensional potential which satisfies the Laplace equation. It is expediently modeled by a field of current in a volumetric bath. Consequently, the model should contain two main parts — a recurrent circuit and volumetric bath filled with a conducting composition to replacing ground. Both parts have to be interconnected in such a manner so as to preserve values of potential on border of connection of the models corresponding to the outer surface of the separated layer of ground. Potential U_1 on this surface is changed only along the axis of the pipe. Therefore, to preserve its values it is necessary to make the surface metallic. In order to ensure a change of potential along the axis of the pipe the metallic surface must be cut into on small element of identical length with cross sections normal to the axis and to insulate the metallic element from each other with thin insulating separators (Fig. 82). To each element of length l is coupled a conductivity $g = g_0 l$ of the recurrent circuit.

We have seen that a line of equal potential remote from axis of pipe by a distance greater than $20R$ is close to a semicircle. A line of equal potential near a railroad has the same form. Therefore element for connection of both parts of the model are expediently prepared from segments of metallic tube. The radius

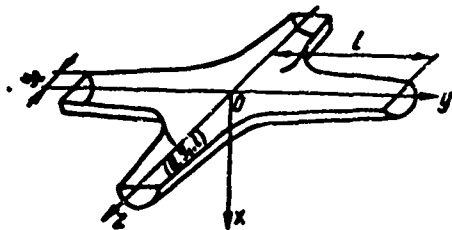


Fig. 83.

of the semicircles y_1 should be selected such that in the scale of the model the radius of tubes of element be not less than 3-4 mm. In the bath the tubes are emersed in conducting composition to one half of their diameter.

In place of branching of pipes, the form of element can be found replacing the pipeline and its mirror image in the surface of the ground by two charged filaments coinciding with axes oz and oy (Fig. 83). At great distances from the pipes such replacement is permissible. The potential of the field of intersecting filaments equals:

$$U(x, y, z) = \frac{l_0}{2\pi\gamma} \ln \sqrt{(x^2 + y^2)(x^2 + z^2)} + c_1. \quad (41.23)$$

The equation of the surface of equal potential is

$$(x^2 + y^2)(x^2 + z^2) = c. \quad (41.24)$$

Constant c we find from the condition that point $(0, y_1, l)$ belongs this surface

$$c = y_1^2 l^2$$

Consequently, the equation of the surface will be

$$y = \pm \sqrt{\frac{y_1^2 l^2}{x^2 + z^2} - x^2} \quad \text{or} \quad z = \pm \sqrt{\frac{y_1^2 l^2}{x^2 + y^2} - x^2}. \quad (41.25)$$

The form of a surface plotted according to this equation is shown in Fig. 83.

The distribution of voltage on the insulation of the pipes which is of interest to us will be modelled by the distribution of voltage on conductivities g of the recurrent circuit. Each of conductivities g replaces the joint conductivity of insulation and ground present on a section of pipe of length l . The value of g is defined thus:

$$g = \frac{g_n g_{rp}}{g_n + g_{rp}}. \quad (41.26)$$

Here

$$g_{\text{us}} = 2\pi R / \gamma_{\text{us}}, \quad (41.27)$$

g_{us} is the conductivity of insulation present on length l of a pipe of radius R ;

$$g_{\text{rp}} = \frac{2\pi \gamma_{\text{is}}}{\frac{\operatorname{ch}\left(\frac{a}{2h} \operatorname{arctg} \frac{2by_1}{y_1^2 - b^2}\right) + 1}{\ln \frac{\operatorname{ch}\left(\frac{a}{2h} \operatorname{arctg} \frac{2by_1}{y_1^2 - b^2}\right) - 1}}}, \quad (41.28)$$

g_{rp} is the conductivity of a separated layer of ground; γ_{us} is the conductivity of a unit of an area of insulation.

Knowing the value of conductivities g_{us} and g_{rp} , it is easy to find the voltage on a section of insulation of the pipe u_{us} by the formula

$$u_{\text{us}} = \frac{g_{\text{rp}}}{g_{\text{rp}} + g_{\text{us}}} u, \quad (41.29)$$

where u is the voltage on conductivity g of a link of the recurrent circuit.

If a gas conduit consists of two closely located pipes electrically interconnected, the form of element will be the same as for a single pipe but in this case the conductivity of the separated layer of ground cannot be calculated by the formula (41.28). The value of conductivity is most easily found by simulation

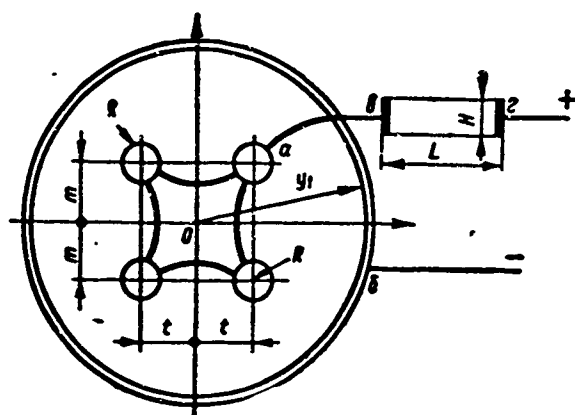


Fig. 84.

The model is connected in a dc circuit in series with a rectangular band measuring $L \times H$ cut from the same paper as was the circle and the voltage between contacts of the model U_{ag} and line U_{ar} are

measured. Conductivity is calculated by the formula

$$\epsilon_{rp} = \gamma_s' \frac{U_{\pi} H}{U_{\infty} L}. \quad (41.30)$$

Replacement of the separated layer of ground and insulation of the pipes by conductivities of a recurrent circuit permits practically a 100 fold decrease in scale of simulation, however for too large an extent of the pipeline network the entire field cannot be modelled, immediately. It is necessary to model the field by sections. The model constitutes volumetric bath filled with a conducting composition with adjoint recurrent circuits. So that the field of current in the model will be similar to the field of current in the modelled section of the network it is necessary on the borders of the modelled section to assign values of potential proportional to those occurring in the actual field. These values are not beforehand known and can be determined only by solving the entire problem. In order to avoid this uncertainty it was necessary to prepare the model in such a manner so that during simulation in it any section is considered to always influence the entire remaining pipeline and railroad network with the ground surrounding it. This can be achieved with the help of a model of an element of unlimited space. The depth of laying of the pipes in the ground is negligibly small as compared to the dimensions of the modelled sections of the network. For planning only the voltage on the insulation of the pipes is of interest. Consequently, it is important to ensure conformity of the field of current in the model and object only on the surface of the conducting composition of the model. Therefore as an element of unlimited space it is expedient to select a square.

The metallic housing of a model of an element of unlimited space is equivalent to an infinitely remote surface of zero potential. Replacing the branches of pipeline and railroad network extending beyond the limits of the modelled section by equivalent resistances connecting the ends of the chain diagram with the metallic housing of the model we will consider thereby an influence of all remaining parts of the network on the field of current from sources located within the limits of area of the given section. The value of resistances equivalent to branches of the network exceeding the limits of the modelled section can be measured collecting for this on the model a circuit of substitution of each of the branches.

The field in the part of interest to us, that is near to the surface of the pipes, is determined by the current flowing through the insulation of the pipes. Sources of opposite sign located in a neighboring section are removed to comparatively great distances and their influence on the value of voltage on the insulation of pipes of a given cross section is the same as if they were infinitely distant. Therefore, for simulation of a field of sources located in a neighboring section it is sufficient on the ends of the circuits of substitution of the branches of a pipeline and a railroad network, at the intersections with these branches of the border between sections, to set the value of currents, equal to earlier occurring resistances, equivalent to the same branches during simulation of a field in a cross section with sources. Connecting sources of current with one pole to the metallic housing, the second to the ends of the circuits of substitution of branches, serving as a continuation of branches of the section with sources and setting the necessary values of currents, we ensure thereby boundary conditions close reality [32].

In such a way it is possible to model by sections the field of the entire pipeline net created by sources located in only one section. Modelling in series a field created by sources of each of the sections separately, and superimposing the results of simulation, we find the resultant field during simultaneous action of all sources.

§ 42. Model for Calculating Electrotection of Underground Constructions from Corrosion

In preceding paragraph we clarified the possibility of simulation of a field of stray currents in a network of underground pipelines and railroads and showed that the modelling device must consist of the model of an element of unlimited space having the form of a section of a plane, and a set of chain circuits with sources of current. In § 37 is examined a model with a zero mean value of potential of distortion on the section of free surface of the conducting composition. Let us give consideration in favor of application of it for simulation of a field of stray currents. During simulation the ends of branches of chain circuits replacing sections of branches of the pipeline network exceeding the limits of the given section are joined to the metallic housing of the model through resistances. The current

in these resistances are measured and during subsequent simulation of the field in neighboring sections the measured value of it is set in continuations of the same branches. This current basically also determines the intensity of the field in neighboring sections. The value of current is proportional to the potential difference between the end of the branch of the chain circuit and the housing of model. Inasmuch as the potential of the model housing is equal to zero, the value of current is proportional to the potential of the end of the branch.

We saw that it is impossible to destroy completely the distortion inserted by the wall of the model onto the field. The field of the sources is partially reflected from the wall of the model and affects the value of potential of the branches of the chain circuits replacing the pipelines. This influence will be reflected in the value of current in the branches and will lead to error during simulation. Properties of model have to be such that this error is as small as possible.

The reflected field in the model can be regarded as a field of sources distributed over its wall. Let us estimate the influence of this field on the value of potential of a branch of the chain circuit replacing a metallic pipeline. Let us assume that in the field of sources is introduced an uncharged conductor (pipeline). Free charges migrate to the surface of the conductor and create their own field. Inside the conductor it is equal to and opposite in sign to the external field of the sources and the potential of the resultant field there is constant. Outside the conductor the field of charges induced on it is similar to the field of a dipole since the total induced charge of the conductor is equal to zero. The zero equipotential surface of this field necessarily will pass inside the conductor and will dissect it into two approximately identical parts. Inside the conductor it coincides with one of the equipotentials of the external field of sources, outside the conductor it goes to infinity. Inasmuch as the resultant potential is equal to the sum of potentials of the field of sources and the field of charges induced on the conductor, the constant value of potential of the conductor $U = C$ will be equal to that value of field potential of external sources which it takes inside the conductor on the section of the surface of zero potential of the field of induced charges. As was shown by G. A. Grinberg¹ potential induced on a

¹G. A. Grinberg, "Izbrannyye voprosy matematicheskoy teorii elektricheskikh i magnitnykh yavleniy, Izd-vo AN SSSR, 1948.

long thin straight wire introduces in an arbitrary external field, is very close to the mean value of potential of this external field on the length of the wire. In our case the modelled pipeline constitutes a totality of long thin conductors located on the surface of the conducting composition of the model. The error introduced by the wall of the model in the value of potential of the circuits of substitution of the pipeline will also be close to the mean value of potential of distortion in the volume occupied by the pipeline. Therefore, it is expedient to study such a model in which the mean value of potential of distortion will equal zero. The model examined in § 37 possesses, besides this, one more valuable property, namely: a small value of potential of distortion in the entire region.

During design of electroshielding of pipelines the field only on the surface of the conducting composition of model is of interest, therefore, it is possible to apply a solid medium for simulation of the field. A solid solution of gelatin in glycerine is most suitable. The solution is poured into a tank in the liquid state and it fills all openings in the walls. After that it is cooled and its surface leveled.

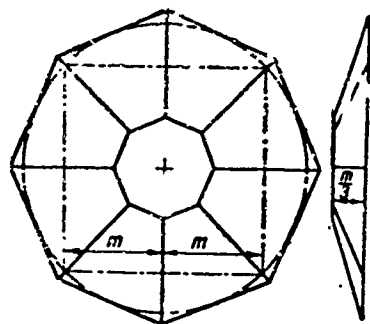


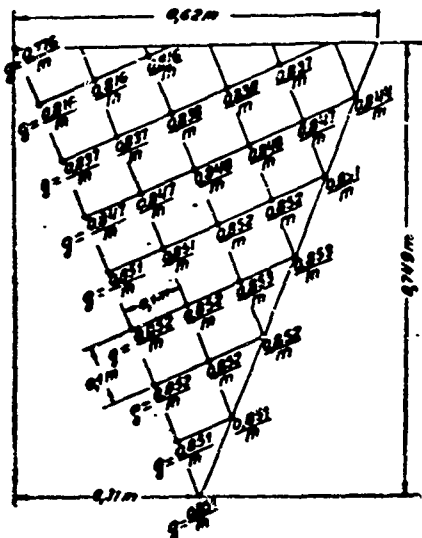
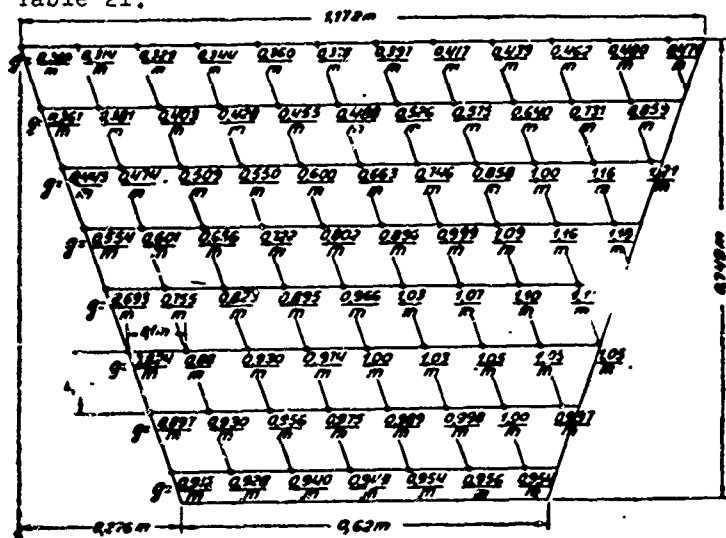
Fig. 85.

The least value of potential of distortion is attained with a spherical surface of model wall. However, to prepare such a surface is difficult and can be replaced with the surface of an octahedral truncated pyramid embracing a spherical segment (Fig. 85). The conductivity of holes in the wall of the model is determined by the formula (37.3). As region D it is expedient to take a square (Fig. 68). Here integrals in formula (37.3) are expressed in terms of elementary

functions. Calculation of conductivity g can be performed on a digital computer programed for calculation of multiple integrals. Results of calculation of conductivity g for the model shown in Fig. 85 are given in Table 21.

The second part of the model — a set of chain circuits and sources of current — is composed of wire adjustable resistances and assembled on a special frame. Values of conductivities and resistances replacing joint conductivity of the insulation and separated layer of ground, and the longitudinal resistance of the pipes, are set in a selected scale depending on the ratio of conductivities of ground and the conducting composition of the model.

Table 21.



In accordance with the plan of pipeline and railroad networks on the surface of the conducting composition of the model, semicircular grooves are cut with a special cutter in which are fused preliminarily heated tubular elements dividing them by thin insulating separators. Then to them are joined conductive wires of the chain circuits. Toward the end of a branch of the chain circuit, it replaces itself a part of a branch of the pipeline or railroad intersecting the border of the modelled section, a resistance is connected equivalent to the part of the branch not included in the model.

Nodes of the chain circuit replacing a railroad line are joined to the contacts of a step switch, at the input of which a source of current is included. Level of ar

electric locomotive along the line is imitated by series switching of contacts of the stepping switch.

The problem at hand is solved thus:

A source of current, one end of which is connected to the input of a stepping switch, is connected by the other end to the node of the circuit of substitution of the railroad corresponding to the point of connection of a traction substation. Current is set in the source in a selected scale proportional to the current consumed by the electric train. After that the stepping switch is activated and the voltage u on conductivity g of a link of the chain circuit replacing a pipeline with insulation and a layer of ground and the value of currents in resistances connected to the housing of the model are measured. Knowing the values of conductivity g_{rp} and g_m (41.27), (41.28), voltage drops on the corresponding section of insulation u_m are calculated by the formula (41.29). Making measurements on all conductivities and calculating the voltage on the insulation, distribution curves of voltage along branches of the pipeline are traced. The same is done for all neighboring sections of the pipeline network however in this case sources of current are connected to beginnings of the branches of the pipeline and railroad networks which are a continuation of branches of the basic section and to the housing of the model and with these sources is provided a current of the same value as was measured on the first model in corresponding resistances. The stepping switch in this case is not included but the current in the sources connected to the beginnings of the branches change in the same stepwise fashion as in the first model during operation of the stepping switch.

Performing similar operations as many times as there are sections of the modelled pipeline network, we obtain a series of distribution curves of voltage on the insulation of the pipeline during action of sources of each of the sections separately. Summing these curves we obtain resultant distribution curves of voltage on the insulation of the pipes of the network. The form of the curves and value of their ordinates will permit finding sections of the pipeline subjected to destruction and to select a device for their protection. Placing stations of cathodic protection and drainages along the pipeline we go on to simulation of the field taking into account the influence of safety devices. Stations of cathode protection on the model will correspond to sources of current connected to nodes of

the chain circuit of substitution of the pipeline, and the point of the surface of conducting composition of the model corresponding to the grounding point. Drainages are modelled by connecting wires of definite resistance between nodes of the chain circuits of substitution of the pipeline and railroad. Having made all necessary connections on the model we begin to take new measurements and plot curves of distribution of voltage on the insulation. If obtained results are unsatisfactory, a new location for the safety devices is selected and modeling is repeated until the optimum variant of shielding is selected.

LITERATURE

1. Alekhin, V. M. "Sravneniye i otsenka razlichnykh metodov elektricheskogo rascheta tokoprovodov" (Comparison and appraisal of different methods of electrical calculation of conductors), Izvestiya vuzov, elektromekhanika, 1960, No. 11.
2. Alekhin, V. M., Tozoni, O. V. "Elektromodelirovaniye magnitnogo polya nasyshchennykh mashin polem postoyannogo toka v provodyashchem liste" (Electrosimulation of magnetic field of saturated machines with a dc field in a conducting sheet), Izvestiya vuzov, elektromekhanika, 1959, No. 4.
3. Alekhin, V. M. "Primer rascheta elektromagnitnogo polya v trekhfaznoy sisteme tokoprovodov pryamougol'nogo secheniya" (Example of calculation of electromagnetic field in a three-phase system of conductors of rectangular cross section). Izvestiya vuzov, elektromekhanika, 1961, No. 4.
4. Akhiyezer, N. I. Elementy teorii ellipticheskikh funktsiy (Element of the theory of elliptic functions), Lostekhizdat, 1948.
5. Bogolyubov, V. Ye., Shamaev, Yu. M. "Elektroliticheskaya vanna s minimal'no iskazhayushchimi stenkami" (Electrolytic bath with minimum distorting walls), "Elektrichestvo", No. 10, 1954.
6. Bogolyubov, V. Ye., Shamyev, Yu. M. "Elektricheskaya vanna s poluprovodyashchimi stenkami" (Electrical bath with semiconducting walls), DAN SSSR, t. 98, No. 3, 1954.
7. Bukhgal'ts, G. Raschet elektricheskikh i magnitnykh poley (Calculation of electrical and magnetic fields), IL, 1961.
8. Vorob'yev, Yu. V. Metod momentov v prikladnoy matematike (Method of moments in applied mathematics), GIFML, 1958.
9. Gavurin, M. K. "Primeneniye polinomov nailuchshego priblikzheniya k uluchsheniyu skhodimosti itepativnykh protsessov" (Application of polynomials of best approximation to improvement of convergence of iterative processes), UMN, t. V, v. 3, 1950.
10. Gel'fond, A. O. Ischisleniye konechnykh raznostey (Calculus of finite differences), GITTL, 1952.
11. Yegorov, P. M. "Eksperimental'noye issledovaniye potentsial'nykh poley posredstvom konformno-preobrazovannykh modeley" (Experimental investigation of potential fields by means of conformally-converted models), "Elektrichestvo", 1954, No. 3.
12. Kantorovich, L. B. i Krylov, V. I. Priblikhennyye metody vysshego analiza (Methods of approximation of higher analysis), GITTL, 1952.

13. Lavrent'yev, M. A. i Shabat, B. V. Metody teorii funktsiy kompleksnogo peremennogo (Methods of theory of functions of complex variable), GIFML, 1958.
14. Mikhlin, S. G. "Lektsii po lineynym integral'nym uravneniyam" (Lecture on linear integral equations), Fizmatgiz, 1959.
15. Muskhelishvili, N. I. "Singulyarnyye integral'nyye uravneniya" (Singular integral equations), OGIZ, Gostekhnizdat, 1946.
16. Markushevich, A. I. "Teoriya analiticheskikh funktsiy" (Theory of analytic functions), GITTL, 1950.
17. Nitsetskiy, L. V. "Uproshchennyye udliniteli kruglykh modeley dlya resheniya uravneniya Laplasa v bezgranichnykh oblastyakh" (Simplified attenuators of round models for solution of the Laplace equation in infinite regions), Trudy seminar "Matematicheskoye modelirovaniye i elektricheskoye tsepi", t. I, Izd-vo AN USSR, 1963.
18. Neyman, L. R. i Kalantarov, P. L. "Teoreticheskiye osnovy elektrotekhniki" (Theoretical bases of electrical engineering), t. III, Gosenergoizdat, 1954, str. 49-148.
19. Ostapenko, V. N. "Matematicheskiye voprosy katodnoy zashchity" (Mathematical questions of cathodic protection), Izd-vo AN USSR, 1961.
20. Polozhiy, G. N. "Effektivnoye resheniye zadachi o priblizhennom konformnom otobrazhenii odnosvyaznykh i dvusvyaznykh oblastey i opredeleniye postoyannykh Kristoffelya-Shvartsa pri pomoshchi elektrogidrodinamicheskikh analogiy" (Effective solution of the problem of approximate conformal mapping of simply connected and doubly connected region and determination of Christoffel-Schwarz constants with the help of electrohydrodynamic analogs), Ukr. Matem. zhurn., t. VII, No. 4, 1955.
21. Polivanov, K. M. "Ferromagnetiki" (Ferromagnetic materials), Gosenergoizdat, 1957.
22. Smirnov, V. I. "Kurs vysshey matematiki" (Course in higher mathematics), t. III, ch. 2, GITTL, 1953, str. 595.
23. Samoylova-Yakhontova, N. "Tablitsy ellipticheskikh integralov" (Table of elliptic integrals), ONTI, 1953.
24. Sinel'nikov, Ye. M. "Analiticheskiy metod rascheta ploskogo magnitnogo polya v odnorodnoy srede ot tokov, protekayushchikh po provodnikam proizvol'nogo secheniya" (Analytic method of calculation of a flat magnetic field in a uniform medium from currents flowing in conductors of arbitrary cross section), Trudy NPI, t. 43/57, 1956.
25. Sinel'nikov, Ye. M. i Tozoni O. V. "Prakticheskoye ispol'zovaniye konformnogo otobrazheniya dlya rascheta magnitnogo polya nenasyschennykh mashin postoyannogo toka" (Practical application of conformal mapping for calculation of the magnetic field of unsaturated dc machines), Izvestiya vuzov, elektromekhanika, 1958, No. 2.
26. Sinel'nikov, Ye. M. i Tozoni, O. V. "Eksperimental'no-analiticheskiy metod rascheta magnitnogo polya v vozdukhom promezhtutke mashinpostoyannogo toka" (Experimental-analytic method of calculation of magnetic field in air interval of dc machines), Trudy NPI, 43/57, 1956.
27. Tozoni, O. V. "Elektrointegrator dlya modelirovaniya chastnogo resheniya uravneniya Puassona" (Electrointegrator for simulation of particular solution of the Poisson equation), Izvestiya vuzov, elektromekhanika, 1961, No. 3.

28. Tozoni, O. V. "Magnitnoye pole mashin postoyannogo toka" (Magnetic field of dc machines), Izvestiya vuzov, elektromekhanika, 1958, No. 3.

29. Tozoni, O. V. "Obosnovaniye eksperimental'no-analiticheskogo metoda resheniya zadachi Dirikhle dlya odnosvyaznoy i dvusvyaznoy oblastey" (Foundation of experimentally-analytic method of solution of the Dirichlet problem for simply connected and two-connected regions), Trudy NPI, t. 43/57, 1956.

30. Tozoni, O. V. "Modelirovaniye funktsii beskonechnolistno konformno otobrazhayushchey dvukhsvyaznuyu oblast' na polosyu" (Modeling the function of an infinite-sheet conformally mapping two-connected region onto a band), Izvestiya vuzov, elektromekhanika, 1958, No. 5.

31. Tozoni, O. V. "Razreshayushchaya sposobnost' elektrointegratora dlya resheniya zadach Dirikhle i Heymana na polose" (Resolving power of electrointegrator for solution of the Dirichlet and Neumann problems onto a band), Izvestiya vuzov, elektromekhanika, 1960, No. 5.

32. Tozoni, O. V. "Modelirovaniye polya tokov v seti podzemnykh sooruzheniy po uchastkam" (Modeling of a field of currents in a network of underground constructions by sections), sb. "Zashchita truboprovodov ot korrozii," v. 6, ITEI, Neftegaz, 1963.

33. Tozoni, O. V. "O vozmozhnosti rascheta raspredeleniya sinusoidal'nogo toka v tokovodakh pri pomoshchi elektromodelirovaniya" (On the possibility of calculation of the distribution of sinusoidal current in current carries with the help of electrosimulation), Izvestiya vuzov, elektromekhanika, 1962, No. 2.

34. Tozoni, O. V. "Elektroliticheskaya vanna s minimal'no iskazhayushchimi stenkami" (Electrolytic bath with minimum distorting walls), "Metody matematicheskogo modelirovaniya i teoriya elektricheskikh tsepy", K., 1963.

35. Tozoni, O. V. "Modelirovaniye polya tokov v seti podzemnykh sooruzheniy" (Simulation of a field of currents in a network of underground constructions), sb. "Matematicheskoye modelirovaniye i elektricheskkiye tsepi", v. 1, Izd-vo AN USSR, 1962.

36. Tozoni, O. V., Khlebnikov, C. D., Sinel'nikov, Ye. M., Kolesnikov, F. V. "Elektrointegrator dlya resheniya zadach Dirikhle i Heymana na polose" (Electrointegrator for solution of the Dirichlet and Neumann problems on a band), Izvestiya vuzov, elektromekhanika, 1959, No. 12.

37. Ugodchikov, A. G. "Elektromodelirovaniye zadachi konformnogo preobrazovaniya kruga na napered zadannuyu odnosvyaznuyu oblast'" (Electrosimulation of the problem of conformal transformation of a circle onto a prescribed simply connected region), Ukr. matem. zhurn., t. VII, No. 2, 1955.

38. Ugodchikov, A. G. "Elektromodelirovaniye konformnogo preobrazovaniya krugovogo kol'tsa na zadannuyu dvusvyaznuyu oblast'" (Electrosimulation of conformal transformation of an annulus onto an assigned two-connected region), Ukr. matem. zhurn., t. VII, No. 3, 1955.

39. Ugodchikov, A. G., Krylov, A. Ya. "Elektromodelirovaniye konformnogo otobrazheniya polubeskonechnykh oblastey" (Electrosimulation of conformal mapping of semi-infinite regions), Izvestiya vuzov, elektromekhanika, 1960, No. 11.

40. Fil'chakov, P. F., Panchishin, V. I. "Integratory EGDA. modelirovaniye potentsial'nykh poley na elektroprovodnoy bumage" (Integrators EGDA. Simulation of potential fields on resistance paper), Izd. AN USSR, 1961.

41. Khag, B. "Elektromagnitnyye raschety" (Electromagnetic calculation), Gosenergoizdat, 1934.

42. Shamanskiy, V. Ye. "K voprosu o konformnom otobrazhenii pr' pomoshchi elektromodelirovaniya" (Concerning the question of conformal mapping with the help of electrosimulation), Ukr. matem. zhurn., t. VIII, No. 1, 1956.

U. S. BOARD ON GEOGRAPHIC NAMES TRANSLITERATION SYSTEM

Block	Italic	Transliteration	Block	Italic	Transliteration
А а	<i>А а</i>	A, a	Р р	<i>Р р</i>	R, r
Б б	<i>Б б</i>	B, b	С с	<i>С с</i>	S, s
В в	<i>В в</i>	V, v	Т т	<i>Т т</i>	T, t
Г г	<i>Г г</i>	G, g	У у	<i>У у</i>	U, u
Д д	<i>Д д</i>	D, d	Ф ф	<i>Ф ф</i>	F, f
Е е	<i>Е е</i>	Ye, ye; Ё, ё*	Х х	<i>Х х</i>	Kh, kh
Ж ж	<i>Ж ж</i>	Zh, zh	Ц ц	<i>Ц ц</i>	Ts, ts
З з	<i>З з</i>	Z, z	Ч ч	<i>Ч ч</i>	Ch, ch
И и	<i>И и</i>	I, i	Ш ш	<i>Ш ш</i>	Sh, sh
Й й	<i>Й й</i>	Y, y	Щ щ	<i>Щ щ</i>	Shch, shch
К к	<i>К к</i>	K, k	Ъ ъ	<i>Ъ ъ</i>	"
Л л	<i>Л л</i>	L, l	Ы ы	<i>Ы ы</i>	Y, y
М м	<i>М м</i>	M, m	Ь ь	<i>Ь ь</i>	'
Н н	<i>Н н</i>	N, n	Э э	<i>Э э</i>	E, e
О о	<i>О о</i>	O, o	Ю ю	<i>Ю ю</i>	Yu, yu
П п	<i>П п</i>	P, p	Я я	<i>Я я</i>	Ya, ya

* ye initially, after vowels, and after ъ, ь; e elsewhere.
 When written as ё in Russian, transliterate as yë or ë.
 The use of diacritical marks is preferred, but such marks
 may be omitted when expediency dictates.

FOLLOWING ARE THE CORRESPONDING RUSSIAN AND ENGLISH
DESIGNATIONS OF THE TRIGONOMETRIC FUNCTIONS

Russian	English
sin	sin
cos	cos
tg	tan
ctg	cot
sec	sec
cosec	csc
sh	sinh
ch	cosh
th	tanh
cth	coth
sch	sech
csch	csch
arc sin	\sin^{-1}
arc cos	\cos^{-1}
arc tg	\tan^{-1}
arc ctg	\cot^{-1}
arc sec	\sec^{-1}
arc cosec	\csc^{-1}
arc sh	\sinh^{-1}
arc ch	\cosh^{-1}
arc th	\tanh^{-1}
arc cth	\coth^{-1}
arc sch	sech^{-1}
arc csch	csch^{-1}
<hr/>	
rot	curl
lg	log

DISTRIBUTION LIST

[illegible]